Development of Novel Cereblon-Based E3 Ligase Ligand-Linker Libraries for Targeted Protein Degradation

by

Chelsi M. Almodóvar Rivera

A dissertation submitted in partial fulfillment of
the requirements for the degree of

Doctor of Philosophy
(Pharmaceutical Sciences)

at the

UNIVERSITY OF WISCONSIN-MADISON

2024

Date of final oral examination: 05/06/2024

The dissertation is approved by the following members of the Final Oral Committee:

Weiping Tang, Professor, Pharmaceutical Sciences Division
Arash Bashirullah, Professor, Pharmaceutical Sciences Division
Cody Wenthur, Assistant Professor, Pharmaceutical Sciences Division
Jennifer Schomaker, Professor, Chemistry

ABSTRACT

Traditional drug discovery has focused on using small molecules to block the function of various proteins. However, almost 80% of the human proteome is considered “undruggable” due to the lack of a defined functional site for small molecules to bind. Proteolysis Targeting Chimeras (PROTACs) are a promising therapeutic strategy that do not require the binding to functional sites. PROTACs promote the degradation of protein targets selectively by exploiting the ubiquitin-proteasome system. Among the limited number of E3 ligase ligands discovered for the PROTAC technology, ligands of the cereblon (CRBN) E3 ligase such as pomalidomide, thalidomide, or lenalidomide are the most frequently used due to their favorable pharmacological properties compared with others. Moreover, although PROTACs have been used for a variety of protein targets, the rapid optimization and SAR evaluation of PROTAC libraries still experience many challenges, including the time-consuming lengthy synthesis and purifications before biological screening. In the first chapter, recent progresses to address this issue are discussed.

Our group previously reported that a phenyl group could be tolerated on the C4-position of lenalidomide as the ligand of CRBN to develop PROTACs. In the second chapter, we will present a recently published modular chemistry platform for the efficient attachment of various ortho, meta, and para-substituted phenyls to the C4-position of the lenalidomide via Suzuki cross-coupling reaction. Accordingly, we employed these new chiral CRBN E3 ligase ligands to create a partial PROTAC library that was further converted into full PROTAC libraries for androgen receptor (AR) degradation using a Rapid-TAC platform. Our results showed significant degradation of AR with three hit degraders as analyzed with a HiBiT and antiproliferation assay. In the third chapter, we will be discussing our efforts for generating a partial PROTAC library based on achiral CRBN E3 ligase ligands and a full PROTAC library for the degradation of the

Bruton's Tyrosine Kinase (BTK) using the Rapid-TAC strategy. Our initial BTK-HiBiT results suggest significant degradation of the BTK protein using nine BTK degraders with para and meta phenyl substitutions to the achiral CRBN E3 ligase ligand. Lastly, we will be presenting our prelimiary efforts in the development of a third-generation Rapid-TAC using a thiol-ene "click" chemistry. Specificially, we worked on optimizing the reaction conditions that could be used for the fast creation and biological evalution of full PROTAC libraries for any protein of interest.

DEDICATION

In loving memory of my grandmother

ACKNOWLEDGMENTS

I want to express my sincerest appreciation to all those who supported me throughout my journey in graduate school.

First and foremost, I thank my research advisor, Dr. Weiping Tang, for his wisdom, endless guidance, patience, and trust during my graduate studies. I could not have asked for a more understanding and supportive mentor. I will be forever grateful to him for laying the basis of my scientific career and inspiring me to be a better scientist and chemist every day.

To my thesis committee members, Dr. Arash Bashirullah, Dr. Cody Wenthur, and Dr. Jennifer Schomaker, for their invaluable advice and direction on my research and future career.

To all my lab members and collaborators, without them, I would not have the opportunity to write and display my research today. I am thankful for taking the time to help me, teach me, hear me, and support me during my projects. I will forever cherish my moments with all of them.

To my funding sources, the Chemistry-Biology Interface Training Program and SciMed GRS, for their financial and academic support.

To my beloved parents, siblings, and family, I cannot express enough how fortunate I am to have their unconditional love and support. I thank them for their sacrifices, care, and faith in me. I am grateful for having them as my rock when times get rough. They are the reason why I get to celebrate my doctorate and all my achievements.

Lastly, to my boyfriend and dear friends, my deepest gratitude. Their affection, encouragement, and comfort always filled me with the fuel I needed to complete my academic journey.

TABLE OF CONTENTS

LIST OF ABBREVIATIONS

AhR	Aryl Hydrocarbon Receptor
AR	Androgen Receptor
BRD4	Bromodomain Containing Protein 4
BTK	Bruton's Tyrosine Kinase
CLL	Chronic Lymphocytic Leukemia
CRBN	Cereblon
Cul4	Cullin 4
D2B	Direct-to-Biology
DDB1	DNA Damage-Binding Protein-1
DLBCL	Diffuse Large B-cell Lymphoma
ERα	Estrogen Receptor alpha
GSK	Glaxo Smith Kline
HRMS	High Resolution Mass Spectrometry
IMiDs	Immunomodulatory Imide Drugs
LC–MS	Liquid Chromatography Mass Spectrometry
MCL	Mantle Cell Lymphoma
MetAP-2	Methionine Aminopeptidase-2
MM	Multiple Myeloma
NMR	Nuclear Magnetic Resonance
PDHU	Phenyl Dihydrouracil
PEG	polyethylene glycol
PG	Phenyl Glutarimides

POI	Protein of Interest
PROTACs	Proteolysis Targeting Chimeras
Rapid-Glue	Rapid Synthesis of Molecular Glues
Rapid-TAC	Rapid Synthesis of PROTACs
Roc1	Regulator of Cullins 1
SAR	Structure-Activity Relationship
SCFβ	Skp-1-Cullin-F box complex containing Hrt1
TLC	Thin Layer Chromatography
TPD	Targeted Protein Degradation
Ub	Ubiquitin
ultra HTE	Ultra High Throughput Experimentation
VHL	vol Hippel-Lindau
WM	Waldenström Macroglobulinemia

CHAPTER 1

Recent Chemistry Advances for Accelerating the Optimization of Proteolysis Targeting Chimeras (PROTACs) for Targeted Protein Degradation

1.1 Introduction

Traditional drug discovery approaches have focused on using small molecules to occupy the active site or allosteric site to modulate the function of proteins. However, almost 80% of the human proteome is considered “undruggable” due to the lack of defined active or allosteric binding sites on the protein for small molecules to bind and control its activity.[1] Targeted protein degradation (TPD) was first discovered as a promising therapeutic strategy to degrade a protein of interest (POI) by employing the Ubiquitin (Ub) proteasome system using molecules that induce a proximity-based pharmacology.[2] Ubiquitination is known as one of the major posttranslational modifications involved in many cellular pathways.[3]

Proteolysis Targeting Chimeras (PROTACs) selectively promote the degradation of proteins by using the targeted protein degradation strategy. PROTACs are heterobifunctional small molecules consisting of two ligands connected by a short linker. One ligand binds to an E3 ubiquitin ligase, while the other binds to a protein of interest. Consequently, the PROTAC small molecule degrader induces the proximity of the POI and an E3 ligase creating an essential ternary complex. The ternary complex enables protein-protein interactions between the two proteins.[2]

The concept of PROTACs was first published in 2001, and significant progress has been witnessed in recent years.[4,5] The first heterobifunctional degrader , Protac-1, was created to promote the degradation of methionine aminopeptidase-2 (MetAP-2).[4] Protac-1

consisted of a chimeric molecule that employed the IκBα phosphopeptide, which recruits the Skp-1-Cullin-F box complex containing Hrt1 (SCFβ-TRCP) E3 ubiquitin ligase, and ovalicin, a ligand that recognizes MetAP-2.[4] Although the study served as a proof-of-concept for targeted elimination of specific proteins, its potential as a therapeutic tool needed further development. Particularly, the delivery of Protac-1 to cells was prevented by cell permeability difficulties owing to its peptidic nature and potential hydrolysis.[4,5] Hence, small molecules have been the main focus of more recent PROTACs, comprising ligands that can bind to various target protein of interest and E3 ligases.

In 2023, it was estimated that at least more than 20 PROTACs entered clinical trials worldwide.[6] Specifically, Vepdegestrant (ARV-471), a collaboration between Arvinas and Pfizer, was granted Fast Track in February 2024 as a monotherapy in the treatment of adults with estrogen receptor positive /human epidermal growth factor receptor 2 negative (ER+/HER2-) locally advanced or metastatic breast cancer.[7] More precisely, the Fast Track process helps advance the development and review of potential drugs in cases of serious medical needs.

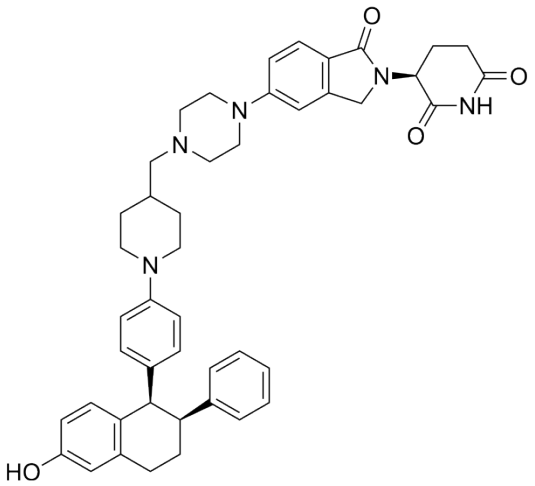

Figure 1. Structure of Vepdegestrant (ARV-471) developed by Arvinas and Pfizer for the treatment of locally advanced or metastatic breast cancer.

Notably, the PROTAC technology has also the capacity of degrading traditionally known as “undruggable” protein targets such as STAT3, which is currently being investigated in clinical trials for the treatment of solid tumors.[8,9] Consequently, although PROTACs have proven to be a suitable drug paradigm, several questions still required to be address.

For instance, the clinical application of PROTACs is still limited mainly due to their high molecular weight (>800 Da). These molecules show a relatively high polar surface, low cell permeability, and low oral bioavailability. However, optimization of PROTACs holds several challenges. The binary complex binding assays do not take into account the effects of the ternary complex formation.[10] Likewise, various complexes are possible in solution and they can only be properly assessed through cell-based assays, where permeability effects may affect the results.[10] Therefore, structure-activity relationship (SAR) studies are mainly guided by the data acquired from individually screening multiple important parameters, including length and types of linkers, of the synthesized compounds.[10,11]

Nonetheless, the large number of lengthy synthetic steps involved for preparing the POI ligand, E3 ligase ligand, and linkers, makes the development of PROTACs very time-consuming, a major obstacle for the rapid optimization of PROTAC molecules.[11] Due to these reasons, here we discuss the recent chemistry progress on the rapid development

of PROTACs, including the considerations for their design. Ultimately, the goal of this review is to provide a comprehensive analysis of the different strategies that have been explored for the fast optimization of PROTACs, which could serve as a valuable guide to quickly develop potent and selective PROTACs than can benefit patients in the clinic.

1.1 Development of PROTACs

1.1.1 E3 Ligase Ligands

There are more than 600 E3 ligases discovered in the human genome. However, only a handful are currently used for PROTACs. Among them, cereblon (CRBN) and von Hippel-Lindau (VHL) are the most widely applied in PROTACs. Apart from CRBN and VHL, other E3 ligands have also been applied to the development of PROTACs, such as the mouse double minute 2 (MDM2)[12], cellular inhibitor of apoptosis (cIAP), RING type zinc-finger protein 114 (RNF114), RING type zinc-finger protein 4 (RNF4), aryl hydrocarbon receptotor (AhR), FEM1B, damage-specific DNA binding protein 1 (DDB1)-CUL4 associated factor 16 (DCAF16), damage-specific DNA binding protein 1 (DDB1)-CUL4 associated factor 15 (DCAF15), damage-specific DNA binding protein 1 (DDB1)-CUL4 associated factor 11 (DCAF11), and Kelch-like ECH-associated protein 1 (KEAP1) (**Figure 2**).[13] Some of the discovered E3 ligase ligands operate through molecular glue mechanism and are able to recruit different E3 ligases. However, although DCAF15-ligand containing PROTACs are reported[14,15], the recruitment of DCAF15 has not been validated for any of them.

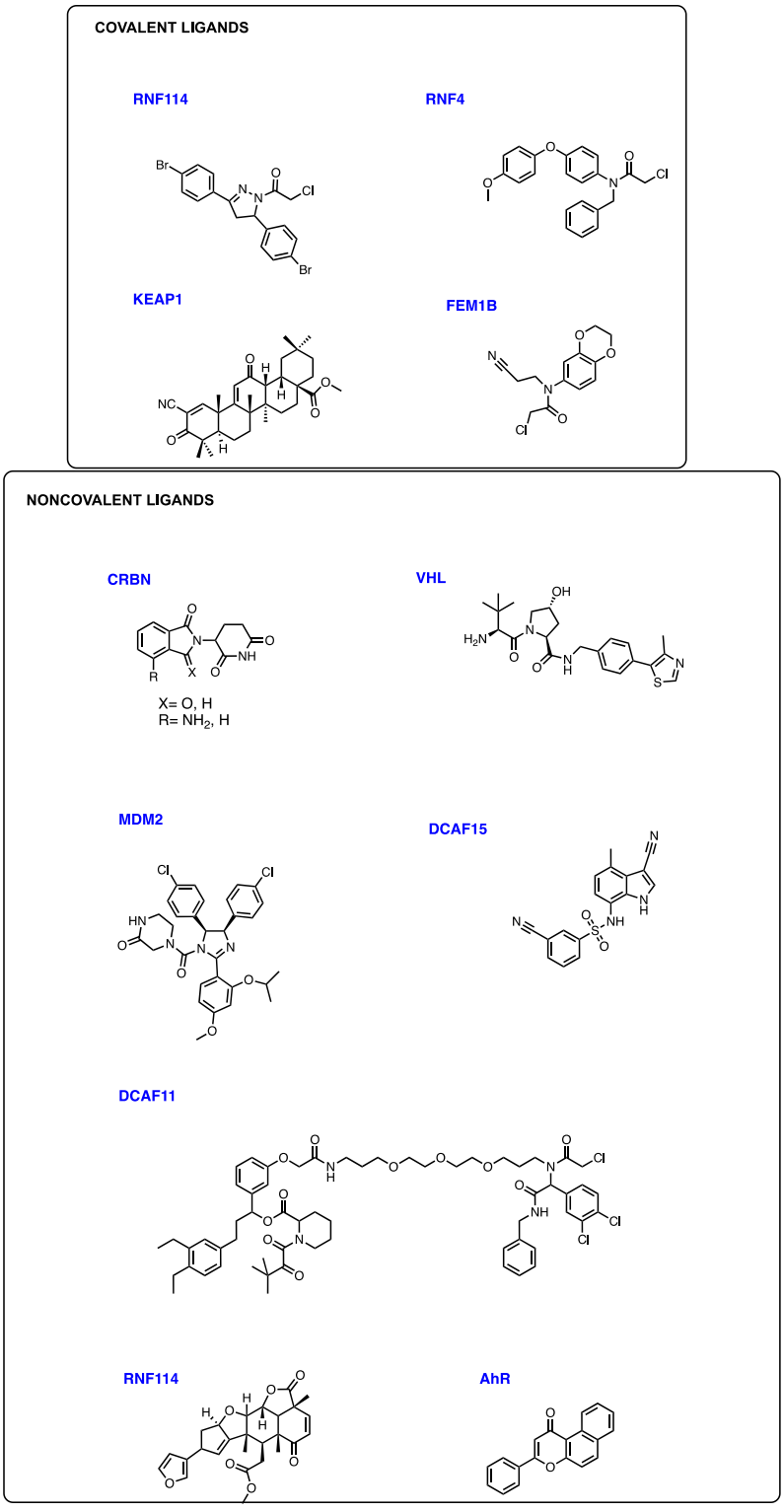

Figure 2. Examples of ligands used in targeted protein degradation.

Nonetheless, it is still not clear how the recruitment of different E3 ligases can affect the degradation efficiency of a PROTAC.[13] More studies should be considered to examine how the ternary complex is affected by distinct E3 ligases.[13] Moreover, different E3 ligases are also expressed in distinct cells or tissue types.[13] Consequently, expanding the toolbox for E3 ligases available for PROTACs and the discovery of new small-molecule E3 ligase ligands is a growing area of interest in TPD.[16] The discovery of new E3 ligase ligands for different E3 ligases could significantly impact the therapeutic potential of PROTACs.

1.1.2 POI targets

Proteolysis Targeting Chimeras are applied to a variety of protein targets. Specifically, PROTACs have been studied for treating diseases such as cancer, immune disorders, and neurodegenerative and cardiovascular diseases.[17] For example, the estrogen receptor α (ER α) and androgen receptor (AR) have been targeted by PROTACs for the treatment of breast cancer and prostate cancer, respectively.[17] Similarly, IRAK3/4, HDAC6, and Sirt2 were studied for the treatment of immune or inflammatory disorders.[17] More recently, PROTACs that target neurodegenerative or cardiovascular disease-causing proteins have been also reported.[17] In addition, the capacity of PROTACs to degrade “undruggable” targets has been proven by different proteins such as STAT3, Tau, and α-synuclein.[17] **Figure 3** shows a few examples of the different PROTACs that have been created for a variety of proteins.

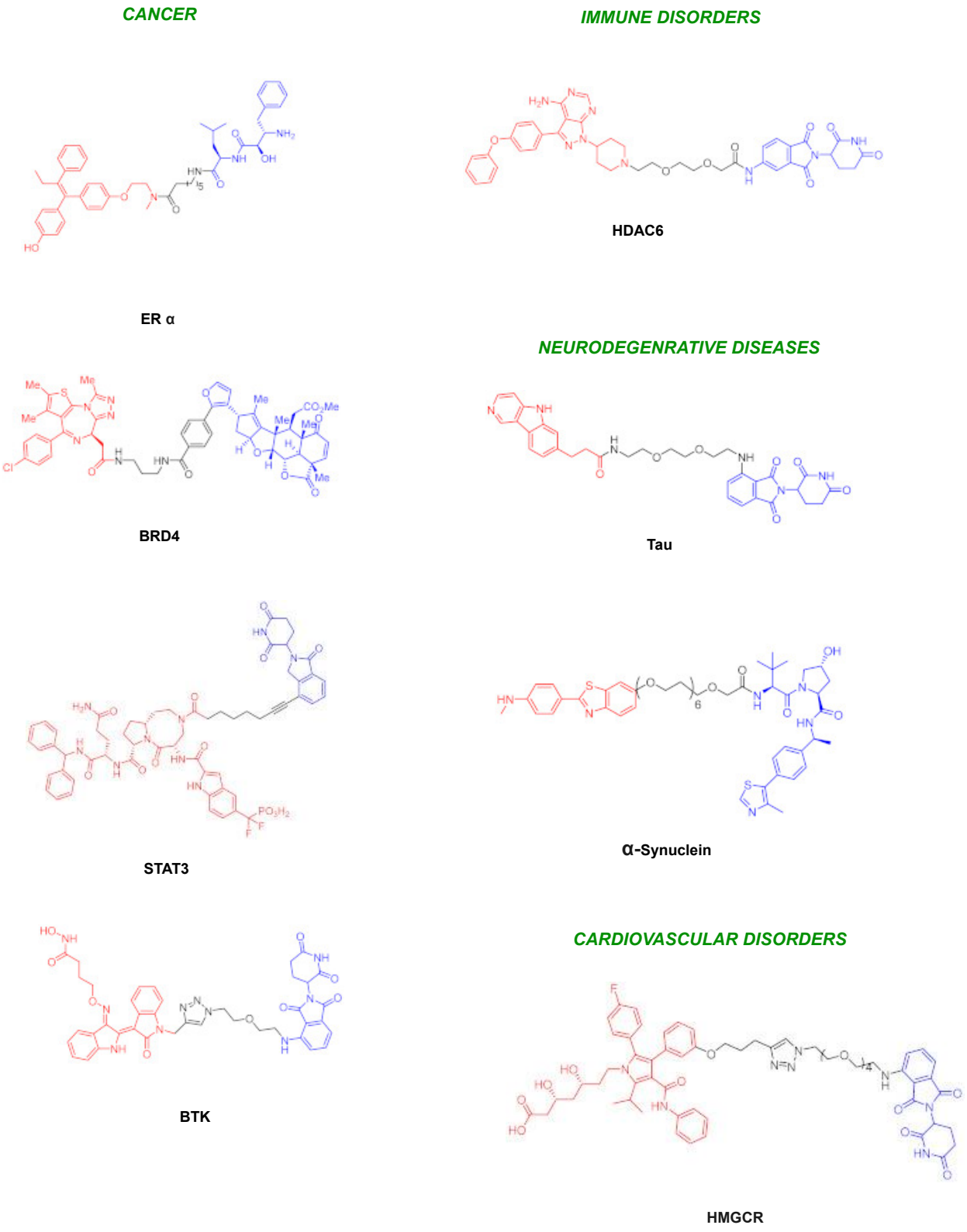

Figure 3. Examples of PROTACs applied for different diseases with their targeted proteins highlighted in black. *The figure was adapted from Yao et al.*[17]

1.1.3 Linkers

It is believed that the degradation efficiency of PROTACs is dependent not only on the affinities of the ligands for the E3 ligase or POIs[18] but also on the combination of ligands with an appropriate linker that can allow the most stable ternary complex formation, which leads to POI polyubiquitination.[18] The composition of the linkers permits a proper spatial orientation that supports the protein-protein interactions between the POI and E3 ligase.[19] Precisely, an arrangement between the length and type of linker composes an essential role in the success of a heterobifunctional PROTAC degrader.[19]

Most of the time, the development of PROTACs begins with the generation of a library of PROTACs containing diverse set of unsubstituted aliphatic linkers between the POI and E3 ligase ligands.[19] Various length of flexible (e.g. PEG or alkyl) or restricted/rigid linkers (e.g. alkyne, piperidine, piperazine, and triazoles) have been employed in PROTAC degraders for the exploration of improved physiochemical, pharmacokinetics properties, and biological activity.[19] However, there is still not a general rule that condenses the PROTAC linker design.

In general, in order to achieve an effective protein degradation, there is an optimal distance required between the E3 ligase and the POI.[18] If the linker is too short, binary steric repulsions between the ligands and the proteins may occur. If the linker is too long, optimal protein-protein interactions cannot be enforced. Thus, the linker length of current PROTACs is usually between 3 and 19 atoms.[18] In addition to the length of linker, it is worth to mention that the orientation and hydrophilic/hydrophobic property of the linker

may affect the potency and selectivity of the PROTAC. Subtle changes in the linker length and composition can often significantly affect the degradation efficiency. Therefore, linker optimization is a key feature of modulating the activity of the small molecule PROTAC degraders.

Nevertheless, the linker optimization can be a time-consuming and challenging process because each degrader must be individually synthesized and multiple rounds of SAR studies need to be conducted. In turn, researchers have been trying to develop innovative strategies to accelerate the development and screening of active PROTAC degraders. In the next section, we will describe the latest strategies that have been developed for accelerating the development of small molecule heterobifunctional PROTAC libraries.

1.2 High-throughput Development of PROTACs

1.2.1 Click Chemistry

Click Chemistry has been utilized for the rapid synthesis of PROTAC libraries.[20,21] Previous work by Lebraud and colleagues incorporated a bio-orthogonal click combination of two small ligand precursors containing a tetrazine or a *trans*-cyclo-octane to develop a cell penetrating PROTAC molecule *in situ*.[22] Inspired by this work, the Jung group reported the creation of a triazole-containing PROTAC molecule for targeting the histone deacetylases sirtuins (Sirt) family of proteins.[20] Specifically, using this “click” chemistry approach they discovered the first highly-potent and Sirt2 selective triazole-

PROTAC degrader.[20] At the same time, Wurz and coworkers assembled PROTACs using similar “click” chemistry based on VHL or CRBN E3 ligase ligands modified with terminal alkynes and varied polyethylene glycol (PEG) linkers able to react with a JQ1-containing-azide to target the BRD4 protein.[21] However, the products need to be purified in order to remove the toxic copper catalyst from the reaction system. Nevertheless, these studies pioneered the first proof-of-concept application of using bio-orthogonal chemistry strategies to create full PROTAC libraries and comprehensively examine the effects linker length.[20,21]

1.2.2 Direct-to-Biology and Rapid-TACs

In 2022, the term of “direct-to-biology” (D2B) first appeared in the literature.[10] It is a process for which large libraries of compounds can be synthesized at a small scale and assay them as a crude mixture with minimal amount of manipulations. High throughput chemistry and high throughput biology strategies are used to accelerate the optimization of molecules and reduce overall costs. Thus, it can provide the opportunity for examining and optimizing preassembled libraries of compounds in just a few days.

Our lab reported the first generation of the rapid synthesis of PROTAC (Rapid-TAC) platform in 2020.[11] It consisted of a combinatorial strategy that allow the couple a preassembled E3 ligase ligand library containing a terminal aldehyde moiety with a library of the POI ligands with a terminal hydrazide group to yield PROTACs with an acylhydrazone linkage that can be directly used for screening without any further

manipulations including purifications.[11] The reaction permits a faster access to full PROTAC products with more than 90% purity in most cases and direct biological screening. However, one key limitation of the approach is the hydrolysis of the acylhydrazone linkage in assays requiring longer time, such as 24 h.[11]

For this reason, a second stage is required after identifying the most active compound, where the acylhydrazone is change to its isostere such as an amide bond for improved stability and drug-like properties.[11] During the study, our group created a full PROTAC library bearing VHL or CRBN E3 ligase ligands and Estrogen Receptorα (ERα) ligands. Importantly, the library achieved nearly 100 compounds in just a few days. Finally, one compound, namely **A3**, was identified as the most potent ERα degrader. Moreover, an amide version of **A3** was created to yield compound **AM-A3** as a more stable compound with degradation and potency comparable to the parent compound. Moreover, in a subsequent study our lab reported the construction of a fibroblast growth factor receptor 1 (FGFR1) degraders using the Rapid-TAC platform.[23] Eventually, PROTAC **LG1188** was identified as a potent and selective FGFR1 degrader.[23] Consequently, the study set the idea of using a direct-to-biology approach for generating and screening PROTAC compounds quickly.

Due to the liability issue of the acylhydrazone linkage, a second generation of Rapid-TAC was also described by our group in 2022. It involves a one-step strategy that allows the creation of active and stable PROTACs while maintaining the advantages of the previous Rapid-TAC platform.[24] The approach relies on the formation of a phthalimidine moiety

from *ortho* phthalaldehyde and a primary alkyl amine. [24] Significantly, the reaction can also be done under miniaturized conditions without further purification required.[24] The utility of the strategy was evaluated by the development of two PROTAC libraries, one for the androgen receptor (AR) and the other for the bromodomain containing protein 4 (BRD4).[24]

In 2022, the Janssen Research & Development Discovery Chemistry team reported a study providing another approach for the synthesis and evaluation of PROTACs using the direct-to-biology strategy.[10] The platform focused on linker effects involving a combination of a high-throughput chemistry with high-throughput cell based assays such as target engagement, protein degradation potency, permeability, and cell toxicity.[10]

They created a library composed of 91 PROTACs, where the synthesis consisted on attaching mono-*N*-Boc diamines building blocks with JQ1 and CRBN-based E3 ligase ligands.[10] Specifically, an amide bond formation, TFA-mediated Boc deprotection, and a second amide bond formation was used to couple the linker portion.[10] Particularly, the investigators used resin-bound scavengers to remove unreacted starting materials during the amide formation reactions.[10] The compounds were then directly dissolved in DMSO and used in biological assay where they identified hit PROTACs with DC_{50} as low as 6 nM.[10] However, compared to our group's previous Rapid-TAC platforms, these diamines coupling reactions still required some types of purification.

Automation is an alternative advantageous tool in drug discovery for high-throughput screening and optimization of drug molecules. In 2023, Glaxo Smith Kline (GSK) published an ultra-high throughput experimentation (ultra HTE) for PROTAC synthesis.[25] The approach incorporated automation on each step of the synthesis, evaluation, and biological screening of PROTACs.[25] It involved a D2B workflow following a 5 μL scale amide coupling synthesis and crude evaluation exploiting a HiBiT assay to quantify the protein degradation.[25] The researchers achieved the synthesis and evaluation of more than 600 PROTACs in a 1536-well plate.[25] Moreover, they were able to identify various potent picomolar BRD4 degraders.[25] Nevertheless, the need for highly expensive liquid handling robots for each step of the experimentation, makes it inaccessible for wide application of this method in PROTAC development.

1.2.3 Molecular Glues and Rapid-Glues

Apart from PROTACs, molecular glues have been widely studied in targeted protein degradation. Molecular glues have a similar mechanism of action to PROTACs by recruiting a protein of interest and E3 ligase simultaneously.[26] However, molecular glues and PROTACs differ structurally, since molecular glues are similar to traditional small molecule drugs (<500 Da).[26] Nonetheless, there are still not general methods available for discovering molecular glues.[26] For this reason, most of the molecular glues have been currently discovered serendipitously and by chemical library screening.[26,27]

In 2023, our group reported a novel approach to identify new molecular glues by a rapid synthesis (Rapid-Glue) in DMSO under miniaturized conditions.[26] Inspired by our first reported Rapid-TAC platform[11], this Rapid-Glue strategy consisted on having the hydrazide attached to different positions of the E3 ligase ligands (lenalidomide derivatives) to react with more than 300 diverse commercially available aldehydes.[26] The feasibility of the platform was assessed by creating a high throughput pilot library of more than 1000 compounds without further purifications or other manipulations.[26] Thus, the compounds were then analyzed by direct screening in cell-based assays.[26]

Using the Rapid-Glue approach, our group was able to identify two highly selective GSPT1 molecular glues hits.[26] Moreover, three stable analogues were also developed by replacing the acylhydrazone linker with an amide motif.[26] These compounds showed significant GSPT1 degradation and two of them are comparable to the parent acylhydrazone-containing compounds.[26] Hence, the Rapid-Glue platform presents a proof-of-principle study to rationally develop molecular glues through rapid synthesis, phenotypic screening, proteomic profiling, target validation and hit optimization.[26]

1.2.4 Computational Methods

Computational tools can benefit the advancement and rapid design of PROTACs. First, virtual screening aids the identification of ligands for a protein target or E3 ligases using large databases.[28] Several protein binders have been discovered through this approach.[28] Computational strategies are also used to investigate the interactions between PROTACs, E3 ligases, and the protein of interest.[2,28] For instance, molecular

docking provides opportunity to evaluate the binding between protein-PROTAC-E3 ligase by docking the PROTAC into a pocket of one of the proteins and then adding the other protein.[28] Our lab reported a method that distinguishes native vs non-native PROTAC complex poses via MD-based scoring enabled by pose thermal durability.[29] Nevertheless, predicting the ternary complex formation remains to be a challenge due to the complexity between protein-small molecule and protein-protein interactions.[2] Thus, additional constraints are often required for simplification.[2]

1.3 Conclusions

In conclusion, PROTACs are rapidly advancing in the fields of chemical biology and medicinal chemistry. As a promising drug discovery strategy, targeted protein degradation offers a way to surmount some of the limitations associated with traditional small molecules. The therapeutic benefits of PROTACs have been demonstrated by targeting numerous disease-related proteins and their clinical applications are expected to expand quickly.

The synthesis of PROTACs is often complex, time-consuming, and challenging, with linker optimization being a crucial aspect in developing effective PROTACs. Consequently, there is significant interest in innovative approaches for the rapid development and screening of PROTAC libraries. Techniques such as click chemistry, direct-to-biology strategies, Rapid-TACs, automation, and computational methods have facilitated the swift design and synthesis of PROTACs targeting various proteins. Similarly, our group has developed the Rapid-Glue approach, which expedites the design

and discovery of molecular glues. Therefore, enhancing the development of small molecule degrader libraries holds considerable promise for quickly identifying potent and selective PROTACs with potential therapeutic applications.

CHAPTER 2

A Modular Chemistry Platform for the Development of a Cereblon (CRBN) E3 Ligase-Based Partial PROTAC Library and Androgen Receptor Full PROTAC Library for Targeted Protein Degradation

Part of this chapter was taken from the following published article.

Almodóvar-Rivera CM, Zhang Z, Li J, Xie H, Zhao Y, Guo L, Mannhardt MG, Tang W. A Modular Chemistry Platform for the Development of a Cereblon E3 Ligase-Based Partial PROTAC Library. Chembiochem. 2023 Oct 17;24(20):e202300482. doi: 10.1002/cbic.202300482. Epub 2023 Aug 22. PMID: 37418320; PMCID: PMC10591699.

2.1 Introduction

Proteolysis targeting chimeras (PROTACs) are heterobifunctional small molecules that can degrade a protein of interest (POI) by employing the ubiquitin (Ub)-Proteasome System.[30] These molecules consist of a linker bound by two ligands. One of the ligands binds to the POI and the other one binds to an E3 ubiquitin ligase.[31] The simultaneous binding forms a ternary complex which initiates an E1-E2-E3 ubiquitin ligase cascade to enable targeted protein's polyubiquitination followed by proteasome degradation of the POI.[31] Since the PROTAC molecule is used catalytically, the PROTAC molecule recycles and promotes the process continuously.

Although the PROTAC technology has been applied to a variety of disease-associated proteins, only a handful of cell permeable small molecule E3 ligase ligands have been successfully discovered. Among them, CRBN and von Hippel-Lindau (VHL) are the two most widely used E3 ligase ligands for the development of PROTACs.[32] Specifically, CRBN E3 ligase ligands have been more commonly used in PROTACs for the degradation of protein targets related to many diseases, such as cancer, neurodegenerative diseases like Alzheimer's disease, and immune disorders.[33,34] Although there are extensive patent literature on various CRBN ligands,[35] no detailed structure activity relationship were disclosed in these patents. Most of the frequently used CRBN ligands still hold limitations[36] such as low potency, low permeability, or poor selectivity and efforts on improving them are actively pursued.[37,38] Moreover, the chemistry developed for the assembly of CRBN ligands with various linkers bearing diverse properties is also limited.[30,32,39,40] This is particularly important for the

development of PROTACs, as the types of linkers and their attachment points are essential for the pharmacological properties of PROTACs, such as potency, selectivity, solubility, and metabolic stability.[41]

To date, most of the CRBN E3 ligase ligands in PROTACs rely on pomalidomide, 4-hydroxythalidomide, alkyl-based thalidomide, and lenalidomide derivatives (Figure **1**).[34] Because lenalidomide lacks a carbonyl group in the phthalimide ring, which contributes to the better chemical and metabolic stability over pomalidomide or thalidomide,[42] lenalidomide-based ligands are found more often over pomalidomide-derived ligands in the development of PROTAC type of degraders, when higher stability is more important than other parameters.[30,34]

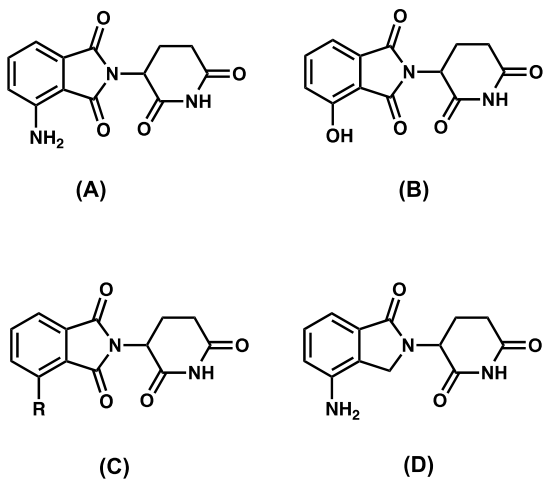

Figure 1. Structures of pomalidomide (**A**), 4-hydroxythalidomide (**B**), alkyl-based thalidomide (**C**), and lenalidomide (**D**).

A recent study involving the development of a cell-based target engagement assay by our group suggests that lenalidomide-based analogs with a phenyl substituent displayed

high affinity and better selectivity to CRBN over thalidomide (**Figure 2**).[43] These compounds containing the phenyl substituent had an activity comparable to pomalidomide, yet they do not degrade neo-substrates such as IKZFs like pomalidomide or thalidomide.[43] Moreover, ortho, meta, or para substitutions of the phenyl ring did not decrease the activity significantly[43] indicating the possibility of the introduction of new phenyl-connected linkers at any of these positions for the development of PROTACs, which will allow the systematic evaluation of the effect of linker to the activity of PROTACs.

Optimizing commonly used synthetic conditions for PROTACs could benefit their applications as chemical probes and therapeutics. Most current lenalidomide-based E3 ligase ligands have linkers attached to the C4- or C5- position of the phthalimide ring.[39] However, compared to pomalidomide-based ligands, the synthesis of lenalidomide-based PROTACs can be limited since the decrease of the phthalimide ring's electrophilicity made some methods such as S_NAr not accessible.[39] In addition, some cross-coupling reactions, which are widely used in PROTAC synthesis to attach linkers to the bicyclic ring, can lead to the hydrolysis of the cyclic imides.

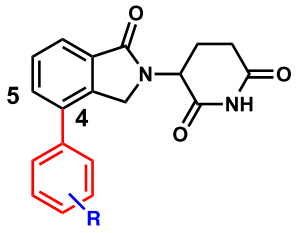

Figure 2. Structure of C4-lenalidomide-derived substituted phenyl ring.

Existing alkyl linkers in lenalidomide-based PROTACs have been focused on introducing alkynes followed by reduction.[34] Recently, a palladium-catalyzed Buchwald-Hartwig amination protocol was reported for the synthesis of lenalidomide-based PROTACs from aryl bromides (**Scheme 1A**).[39] A similar Suzuki cross-coupling strategy was reported by using an isoindolinone boronic acid intermediate to introduce an ester to the phthalimide ring of lenalidomide-based analogs, which can be used for the attachment of amine linkers after hydrolysis (**Scheme 1B**).[44]

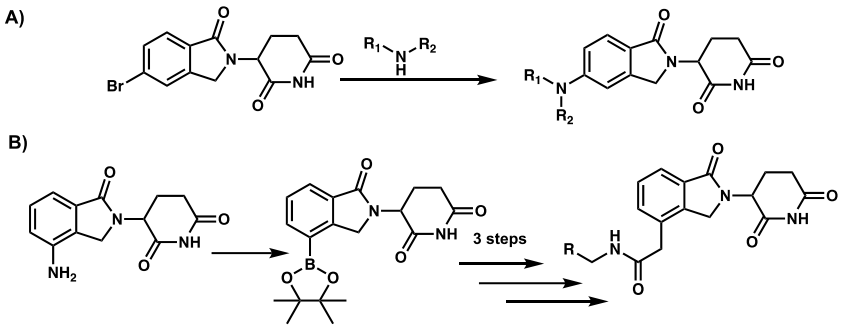

Scheme 1. Current methods for the synthesis of lenalidomide-derived CRBN E3 ligase ligands with an attachment.

We herein describe the development of a modular chemistry platform for the direct attachment of phenyl groups to the phthalimide moiety of lenalidomide-based ligands by Suzuki cross-coupling. This strategy provides an opportunity to introduce ortho, meta, and para substituted phenyl groups to lenalidomide, which allows systematic evaluation of the effect of the attachment positions to the property of PROTACs against various targets. Finally, we applied some of the lenalidomide-based ligands with phenyl substitutions to the creation of a pre-assembled partial PROTAC library composed of

twelve compounds that can later be used in the synthesis of full PROTAC libraries for any protein of interest.

2.2 Results and Discussion

We first prepared the iodolenalidomide derivative **2**, a key intermediate for the Suzuki cross-coupling reaction. The synthesis of the iodo-lenalidomide intermediate **2** was achieved in three steps as previously reported[43,45] from commercially available starting material **1** (**Scheme 2**). Because more diverse aryl iodides are available than aryl boronic acids, we decided to replace the iodide in **2** by a boronic ester functional group so that we can couple it with various functionalized aryl iodides if necessary. We adapted the cross-coupling reaction condition reported in the literature for this transformation[46] (**Scheme 3**). Essentially, a palladium-catalyzed coupling reaction using a pinacol ester diboron and aryl halides can afford various arylboronic esters.[46]

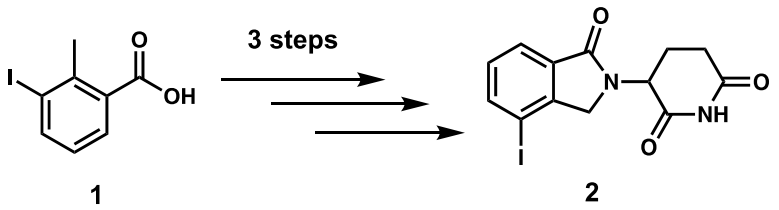

1 **2**

Scheme 2. Synthesis of key iodide-lenalidomide starting material **2**.

First, applying the previously published standard conditions[46] with iodo-lenalidomide **2** as starting material led to no reaction after 24 h (**Scheme 3**). Thus, we decided to start our optimization process by examining various parameters. Increasing the temperature from 80 ˚C to 100 ˚C gave a major byproduct. Careful analysis of this byproduct suggests that

a Suzuki cross-coupling was taking place under these conditions and a dimerization product **3** was formed as indicated by LC-MS (**Scheme 3**)

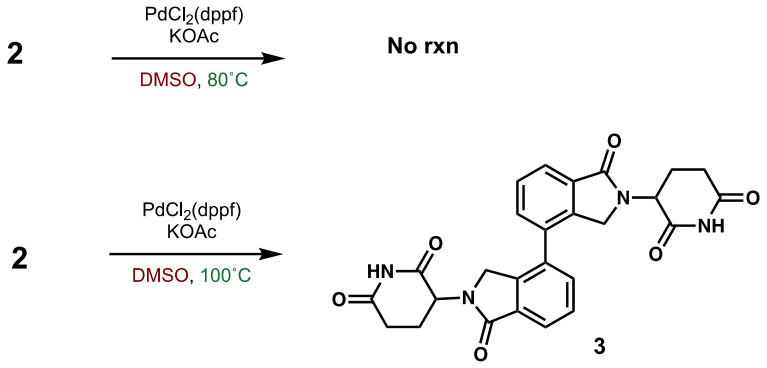

Scheme 3. Optimization of the Suzuki cross-coupling reaction using **2** (1 eq), bis(pinacolato) diboron (2 eq), $PdCl_2$(dppf) (5 mol %), KOAC (3 eq), and DMSO or 1,4-dioxane as solvents (0.2 M).

The observation of dimerization product **3** suggests that Suzuki cross-coupling reaction between an aryl iodide and an aryl boronic ester can occur under the above condition with a mild base. Previously, we had to use a strong base such as potassium carbonate and aqueous solution to promote the cross-coupling reaction and significant amount of hydrolysis byproduct was observed (**Scheme 4A**),[43] which has also been reported by others.[47] We had to treat the resulting mixture with CDI to re-cyclize the hydrolysis product to imide.[43] Not surprisingly, a low yield (~20%) was often obtained for the final product. To test the applicability of the new Suzuki coupling condition with a mild base, we synthesized a model CRBN E3 ligase ligand **4** based on the phenyl linker (**Scheme 4B**). Since in our previous conditions we had set the temperature to 90 ˚C, we decided to test

our new Suzuki cross-coupling conditions using the same temperature for comparison. Excitingly, our results showed that the new Suzuki coupling conditions improved the yield of product **4** from 20% to 58%. Compared to our previously used Suzuki coupling conditions (**Scheme 4A**), the new condition with a mild base (**Scheme 4B**) did not lead to any hydrolysis product.

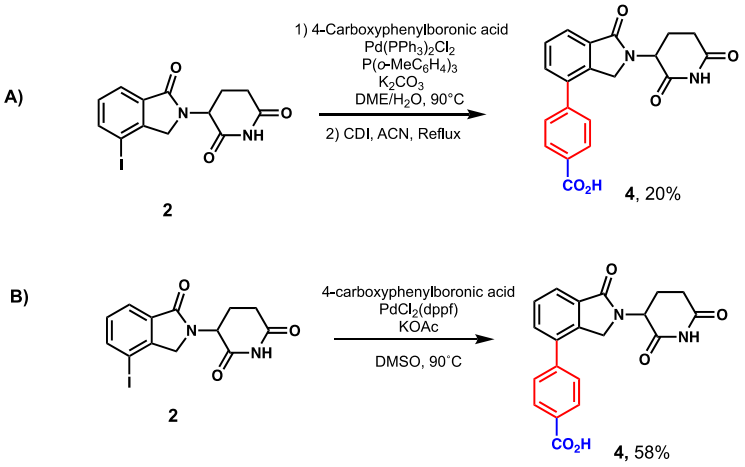

Scheme 4. Suzuki cross-coupling model reaction.

Next, we synthesized a small library of twelve lenalidomide derived-compounds with linkers on the ortho-, meta-, or para- positions to the terminal phenyl ring (**Scheme 5**). Most strategies for PROTAC linker synthesis rely on amines, amides, ethers, or C-C bonds.[48] Our strategy would allow the introduction of various linkers to the ortho-, meta-, and para- position of the phenyl ring by incorporating a Boc-amine or tert-butyl ester, phenol, or aldehyde to the phenyl boronic ester or boronic acid motif, which can then be further elaborated to PROTAC linkers. Notably, since most of the twelve compounds were relatively polar, we changed the solvent from DMSO to DMF to avoid any extraction

workup procedure to remove the solvent after completing the reaction. Moreover, setting the temperature to 100°C allowed for reaction completion after 12 h.

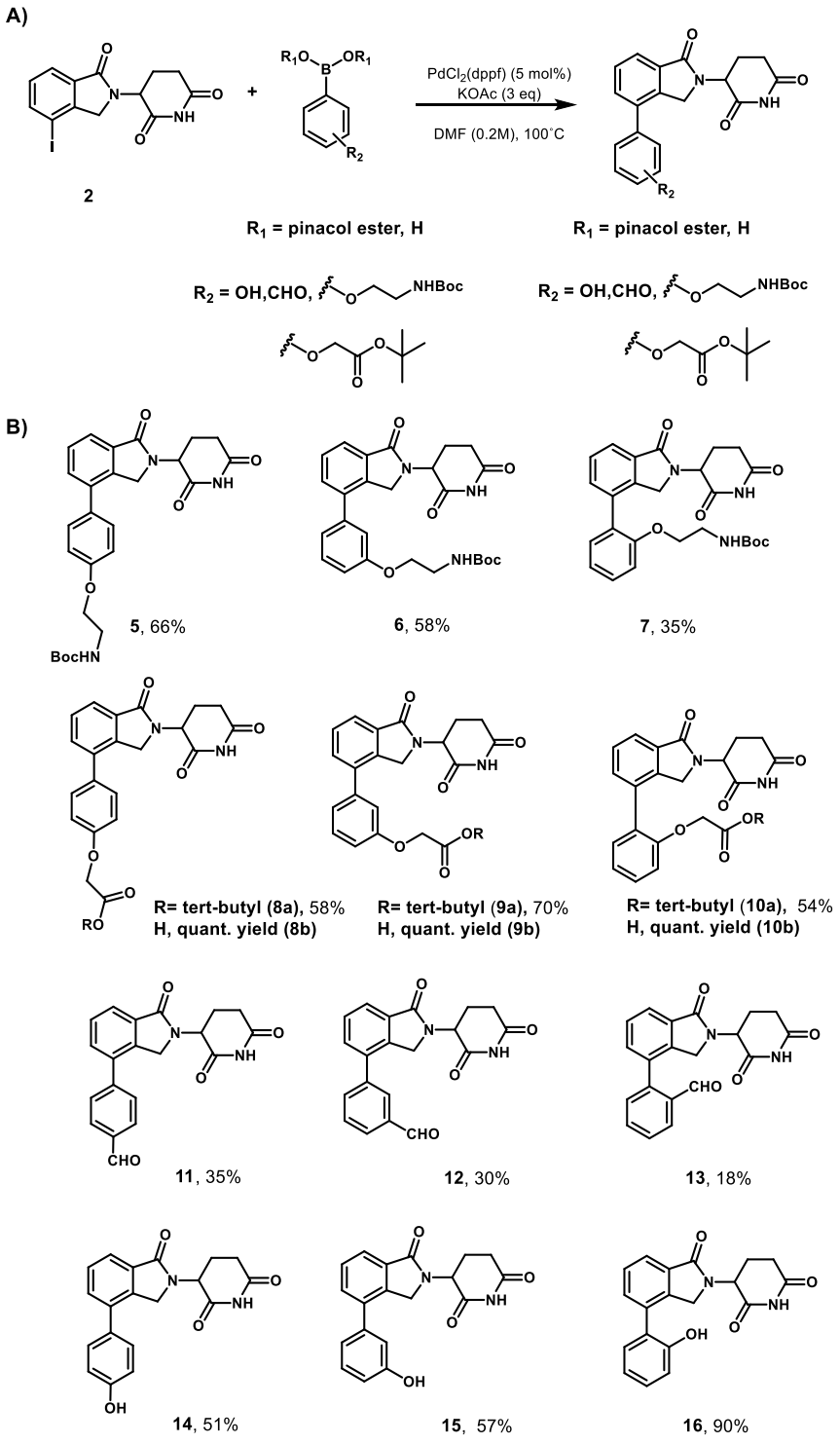

Scheme 5. Suzuki cross-coupling conditions and substrate scope of lenalidomide-derived CRBN E3 ligase ligands. [a] Isolated by flash column chromatography. The Suzuki cross-coupling conditions and lenalidomide-derived substrates were performed with Dr. Zhen Zhang, Dr. Jinyao Li, Dr. Yu Zhao and Dr. Le Guo.

Finally, we selected three compounds (**5, 6,** and **7**) from the small library as building blocks to create a partial PROTAC library. Specifically, we designed our partial PROTAC library based on the Rapid Synthesis of PRTAC (Rapid-TAC) strategy recently reported by our group.[11,23] Although many PROTACs have been successfully developed for a wide range of protein targets, the synthesis of these types of bifunctional molecules can be very time-consuming. The Rapid-TAC approach can significantly speed up the synthesis process and facilitate the rapid screening of E3 ligase ligands with a variety of different linkers.[11,23]

The Rapid-TAC strategy involves the reaction of a pre-assembled library of E3 ligase ligands with linkers containing a terminal aldehyde in a 1:1 ratio with a POI ligand containing a hydrazide moiety to form PROTACs with an acylhydrazone linkage.[11] Importantly, the resulting products in DMSO solution can be used for screening without any further manipulation including purification step since water is the only byproduct.[11] The acylhydrazone bond can then be changed to an amide bond for higher stability and more drug-like properties in the later stage.[11]

Before initiating the synthesis, we confirmed the binding affinity of compounds **5**, **6**, and **7** to CRBN using a well-established fluorescent polarization assay.[49] These three compounds showed K_ds of 231 nM for **5**, 218 nM for **6**, and 100 nM for **7**, respectively, while the the thalidomide-based probe has a K_d of 122 nM (**Figure 3**). It is consistent with our previous results from the cell-based assay.[43]

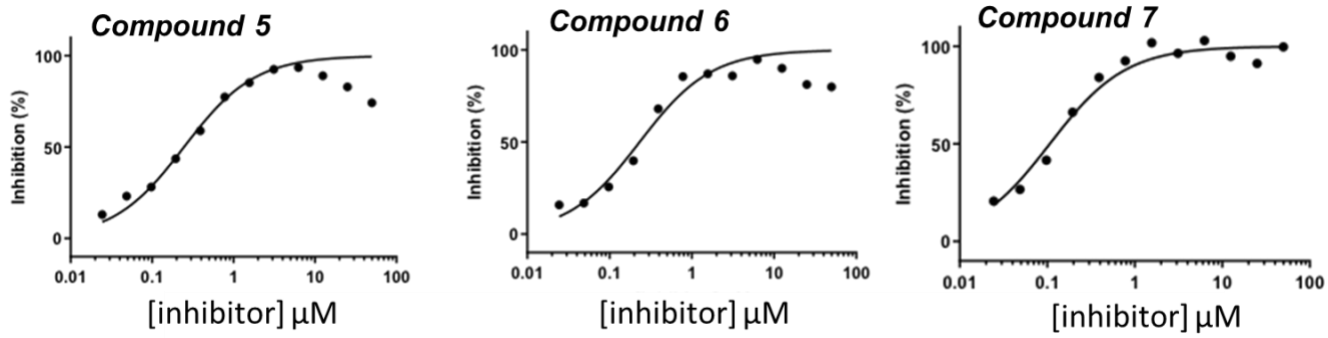

Figure 3. K_ds of compounds **5**, **6**, and **7**. The fluorescence polarization assay was performed by Dr. Haibo Xie.

It is well known that the linker plays a significant role in the ternary complex formation and activity of PROTACs.[11,18] We sought to choose compounds **5**, **6**, and **7** for the synthesis of a pre-assembled CRBN E3 ligase partial PROTAC library by systematically examining the length and orientation of the linker. Compounds **5, 6** and **7** contained a terminal Boc-protected amine, which could be easily deprotected and used to attach an alkyl linker containing a terminal aldehyde via an amide coupling reaction. Particularly, we considered that the relatively short partial linker length of these compounds provides the opportunity for systematic examining the substitution pattern on phenyl groups at both ends of the alkyl group. We then removed the Boc group to form a primary amine followed by an amide coupling with a ortho-, meta-, or para- formylbenzoic acid (**Scheme 6**). We

then prepared a small CRBN partial PROTAC library with a relatively short alkyl linker containing a meta or para terminal benzaldehyde that can be further used to react with a hydrazide group in any protein of interest ligand.

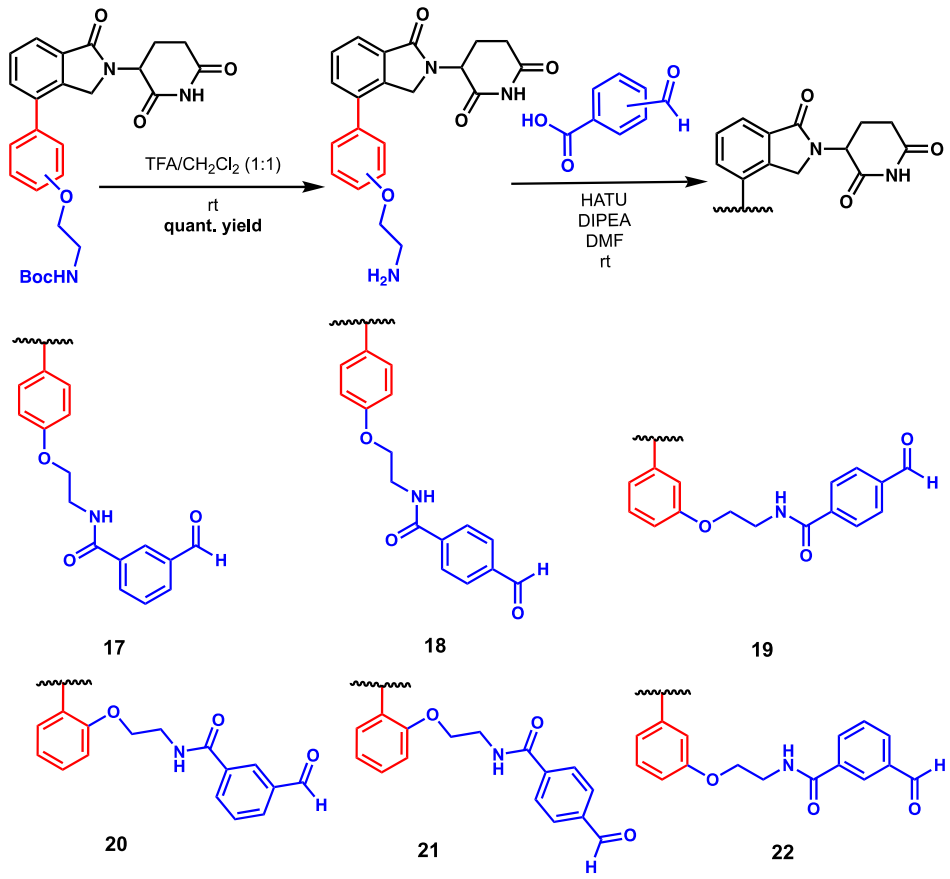

Scheme 6. Partial PROTAC library synthesis and substrate scope starting from compounds **5**, **6**, or **7** obtained from the Suzuki cross-coupling reactions.

2.2.1 Androgen Receptor (AR) Degraders based on the Chiral Cereblon E3 Ligase Ligands

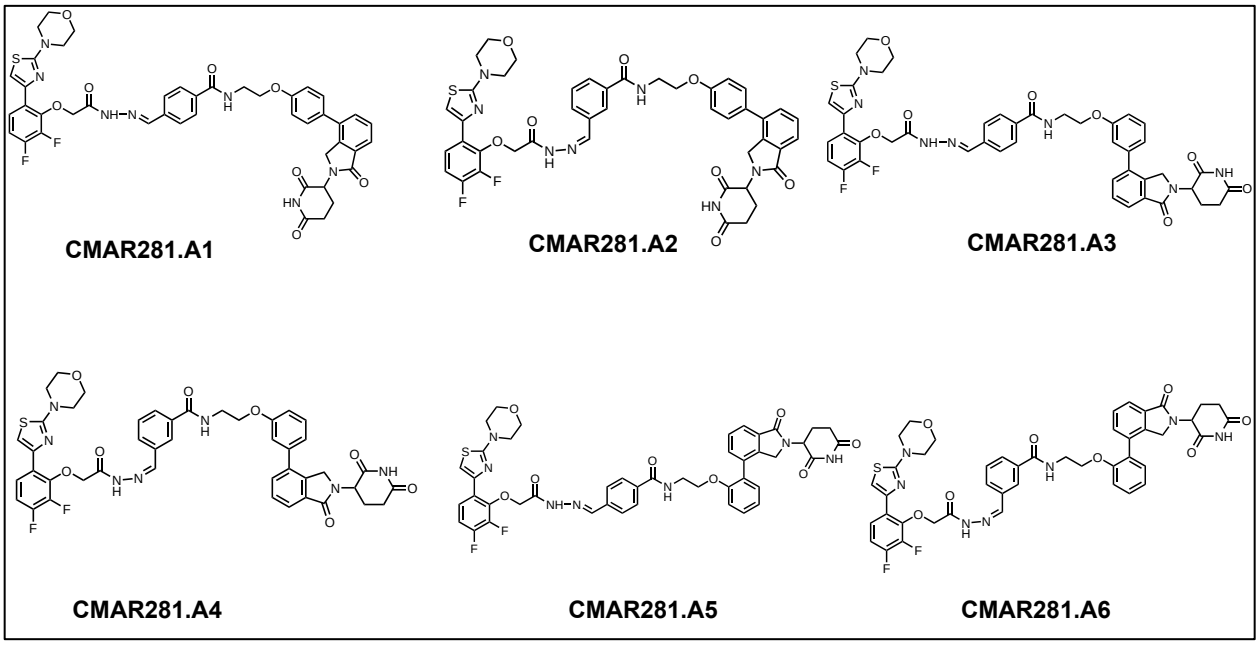

CMAR281.A1 CMAR281.A2 CMAR281.A3

CMAR281.A4 CMAR281.A5 CMAR281.A6

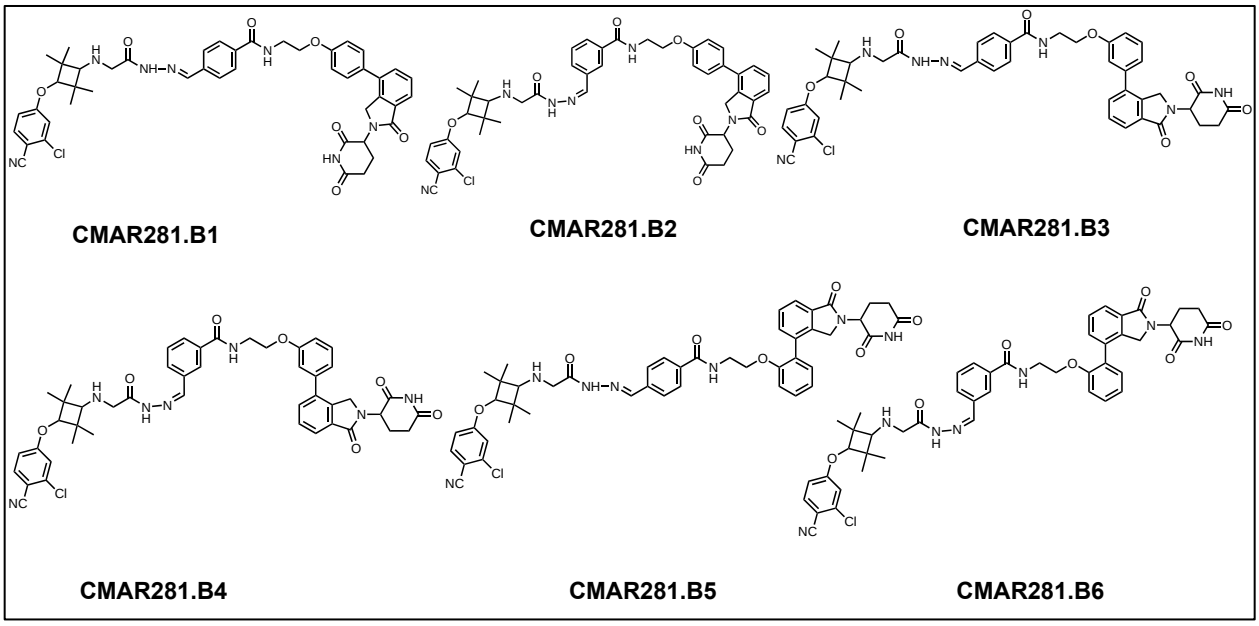

CMAR281.B1 CMAR281.B2 CMAR281.B3

CMAR281.B4 CMAR281.B5 CMAR281.B6

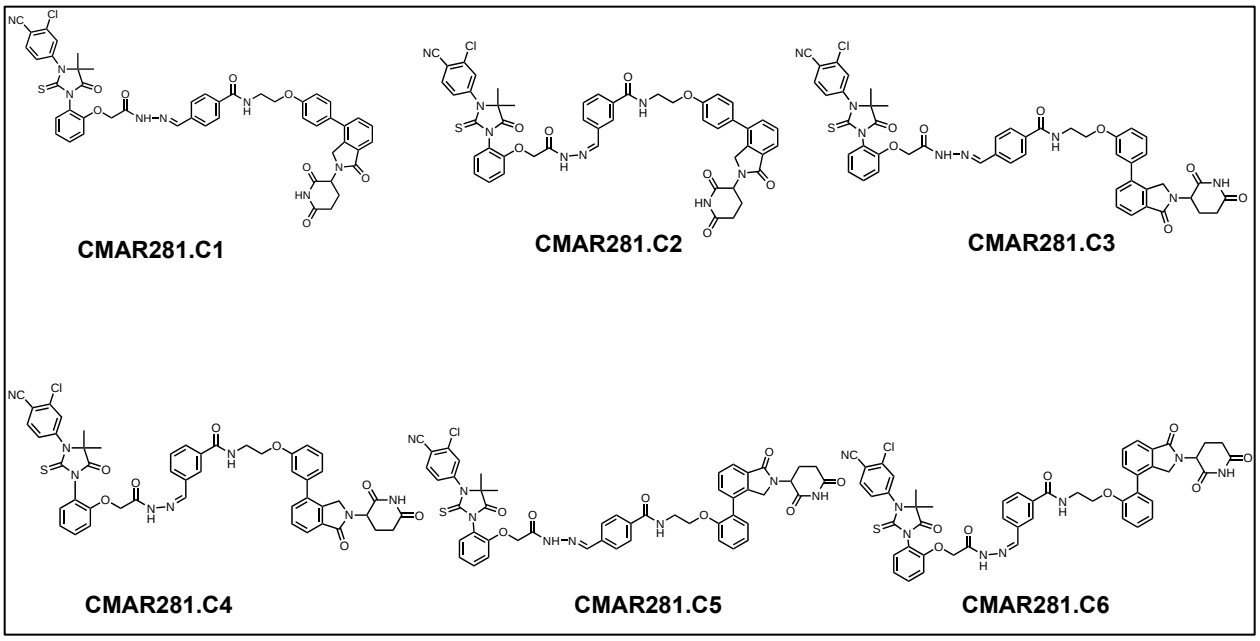

Figure 4. Structures of AR degraders employing the partial PROTAC library based on the chiral CRBN E3 ligase ligands.

We synthesized of Androgen Receptor (AR) degraders based on the aldehyde-hydrazide Rapid-TAC strategy (**Figure 4**). Analysis of the reaction by HPLC suggested the formation of product as shown by the changed in retention time from the starting material. We created a small library of CRBN-based AR degraders composed of ligand-binding domain and DNA-binding domain ligands for the androgen receptor. The degradation assay was completed by Dr. Chunrong Li.

A. **LNCAP-AR-HiBiT (20h, % normalized to DMSO)**

	10µM			5µM			1µM		
	A	B	C	A	B	C	A	B	C
1	101.37	65.35	74.79	89.54	67.41	72.21	93.83	74.27	80.27
2	103.09	68.44	73.76	87.65	71.18	79.76	96.57	72.38	88.16
3	88.85	73.24	72.73	94.34	69.47	77.36	95.71	78.56	72.21
4	99.31	58.66	82.33	92.62	59.18	75.13	91.77	70.67	76.16
5	100.17	64.84	73.93	105.32	69.98	78.73	106.52	78.22	80.79
6	94.68	64.49	80.96	113.72	66.04	78.73	107.55	74.44	87.99
LG2138	35.51	35.33	37.74	25.56	26.07	26.42	39.97	39.28	39.28
DMSO	90.05	99.66	97.08	98.63	100.17	98.80	102.57	108.23	104.46

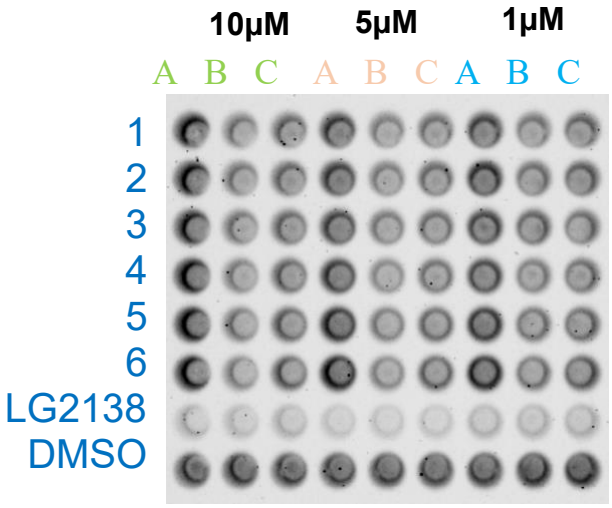

	1	2	3	4	5	6	7	8	9
A	591	381	436	522	393	421	547	433	468
B	601	399	430	511	415	465	563	422	514
C	518	427	424	550	405	451	558	458	421
D	579	342	480	540	345	438	535	412	444
E	584	378	431	614	408	459	621	456	471
F	552	376	472	663	385	459	627	434	513
G	207	206	220	149	152	154	233	229	229
H	525	581	566	575	584	576	598	631	609

B. **LNCAP (5 days, Alamar Blue)**

	10µM			5µM			1µM		
	A	B	C	A	B	C	A	B	C
1	104.85	104.48	104.68	103.09	102.45	102.31	100.23	100.85	99.96
2	101.67	100.66	99.70	100.17	101.52	98.41	100.23	100.18	99.33
3	101.74	99.63	98.22	99.81	100.36	99.49	100.55	100.42	99.62
4	102.00	**77.30**	95.79	101.26	**80.73**	98.38	100.37	**99.27**	98.25
5	101.22	96.61	96.57	100.44	96.59	109.38	99.74	99.96	99.18
6	101.45	97.30	95.07	111.16	98.00	96.32	99.91	99.24	98.71
LG2138	**100.24**	**101.01**	**97.51**	**110.51**	**99.51**	**98.04**	**99.59**	**99.92**	**99.14**
DMSO	100.50	100.57	98.73	100.34	99.44	98.25	98.43	98.80	98.80

Figure 5. A) Degradation assay of AR degraders based on CRBN chiral E3 ligase ligands using the LNCAP-AR-HiBiT cell line. B) Degradation assay of AR degraders based on CRBN chiral E3 ligase ligands using the LNCAP cell line. (The assays were performed by Dr. Chunrong Li)

These degraders were evaluated at three different concentrations ($10\mu M$, $5\ \mu M$, $1\ \mu M$) using a LNCAP-AR-HiBiT and LNCAP cell lines. Specifically, the HiBiT assay was designed and developed by Promega as an alternative bioluminescence protein detection method.[50,51] It allows the quantification of a protein of interest by complementary binding of a HiBiT tag genetically fused to the endogenous POI and a LgBiT subunit to create a functional NanoLuc luciferase enzyme.[50] Overall degradation results suggested three potential hits containing the ligand-binding domain ligand for AR, but no hits were identified with the DNA-binding domain ligand (**Figure 5**).

The three identified hits were further confirmed by western blot analysis (**Figure 6**). Western blot analysis indicates significant degradation of the AR with CMAR281.C4 at all three concentrations and some degradation at $10\mu M$ with CMAR281.B5. It is interesting that only PROTAC CMAR281.C4 with the combination of meta/meta substitution pattern on the two benzene rings in the linker region provides potent degradation activity among the six compounds derived from one AR ligand (**Figure 5**). Our results support the hypothesis that small differences in length and orientation can significantly affect the degradation efficiency.

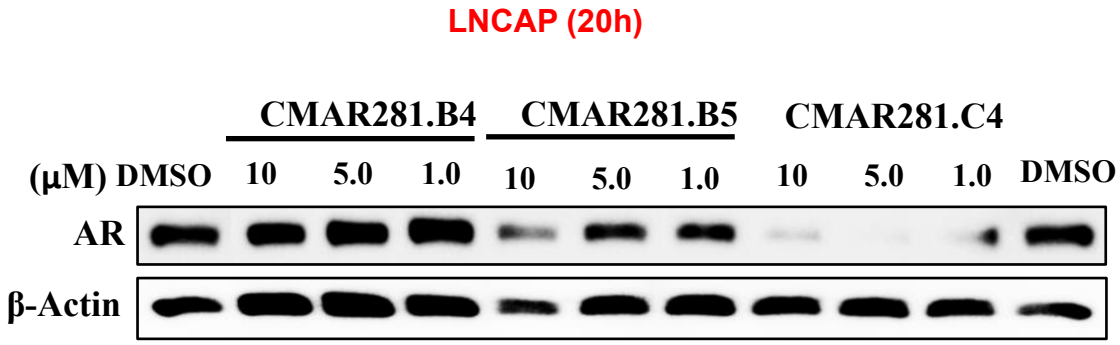

Figure 6. Western blot analysis for degradation of AR using the three top hit degraders based on CRBN chiral E3 ligase ligands.

2.3 Conclusion

In summary, we described a modular chemistry platform for the introduction of substituted phenyls to the C4-position of the lenalidomide-derived analogs under an improved Suzuki cross-coupling condition. We demonstrated that the formation of Suzuki-cross coupling product without hydrolysis of the imide was possible with a mild base. This provides quick access to various phenyl substituted lenalidomide analogues. The creation of a partial PROTAC library can be used for the synthesis of a full PROTAC library for any protein target and allow us to systematically examine the effect of length and orientation of the linkers with a relatively short distance. To demonstrate the utility of the partial PROTAC library, we examined the degradation of Androgen Receptor (AR) using the preassembled partial PROTAC library using the Rapid-TAC strategy. We observed only significant degradation of AR with CMAR281.C4 and some degradation at 10μM with CMAR281.B5 through Western Blot analysis. Further testing should be considered to confirm the

degradation of AR using these compounds. Our results indicate that small differences in length and orientation using a short linker significantly affect the degradation efficiency.

2.4 Experimental Procedures

2.4.1 Chemical Synthesis

All solvents and reagents were purchased from commercially available sources. Thin-layer chromatography (TLC) was used with precoated silica gel plates. Flash column chromatography was performed using silica gel. The ^{1}H and ^{13}C nuclear magnetic resonance (NMR) spectra were recorded using a Bruker AV-400 MHz in parts per million (ppm) (δ) downfield of TMS (δ = 0). Signal splitting patterns were described as singlet (s), doublet (d), triplet (t) or multiplet (m), with coupling constants (*J*) in hertz. The liquid chromatography–mass spectrometry (LC–MS) analysis of final products was processed on an Agilent 1290 Infinity II LC system using a Poroshell 120 EC-C18 column (5 cm × 2.1 mm, 1.9 μm) for chromatographic separation. Agilent 6120 Quadrupole LC/MS with multimode electrospray ionization plus atmospheric pressure chemical ionization was used for detection. The mobile phases were 5.0% methanol and 0.1% formic acid in purified water (A) and 0.1% formic acid in methanol (B). The gradient was held at 5% (0–0.2 min), increased to 100% at 2.5 min, then held at isocratic 100% B for 0.4 min, and then immediately stepped back down to 5% for 0.1 min re-equilibration. The flow rate was set at 0.8 mL/min. The column temperature was set at 40 °C. High resolution mass spectra (HRMS) were performed by Analytical Instrument Center at the School of Pharmacy or Department of Chemistry on an Electron Spray Injection (ESI) mass spectrometer.

2.4.2 Synthesis of intermediates 2

Intermediate **2** was synthesized according to the literature reported method. [1]

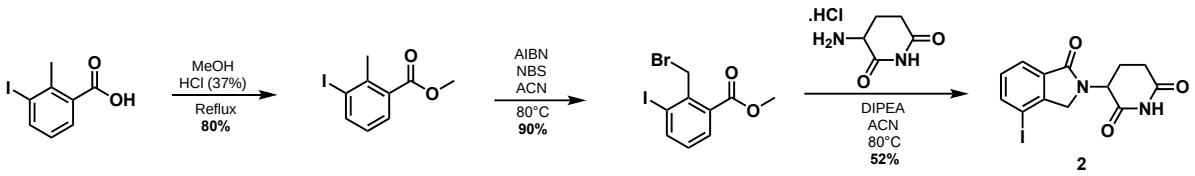

To a mixture of 3-iodo-2-methylbenzoic acid (2.0 g, 7.63 mmol), 4 ml of HCl (37%) and 76 ml of MeOH were added in a flask. The solution was stirred at 65°C for 8 h. Afterwards, the reaction mixture was quenched with a solution of saturated sodium bicarbonate reaching a pH of ~5-6 and concentrated in vacuo to achieve 1.67 g of an orange oil.

To a solution of methyl 3-iodo-2-methylbenzoate (1.67 g, 6.05 mmol) in 40 ml ACN, n-Bromosuccinimide (1.3 g, 7.26 mmol) and 2,2'-Azobis(2-methylpropionitrile) (60 mg, 0.36 mmol) were added. The solution was stirred at 80 °C for 4 h. The reaction was concentrated to achieve 1.95 g of a red solid product that was directly used in the next step.

To a solution of methyl 2-(bromomethyl)-3-iodobenzoate (1.95 g, 5.50 mmol) and ACN (27.5mL), 3-aminopiperidine-2 6-dione hydrochlorid (815 mg, 4.95 mmol) and DIPEA (1.92 mL, 11.0 mmol) were added. The solution was stirred at 95 °C for 3 h and then filtered. The solid was washed with ethyl acetate (3X30ml) to afford 1.06 g of a purple solid.

2.4.3 General Procedure of *tert*-butyl (2-bromoethyl)carbamate Alkylation

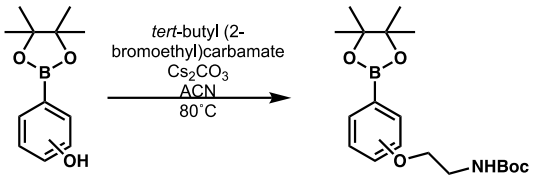

Modified boronic esters were synthesized according to the literature reported method. [2]

To a solution of 4, 3, or 2-(4,4,5,5-tetramethyl-1,3,2-dioxaborolan-2-yl)phenol (2 g, 9.08 mmol) in ACN (44 mL), t*ert*-butyl (2-bromoethyl)carbamate (3 g, 13.64 mmol) and Cs_2CO_3 (6 g, 18.16 mmol) were added. The solution was stirred at 80°C overnight. The reaction mixture was then cooled at room temperature and an extraction was done using H_2O and ethyl acetate (3 x 50 mL). The organic layer was separated, dried with Na_2SO_4 and concentrated. The crudes were later purified using flash column chromatography DCM/MeOH 0-10% to achieve the desired products.

2.4.4 General Procedure of Suzuki-Cross Coupling (5-16)

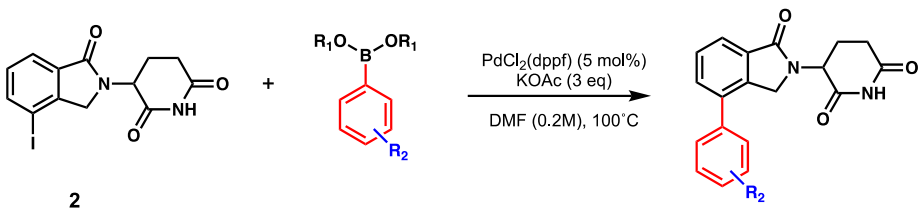

To a solution of **2** (100 mg, 0.270 mmol) in DMF (1.3 mL, 0.2 M) was added the corresponding boron pinacolester or boronic acid compounds (0.540 mmol), $PdCl_2$(dppf) (10 mg, 0.0135 mmol) and KOAc (79 mg, 0.81 mmol) at room temperature. Then, the reaction mixture was stirred for 12 h at 100 ^oC. Afterwards, the solvent was concentrated by rotovapor and the sample was diluted with DCM. The crude was later purified by flash

column chromatography using an elution gradient of 0-10% MeOH in DCM as mobile phase and a 12 g silica column as stationery phase. Finally, the desired fractions were combined and concentrated to afford the desired compounds.

2.4.5 General Procedure for the Amide Formation (18-22)

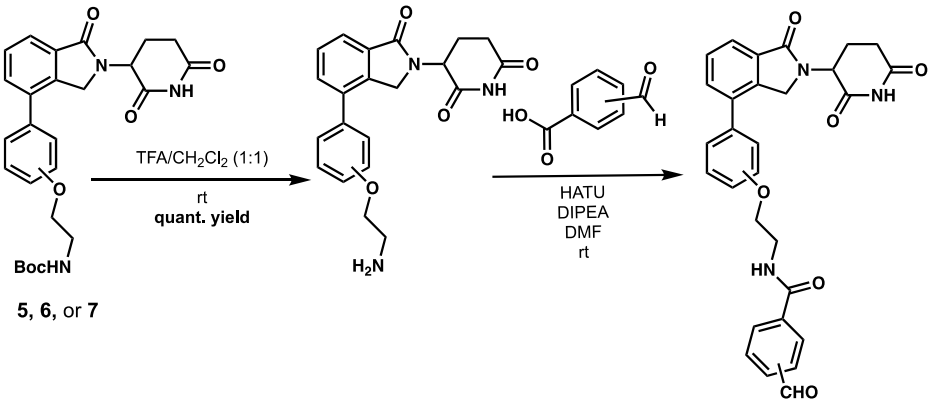

To a solution of **5, 6** or **7 (**300 mg, 0.626 mmol) in DCM (1.5 mL) was added TFA (1.5 mL) at 0 ^{o}C. The reaction mixture was stirred at room temperature for 1 h. Finally, the solvent and TFA were evaporated in vacuo to give the crude product which was directly used in the next step.

To a solution of the corresponding protected Boc-amine (124 mg, 0.327 mmol) in DMF (1.5 mL) was added HATU (124 mg, 0.327 mmol), DIPEA (114 μL, 0.654 mmol) and the corresponding benzaldehyde-COOH (98 mg, 0.654 mmol). The reaction mixture was stirred at room temperature until the staring material was gone by TLC. The mixture was then extracted with ethyl acetate (3 x 10 mL). The combined organic fractions were dried over Na_2SO_4 and concentrated. The crude was later purified by flash column

chromatography (elution gradient of 0-10% MeOH in DCM). The desired fractions were combined and concentrated to yield our desired compounds.

2.5 Characterization Data

2.5.1 Synthesized using the general procedure of tert-butyl (2-bromoethyl)carbamate alkylation

tert-butyl (2-(4-(4,4,5,5-tetramethyl-1,3,2-dioxaborolan-2-yl)phenoxy)ethyl)carbamate

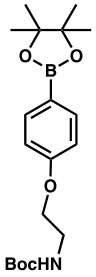

Yield: 1.8 g, 55 %

^{1}H NMR (400 MHz, $CDCl_3$) δ 7.78 – 7.72 (m, 1H), 7.73 (s, 1H), 6.92 – 6.83 (m, 2H), 4.98 (s, 1H), 4.12 – 4.01 (m, 2H), 3.54 (q, *J* = 5.5 Hz, 2H), 1.45 (s, 9H), 1.33 (s, 12H).

tert-butyl (2-(3-(4,4,5,5-tetramethyl-1,3,2-dioxaborolan-2-yl)phenoxy)ethyl)carbamate

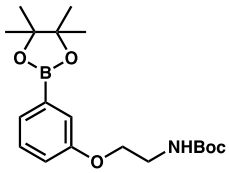

Yield: 1.4 g, 56%

^{1}H NMR (400 MHz, $CDCl_3$) δ 7.41 (dt, *J* = 7.2, 1.1 Hz, 1H), 7.36 – 7.25 (m, 2H), 6.99 (ddd, *J* = 8.2, 2.8, 1.1 Hz, 1H), 5.00 (s, 1H), 4.05 (t, *J* = 5.1 Hz, 2H), 3.52 (q, *J* = 5.4 Hz, 2H), 1.45 (s, 9H), 1.34 (s, 12H).

tert-butyl (2-(2-(4,4,5,5-tetramethyl-1,3,2-dioxaborolan-2-yl)phenoxy)ethyl)carbamate

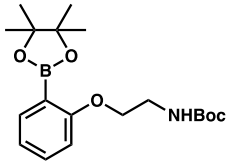

Yield: 147 mg, 41%

^{1}H NMR (400 MHz, $CDCl_3$) δ 7.64 (dd, *J* = 7.3, 1.8 Hz, 1H), 7.33 (ddd, *J* = 8.3, 7.3, 1.8 Hz, 1H), 6.91 (td, *J* = 7.3, 0.9 Hz, 1H), 6.77 (dd, *J* = 8.3, 0.8 Hz, 1H), 6.13 (s, 1H), 3.97 (t, *J* = 4.9 Hz, 2H), 3.49 (d, *J* = 5.1 Hz, 2H), 1.39 (s, 9H), 1.31 (s, 12H).

2.6.3. Synthesized using the Suzuki Cross-Coupling General Procedure:

4-(2-(2,6-dioxopiperidin-3-yl)-1-oxoisoindolin-4-yl)benzoic acid

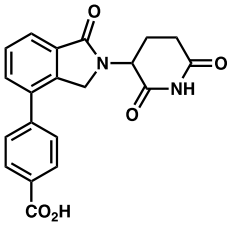

Yield: 232 mg, 58%

^{1}H NMR (400 MHz, DMSO) δ 10.98 (s, 1H), 8.15 – 8.08 (m, 2H), 7.79 (ddd, *J* = 35.5, 18.4, 8.2 Hz, 5H), 5.13 (d, *J* = 13.0 Hz, 1H), 4.65 (d, *J* = 17.5 Hz, 1H), 4.44 (d, *J* = 17.5 Hz, 1H), 2.89 (t, *J* = 15.2 Hz, 1H), 2.58 (d, *J* = 26.5 Hz, 3H), 2.05 – 1.97 (m, 1H).

^{13}C NMR (101 MHz, DMSO) δ 173.44, 171.40, 168.37, 167.63, 142.55, 139.99, 136.25, 132.94, 132.27, 130.96, 130.50, 130.35, 129.58, 128.76, 127.59, 123.35, 52.16, 47.78, 31.60, 22.80.

LC-MS (ESI) calculated for $C_{20}H_{17}N_2O_5$ $[M+H]^+$= 365.1. Found: 365.1

tert-butyl (2-(4-(2-(2,6-dioxopiperidin-3-yl)-1-oxoisoindolin-4-yl)phenoxy)ethyl)carbamate

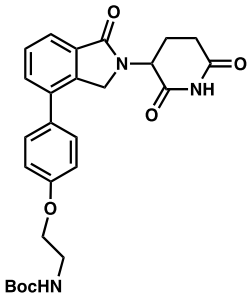

Yield: 456 mg, 66%

^{1}H NMR (400 MHz, $CDCl_3$) δ 8.21 (s, 1H), 7.87 (dd, *J* = 5.0, 3.7 Hz, 1H), 7.60 – 7.52 (m, 2H), 7.42 – 7.33 (m, 2H), 7.03 – 6.95 (m, 2H), 5.26 (dd, *J* = 13.3, 5.2 Hz, 1H), 5.01 (s, 1H), 4.56 (d, *J* = 16.3 Hz, 1H), 4.35 (d, *J* = 16.3 Hz, 1H), 4.07 (t, *J* = 5.2 Hz, 2H), 3.57 (d, *J* = 6.8 Hz, 2H), 2.98 – 2.79 (m, 2H), 2.41 – 2.27 (m, 1H), 2.20 (ddq, *J* = 10.1, 5.1, 2.4 Hz, 1H), 1.46 (s, 9H).

^{13}C NMR (101 MHz, $CDCl_3$) δ 171.05, 169.55, 169.36, 158.51, 139.03, 137.03, 132.09, 131.90, 131.28, 129.30, 128.96, 122.80, 114.91, 67.32, 51.79, 47.04, 40.09, 31.56, 28.41, 23.44.

ESI-MS calculated for $C_{26}H_{30}N_3O_6$ $[M + H]^+$= 480.2. Found: 480.2

tert-butyl (2-(3-(2-(2,6-dioxopiperidin-3-yl)-1-oxoisoindolin-4-yl)phenoxy)ethyl)carbamate

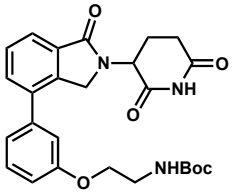

Yield: 340 mg, 58%

^{1}H NMR (400 MHz, DMSO) δ 10.97 (s, 1H), 7.77 (dd, *J* = 7.4, 1.2 Hz, 1H), 7.71 (dd, *J* = 7.6, 1.2 Hz, 1H), 7.64 (t, *J* = 7.5 Hz, 1H), 7.41 (t, *J* = 7.9 Hz, 1H), 7.21 – 7.09 (m, 2H),

7.01 (ddd, *J* = 8.2, 2.6, 0.9 Hz, 2H), 5.14 (dd, *J* = 13.3, 5.1 Hz, 1H), 4.63 (d, *J* = 17.3 Hz, 1H), 4.40 (d, *J* = 17.3 Hz, 1H), 4.04 (t, *J* = 5.9 Hz, 2H), 3.32 (q, *J* = 6.0 Hz, 2H), 2.91 (ddd, *J* = 17.2, 13.6, 5.4 Hz, 1H), 2.58 (ddd, *J* = 17.2, 4.5, 2.3 Hz, 1H), 2.44 (td, *J* = 13.2, 4.5 Hz, 1H), 2.00 (dtd, *J* = 12.5, 5.1, 2.1 Hz, 1H), 1.38 (s, 9H).

^{13}C NMR (101 MHz, DMSO) δ 173.32, 171.42, 168.34, 159.27, 156.16, 139.94, 139.91, 137.17, 132.87, 132.18, 130.54, 129.34, 122.75, 120.93, 114.71, 114.65, 78.26, 67.00, 52.10, 47.72, 40.62, 40.41, 40.21, 40.00, 39.79, 39.58, 39.37, 31.66, 28.69, 22.85.

ESI-MS calculated for $C_{26}H_{30}N_3O_6$ $[M + H]^+$= 480.2. Found: 480.2

tert-butyl (2-(2-(2-(2,6-dioxopiperidin-3-yl)-1-oxoisoindolin-4-yl)phenoxy)ethyl)carbamate

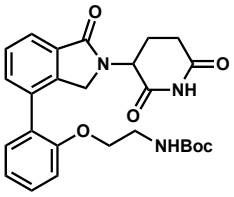

Yield: 60 mg, 35%

^{1}H NMR (400 MHz, $CDCl_3$) δ 8.07 (s, 1H), 7.90 (dd, *J* = 7.4, 1.3 Hz, 1H), 7.56 (t, *J* = 7.5 Hz, 1H), 7.51 (d, *J* = 7.7 Hz, 1H), 7.38 (td, *J* = 7.9, 1.8 Hz, 1H), 7.29 – 7.23 (m, 2H), 7.07 (td, *J* = 7.5, 1.0 Hz, 1H), 7.02 (d, *J* = 8.3 Hz, 1H), 5.25 (dd, *J* = 13.2, 5.4 Hz, 1H), 4.96 (s, 1H), 4.51 – 4.39 (m, 1H), 4.20 (d, *J* = 16.4 Hz, 1H), 4.05 (d, *J* = 7.0 Hz, 1H), 3.93 (s, 1H), 3.44 – 3.25 (m, 2H), 2.94 – 2.71 (m, 2H), 2.31 (td, *J* = 12.8, 4.9 Hz, 1H), 2.20 (dtd, *J* = 13.3, 5.4, 2.9 Hz, 1H), 1.41 (s, 9H).

^{13}C NMR (101 MHz, $CDCl_3$) δ 171.20, 170.07, 169.53, 155.91, 155.39, 140.88, 134.30, 133.32, 131.17, 130.85, 129.74, 128.25, 127.81, 123.04, 121.56, 113.34, 68.52, 51.77, 47.22, 40.12, 31.47, 28.35, 23.30.

ESI-MS calculated for $C_{26}H_{30}N_3O_6$ $[M + H]^+$= 480.2. Found: 480.2

2-(2-(2-(2,6-dioxopiperidin-3-yl)-1-oxoisoindolin-4-yl)phenoxy)acetic acid

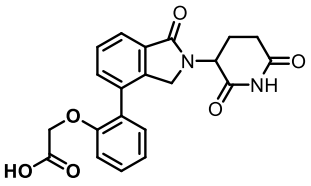

^{1}H NMR (400 MHz, DMSO-*d*) δ 13.09 (s, 1H), 10.87 (s, 1H), 7.67 (dd, *J* = 6.4, 2.3 Hz, 1H), 7.56 – 7.48 (m, 2H), 7.32 (ddd, *J* = 8.6, 7.4, 1.8 Hz, 1H), 7.23 (dd, *J* = 7.5, 1.8 Hz, 1H), 7.00 (td, *J* = 7.4, 0.9 Hz, 1H), 6.93 (d, *J* = 8.4 Hz, 1H), 5.06 (dd, *J* = 13.3, 5.1 Hz, 1H), 4.69 – 4.53 (m, 2H), 4.47 (d, *J* = 17.4 Hz, 1H), 4.11 (d, *J* = 17.4 Hz, 1H), 2.83 (ddd, *J* = 17.3, 13.7, 5.4 Hz, 1H), 2.55 – 2.45 (m, 1H), 2.25 (qd, *J* = 13.3, 4.4 Hz, 1H), 1.95 – 1.84 (m, 1H).

^{13}C NMR (101 MHz, DMSO) δ 173.31, 171.44, 170.70, 168.51, 154.86, 141.74, 134.69, 133.47, 132.04, 131.33, 130.07, 128.65, 127.16, 122.47, 121.57, 112.25, 64.82, 51.90, 47.44, 31.65, 22.98.

ESI-MS calculated for $C_{21}H_{19}N_2O_6$ $[M + H]^+$= 395.1. Found: 395.1

2-(3-(2-(2,6-dioxopiperidin-3-yl)-1-oxoisoindolin-4-yl)phenoxy)acetic acid

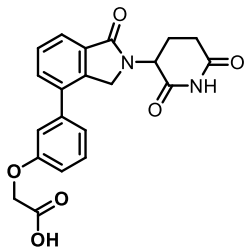

^{1}H NMR (400 MHz, DMSO-*d*) δ 13.07 (s, 1H), 10.97 (s, 1H), 7.77 (dd, *J* = 7.4, 1.2 Hz, 1H), 7.71 (dd, *J* = 7.6, 1.3 Hz, 1H), 7.65 (t, *J* = 7.5 Hz, 1H), 7.42 (t, *J* = 8.0 Hz, 1H), 7.22 – 7.15 (m, 1H), 7.15 – 7.09 (m, 1H), 6.99 (ddd, *J* = 8.3, 2.6, 0.9 Hz, 1H), 5.14 (dd, *J* = 13.3, 5.1 Hz, 1H), 4.76 (s, 2H), 4.63 (d, *J* = 17.3 Hz, 1H), 4.38 (d, *J* = 17.3 Hz, 1H), 2.91 (ddd, *J* = 17.3, 13.6, 5.4 Hz, 1H), 2.64 – 2.54 (m, 1H), 2.49 – 2.39 (m, 1H), 2.07 – 1.95 (m, 1H).

^{13}C NMR (101 MHz, DMSO) δ 173.34, 171.42, 170.68, 168.32, 158.58, 139.91, 139.83, 137.04, 132.91, 132.13, 130.52, 129.38, 122.80, 121.28, 114.80, 114.42, 65.08, 52.09, 47.70, 31.69, 22.83.

ESI-MS calculated for $C_{21}H_{19}N_2O_6$ $[M + H]^+$= 395.1. Found: 395.1

2-(4-(2-(2,6-dioxopiperidin-3-yl)-1-oxoisoindolin-4-yl)phenoxy)acetic acid

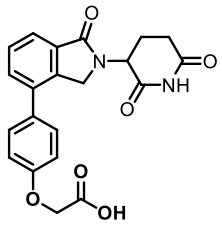

^{1}H NMR (400 MHz, DMSO-*d*) δ 13.09 (s, 1H), 11.00 (s, 1H), 7.85 (t, *J* = 1.1 Hz, 1H), 7.77 (d, *J* = 1.1 Hz, 2H), 7.69 (d, *J* = 8.9 Hz, 2H), 7.05 (d, *J* = 8.8 Hz, 2H), 5.14 (dd, *J* = 13.3, 5.1 Hz, 1H), 4.74 (s, 2H), 4.51 (d, *J* = 17.3 Hz, 1H), 4.38 (d, *J* = 17.4 Hz, 1H), 2.93 (ddd, *J* = 17.2, 13.6, 5.4 Hz, 1H), 2.62 (dt, *J* = 15.8, 3.4 Hz, 1H), 2.43 (qd, *J* = 13.4, 4.7 Hz, 1H), 2.03 (ddd, *J* = 10.6, 5.5, 3.2 Hz, 1H).

^{13}C NMR (101 MHz, DMSO) δ 173.38, 171.55, 170.64, 168.42, 158.48, 143.76, 143.44, 132.72, 130.55, 128.76, 126.73, 123.87, 121.74, 115.53, 65.08, 52.10, 47.72, 31.71, 22.98.

ESI-MS calculated for $C_{21}H_{19}N_2O_6$ $[M + H]^+$= 395.1. Found: 395.1

4-(2-(2,6-dioxopiperidin-3-yl)-1-oxoisoindolin-4-yl)benzaldehyde

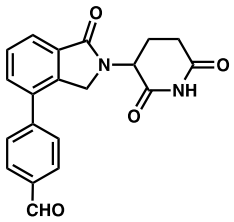

Yield: 33 mg, 35%

^{1}H NMR (400 MHz, DMSO-*d*$_6$) δ 10.98 (s, 1H), 10.10 (s, 1H), 8.07 – 8.01 (m, 2H), 7.89 – 7.78 (m, 4H), 7.70 (t, *J* = 7.6 Hz, 1H), 5.16 (dd, *J* = 13.3, 5.1 Hz, 1H), 2.99 – 2.85 (m, 1H), 2.64 – 2.54 (m, 1H), 2.51 – 2.37 (m, 1H), 2.00 (ddd, *J* = 10.6, 4.8, 2.6 Hz, 1H).

^{13}C NMR (101 MHz, DMSO-*d*$_6$) δ 193.32, 173.34, 171.37, 168.17, 144.31, 140.14, 136.06, 135.94, 133.10, 132.33, 130.48, 129.58, 129.41, 123.59, 52.10, 47.68, 31.63, 22.85.

ESI-MS calculated for $C_{20}H_{17}N_2O_4$ $[M + H]^+$= 349.1. Found: 349.1

3-(2-(2,6-dioxopiperidin-3-yl)-1-oxoisoindolin-4-yl)benzaldehyde

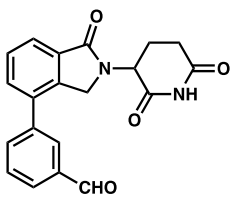

Yield: 28 mg, 30%

^{1}H NMR (400 MHz, DMSO-*d*$_6$) δ 10.98 (s, 1H), 10.12 (s, 1H), 8.13 (t, *J* = 1.8 Hz, 1H), 8.01 – 7.93 (m, 2H), 7.86 – 7.66 (m, 4H), 5.15 (dd, *J* = 13.2, 5.1 Hz, 1H), 4.66 (d, *J* = 17.4 Hz, 1H), 4.45 (d, *J* = 17.4 Hz, 1H), 2.91 (ddd, *J* = 18.0, 13.6, 5.4 Hz, 1H), 2.59 (d, *J* = 17.7 Hz, 1H), 2.43 (td, *J* = 13.2, 4.4 Hz, 1H), 2.05 – 1.96 (m, 1H).

^{13}C NMR (101 MHz, DMSO-*d*$_6$) δ 193.65, 173.34, 171.39, 168.25, 140.06, 139.36, 137.25, 136.04, 134.50, 133.03, 132.29, 130.36, 130.32, 129.57, 128.65, 123.26, 52.11, 47.63, 31.63, 22.84.

ESI-MS calculated for $C_{20}H_{17}N_2O_4$ $[M + H]^+$= 349.1. Found: 349.1

2-(2-(2,6-dioxopiperidin-3-yl)-1-oxoisoindolin-4-yl)benzaldehyde

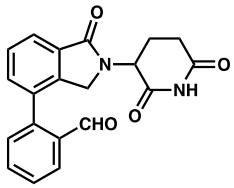

Yield: 17 mg, 18%

^{1}H NMR (400 MHz, DMSO) δ 10.94 (s, 1H), 9.79-9.76 (m, 1H), 8.03-7.97 (m, 1H), 7.87 – 7.76 (m, 2H), 7.64 – 7.57 (m, 5H), 5.15-5.11 (m, 1H), 4.38 – 4.09 (m, 2H), 2.97 – 2.78 (m, 1H), 2.57-2.54 (m, 1H), 2.45 – 2.31 (m, 1H), 1.97-1.94 (m, 1H).

^{13}C NMR (101 MHz, DMSO) δ 191.88, 173.29, 171.35, 168.27, 141.44, 141.35, 134.62, 133.92, 133.76, 132.54, 132.01, 131.10, 129.29, 129.18, 128.88, 123.34, 52.04, 47.21, 31.60, 22.76.

ESI-MS calculated for $C_{20}H_{17}N_2O_4$ $[M + H]^+$= 349.1. Found: 349.1

3-(4-(4-hydroxyphenyl)-1-oxoisoindolin-2-yl)piperidine-2,6-dione

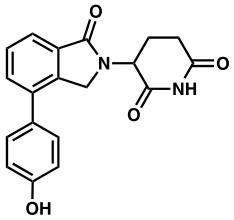

Yield: 46 mg, 51%

^{1}H NMR (400 MHz, DMSO) δ 11.03 (s, 1H), 9.74 (s, 1H), 7.76 – 7.63 (m, 3H), 7.50 – 7.45 (m, 2H), 6.98 – 6.90 (m, 2H), 5.20 (dd, *J* = 13.2, 5.1 Hz, 1H), 4.65 (d, *J* = 17.3 Hz, 1H), 4.45 (d, *J* = 17.3 Hz, 1H), 2.97 (ddd, *J* = 17.3, 13.6, 5.4 Hz, 1H), 2.64 (ddt, *J* = 16.5, 5.5, 2.7 Hz, 1H), 2.54 – 2.46 (m, 1H), 2.10 – 1.99 (m, 1H).

^{13}C NMR (101 MHz, DMSO) δ 173.36, 171.47, 168.50, 157.90, 139.48, 137.29, 132.84, 131.63, 129.72, 129.27, 129.04, 121.80, 116.18, 52.05, 49.07, 47.84, 31.66, 22.87.

LC-MS (ESI) calculated for $C_{19}H_{17}N_2O_4$ $[M+H]^+$= 337.1. Found: 337.1

3-(4-(3-hydroxyphenyl)-1-oxoisoindolin-2-yl)piperidine-2,6-dione

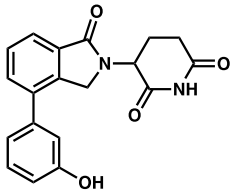

Yield: 52 mg, 57%

^{1}H NMR (400 MHz, DMSO) δ 11.03 (s, 1H), 9.68 (s, 1H), 7.84 – 7.77 (m, 1H), 7.76 – 7.64 (m, 2H), 7.36 (t, *J* = 7.8 Hz, 1H), 7.08 – 7.02 (m, 1H), 7.00 (t, *J* = 2.0 Hz, 1H), 6.89 (dd, *J* = 8.1, 2.4 Hz, 1H), 5.21 (dd, *J* = 13.2, 5.1 Hz, 1H), 4.61 (s, 1H), 4.47 (d, *J* = 17.3 Hz, 1H), 3.03 – 2.90 (m, 1H), 2.64 (d, *J* = 14.9 Hz, 1H), 2.50 (dd, *J* = 13.2, 4.4 Hz, 1H), 2.10 – 2.00 (m, 1H).

^{13}C NMR (101 MHz, DMSO) δ 173.34, 171.48, 168.37, 158.21, 139.77, 139.73, 137.39, 132.85, 131.95, 130.48, 129.36, 122.60, 119.17, 115.46, 115.26, 52.05, 47.69, 31.67, 22.86.

LC-MS (ESI) calculated for $C_{19}H_{17}N_2O_4$ $[M+H]^+$= 337.1. Found: 337.1

3-(4-(2-hydroxyphenyl)-1-oxoisoindolin-2-yl)piperidine-2,6-dione

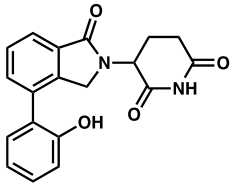

Yield: 82 mg, 90%

^{1}H NMR (400 MHz, DMSO) δ 10.99 (s, 1H), 9.80 (s, 1H), 7.78 (dd, *J* = 7.2, 1.5 Hz, 1H), 7.68 – 7.57 (m, 2H), 7.30 (ddd, *J* = 14.5, 7.3, 1.7 Hz, 2H), 7.09 – 7.00 (m, 1H), 6.96 (td, *J* = 7.4, 1.1 Hz, 1H), 5.19 (dd, *J* = 13.3, 5.1 Hz, 1H), 4.45 – 4.30 (m, 2H), 2.94 (ddd, *J* = 17.3, 13.8, 5.4 Hz, 1H), 2.61 (d, *J* = 7.8 Hz, 1H), 2.47 (td, *J* = 13.1, 4.4 Hz, 1H), 2.06 – 1.95 (m, 1H).

^{13}C NMR (101 MHz, DMSO) δ 173.32, 171.51, 168.61, 154.70, 141.42, 135.34, 133.49, 132.00, 131.11, 129.84, 128.60, 125.54, 122.18, 119.78, 116.34, 51.94, 31.68.

LC-MS (ESI) calculated for $C_{19}H_{17}N_2O_4$ $[M+H]^+$=337.1. Found: 337.1

2.5.2 Partial PROTAC Library

N-(2-(4-(2-(2,6-dioxopiperidin-3-yl)-1-oxoisoindolin-4-yl)phenoxy)ethyl)-4-formylbenzamide

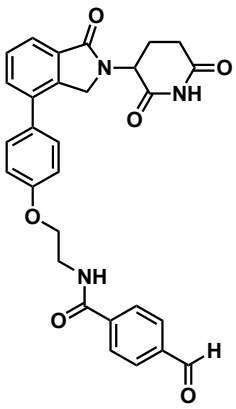

^{1}H NMR (400 MHz, DMSO) δ 10.97 (s, 1H), 10.08 (s, 1H), 8.99 (t, *J* = 5.5 Hz, 1H), 8.76 (dd, *J* = 4.4, 1.5 Hz, 1H), 8.53 (dd, *J* = 8.4, 1.4 Hz, 1H), 8.19 (dt, *J* = 7.8, 1.6 Hz, 1H), 8.08 (dt, *J* = 7.6, 1.4 Hz, 1H), 7.80 – 7.69 (m, 2H), 7.56 – 7.49 (m, 3H), 7.15 – 7.06 (m, 2H), 5.14 (dd, *J* = 13.2, 5.1 Hz, 1H), 4.60 (d, *J* = 17.4 Hz, 1H), 4.40 (d, *J* = 17.3 Hz, 1H), 4.22 (t, *J* = 5.8 Hz, 2H), 3.71 (q, *J* = 5.7 Hz, 2H), 2.91 (ddd, *J* = 17.2, 13.6, 5.4 Hz, 1H), 2.00 (ddp, *J* = 7.7, 5.4, 2.3 Hz, 1H), 1.27 (d, *J* = 2.3 Hz, 2H).

^{13}C NMR (101 MHz, DMSO) δ 193.40, 173.34, 171.44, 168.43, 166.23, 158.78, 151.33, 140.07, 139.70, 139.64, 138.30, 136.89, 135.09, 132.86, 131.82, 130.90, 129.91, 129.81, 129.34, 129.21, 128.45, 122.14, 121.06, 115.44, 66.50, 52.06, 47.77, 40.62, 40.46, 40.41, 40.24, 40.20, 39.99, 39.78, 39.57, 39.36, 31.65, 22.88.

LC-MS (ESI) calculated for $C_{29}H_{26}N_3O_6$ $[M + H]^+$= 512.2. Found: 512.1

N-(2-(4-(2-(2,6-dioxopiperidin-3-yl)-1-oxoisoindolin-4-yl)phenoxy)ethyl)-3-formylbenzamide

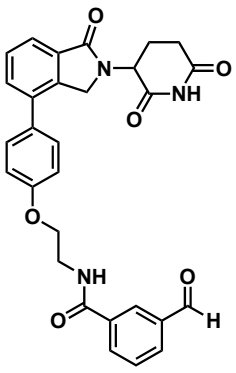

^{1}H NMR (400 MHz, DMSO) δ 10.96 (s, 1H), 10.07 (s, 1H), 8.97 (t, *J* = 5.5 Hz, 1H), 8.77 (dd, *J* = 4.4, 1.4 Hz, 1H), 8.54 (dd, *J* = 8.4, 1.4 Hz, 1H), 8.17 (dt, *J* = 7.8, 1.5 Hz, 1H), 8.07 (dt, *J* = 7.6, 1.4 Hz, 1H), 7.80 – 7.68 (m, 2H), 7.52 (dd, *J* = 8.4, 4.4 Hz, 1H), 7.46 – 7.37 (m, 1H), 7.22 – 7.12 (m, 2H), 7.12 – 7.00 (m, 1H), 5.13 (dd, *J* = 13.2, 5.1 Hz, 1H), 4.63 (d, *J* = 17.3 Hz, 1H), 4.39 (d, *J* = 17.3 Hz, 1H), 4.24 (t, *J* = 5.9 Hz, 2H), 3.70 (q, *J* = 5.7 Hz, 2H), 2.90 (ddd, *J* = 17.0, 13.6, 5.4 Hz, 1H), 2.05 – 1.94 (m, 1H), 1.28 (d, *J* = 3.2 Hz, 2H).

^{13}C NMR (101 MHz, DMSO) δ 193.36, 173.35, 171.44, 168.43, 166.06, 158.79, 151.48, 140.08, 139.63, 136.89, 136.68, 135.53, 135.10, 133.48, 132.86, 131.82, 130.89, 129.84, 129.81, 129.35, 129.28, 128.46, 122.14, 121.14, 115.44, 66.53, 52.06, 31.65, 22.88.

LC-MS (ESI) calculated for $C_{29}H_{26}N_3O_6$ $[M + H]^+$= 512.2. Found: 512.2

N-(2-(3-(2-(2,6-dioxopiperidin-3-yl)-1-oxoisoindolin-4-yl)phenoxy)ethyl)-4-formylbenzamide

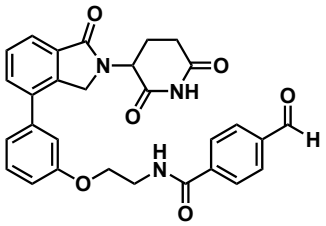

^{1}H NMR (400 MHz, DMSO) δ 11.02 (s, 1H), 10.14 (s, 1H), 9.00 (t, *J* = 5.6 Hz, 1H), 8.07 (q, *J* = 8.3 Hz, 4H), 7.82 (dd, *J* = 7.4, 1.2 Hz, 1H), 7.76 (dd, *J* = 7.6, 1.3 Hz, 1H), 7.69 (t, *J* = 7.5 Hz, 1H), 7.48 (t, *J* = 8.1 Hz, 1H), 7.27 – 7.18 (m, 2H), 7.17 – 7.08 (m, 1H), 5.19 (dd, *J* = 13.2, 5.1 Hz, 1H), 4.69 (d, *J* = 17.4 Hz, 1H), 4.45 (d, *J* = 17.3 Hz, 1H), 4.29 (t, *J* = 5.9 Hz, 2H), 3.74 (q, *J* = 5.6 Hz, 2H), 2.95 (ddd, *J* = 17.6, 13.5, 5.4 Hz, 1H), 2.06 (d, *J* = 4.6 Hz, 1H), 1.39 – 1.20 (m, 2H).

^{13}C NMR (101 MHz, DMSO) δ 193.50, 173.45, 171.43, 168.42, 166.25, 159.24, 139.86, 139.60, 138.22, 137.10, 132.79, 132.25, 130.62, 129.85, 129.39, 128.50, 122.75, 120.98, 119.28, 114.57, 66.38, 52.13, 47.81, 40.35, 40.14, 39.93, 39.72, 39.51, 39.30, 39.09, 31.27, 22.93.

LC-MS (ESI) calculated for $C_{29}H_{26}N_3O_6$ $[M + H]^+$= 512.2. Found: 512.1

N-(2-(3-(2-(2,6-dioxopiperidin-3-yl)-1-oxoisoindolin-4-yl)phenoxy)ethyl)-3-formylbenzamide

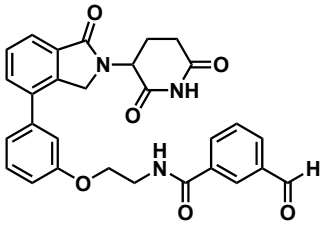

^{1}H NMR (400 MHz, DMSO) δ 10.96 (s, 1H), 10.07 (s, 1H), 8.97 (t, *J* = 5.5 Hz, 1H), 8.77 (dd, *J* = 4.4, 1.4 Hz, 1H), 8.54 (dd, *J* = 8.4, 1.4 Hz, 1H), 8.17 (dt, *J* = 7.8, 1.5 Hz, 1H),

8.07 (dt, *J* = 7.6, 1.4 Hz, 1H), 7.79 – 7.69 (m, 2H), 7.52 (dd, *J* = 8.4, 4.4 Hz, 1H), 7.46 – 7.37 (m, 1H), 7.22 – 7.12 (m, 2H), 7.12 – 7.00 (m, 1H), 5.13 (dd, *J* = 13.2, 5.1 Hz, 1H), 4.63 (d, *J* = 17.3 Hz, 1H), 4.39 (d, *J* = 17.3 Hz, 1H), 4.24 (t, *J* = 5.9 Hz, 2H), 3.70 (q, *J* = 5.7 Hz, 2H), 2.90 (ddd, *J* = 17.0, 13.6, 5.4 Hz, 1H), 2.05 – 1.94 (m, 1H), 1.24 (d, *J* = 7.3 Hz, 2H).

^{13}C NMR (101 MHz, DMSO) δ 193.34, 173.33, 171.43, 168.33, 166.05, 159.27, 151.61, 140.08, 139.98, 139.91, 137.14, 136.66, 135.51, 133.46, 132.86, 132.68, 132.18, 130.58, 129.81, 129.34, 128.45, 122.76, 121.21, 121.01, 114.61, 66.50, 52.10, 31.65, 22.84.

LC-MS (ESI) calculated for $C_{29}H_{26}N_3O_6$ $[M + H]^+$= 512.2. Found: 512.2

N-(2-(2-(2-(2,6-dioxopiperidin-3-yl)-1-oxoisoindolin-4-yl)phenoxy)ethyl)-4-formylbenzamide

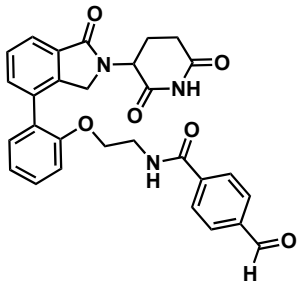

^{1}H NMR (400 MHz, DMSO) δ 10.93 (s, 1H), 10.08 (s, 1H), 8.80 – 8.44 (m, 2H), 7.98 (d, *J* = 8.1 Hz, 2H), 7.90 (d, *J* = 7.9 Hz, 2H), 7.67 (d, *J* = 7.4 Hz, 1H), 7.55 – 7.41 (m, 2H), 7.31 (dd, *J* = 7.5, 1.8 Hz, 1H), 7.25 (d, *J* = 8.4 Hz, 1H), 7.07 (t, *J* = 7.4 Hz, 1H), 5.10 (dd, *J* = 13.2, 5.1 Hz, 1H), 4.40 – 4.25 (m, 1H), 4.24 – 4.10 (m, 3H), 3.66 – 3.43 (m, 1H), 2.92 – 2.79 (m, 1H), 1.95 – 1.85 (m, 1H), 1.26 (q, *J* = 6.9, 6.2 Hz, 3H).

^{13}C NMR (101 MHz, DMSO) δ 193.38, 173.29, 171.57, 168.55, 166.08, 155.58, 151.54, 141.32, 140.09, 139.63, 135.10, 134.52, 133.56, 132.17, 131.15, 130.18, 129.84, 129.31, 128.37, 128.31, 127.44, 122.36, 121.49, 121.17, 113.40, 66.54, 51.97, 31.66, 22.77.

LC-MS (ESI) calculated for $C_{29}H_{26}N_3O_6$ $[M + H]^+$= 512.2. Found: 512.2

N-(2-(2-(2-(2,6-dioxopiperidin-3-yl)-1-oxoisoindolin-4-yl)phenoxy)ethyl)-3-formylbenzamide

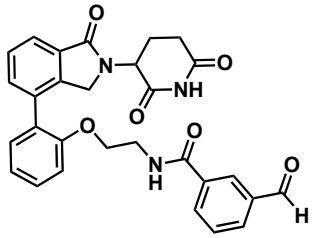

^{1}H NMR (400 MHz, DMSO) δ 10.93 (s, 1H), 10.07 (s, 1H), 8.72 (dt, *J* = 10.9, 3.5 Hz, 1H), 8.51 (dd, *J* = 8.4, 1.4 Hz, 1H), 8.29 (d, *J* = 1.8 Hz, 1H), 8.05 (ddt, *J* = 10.8, 7.7, 1.6 Hz, 2H), 7.79 – 7.61 (m, 2H), 7.42 (ddt, *J* = 7.5, 4.9, 2.5 Hz, 2H), 7.34 – 7.21 (m, 2H), 7.07 (t, *J* = 7.4 Hz, 1H), 5.10 (dd, *J* = 13.2, 5.0 Hz, 1H), 4.35 (d, *J* = 17.2 Hz, 1H), 4.26 – 4.11 (m, 3H), 3.64 – 3.47 (m, 2H), 2.93 – 2.80 (m, 1H), 1.92 (ddq, *J* = 10.5, 5.6, 3.2, 2.7 Hz, 1H), 1.26 (dt, *J* = 9.6, 4.6 Hz, 2H).

^{13}C NMR (101 MHz, DMSO) δ 193.31, 173.30, 171.57, 168.54, 165.89, 155.58, 151.61, 141.31, 140.09, 136.61, 135.44, 134.52, 133.35, 132.14, 131.15, 130.18, 129.75, 129.34, 128.44, 128.36, 127.46, 122.33, 121.50, 121.21, 113.43, 66.59, 51.97, 31.67, 22.76.

ESI-MS calculated for $C_{29}H_{26}N_3O_6$ $[M + H]^+$= 512.2. Found: 512.2

2.5.3 LC-MS Data

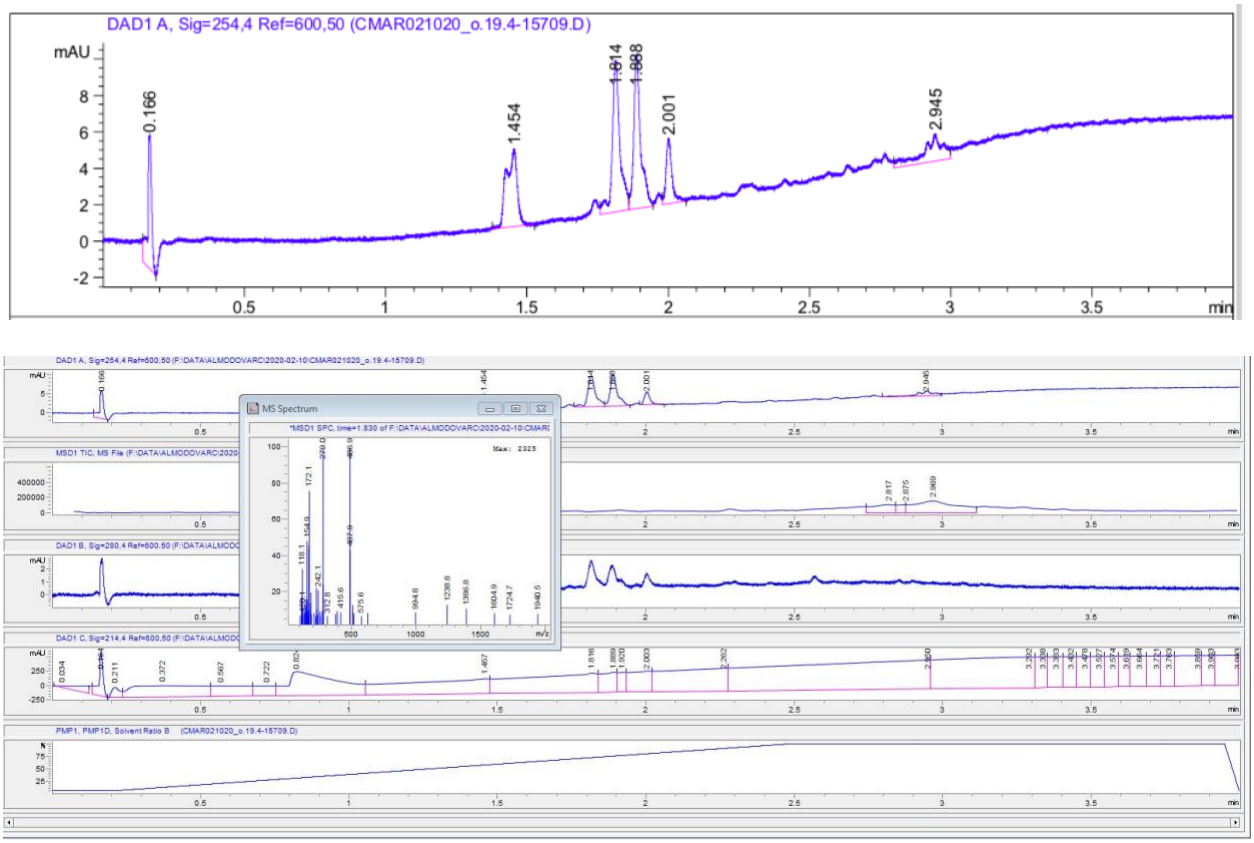

Figure S2. LC-MS Data of Suzuki Cross-Coupling Reaction Optimization.

2.6 NMR Spectra

^{1}H NMR (400 MHz, DMSO) *-4-(2-(2,6-dioxopiperidin-3-yl)-1-oxoisoindolin-4-yl)benzoic acid*

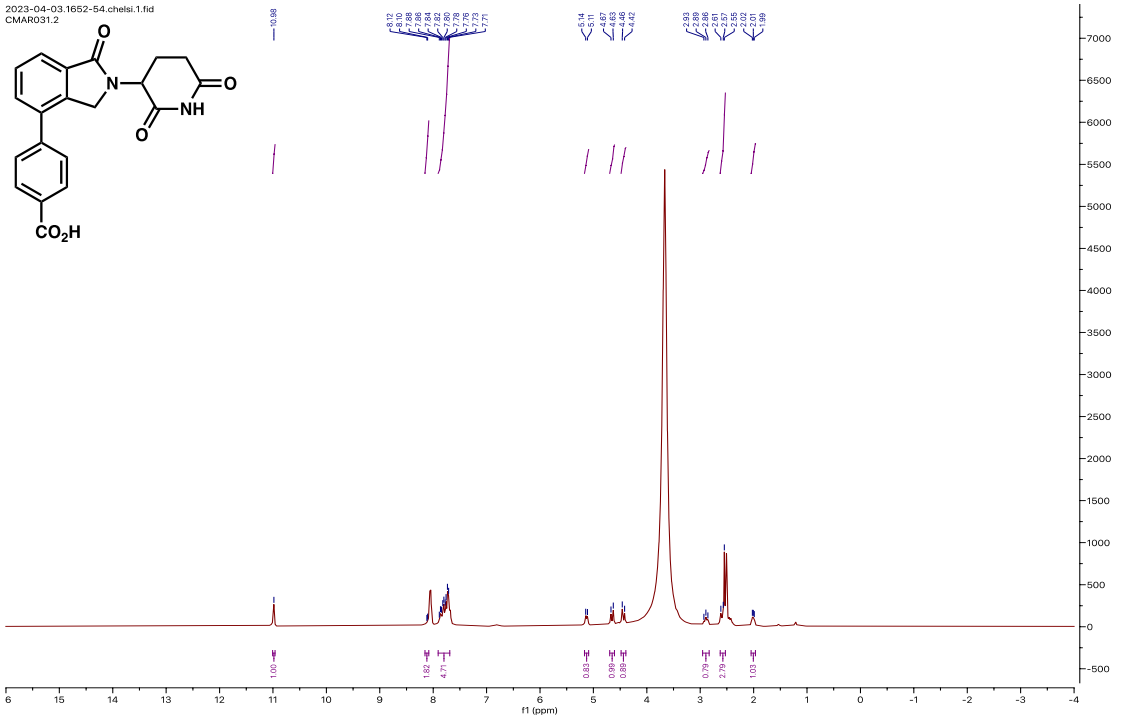

^{13}C NMR (400 MHz, DMSO) *-4-(2-(2,6-dioxopiperidin-3-yl)-1-oxoisoindolin-4-yl)benzoic acid*

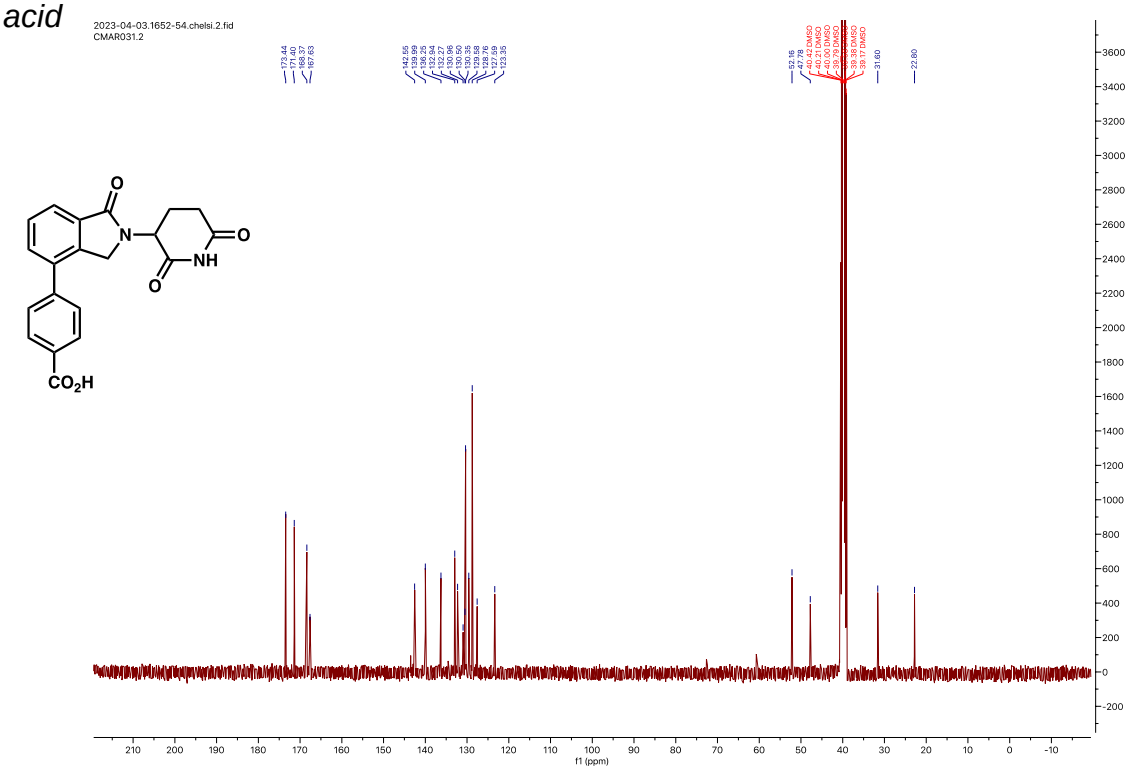

^{1}H NMR(400 MHz, $CDCl_3$) *-tert-butyl (2-(4-(2-(2,6-dioxopiperidin-3-yl)-1-oxoisoindolin-4-yl)phenoxy)ethyl)carbamate*

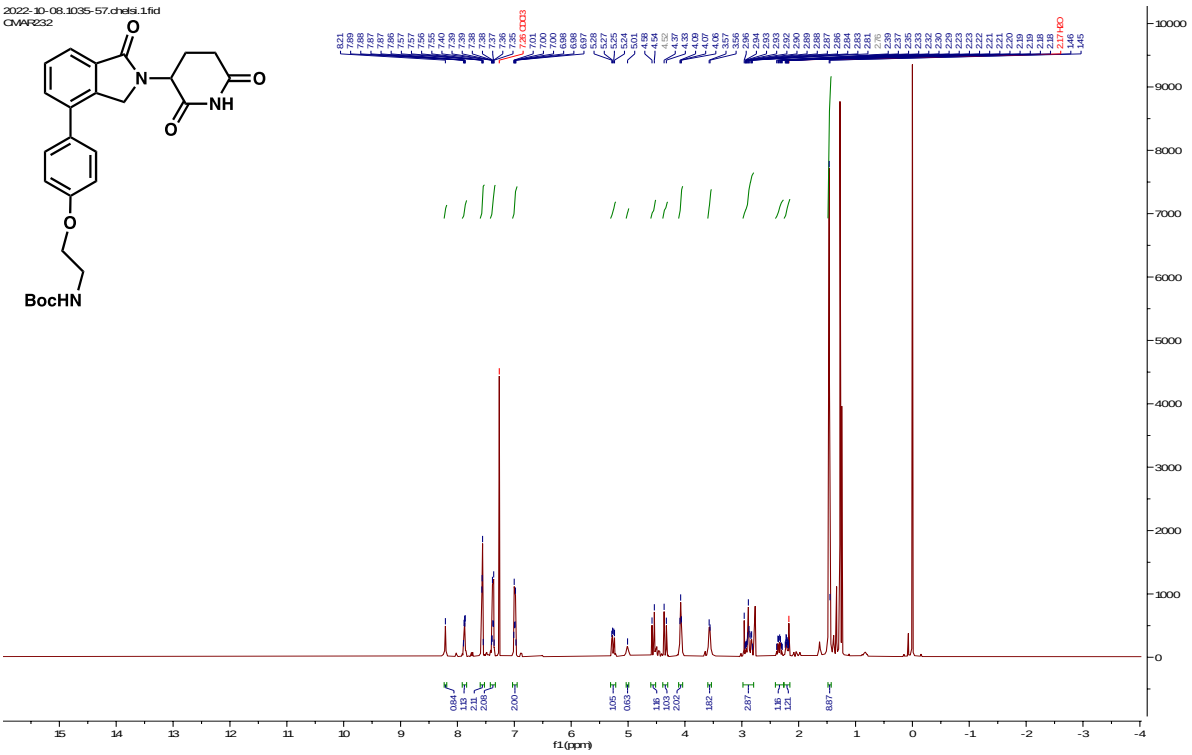

^{13}C NMR (101 MHz, $CDCl_3$) *-tert-butyl (2-(4-(2-(2,6-dioxopiperidin-3-yl)-1-oxoisoindolin-4-yl)phenoxy)ethyl)carbamate*

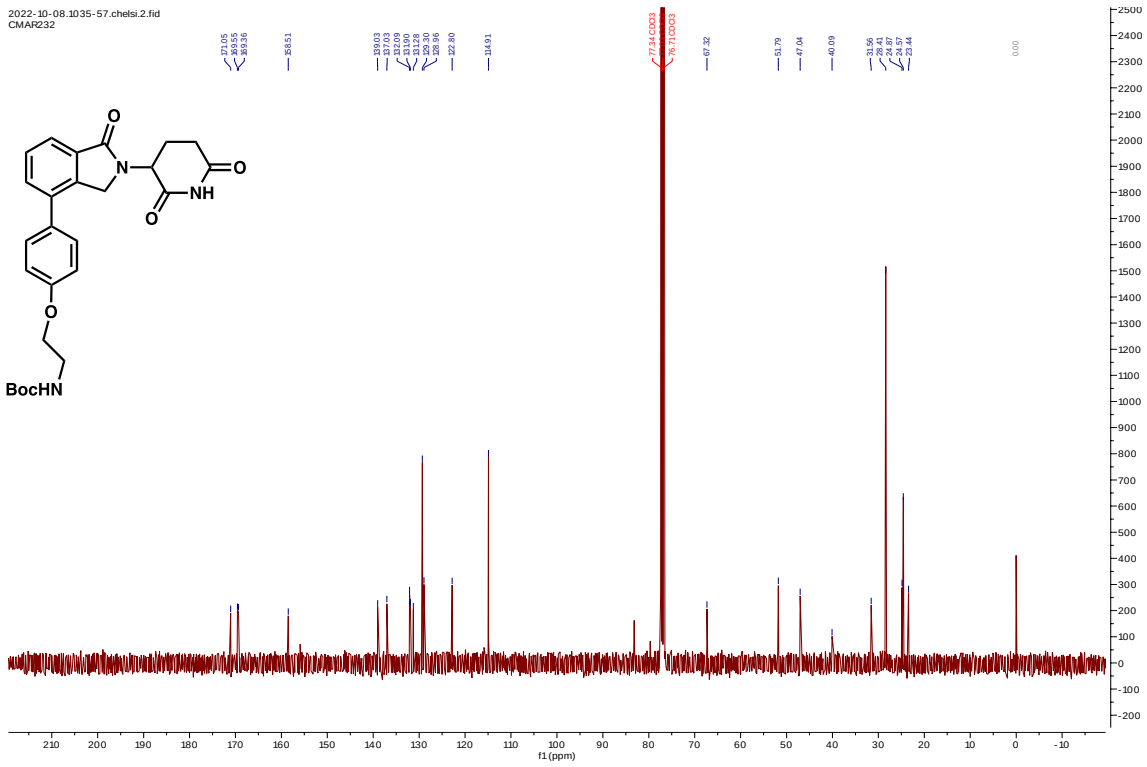

[1]H NMR (400 MHz, DMSO) *-tert-butyl (2-(3-(2-(2,6-dioxopiperidin-3-yl)-1-oxoisoindolin-4-yl)phenoxy)ethyl)carbamate*

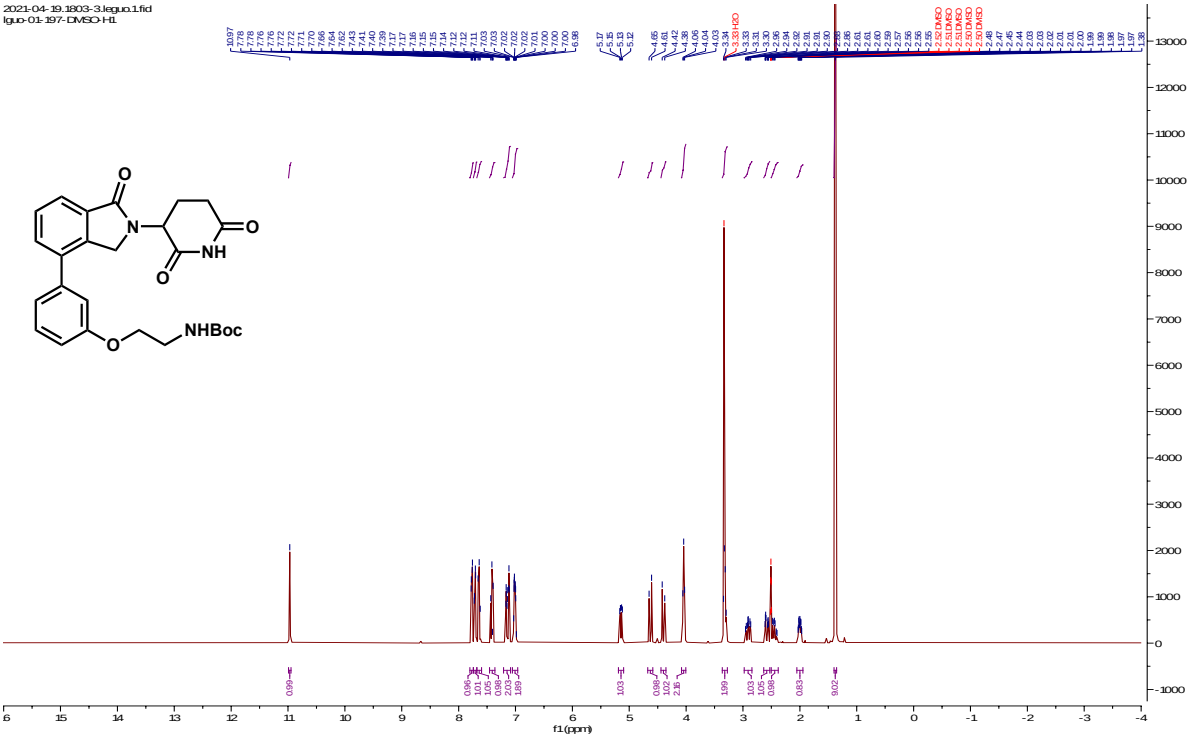

[13]C NMR (101 MHz, DMSO) *-tert-butyl (2-(3-(2-(2,6-dioxopiperidin-3-yl)-1-oxoisoindolin-4-yl)phenoxy)ethyl)carbamate*

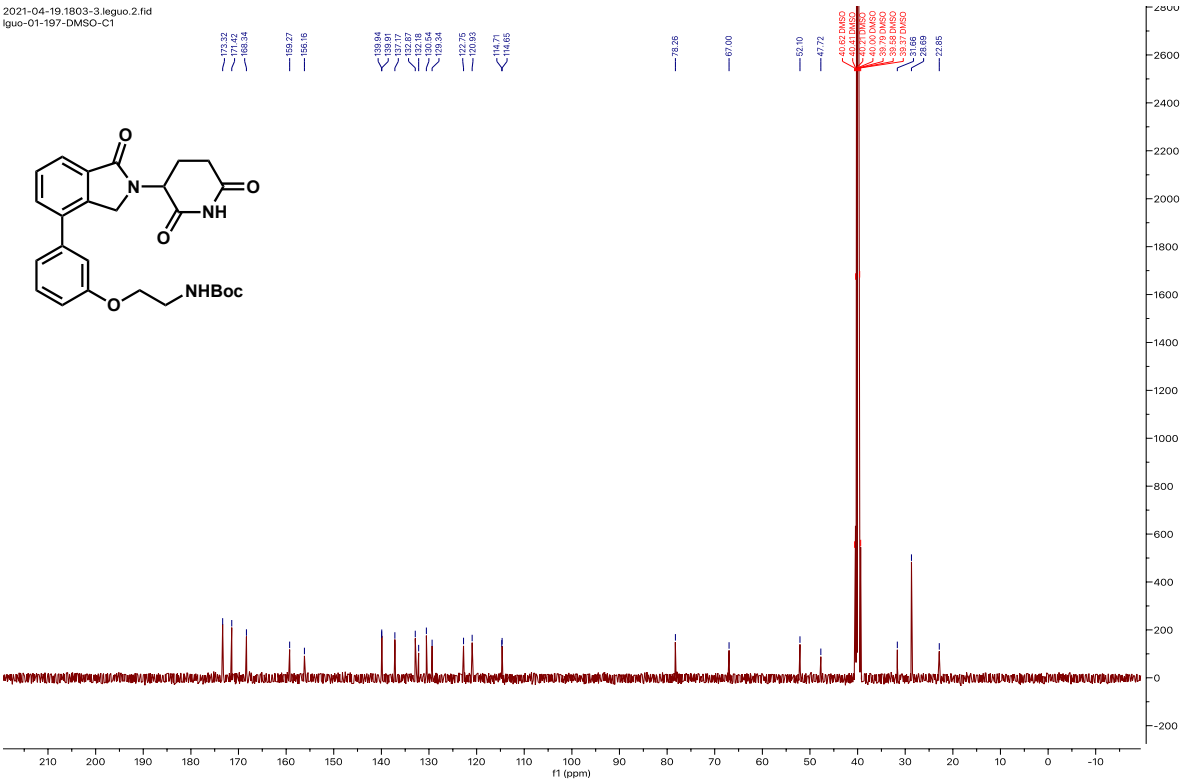

^{1}H NMR (400 MHz, $CDCl_3$) *-tert-butyl (2-(2-(2-(2,6-dioxopiperidin-3-yl)-1-oxoisoindolin-4-yl)phenoxy)ethyl)carbamate*

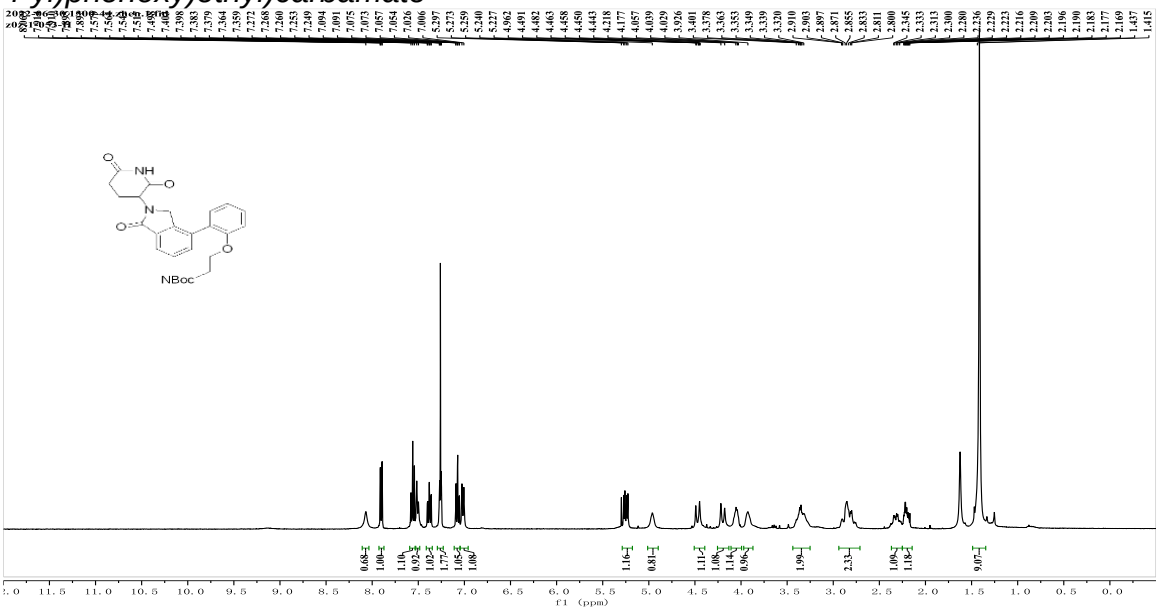

^{13}C NMR (101 MHz, DMSO) *-tert-butyl (2-(2-(2-(2,6-dioxopiperidin-3-yl)-1-oxoisoindolin-4-yl)phenoxy)ethyl)carbamate*

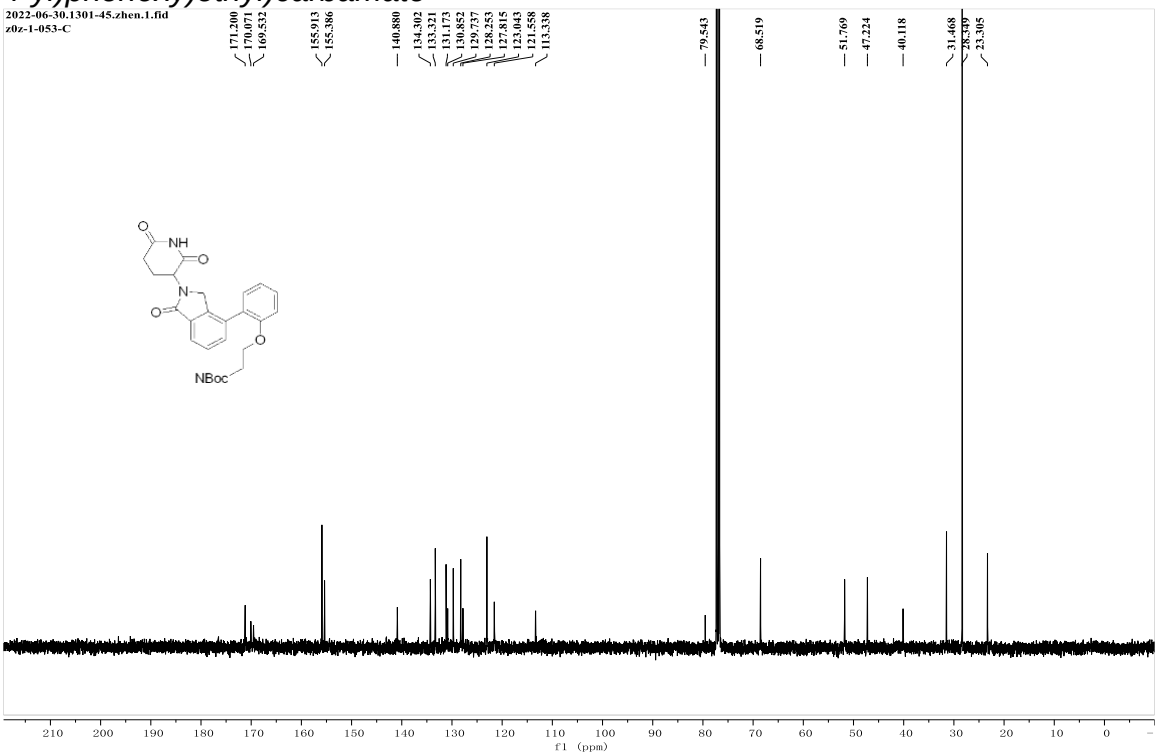

^{1}H NMR (400 MHz, DMSO) **-** 2-(2-(2-(2,6-dioxopiperidin-3-yl)-1-oxoisoindolin-4-yl)phenoxy)acetic acid

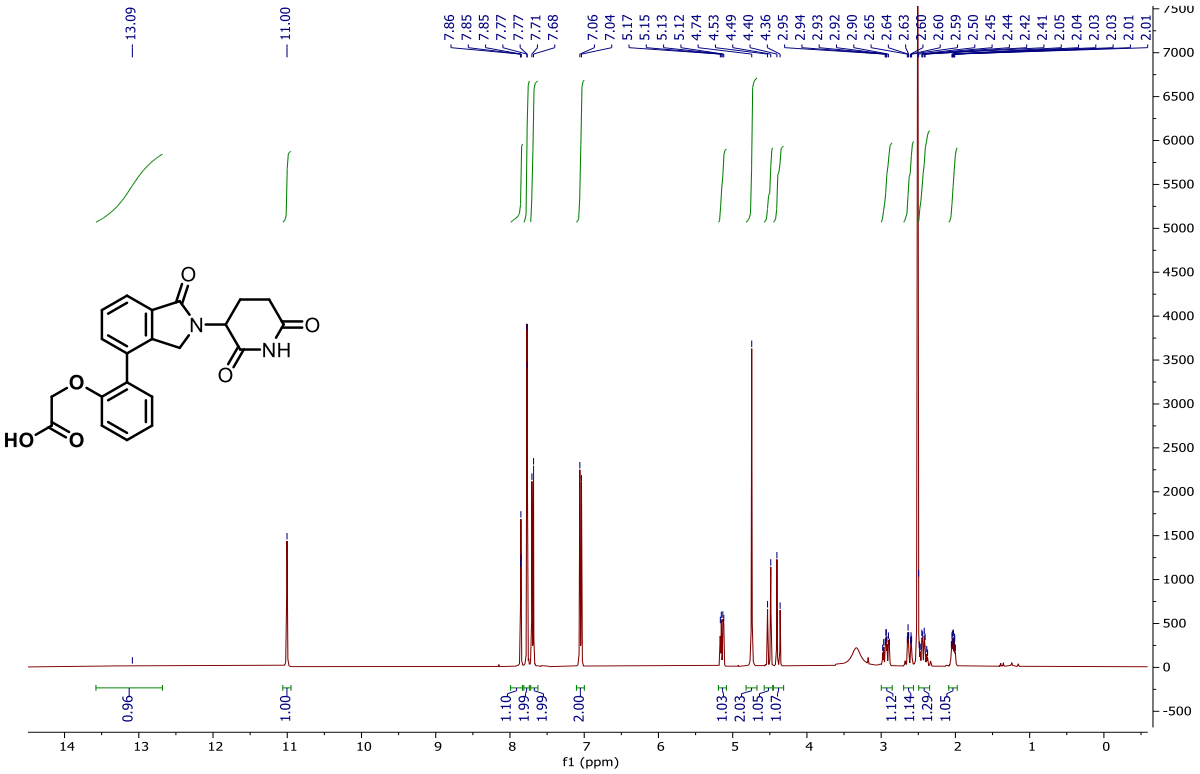

^{13}C NMR (101 MHz, DMSO) **-** 2-(2-(2-(2,6-dioxopiperidin-3-yl)-1-oxoisoindolin-4-yl)phenoxy)acetic acid

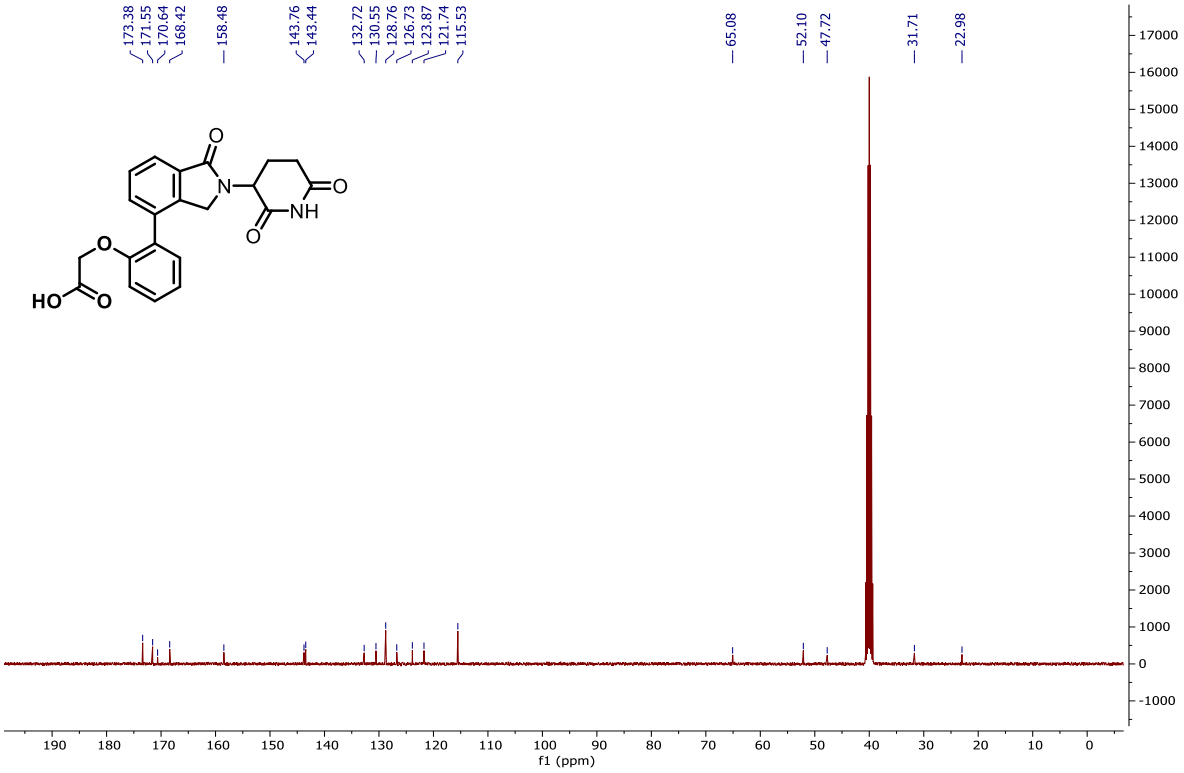

[1]H NMR (400 MHz, DMSO) ***-****2-(4-(2-(2,6-dioxopiperidin-3-yl)-1-oxoisoindolin-4-yl)phenoxy)acetic acid*

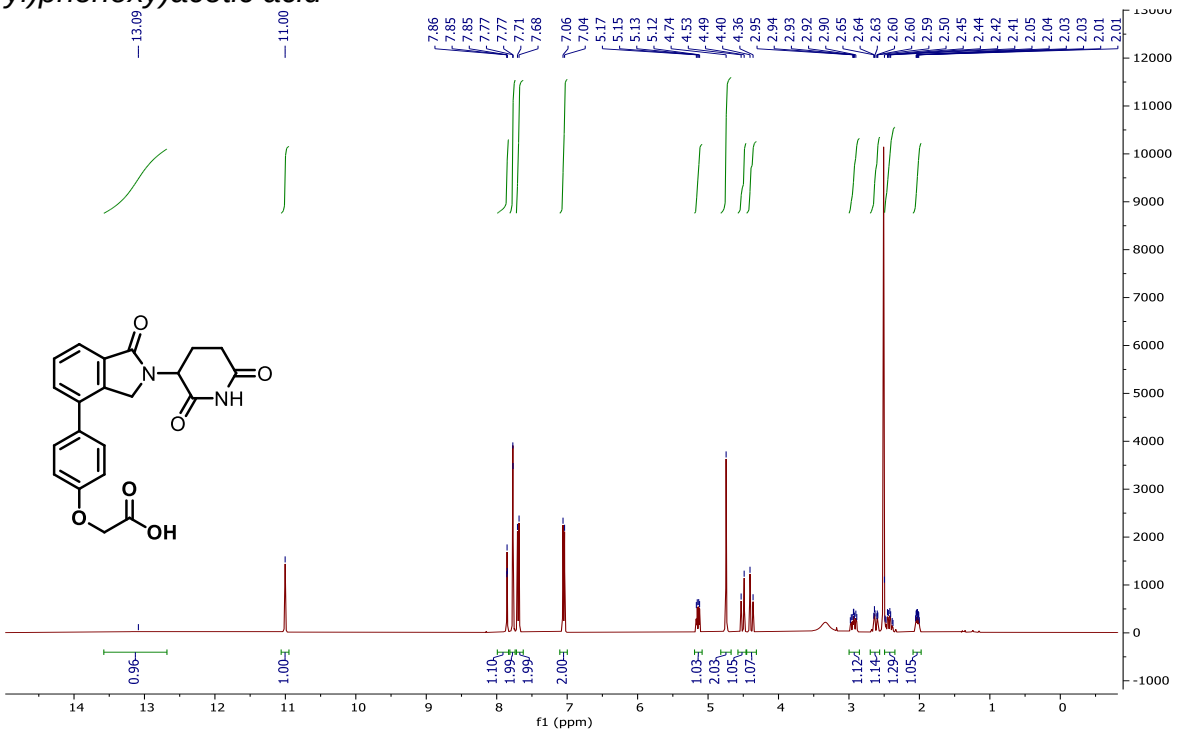

[13]C NMR (101 MHz, DMSO) ***-****2-(4-(2-(2,6-dioxopiperidin-3-yl)-1-oxoisoindolin-4-yl)phenoxy)acetic acid*

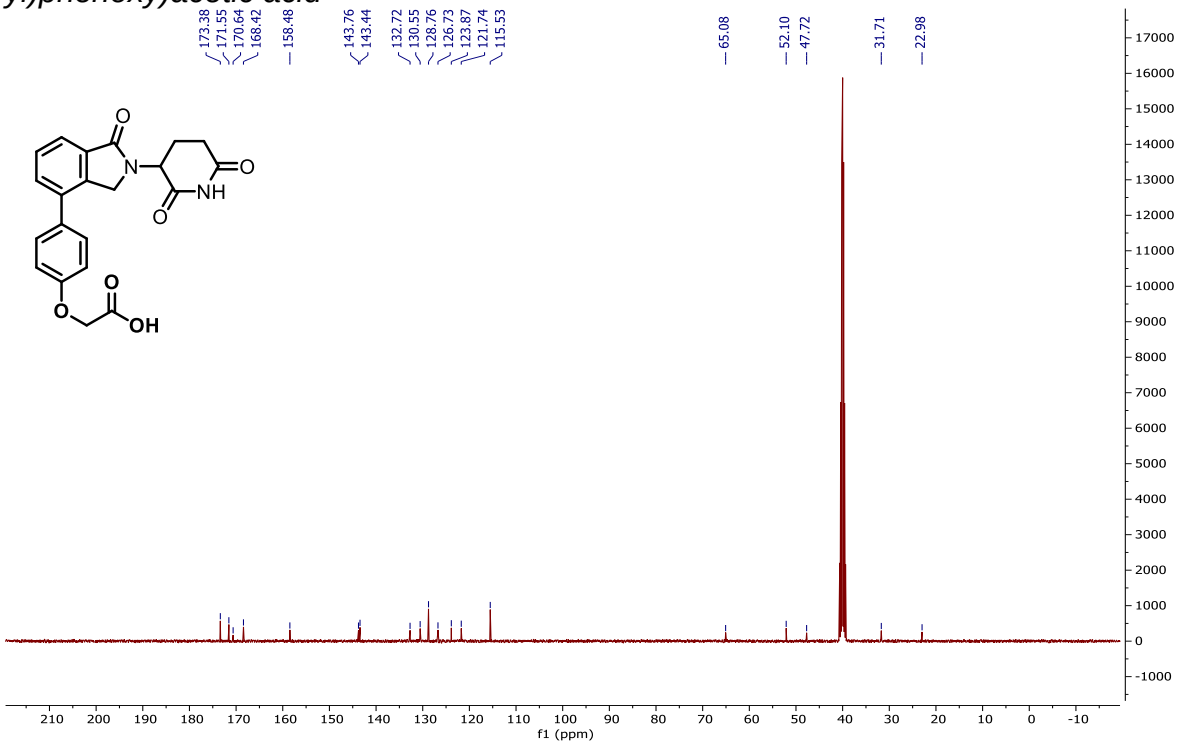

[1]H NMR (400 MHz, DMSO) *-2-(3-(2-(2,6-dioxopiperidin-3-yl)-1-oxoisoindolin-4-yl)phenoxy)acetic acid*

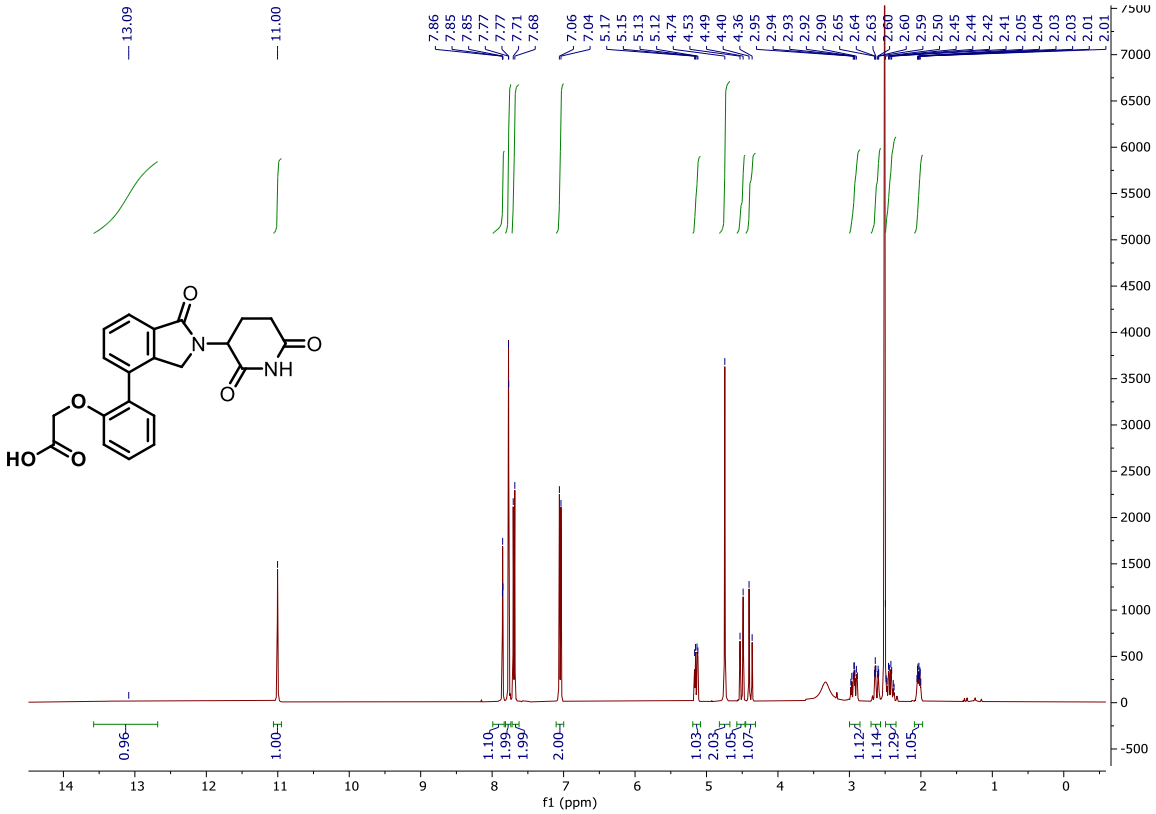

[13]C NMR (101 MHz, DMSO) *-2-(3-(2-(2,6-dioxopiperidin-3-yl)-1-oxoisoindolin-4-yl)phenoxy)acetic acid*

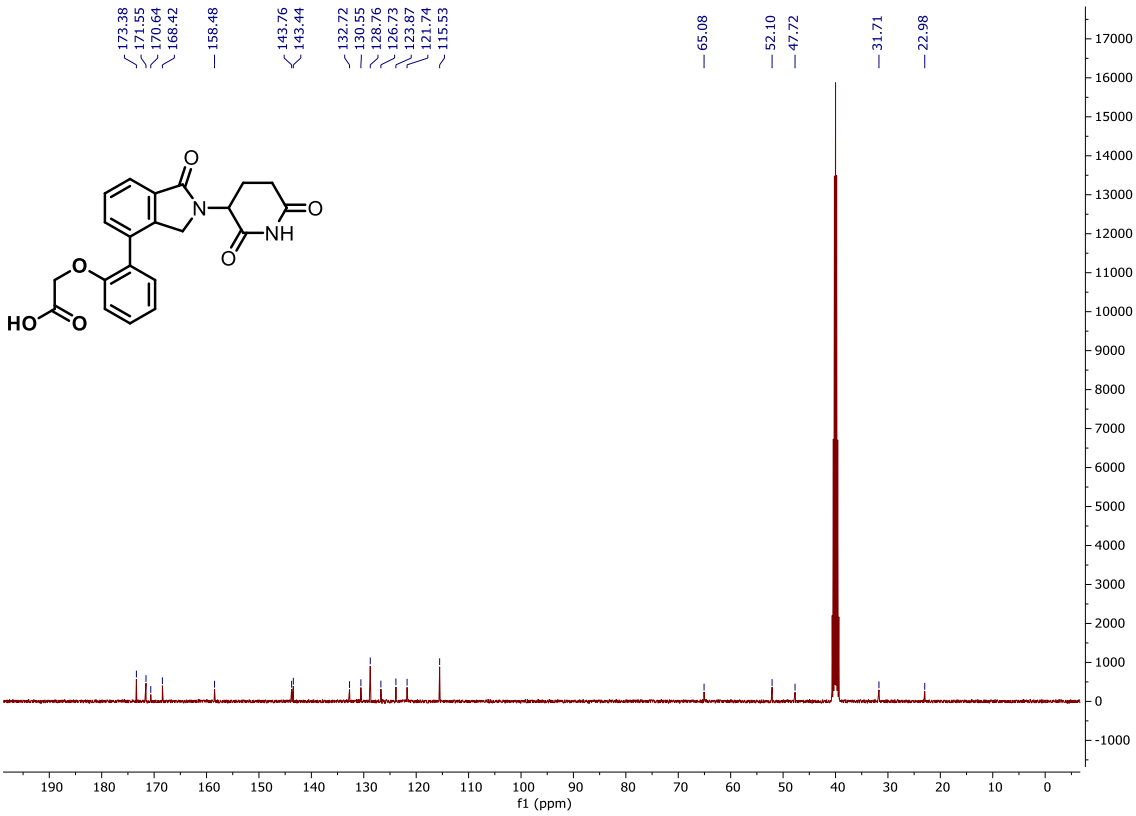

[1]H NMR (400 MHz, DMSO)-*4-(2-(2,6-dioxopiperidin-3-yl)-1-oxoisoindolin-4-yl)benzaldehyde*

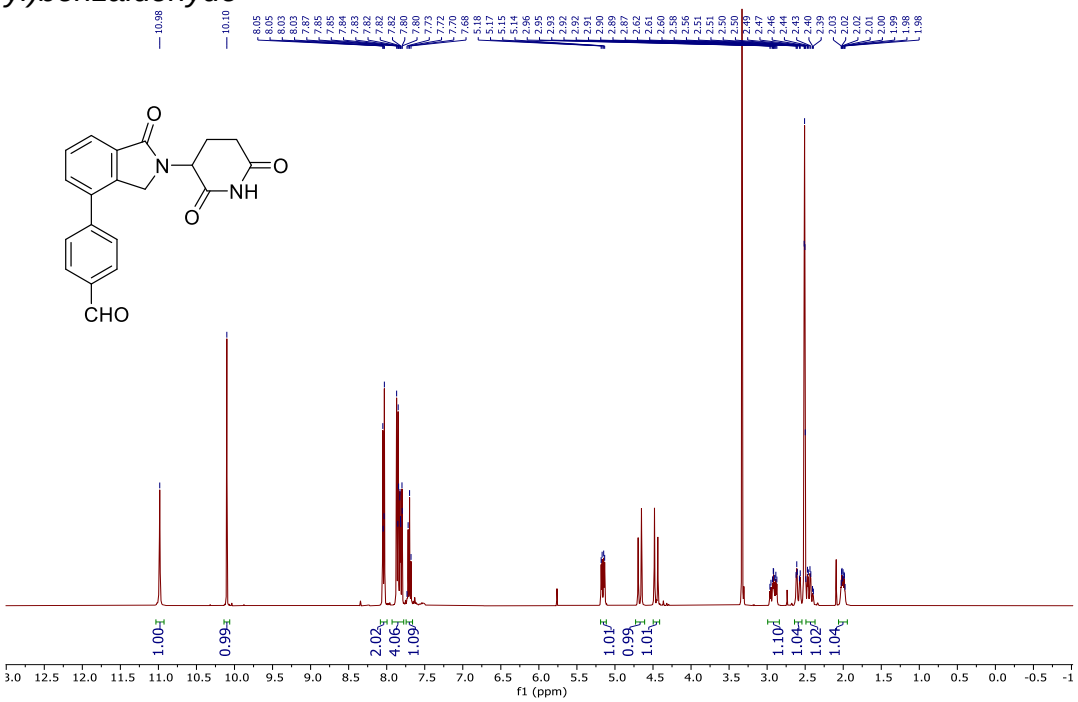

[13]C NMR (101 MHz, DMSO) *-4-(2-(2,6-dioxopiperidin-3-yl)-1-oxoisoindolin-4-yl)benzaldehyde*

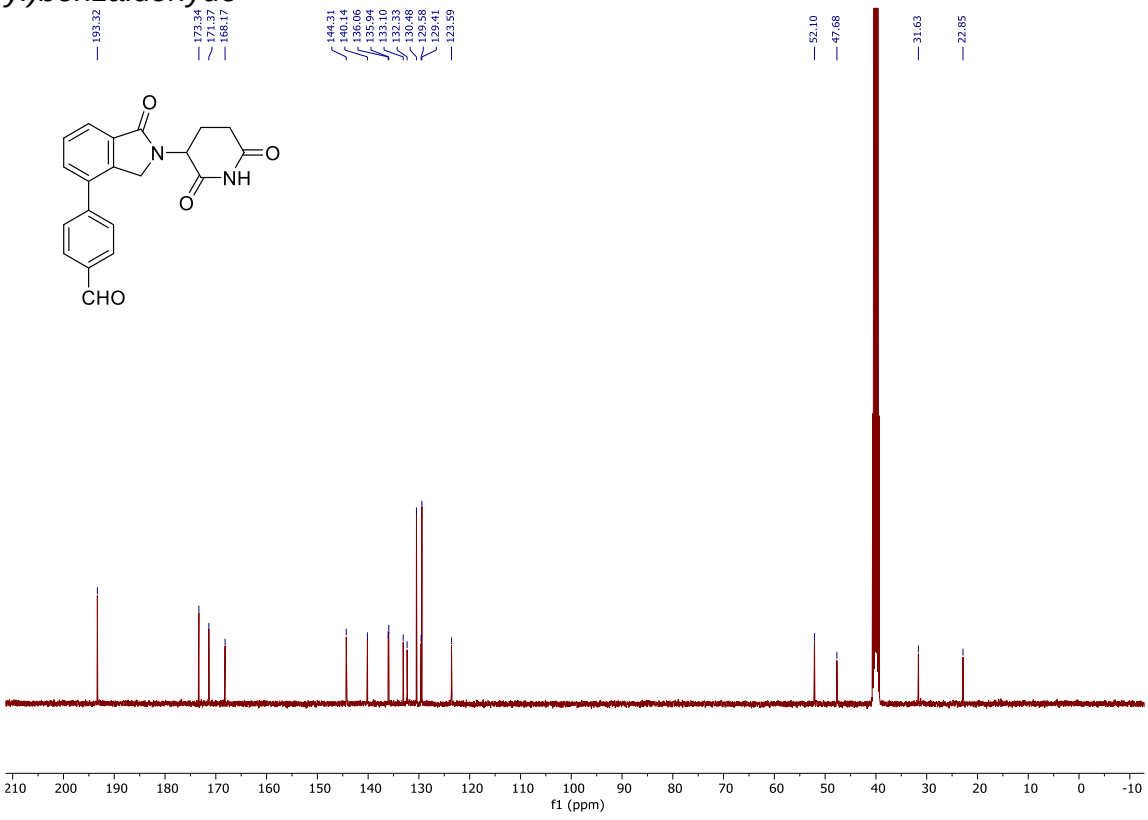

[1]H NMR (400 MHz, DMSO) *-3-(2-(2,6-dioxopiperidin-3-yl)-1-oxoisoindolin-4-yl)benzaldehyde*

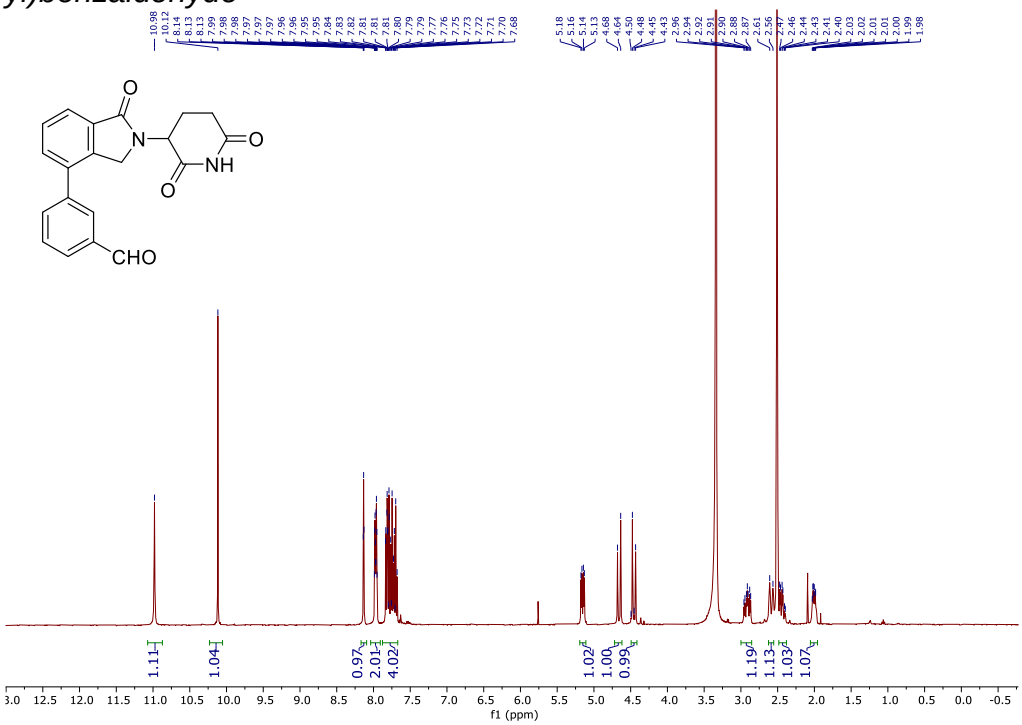

[13]C NMR (101 MHz, DMSO) *-3-(2-(2,6-dioxopiperidin-3-yl)-1-oxoisoindolin-4-yl)benzaldehyde*

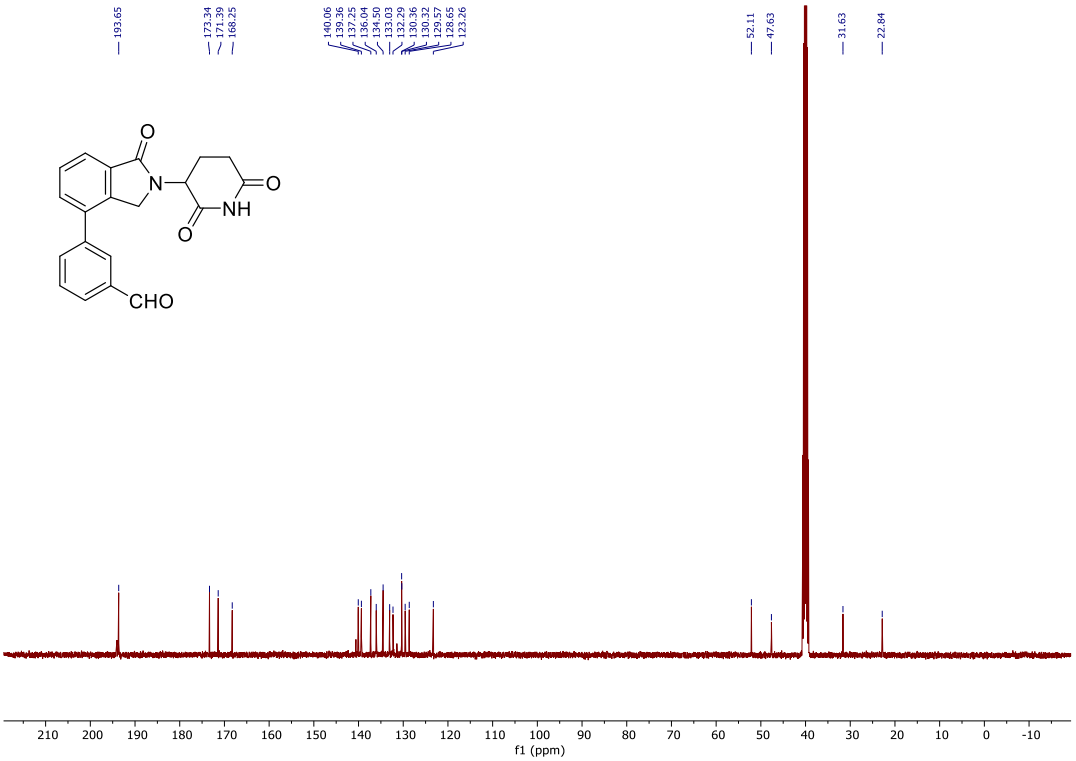

[1]H NMR (400 MHz, DMSO) *-2-(2-(2,6-dioxopiperidin-3-yl)-1-oxoisoindolin-4-yl)benzaldehyde*

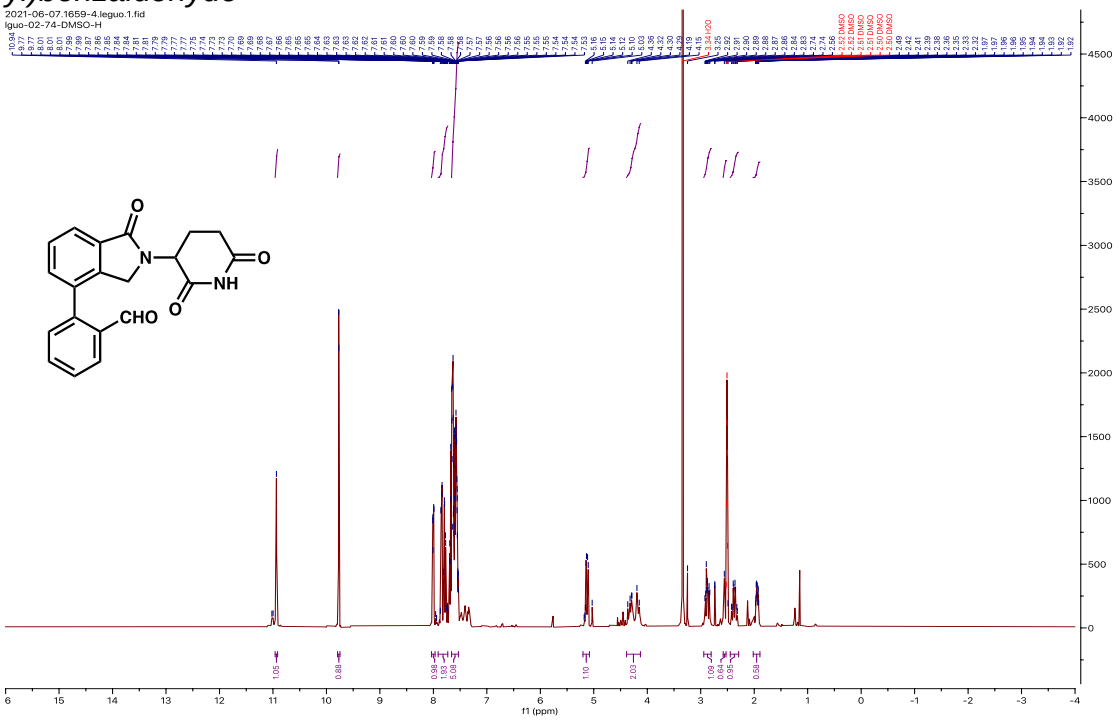

[13]C NMR (101 MHz, DMSO) *-2-(2-(2,6-dioxopiperidin-3-yl)-1-oxoisoindolin-4-yl)benzaldehyde*

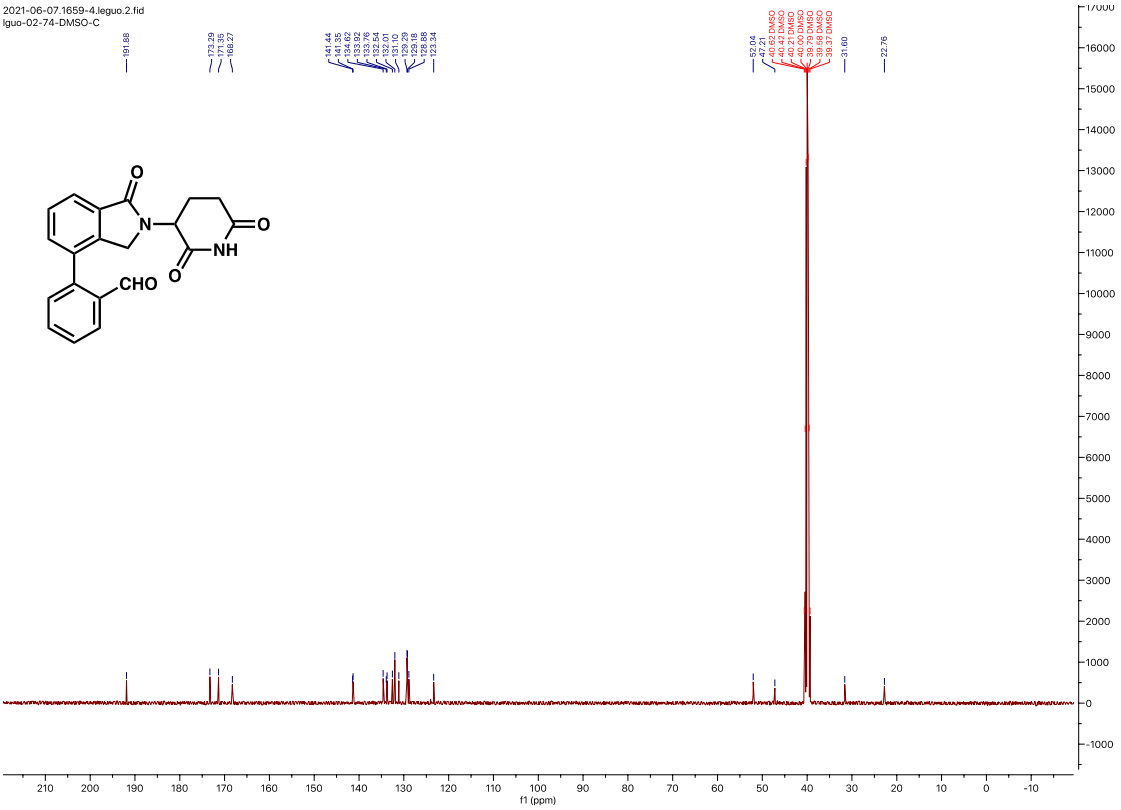

[1]H NMR (400 MHz, DMSO) *-3-(4-(4-hydroxyphenyl)-1-oxoisoindolin-2-yl)piperidine-2,6-dione*

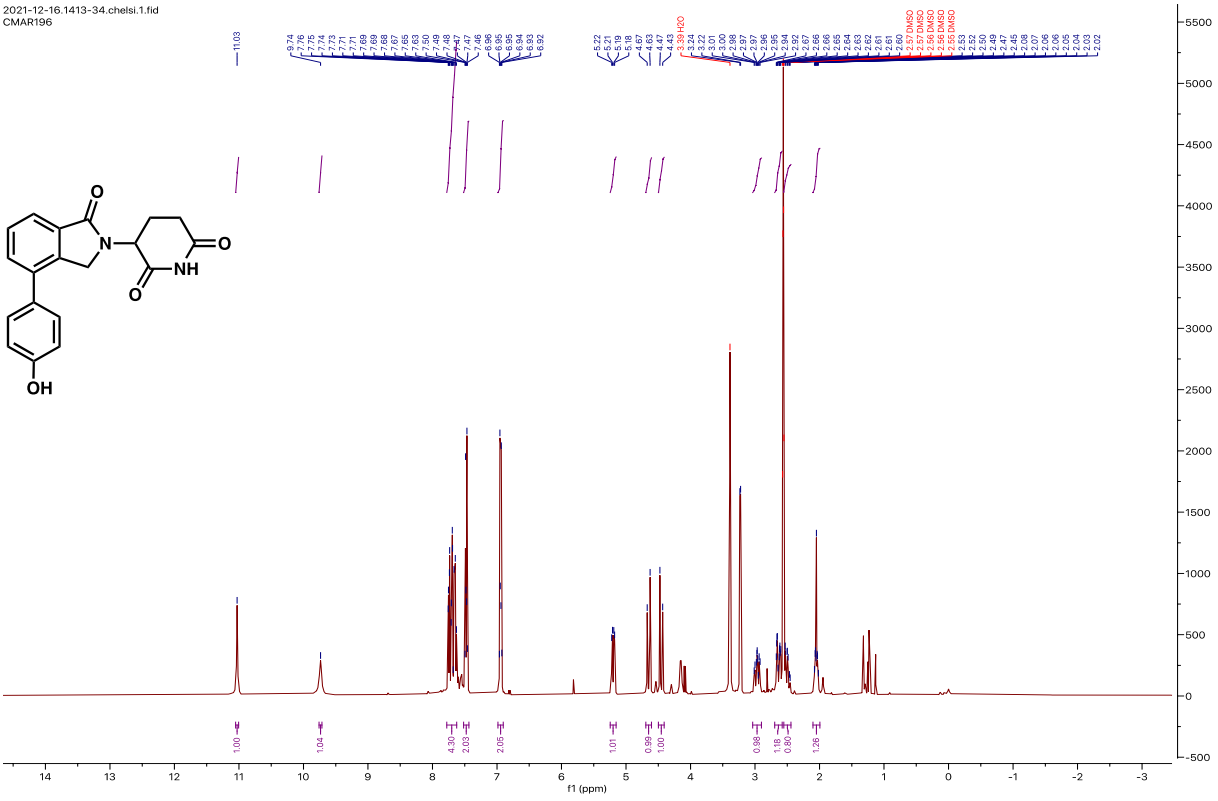

^{13}C NMR (101 MHz, DMSO) *-3-(4-(4-hydroxyphenyl)-1-oxoisoindolin-2-yl)piperidine-2,6-dione*

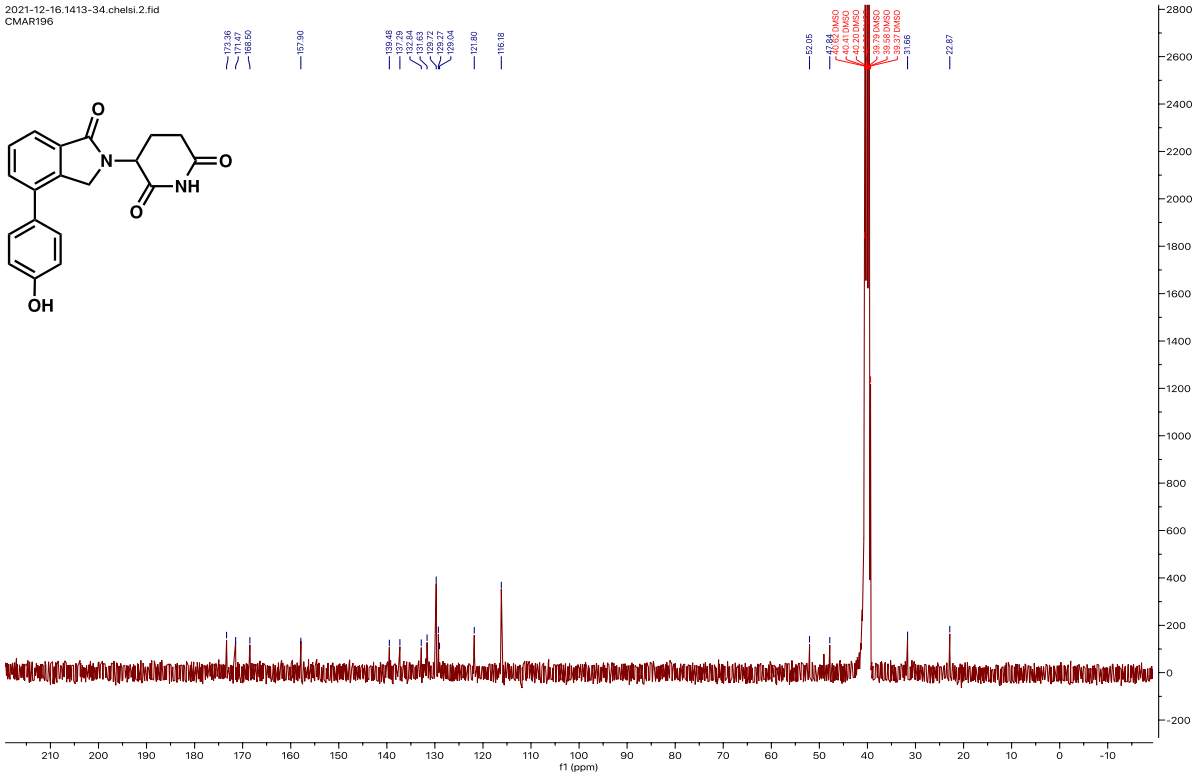

^{1}H NMR (400 MHz, DMSO) *-3-(4-(3-hydroxyphenyl)-1-oxoisoindolin-2-yl)piperidine-2,6-dione*

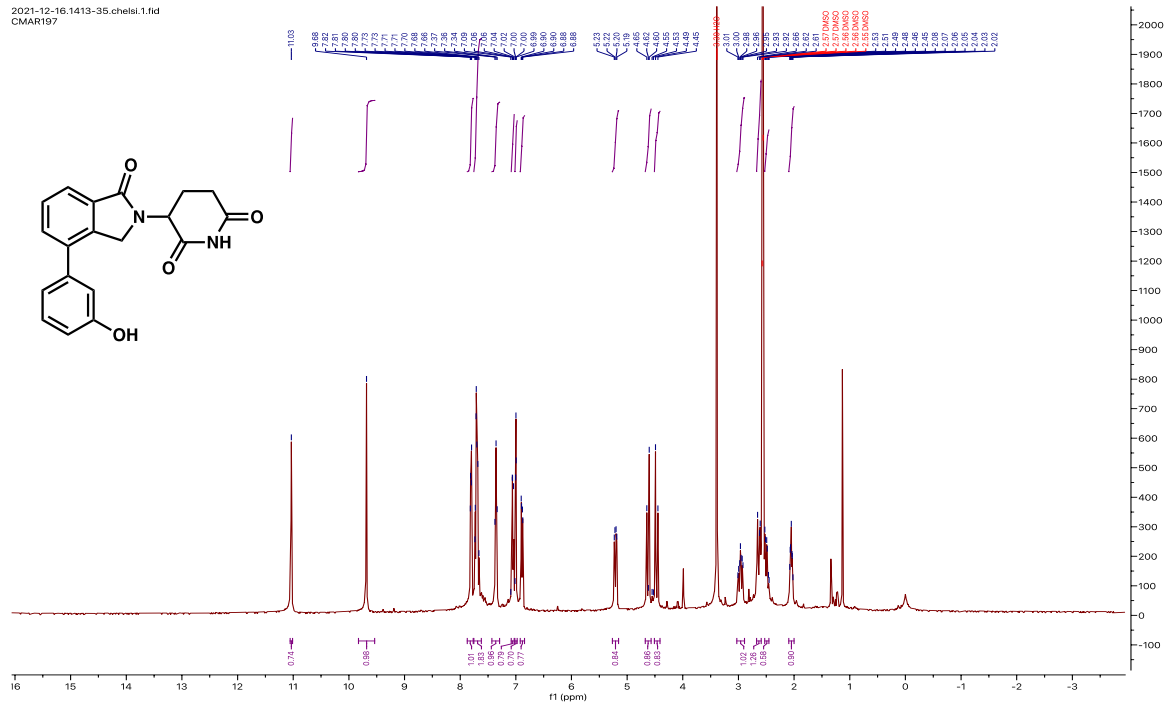

^{13}C NMR (101 MHz, DMSO) - *3-(4-(3-hydroxyphenyl)-1-oxoisoindolin-2-yl)piperidine-2,6-dione*

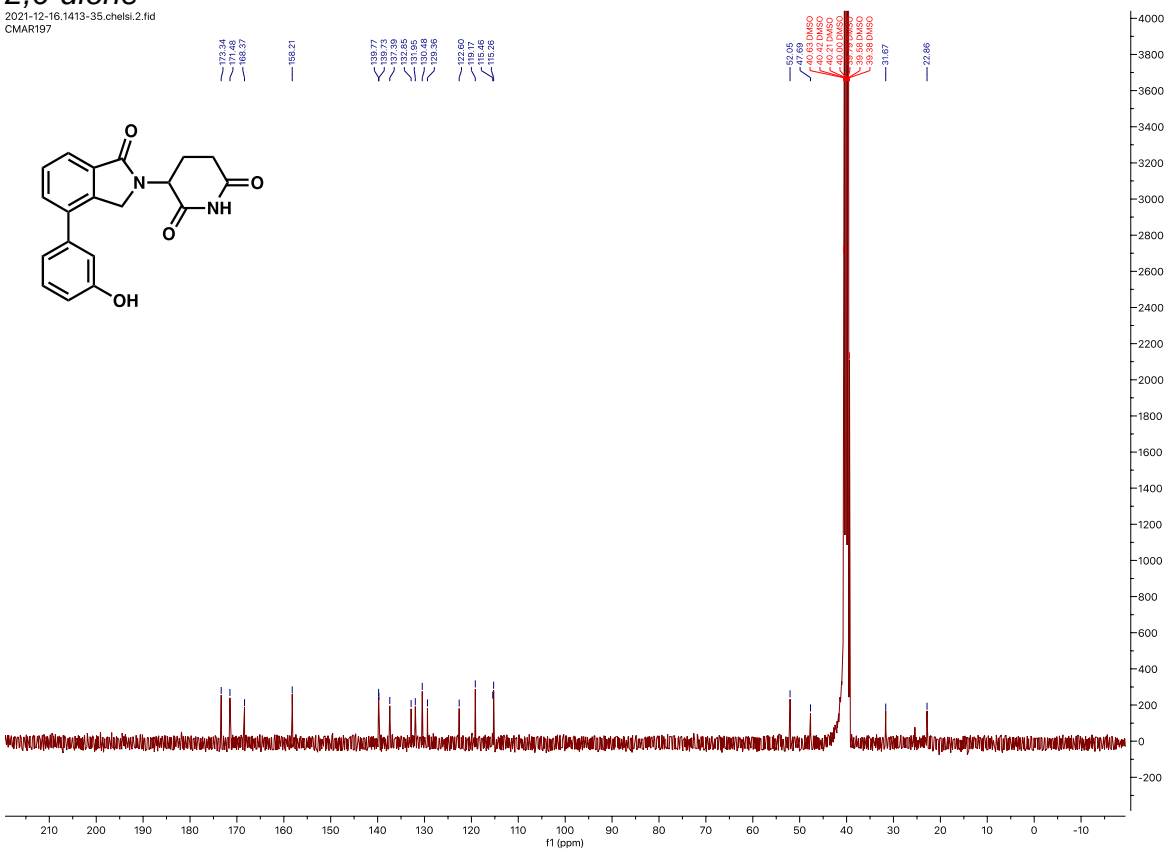

^{1}H NMR (400 MHz, DMSO) *-3-(4-(2-hydroxyphenyl)-1-oxoisoindolin-2-yl)piperidine-2,6-dione*

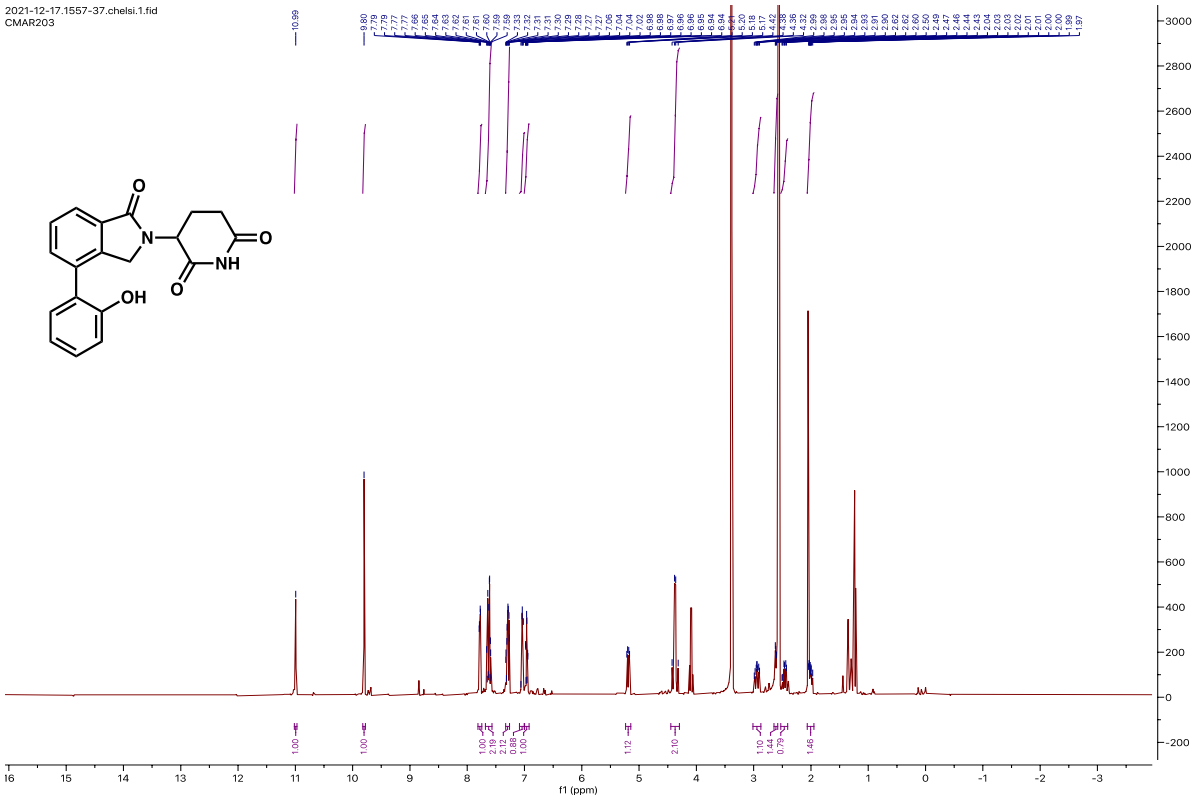

^{13}C NMR (101 MHz, DMSO) *-3-(4-(2-hydroxyphenyl)-1-oxoisoindolin-2-yl)piperidine-2,6-dione*

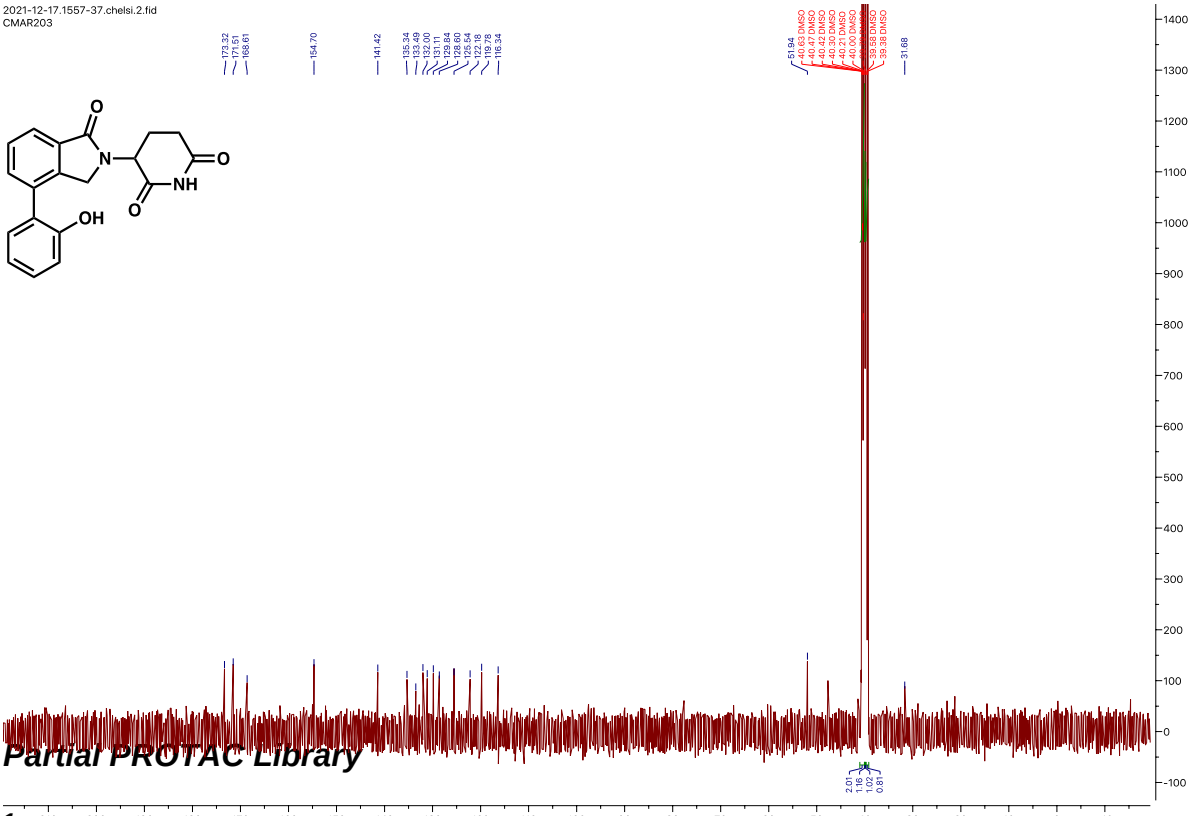

Partial PROTAC Library

^{1}H NMR (400 MHz, DMSO) *-N-(2-(4-(2-(2,6-dioxopiperidin-3-yl)-1-oxoisoindolin-4-yl)phenoxy)ethyl)-4-formylbenzamide*

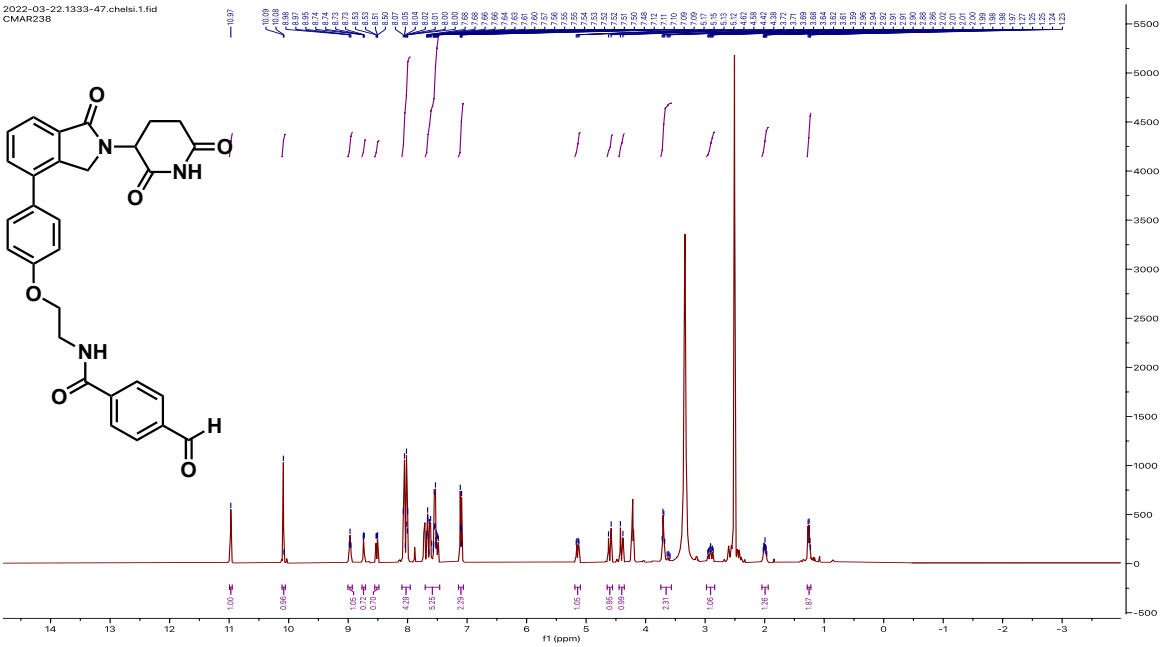

^{13}C NMR (101 MHz, DMSO)-*N-(2-(4-(2-(2,6-dioxopiperidin-3-yl)-1-oxoisoindolin-4-yl)phenoxy)ethyl)-4-formylbenzamide*

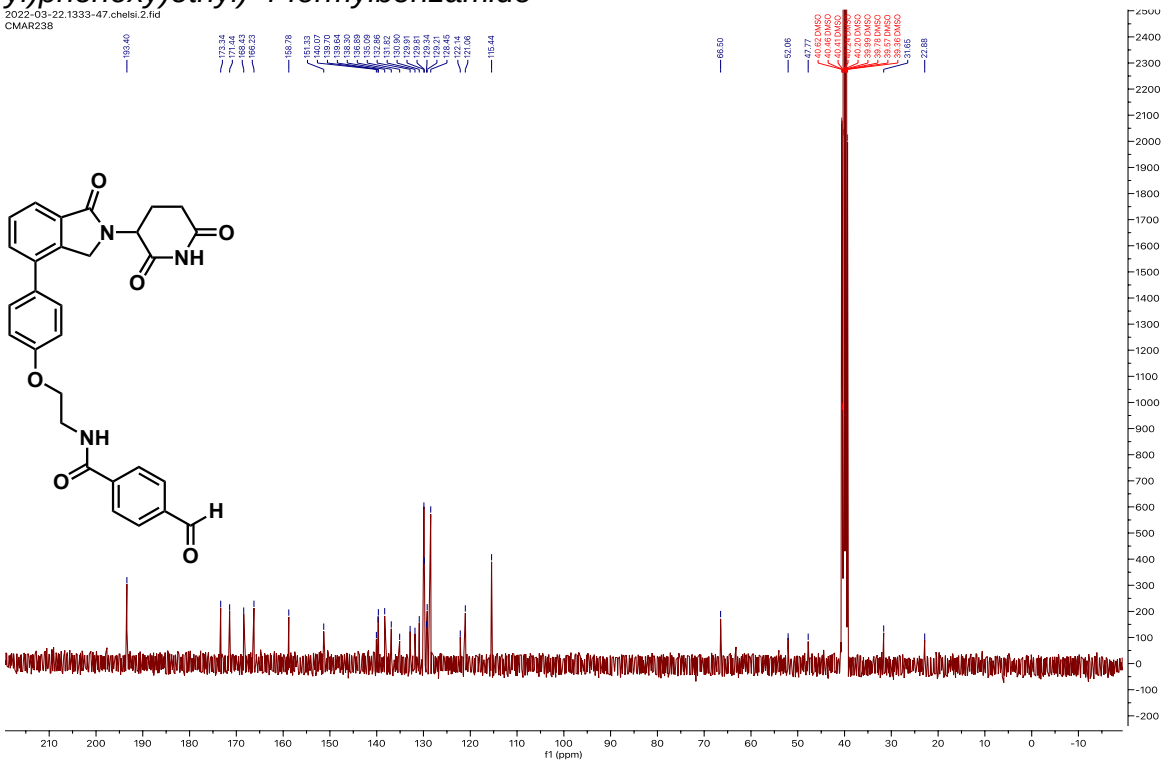

^{1}H NMR (400 MHz, DMSO) *-N-(2-(4-(2-(2,6-dioxopiperidin-3-yl)-1-oxoisoindolin-4-yl)phenoxy)ethyl)-3-formylbenzamide*

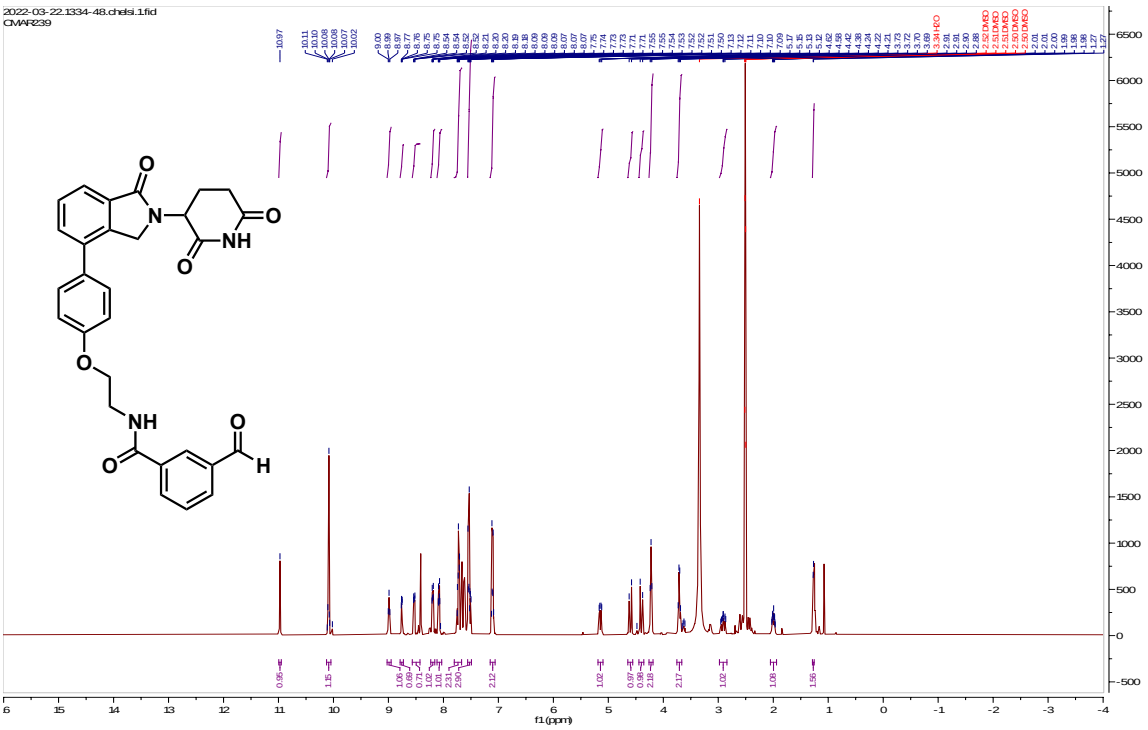

^{13}C NMR (101 MHz, DMSO) *-N-(2-(4-(2-(2,6-dioxopiperidin-3-yl)-1-oxoisoindolin-4-yl)phenoxy)ethyl)-3-formylbenzamide*

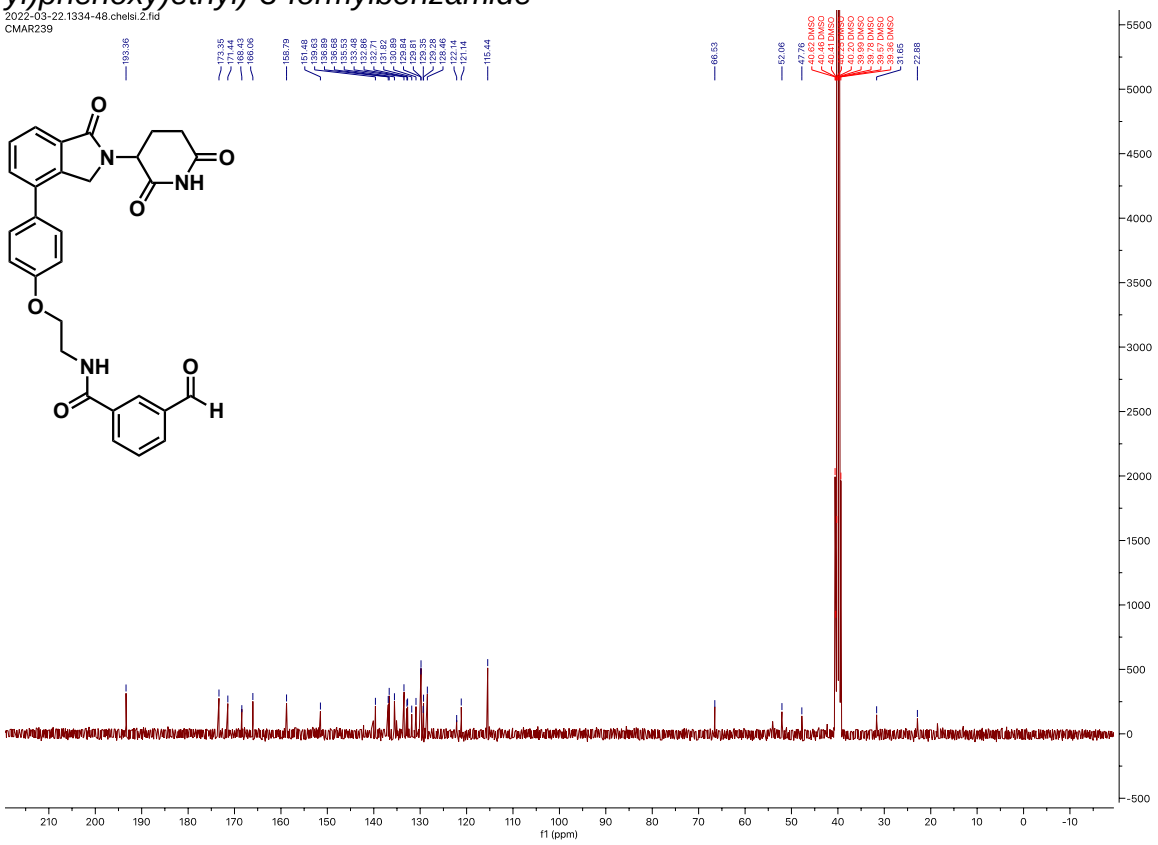

^{1}H NMR (400 MHz, DMSO) *-N-(2-(3-(2-(2,6-dioxopiperidin-3-yl)-1-oxoisoindolin-4-yl)phenoxy)ethyl)-4-formylbenzamide*

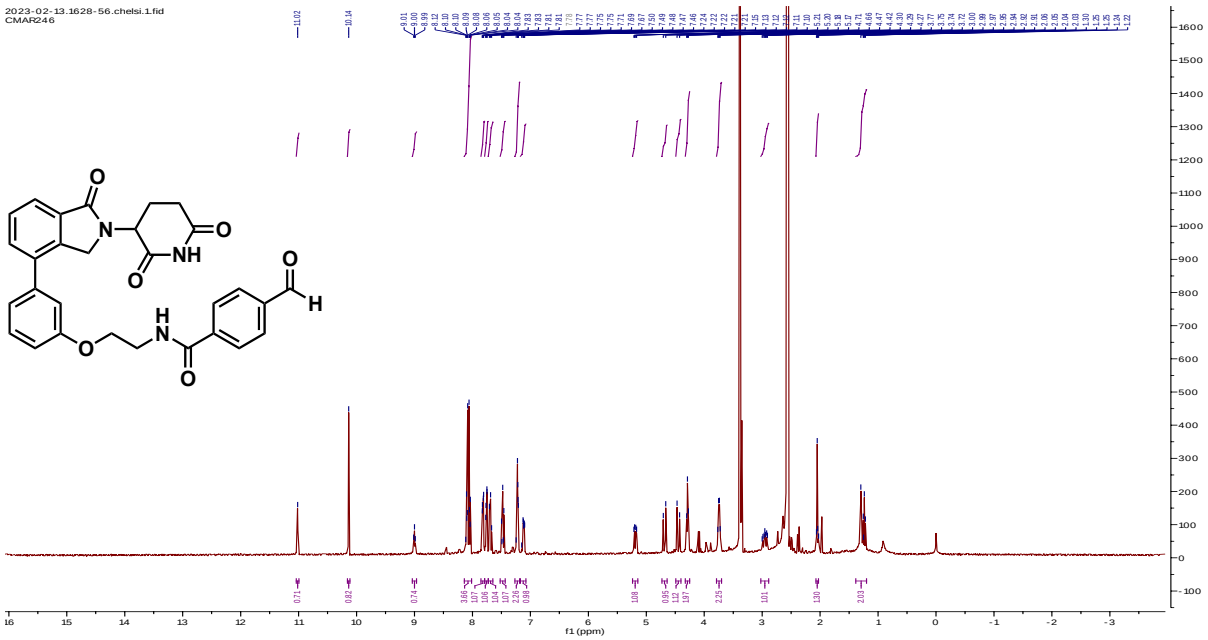

^{13}C NMR (126 MHz, DMSO) *-N-(2-(3-(2-(2,6-dioxopiperidin-3-yl)-1-oxoisoindolin-4-yl)phenoxy)ethyl)-4-formylbenzamide*

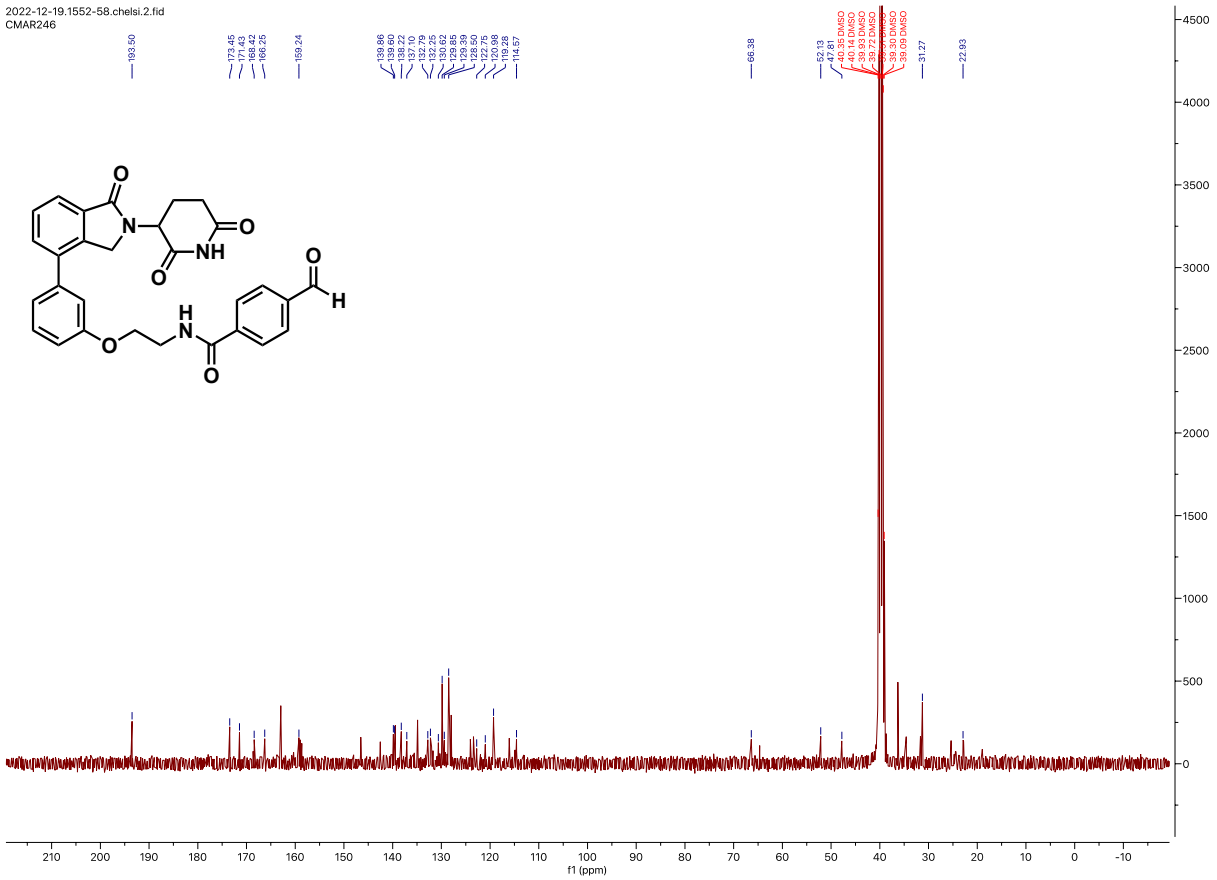

^{1}H NMR (400 MHz, DMSO) *-N-(2-(3-(2-(2,6-dioxopiperidin-3-yl)-1-oxoisoindolin-4-yl)phenoxy)ethyl)-3-formylbenzamide*

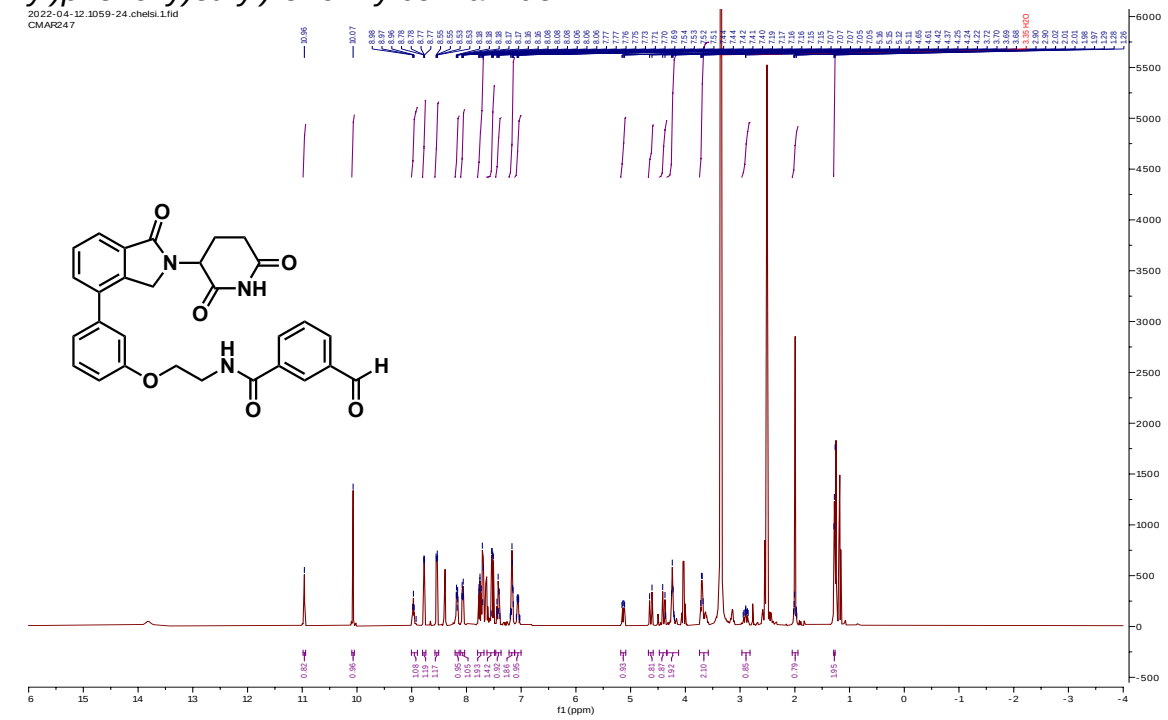

^{13}C NMR (101 MHz, DMSO) *-N-(2-(3-(2-(2,6-dioxopiperidin-3-yl)-1-oxoisoindolin-4-yl)phenoxy)ethyl)-3-formylbenzamide*

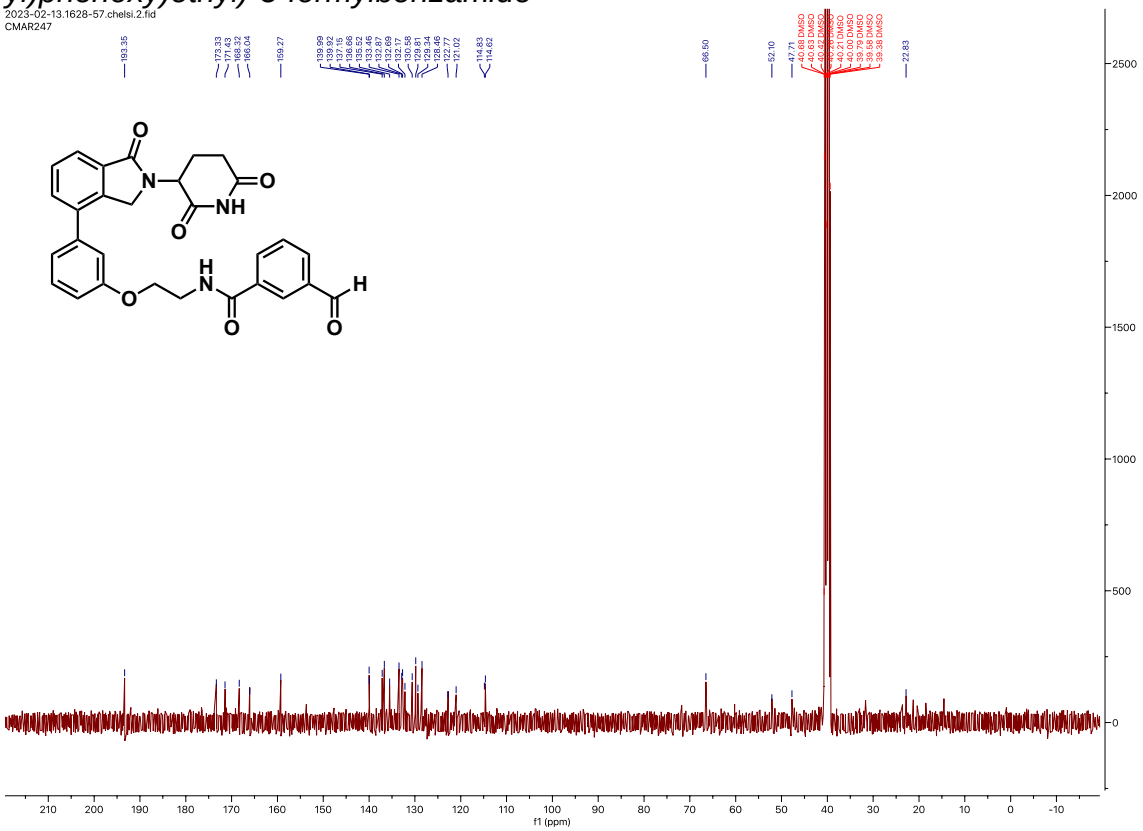

^{1}H NMR (400 MHz, DMSO) *-N-(2-(2-(2-(2,6-dioxopiperidin-3-yl)-1-oxoisoindolin-4-yl)phenoxy)ethyl)-4-formylbenzamide*

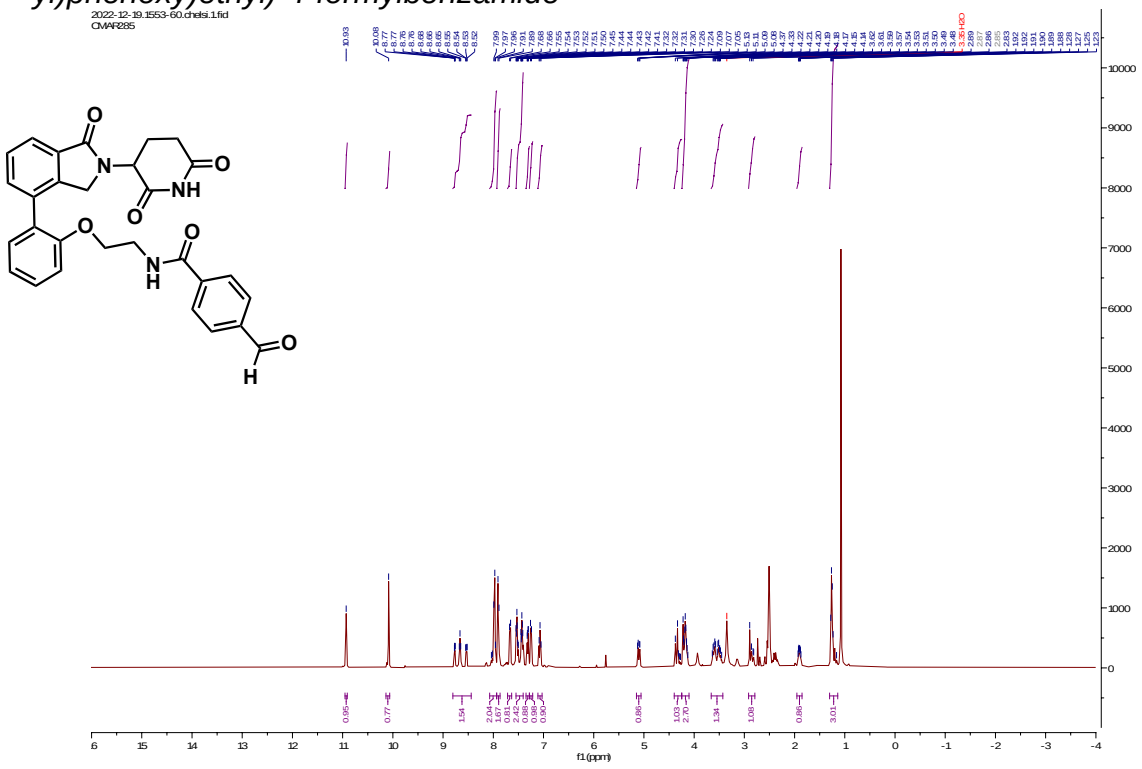

^{13}C NMR (101 MHz, DMSO) *-N-(2-(2-(2-(2,6-dioxopiperidin-3-yl)-1-oxoisoindolin-4-yl)phenoxy)ethyl)-4-formylbenzamide*

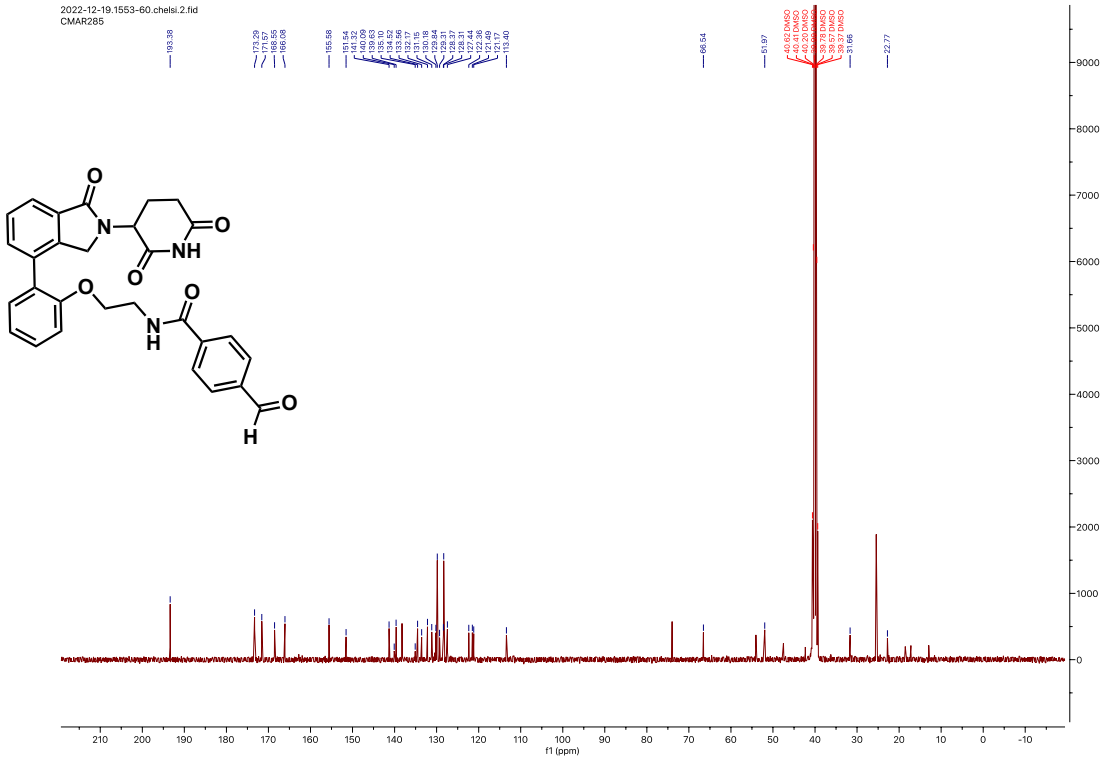

^{1}H NMR (400 MHz, DMSO) *-N-(2-(2-(2-(2,6-dioxopiperidin-3-yl)-1-oxoisoindolin-4-yl)phenoxy)ethyl)-3-formylbenzamide*

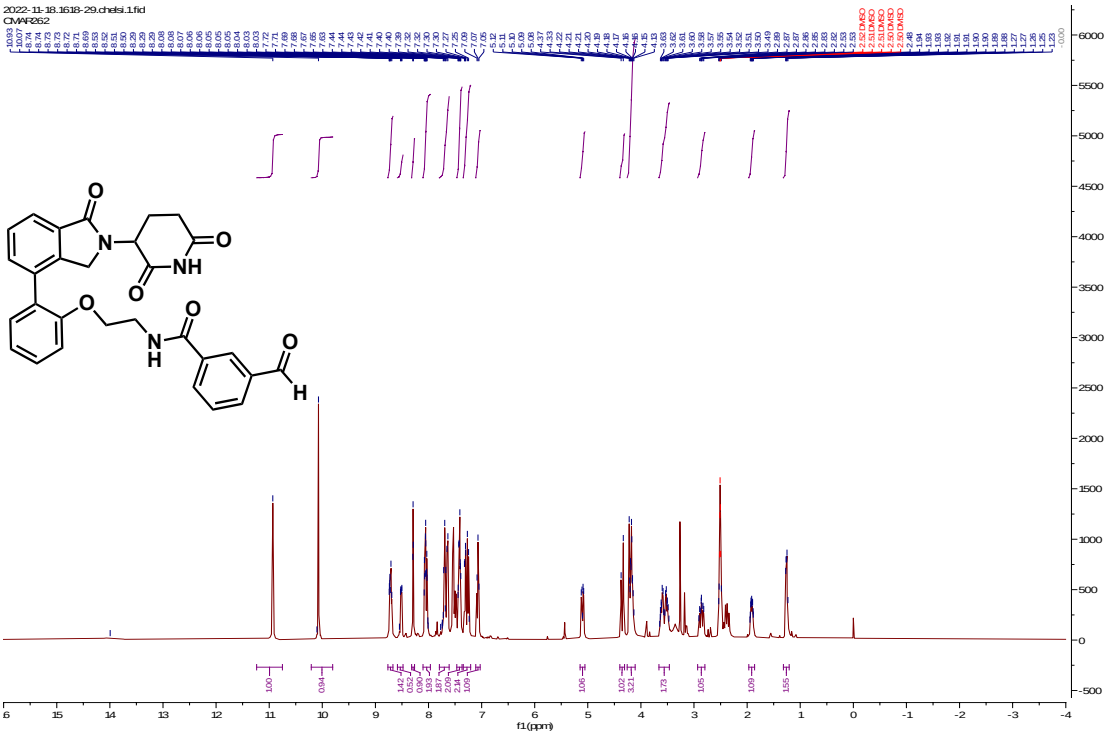

^{13}C NMR (101 MHz, DMSO) *-N-(2-(2-(2-(2,6-dioxopiperidin-3-yl)-1-oxoisoindolin-4-yl)phenoxy)ethyl)-3-formylbenzamide*

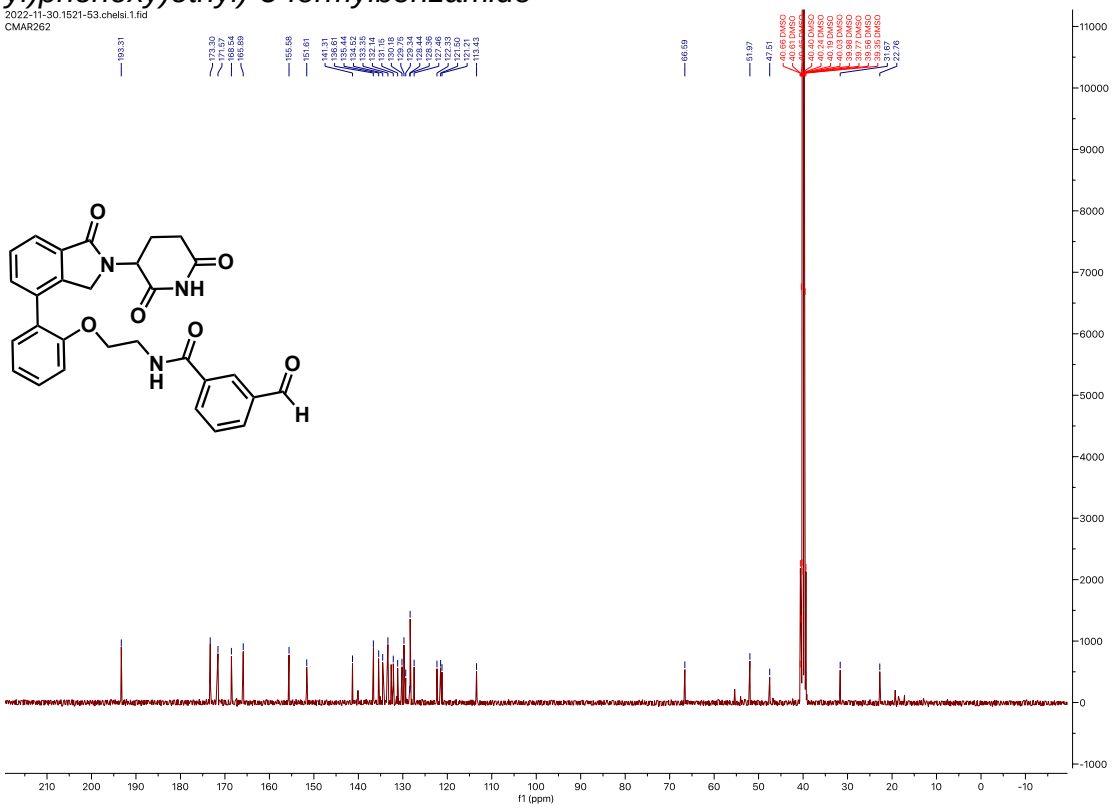

CHAPTER 3

Development of a Partial PROTAC Library based on Achiral Cereblon E3 Ligase Ligands and Bruton's Tyrosine Kinase-Based Full PROTAC Library for Targeted Protein Degradation

3.1 Introduction

Immunomodulatory imide drugs (IMiDs) such as thalidomide, pomalidomide, and lenalidomide are essential treatments for patients with multiple myeloma (MM).[43] During the 1950s, thalidomide was released as an effective sedative to treat morning sickness during pregnancy. However, it was withdrawn from the market due to significant side effects including neuropathy and teratogenicity caused by the drug.[52] After being withdrawn from the market, studies showed that thalidomide improved MM patients outcomes due to successful anti-angiogenic, anti-proliferative anti-inflammatory, and immunomodulation activities leading to the creation of pomalidomide and lenalidomide as more potent analogues.[43,53] Nonetheless, their biological targets and mechanism of action remained unknown until recently.

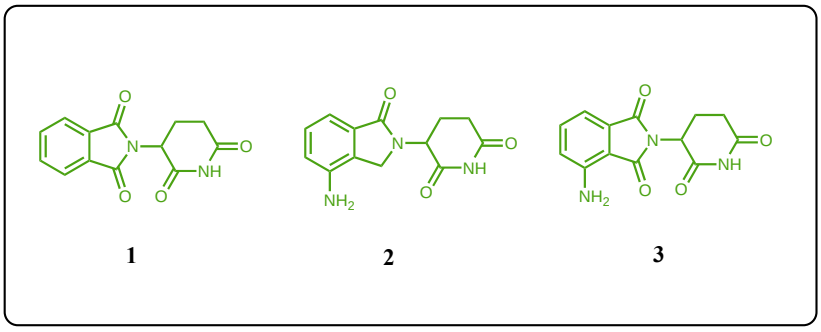

Figure 1. Structures of reported E3 CRBN ligands IMiDs (**1**) thalidomide, (**2**) lenalidomide, and (**3**) pomalidomide.

Evidence suggests that the mechanism of action of thalidomide and its analogues requires binding to the cereblon (CRBN) proteins.[54] Particularly, CRBN serves as a substrate receptor in the E3-ubiquitin ligase complex $CRL4^{CRBN}$ where it associates with

the DNA damage-binding protein-1 (DDB1), Cullin 4 (Cul4), and regulator of Cullins 1 (Roc1) for labelling proteins for ubiquitination and proteasome degradation.[55,56] The binding of IMiDs to CRBN can lead to the degradation of key transcription factors that are essential for the growth of multiple myeloma, such as IKZF1 and IKZF3, two of the neo-substrates for CRBN.[43]

Proteolysis Targeting Chimeras (PROTACs) emerged as a therapeutic strategy to promote the degradation of intracellular proteins. PROTACs consist of a ligand for a target protein, a linker, and a E3 ubiquitin ligase ligand that can induce the degradation of the protein of interest (POI).[38] The heterobifunctional PROTAC degrader brings the POI and E3 ligase ligand into close proximity, leading to polyubiquitination of the target protein and subsequent proteasomal degradation. Since the process is catalytic, the PROTAC molecule recycles to induce another round of degradation.

Although there are more than 600 E3 ligases discovered in humans, only a few have been successfully employed in PROTACs. Specifically, CRBN is the most commonly used E3 ligase in PROTACs due to the low molecular weight and drug-like properties of its ligands, such as thalidomide and its analogs.[38] However, researchers have found that thalidomide and its analogs are unstable and undergo rapid racemization and hydrolysis *in vitro* and *in vivo*.[37,38] Particularly, the (S)-enantiomer is at least 10-fold stronger than the (R)-enantiomer.[38] Moreover, because IMiDs are known to promote the degradation of the CRBN neosubstrates, the selectivity profile of current CRBN E3 ligase ligands requires further optimization. Hence, the stability, racemization, and selectivity of the CRBN

ligands are potential issues for the development of CRBN-based PROTACs as therapeutics.[43] For this reason, there has been a growing need for creating alternative CRBN binders that can be applied for PROTACs.

To date, various efforts have been developed for resolving the above issues of CRBN ligands, including changing the hydrogen in the chiral carbon of thalidomide to deuterium or introducing a quaternary carbon.[38] However, the addition of a methyl group significantly impeded the biological activity of thalidomide to treat multiple myeloma and human leukemia.[38,57,58] Phenyl glutarimides (PG) were later discovered as novel CRBN binders with improved hydrolytic stability and similar binding affinity, when compared to traditional IMiDs (**Figure 2**).[37] The authors applied the phenyl glutarimides ligands to create PG-based BET PROTACs.[37] These degraders showed anti-proliferative efficiency in MV4-11 and HD-MB03 cell lines, and cellular potency IC_{50} of 3 pM in MV4-11.[37] Nonetheless, since these PG ligands still contain a chiral center, they continue to suffer from racemization issue.

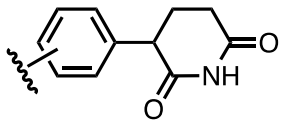

Phenyl Glutarimide (PG)

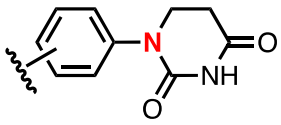

Phenyl Dihydrouracil (PDHU)

Figure 2. Alternative CRBN binders.

Our group recently reported a detailed structure-activity relationship and properties studies of substituted and unsubstituted achiral phenyl dihydrouracil (PDHU) ligands as alternative CRBN binders (**Figure 2**).[38] These ligands showed a similar binding affinity and stronger stability compared to lenalidomide.[38] In addition, five BRD4 PROTACs containing 1,2,3-trisubstituted PDHUs were also designed and synthesized, where significant degradation efficiency was observed in multiple cell lines.[38] Particularly, compounds **4F** and **6F** containing a relatively accessible terminal Boc-protected amine linker, showed stronger binding affinities to CBRN compared to lenalidomide (**Figure 3**). Specifically, **6F** showed the strongest potency and binding affinity compared to all PDHU ligands (**Figure 3**). Accordingly, we believe that it is possible to apply the newly discovered substituted PDHU ligands for the design and synthesis of novel nonracemic PROTACs for any protein of interest.

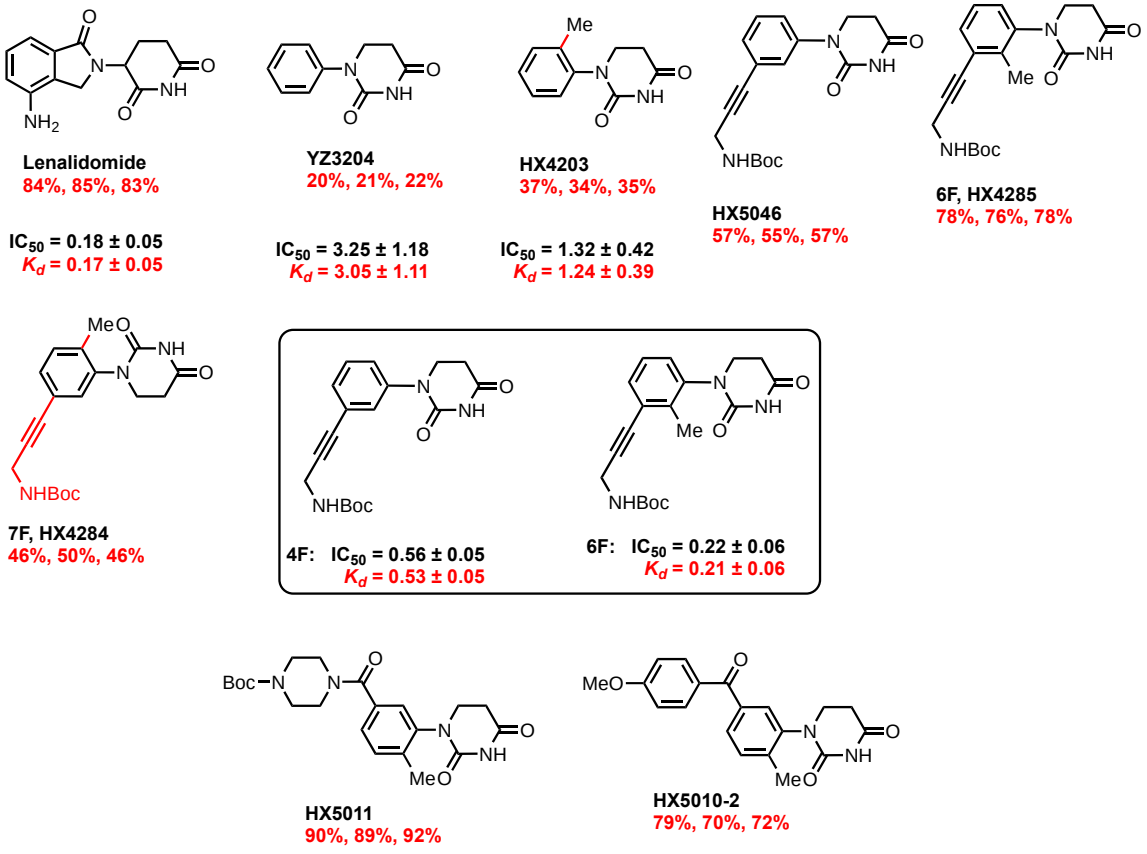

Figure 3. Data previously reported of the relative binding affinities of substituted PDHU ligands using a fluorescence polarization assay.[38]

The Bruton's Tyrosine Kinase (BTK) is a nonreceptor tyrosine kinase part of the Tec family of proteins. BTK plays a key role in the B-cell receptor signaling pathway in the development, activation, differentiation, proliferation, and immune response of B-cells.[59] Apart from B-cells, BTK is also found in other myeloid cells and controls their development through other signaling pathways such as FcγR, CXCR, and TLR.[60] However, aberrant activation of BTK has been shown to drive oncogenic signaling of various B-cell malignancies such as chronic lymphocytic leukemia (CLL), mantle cell lymphoma (MCL), diffuse large B-cell lymphoma (DLBCL), and Waldenström macroglobulinemia (WM). [61,62]

The US Food and Drug administration approved six BTK inhibitors for the treatment of B-cell malignancies (**Figure 4**).[60] Ibrutinib (the first-in class BTK inhibitor), as well as acalabrutinib and zanubrutinib (second-generation BTK inhibitors), target the cysteine residue Cys481 in the noncatalytic site of BTK through an irreversible covalent interaction.[61] Nevertheless, resistance to these inhibitors has been reported in patients with CLL and MCL mainly due to a genetic mutation of the Cys481 residue.[59]

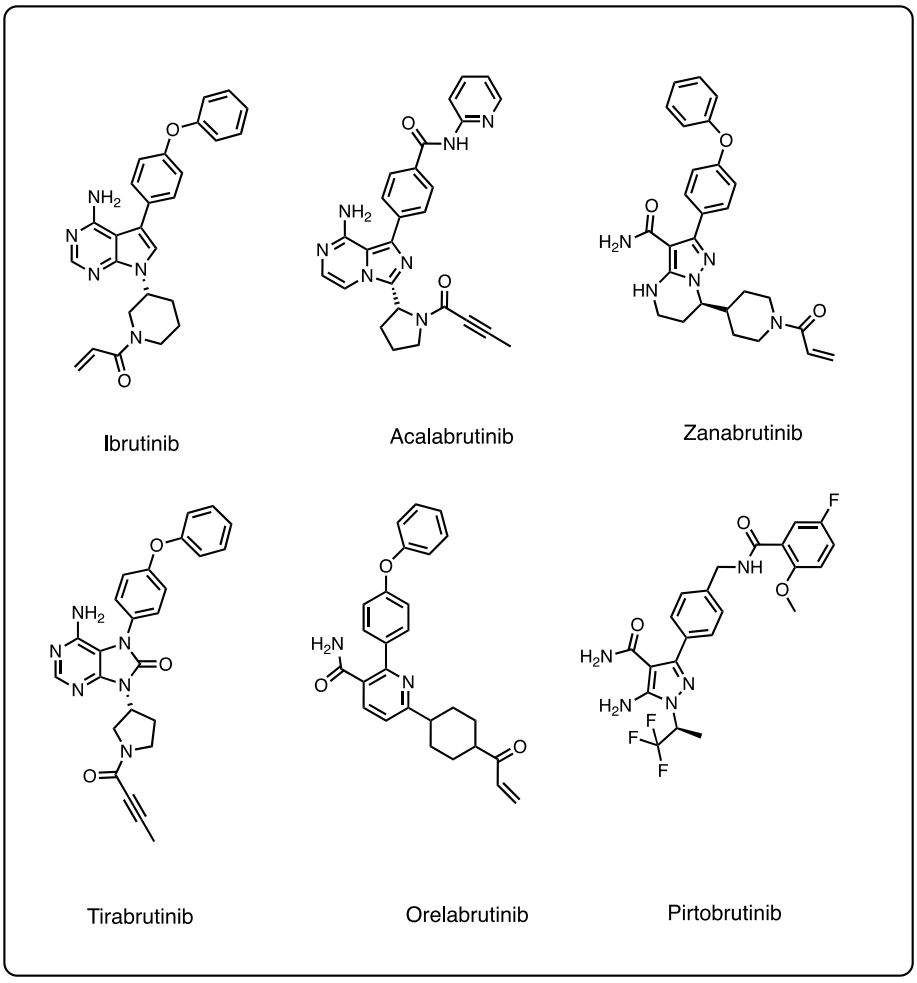

Figure 4. US Food and Drug Administration approved BTK inhibitors for the treatment of B-cell malignancies.

Since drug resistance presents one of the major challenges in treating BTK-related malignancies using irreversible covalent inhibitors, various noncovalent inhibitors have been created.[61] However, many off-target or adverse effects using current BTK inhibitors has been observed in clinical trials, some of them leading to drug discontinuation.[62] Additionally, recent studies reported that deactivation of the kinase activity of BTK still enables the growth, survival, and B-cell receptor signaling of oncogenic cells in CLL and

DLBCL.[63,64] For these reasons, there is an urgent clinical need for alternative therapeutics that can overcome drug resistance, adverse effects, and disrupt the oncogenic signaling related to the nonenzymatic function of BTK in B-cell malignancies.

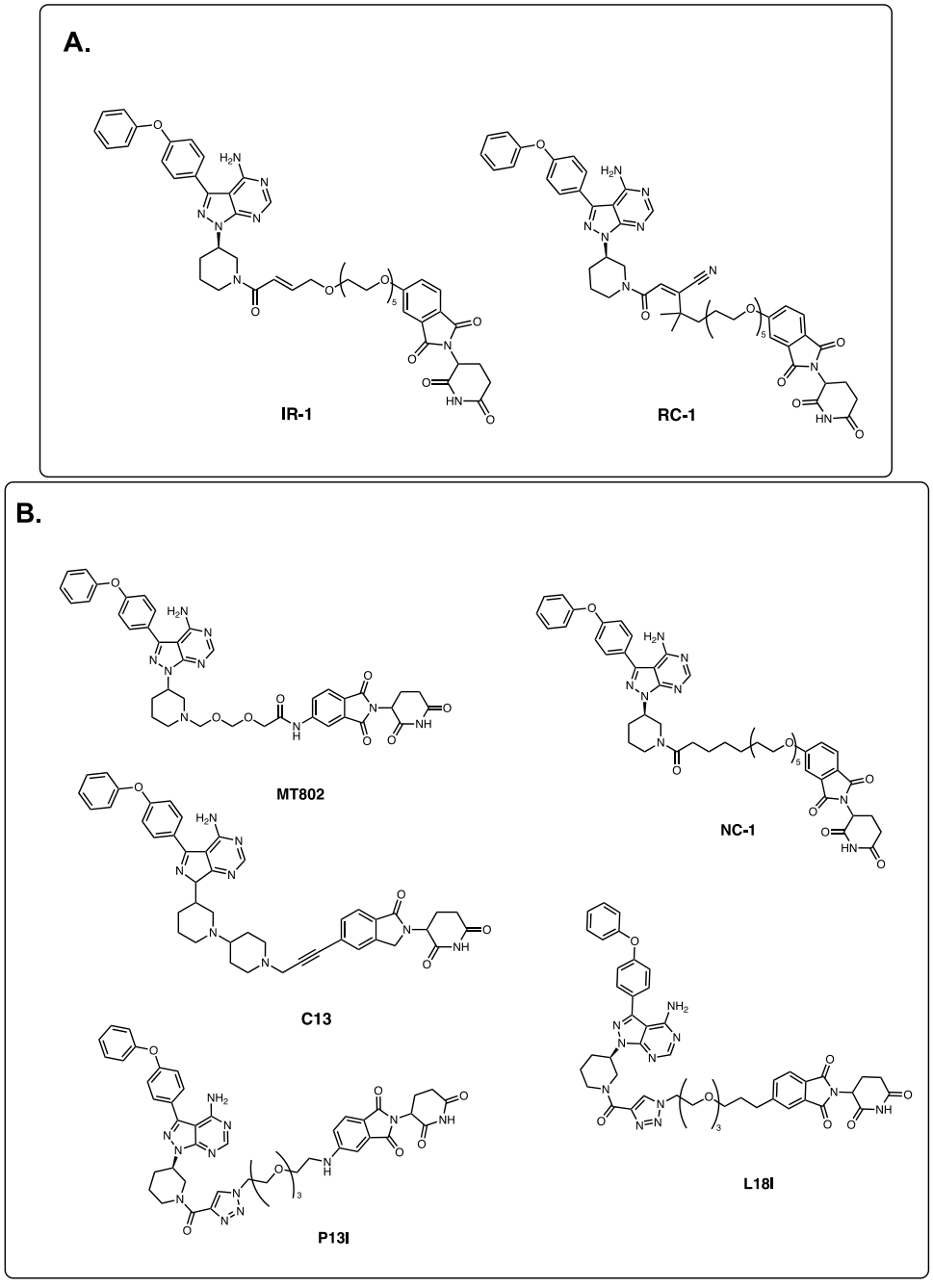

Figure 5. A) BTK PROTACs containing a covalent linker.[60,65] B) BTK PROTACs containing a noncovalent linker.[60,65]

Recently, PROTACs were introduced as a promising strategy for targeting BTK. Most of these PROTACs rely on the ibrutinib inhibitor containing either covalent or noncovalent linkers to interact with the BTK protein and a E3 ligase to promote protein degradation (**Figure 5**).[66,67] Specifically, Nurix Therapeutics and BeiGene developed four CRBN-based BTK-targeting PROTACs currently in clinical trials.[6] However, preclinical data of some these degraders have been only made public by Nurix Therapeutics (**Figure 6**). They showed that NX-2121 induces the degradation of wild-type and ibrutinib-resistant BTK with DC_{50} between 4-6 nM and 13 nM, respectively in DLBCL and MCL.[6,63]

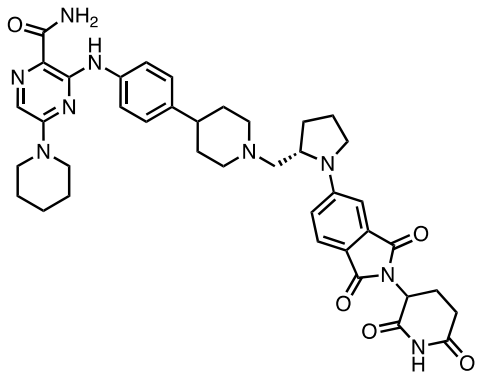

NX-2127

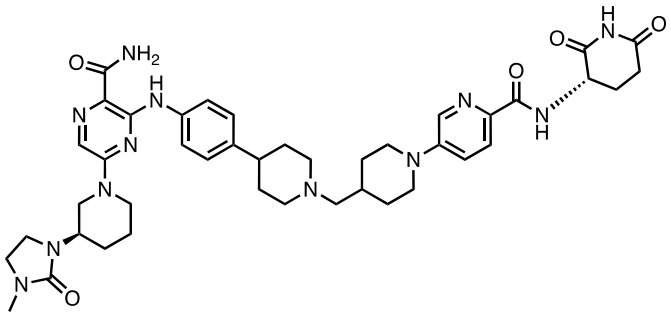

NX-5948

Figure 6. Current BTK PROTACs in Phase I clinical trials developed by Nurix Therapeutics.

Importantly, NX-2121 is also able to disrupt the scaffolding function of BTK-mediated BCR signaling in kinase-impaired BTK mutants.[63] NX-5948 promotes the degradation of wild-type and resistant BTK in DLBCL with DC_{50} of 0.32 nM and 1.0nM, respectively.[6] Although

these results show potential in using the PROTAC technology as a novel way to target BTK, all of these BTK PROTACs still rely on the chiral racemic IMiDs. Due to this, the stability, racemization, and selectivity concerns of exploiting the mixture of stereoisomers should be considered for further development in the clinic. Hence, here we report our efforts in generating BTK-targeting PROTACs based on a partial PROTAC library containing the previously published achiral phenyl dihydrouracil ligands. Comparable to our previous project, our goal here was to identify a potent and selective BTK degrader based on achiral CRBN ligands containing a series of short and restricted linkers to systematically evaluate the effect of small changes in phenyl linker substitutions.

3.2 Results and Discussion

To create the first series of partial PROTAC library based on the achiral phenyl dihydrouracil ligand **6F**, we started with a commercially available 2-methyl iodoaniline. The first step involves a condensation reaction leading to 49% yield. Afterwards, we employed a Sonogashira coupling reaction in 94% yield. Deprotection of the Boc group was accomplished using a mixture of 1:1 TFA/CH_2Cl_2 at room temperature. Finally, an amide coupling reaction was employed leading to a series of six compounds for the achiral partial PROTAC library.

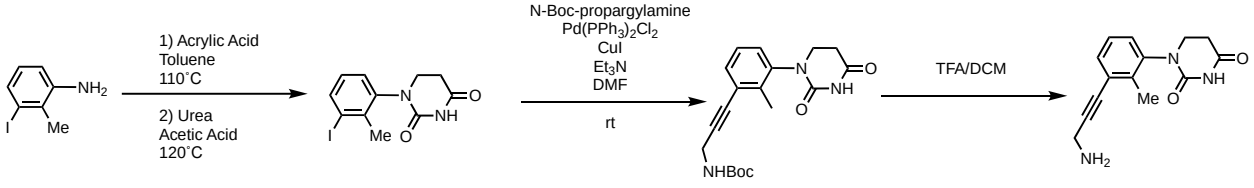

2 g

CMAR299
1.37 g, 49% yield

310 mg

CMAR-2-14

316 mg, 94% yield

CMAR301
quan. yield

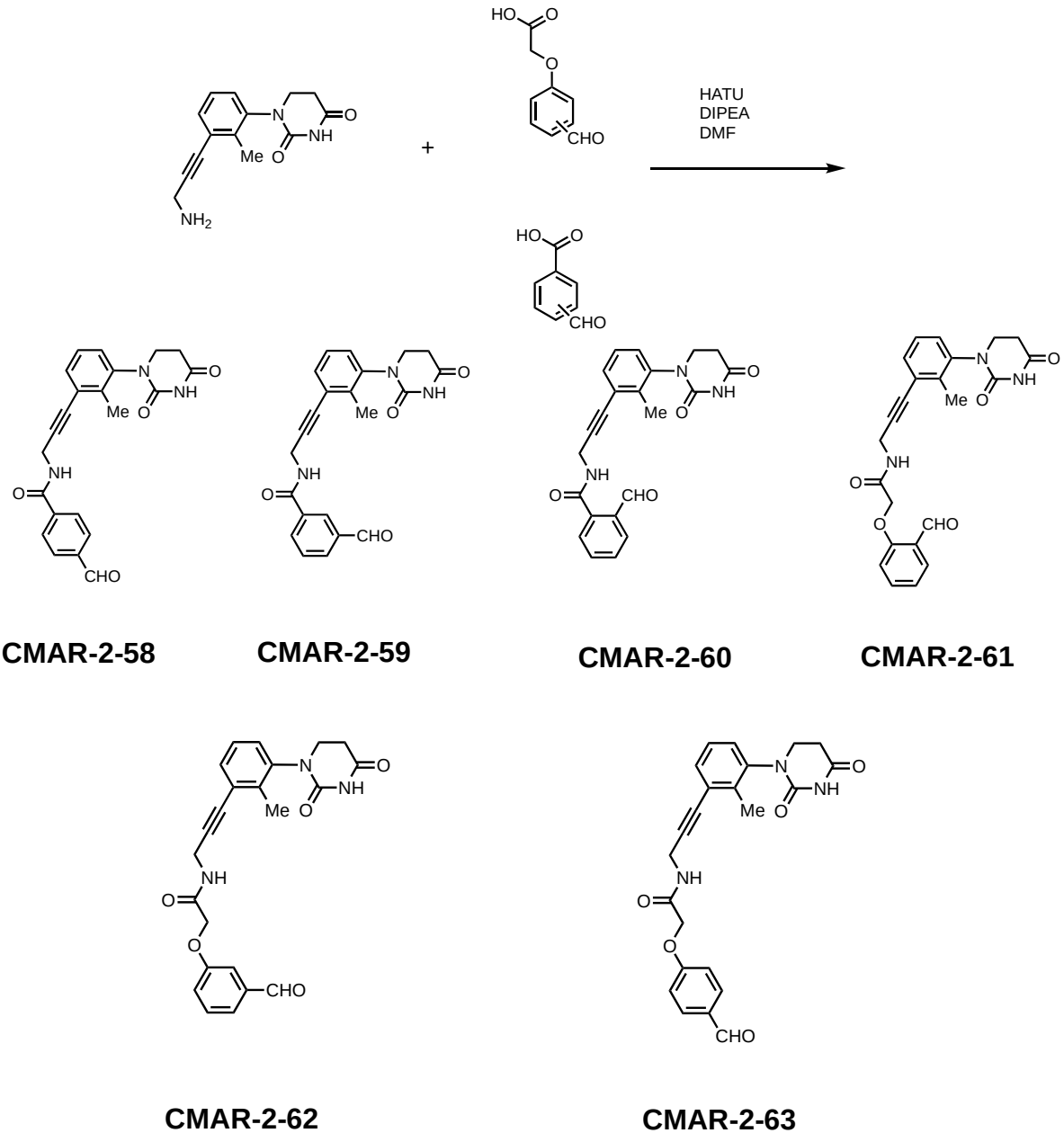

Scheme 1. First set of partial PROTAC Library based on achiral CRBN E3 ligase ligands.

We also developed another series of partial PROTAC library based on the achiral PDHU ligands. We first started with the synthesis of a meta-substituted piperidine moiety directly connected to the achiral CRBN ligand. The first step involves a condensation reaction. Then, we employed a Suzuki coupling reaction under the optimized conditions to obtain our desired compounds in 50% and 37% yield, respectively. Moreover, a hydrogenation reaction was employed followed by deprotection of the Boc group using a mixture of 1:1 TFA/CH_2Cl_2 at room temperature. Finally, an amide coupling reaction was employed leading to another series of six compounds for the achiral partial PROTAC library. The same synthetic route was used for the next set of compounds containing the para-substituted piperidine.

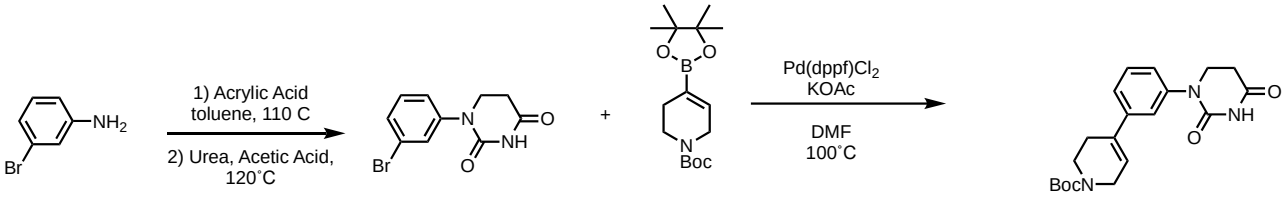

3 g

CMAR-2-28
2.5 g

50 mg
500 mg

CMAR-2-37, 90 mg
CMAR-2-38, 339 mg, 50% yield

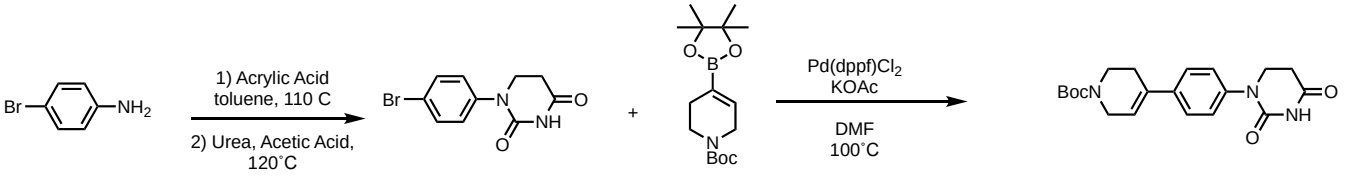

1 g

CMAR-2-30
1.3 g

500 mg

CMAR-2-40, 257 mg, 37% yield

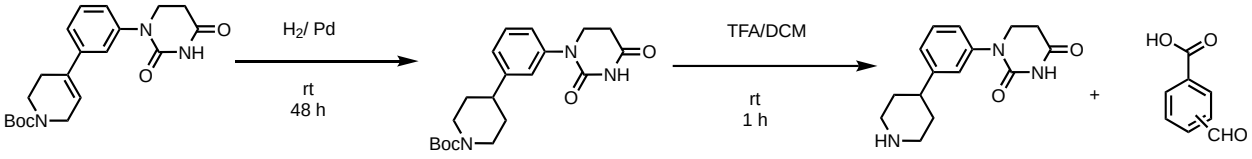

CMAR-2-37, 90 mg
CMAR-2-38, 339 mg, 50% yield

CMAR-2-68
205 mg, 78% yield

CMAR-2-70

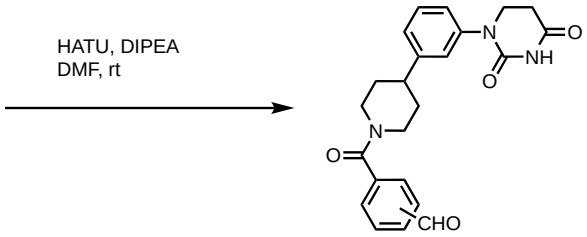

CMAR-2-73,74,75

Scheme 2. Second set of partial PROTAC library synthesis based on achiral ligands.

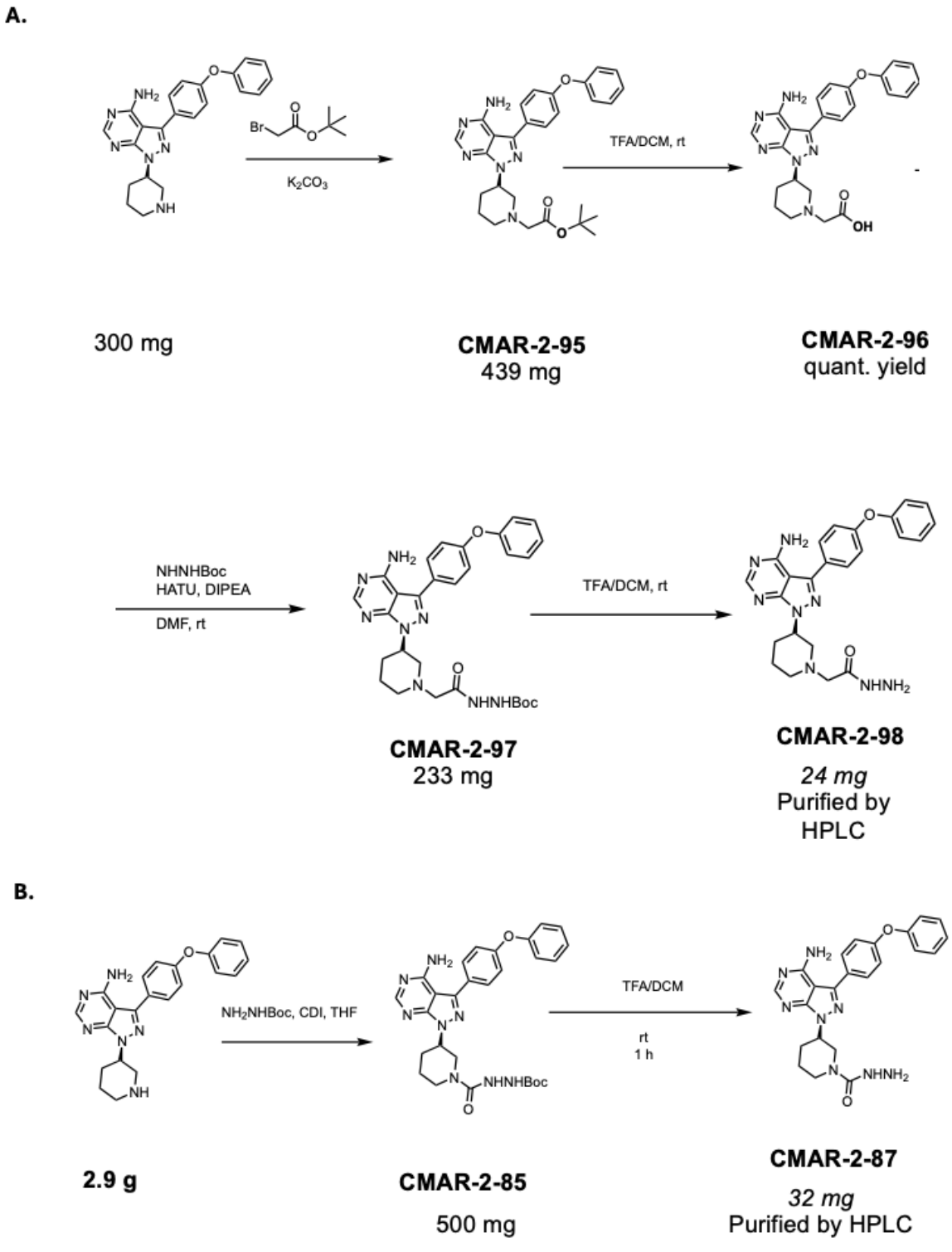

Scheme 3. Synthesis of BTK ligands based on noncovalent linkers.

The original plan for the synthesis of a BTK binder was thought to follow the synthesis route as shown in **Scheme 3**, starting from the commercially available starting material (ibrutinib intermediate) containing a free secondary amine in a piperidine moiety. We selected two functional groups that can readily react with aldehyde – hydrazide and semicarbazide (**Scheme 3**). The synthesis of the first one as shown in **Scheme 3A** involved an alkylation reaction followed by a TFA/DCM Boc deprotection, amide formation, and another Boc deprotection that lead to the formation of desired acylhydrazone or semicarbazone. Analysis of the reaction by TLC and LCMS suggested the formation of product (CMAR-2-98). Similarly, the second BTK ligand involved a one-pot reaction utilizing a primary protected Boc-diamine and CDI at room temperature. Later, the Boc-protected semicarbazide that led to the desired product (CMAR-2-87) as shown in **Scheme 3B**.

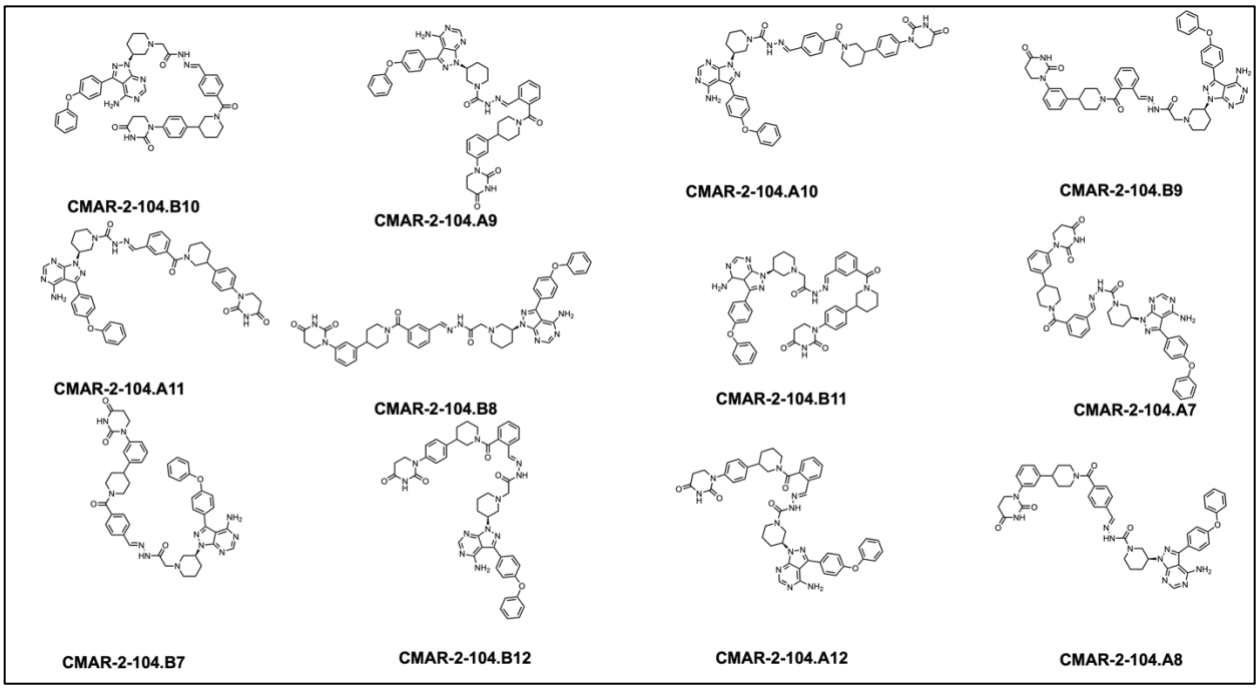

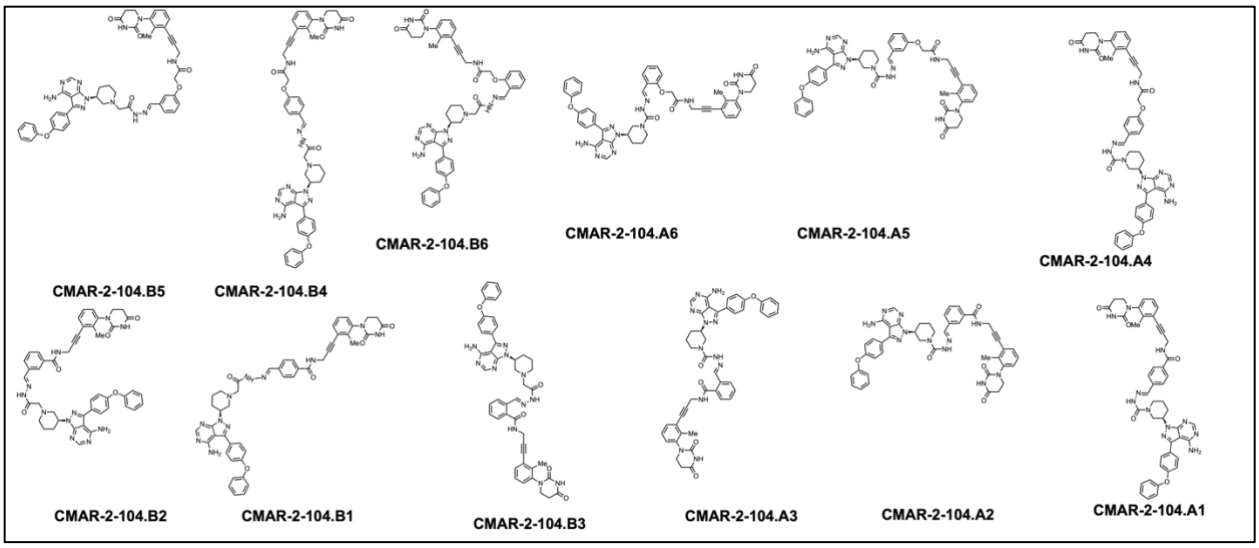

Figure 7. Structures of BTK degraders employing the partial PROTAC library based on the achiral CRBN E3 ligase ligands.

We synthesized of a small library of BTK degraders using the Rapid-TAC strategy (**Figure 7**). We analyzed the reaction progression by LC-MS and the formation of product was observed by the changes of retention time and mass. Specifically, we created CRBN-based BTK degraders composed of two building blocks that contain a BTK binding ligand and a hydrazide or semicarbazide, which differ from each other by a methylene moiety. The HiBiT degradation assay was completed by Ira Tandon.

A.

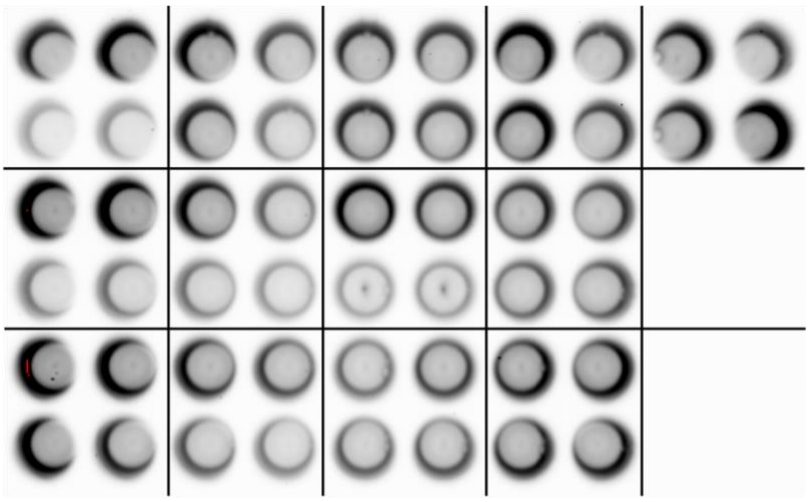

	A1	A1	A4	A4	A7	A7	A9	A9	A12	A12
10 µM	85.96954	109.183663	102.623806	75.3802197	92.1162439	84.8269179	113.946957	82.0637117	93.1605317	74.6675765
1 µM	34.3029045	48.2126588	88.7236482	55.0152985	95.6581481	81.8337664	104.958155	79.7424489	93.3272887	110.414898
	A2	A2	A5	A5	Controls	Controls	A10	A10		
10 µM	117.142385	115.163236	99.2477862	66.6641117	109.597814	90.402186	87.8990858	81.4148798		DMSO
1 µM	53.3777645	57.93741	56.1721286	45.2241187	44.5093567	50.3222972	74.3073913	73.6099531		10 µM JP
	A3	A3	A6	A6	A8	A8	A11	A11		
10 µM	114.180392	103.279866	101.721972	79.5404211	60.2171705	80.9989843	101.991425	101.210235		
1 µM	101.273921	85.5265995	65.9477295	56.0481202	67.5451322	69.679323	93.6786251	89.3881837		

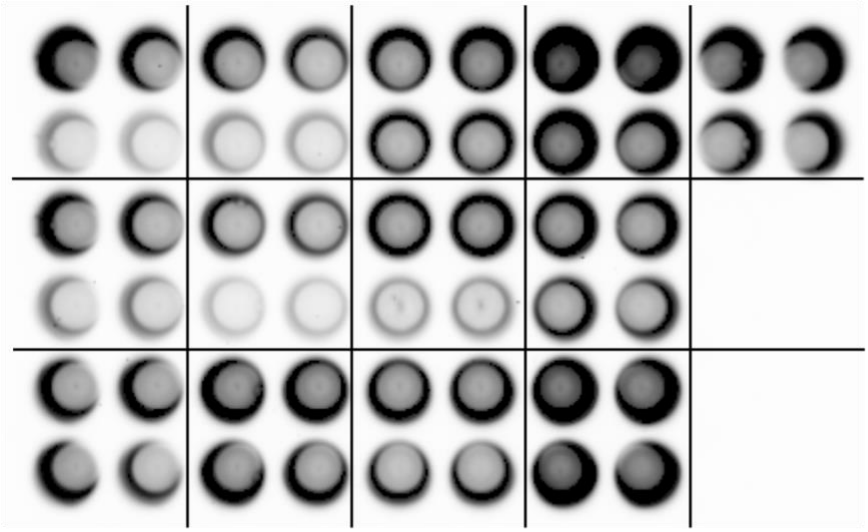

	B1	B1	B4	B4	B7	B7	B9	B9	B12	B12
10 µM	93.87203	77.72283	81.15219	62.12034	92.2145	110.9846	159.3097	159.6599	118.621	102.7863
1 µM	31.75796	23.7952	34.94988	30.84091	80.43501	86.40746	134.3856	108.6476	77.29805	71.80743
	B2	B2	B5	B5	Controls	Controls	B10	B10		
10 µM	82.78294	69.65327	67.92755	65.48395	97.04065	102.9594	96.57743	85.67236		DMSO
1 µM	39.21105	39.43544	23.06776	23.60056	31.11644	35.78778	72.90955	70.12449		10 µM JP
	B3	B3	B6	B6	B8	B8	B11	B11		
10 µM	76.30795	78.73763	103.2349	99.81562	87.67432	92.85775	129.3091	112.9865		
1 µM	77.46348	62.46441	95.76283	84.58624	68.78528	69.53377	129.47	113.7703		

B.

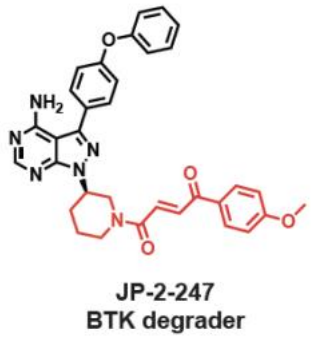

Figure 8. A) Degradation assay completed by Ira Tandon for BTK degraders based on achiral CRBN E3 ligase ligands using a BTK-HiBiT assay. B) BTK degrader JP-2-247 recently developed by the Nomura group used as the positive control.[68]

The degraders were evaluated at two different concentrations (10μM, 1 μM). The HiBiT assay was developed by Promega. Degradation results suggested significant degradation of BTK after 1 μM treatment of nine potential hits A1, A2, A4, A5, A6, B1, B2, B4, and B5 when compared to the positive control JP-2-247 (**Figure 8**).

Interestingly, our preliminary screening suggests that significant degradation was achieved by employing our previously reported **6F**[38] achiral CRBN E3 ligase ligand with meta or para linker on the phenyl group in the linker region. Moreover, although these results showed significant BTK degradation with the degraders containing both hydrazide and semicarbazide, compounds that possess an additional methylene group in the hydrazide achieved slightly better degradation (**Figure 8**). We hypothesized that it may be due to an increase in linker flexibility, allowing the formation of a more stable ternary

complex. Similar to our previous AR degraders, these results support the hypothesis that small differences in length and orientation affect the degradation efficiency.

3.3 Conclusions

In summary, here we described the synthesis of a partial PROTAC library based on achiral phenyl dihydrouracil (PDHU) ligand. The library was composed of twelve PDHU ligands with relatively short and rigid linkers with small differences in the ortho, meta, or para phenyl substitution. The resulting partial PROTAC library can be applied to the rapid synthesis of a full PROTAC library for any protein target. The small diversifications in phenyl substitutions also allows us to systematically examine the effect of length and linker orientation with a relatively short distance. Moreover, we demonstrated the utility of the partial PROTAC library by the development of a full PROTAC library for the BTK protein using the Rapid-TAC strategy. Our results showed significant degradation of BTK with A1, A2, A4, A5, A6, B1, B2, B4, and B5 at 1μM using a BTK-HiBiT assay. Particularly, it was observed that the linkers containing a para and meta substitutions to the phenyl attached to an alkyne-based linker had the highest BTK degradation. In comparison, no significant degradation of BTK was shown using a piperidine-based linker or a linker with ortho-substituted phenyl group. Consequently, these results indicate that the orientation of the PROTAC linker significantly affect the degradation efficiency and it can be examined with relatively short linkers.

3.4 Future Directions

Further testing will be done using the BTK-HiBiT assay to confirm the degradation of BTK using these A1, A2, A4, A5, A6, B1, B2, B4, and B5 at lower concentrations. After

identifying the most potent compounds, stable analogues will be synthesized by changing the acylhydrazone or semicarbazone linkage to a more stable isostere such as an amide bond. Finally, mechanistic studies will be performed to assess the degradation pathway.

3.5 Experimental Procedures

3.5.1 Chemical Synthesis

All solvents and reagents were purchased from commercially available sources. Thin-layer chromatography (TLC) was used with precoated silica gel plates. Flash column chromatography was performed using silica gel. The ^{1}H and ^{13}C nuclear magnetic resonance (NMR) spectra were recorded using a Bruker AV-400 MHz in parts per million (ppm) (δ) downfield of TMS (δ = 0). Signal splitting patterns were described as singlet (s), doublet (d), triplet (t) or multiplet (m), with coupling constants (*J*) in hertz. The liquid chromatography–mass spectrometry (LC–MS) analysis of final products was processed on an Agilent 1290 Infinity II LC system using a Poroshell 120 EC-C18 column (5 cm × 2.1 mm, 1.9 μm) for chromatographic separation. Agilent 6120 Quadrupole LC/MS with multimode electrospray ionization plus atmospheric pressure chemical ionization was used for detection. The mobile phases were 5.0% methanol and 0.1% formic acid in purified water (A) and 0.1% formic acid in methanol (B). The gradient was held at 5% (0–0.2 min), increased to 100% at 2.5 min, then held at isocratic 100% B for 0.4 min, and then immediately stepped back down to 5% for 0.1 min re-equilibration. The flow rate was set at 0.8 mL/min. The column temperature was set at 40 °C. High resolution mass spectra (HRMS) were performed by Analytical Instrument Center at the School of Pharmacy or Department of Chemistry on an Electron Spray Injection (ESI) mass spectrometer.

3.5.2 Synthesis of 1-(3-bromophenyl) dihydropyrimidine-2,4(1H,3H)-dione

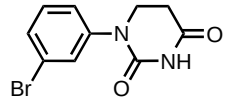

To a solution of 3-bromoaniline (3g, 10.23 mmol) and toluene (22 mL), acrylic acid (1.6g, 22.7 mmol) was added. The solution was stirred at 110 °C for 5 h. Then, the toluene was concentrated in vacuo. Afterwards, acetic acid (26 mL) and urea (3.1 g, 52.2 mmol) were added. The reaction was stirred at 120 °C for 16 h. The acetic acid was later evaporated using the rotovap. The obtained product was then directly used for the next step.

3.5.3 Synthesis of tert-butyl 4-(3-(2,4-dioxotetrahydropyrimidin-1(2H)-yl)phenyl)-3,6-dihydropyridine-1(2H)-carboxylate

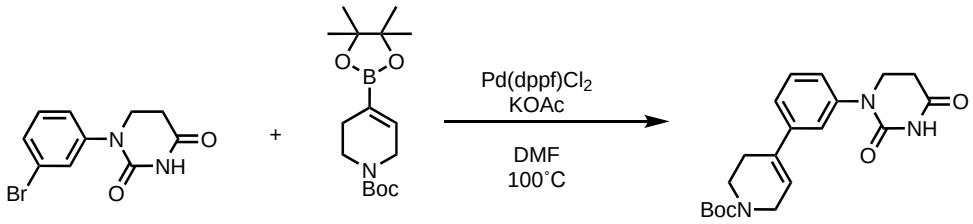

The same method for Suzuki cross-coupling was followed as previously described.[69]

3.5.4 Synthesis of tert-butyl 4-(3-(2,4-dioxotetrahydropyrimidin-1(2H)-yl)phenyl)piperidine-1-carboxylate

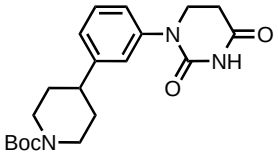

To a solution of in (262 mg, 0.705 mmol) and methanol (40 mL), Pd/c (89 mg) was added. The reaction was purged with Argon and H_2. The solution was stirred at rt for 48 h. Then, the Pd was discarded in an aqueous solution and the reaction was concentrated in vacuo.

3.5.5 General Procedure of Partial PROTAC Library Aldehydes: Example of synthesis of 2,3,4-(4-(3-(2,4-dioxotetrahydropyrimidin-1(2H)-yl)phenyl)piperidine-1-carbonyl)benzaldehyde

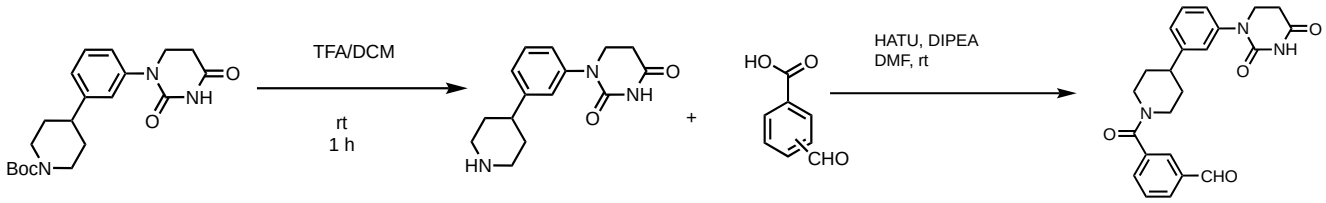

To a solution of 4-(3-(2,4-dioxotetrahydropyrimidin-1(2*H*)-yl)phenyl)piperidine-1-carboxylate (1.0 eq) in DCM was added TFA (1.5 mL) at 0 ^{o}C. The reaction mixture was stirred at room temperature for 1 h. Finally, the solvent and TFA were evaporated in vacuo to give the crude product which was directly used in the next step.

To a solution of the benzaldehyde-COOH (1.0 eq) in DMF was added HATU (1.0 eq), DIPEA (2.0 eq) and the deprotected crude of the amine. The reaction mixture was stirred at rt for 4 h. The mixture was then extracted with ethyl acetate (3 x 10 mL). The combined organic fractions were dried over Na_2SO_4 and concentrated. The crude was later purified by flash column chromatography (elution gradient of 0-10% MeOH in DCM). The desired fractions were combined and concentrated to yield our desired compounds.

3.1.1 Synthesis of tert-butyl (3-(3-(2,4-dioxotetrahydropyrimidin-1(2H)-yl)-2-methylphenyl)prop-2-yn-1-yl)carbamate

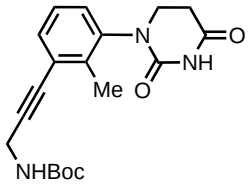

The compound was synthesized as previously described.[38]

3.5.6 Synthesis of N-(3-(3-(2,4-dioxotetrahydropyrimidin-1(2H)-yl)-2-methylphenyl)prop-2-yn-1-yl)-2-(3-formylphenoxy)acetamide

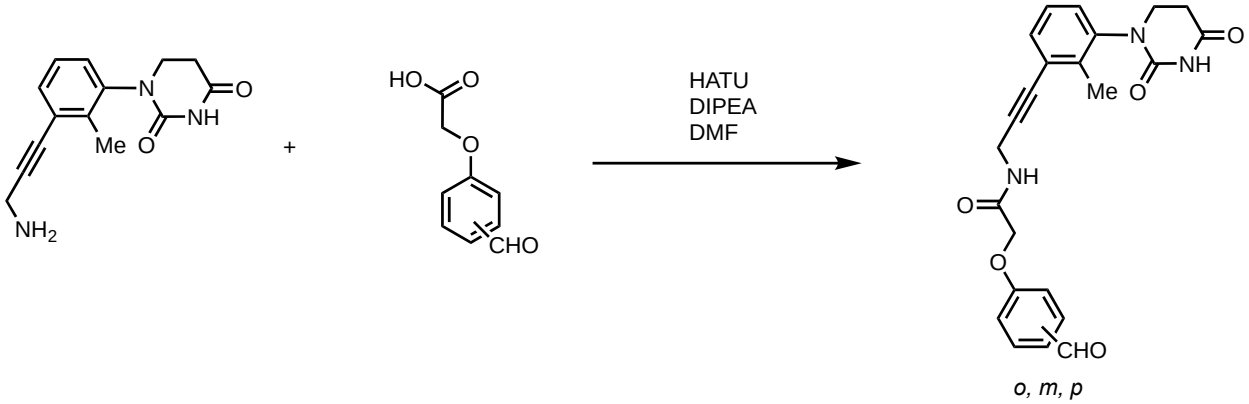

To a solution of 1-(3-(3-aminoprop-1-yn-1-yl)-2-methylphenyl)dihydropyrimidine-2,4(1*H*,3*H*)-dione (1.0 eq) in DCM was added TFA (1.5 mL) at 0 ^{o}C. The reaction mixture was stirred at room temperature for 1 h. Finally, the solvent and TFA were evaporated in vacuo to give the crude product which was directly used in the next step.

To a solution of the benzaldehyde-COOH (1.0 eq) in DMF was added HATU (1.0 eq), DIPEA (2.0 eq) and the deprotected crude of the amine. The reaction mixture was stirred at rt for 4 h. The mixture was then extracted with ethyl acetate (3 x 10 mL). The combined organic fractions were dried over Na_2SO_4 and concentrated. The crude was later purified by flash column chromatography (elution gradient of 0-10% MeOH in DCM). The desired fractions were combined and concentrated to yield our desired compounds.

3.5.7 *Synthesis of* (*S*)-2-(3-(4-amino-3-(4-phenoxyphenyl)-1*H*-pyrazolo[3,4-*d*] pyrimidin-1-yl) piperidin-1-yl)acetic acid

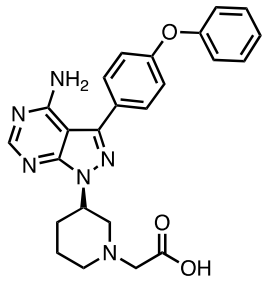

To a solution of *S*)-3-(4-phenoxyphenyl)-1-(piperidin-3-yl)-1*H*-pyrazolo[3,4-*d*]pyrimidin-4-amine (300 mg, 0.776 mmol) in DMF (3.5 mL), 2-(*tert*-butoxy)acetyl bromide (226 mg, 1.16 mmol) and Cs_2CO_3 (214 g, 1.55 mmol) were added. The solution was stirred at 60°C overnight. The reaction mixture was then cooled at room temperature and an extraction was done using H_2O and ethyl acetate (3 x 50 mL). The organic layer was separated, dried with Na_2SO_4 and concentrated. The crudes were later purified using flash column chromatography DCM/MeOH 0-10% to achieve the desired product. After the compound was purified, 1.0 eq was dissolved in DCM and TFA (1:1 mixture, 4 mL) at 0 ^oC. The reaction mixture was stirred at room temperature for 1 h. Finally, the solvent and TFA were evaporated in vacuo to give the crude product which was directly used in the next step.

3.5.8 Synthesis of (S)-2-(3-(4-amino-3-(4-phenoxyphenyl)-1H-pyrazolo[3,4-d] pyrimidin-1-yl)piperidin-1-yl)acetohydrazide

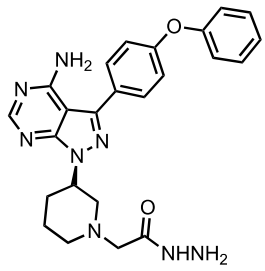

To a solution of the (*S*)-2-(3-(4-amino-3-(4-phenoxyphenyl)-1*H*-pyrazolo[3,4-*d*] pyrimidin-1-yl) piperidin-1-yl)acetic acid (1.0 eq) in DMF was added HATU (1.0 eq), DIPEA (2.0 eq) and 2.0 eq of tert-butyl carbamate. The reaction mixture was stirred at rt for 4 h. The mixture was then extracted with ethyl acetate (3 x 10 mL). The combined organic fractions were dried over Na_2SO_4 and concentrated. The crude was later purified by flash column chromatography (elution gradient of 0-10% MeOH in DCM). The desired fractions were combined and concentrated to yield our desired compounds. After the compound was purified, 1.0 eq was dissolved in DCM and TFA (1:1 mixture, 4 mL) at 0 ^{o}C. The reaction mixture was stirred at room temperature for 1 h. The DCM and TFA were evaporated in vacuo to give the crude product which was directly used in the next step.

3.5.9 Synthesis of (*S*)-3-(4-amino-3-(4-phenoxyphenyl)-1*H*-pyrazolo[3,4-*d*] pyrimidin-1-yl) piperidine-1-carbohydrazide

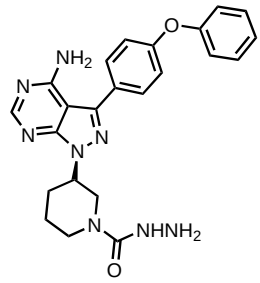

To a round bottom flask, NH_2NHBoc (2 g, 15.13 mmol) and CDI (2.5 g, 15.13 mmol) were dissolved in THF (65 mL). The solution was stirred at room temperature for 2 h. Afterwards, (*S*)-3-(4-phenoxyphenyl)-1-(piperidin-3-yl)-1*H*-pyrazolo[3,4-*d*] pyrimidin-4-amine (2.9 g, 7.55 mmol) was directly added to the reaction mixture. The reaction was stirred at room temperature for 24 h. Finally, the THF was concentrated in vacuo and the crude was later purified by flash column chromatography (elution gradient of 0-10% MeOH in DCM). Then, 1.0 eq was dissolved in DCM and TFA (1:1 mixture, 4 mL) at 0 ^oC. The reaction mixture was stirred at room temperature for 1 h. The DCM and TFA were evaporated in vacuo to give the crude product which was directly used in the next step.

3.5.10 General procedure for the preparation of BTK PROTACs under miniaturized conditions

Solution **A**: A 50 mM DMSO stock solution of the BTK building blocks was prepared by dissolving appropriate amounts in DMSO.

Solution **B**: A 50 mM DMSO stock solution of each member of the aldehyde achiral partial PROTAC library was also prepared similarly to Solution **A**.

We next mixed 20 µL of DMSO solution **A** with 20 µL of DMSO solution **B** in a 96-well plate. The resulting mixture was then heated at 80 °C for 3-4 h on the reaction block. After cooling it to room temperature, another 60 µL of DMSO was added to the solution. The solution was then cooled down to room temperature and the purity of the product was analyzed by LC-MS. All products were directly used for cell-based screening without any further manipulations.

3.6 Characterization

3.6.1 Partial PROTAC Library based on Achiral Ligands

1-(3-bromophenyl) dihydropyrimidine-2,4(1H,3H)-dione

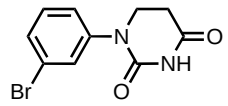

^{1}H NMR (400 MHz, DMSO) δ 10.41 (s, 1H), 7.56 (t, *J* = 1.9 Hz, 1H), 7.43 (dt, *J* = 7.2, 1.9 Hz, 1H), 7.42 – 7.29 (m, 2H), 3.81 – 3.74 (m, 2H), 2.70 (t, *J* = 6.7 Hz, 2H).

^{13}C NMR (101 MHz, DMSO) δ 171.32, 152.58, 143.80, 131.06, 129.14, 128.63, 124.62, 121.47, 44.87, 40.20, 40.04, 39.99, 39.79, 39.58, 39.37, 39.16, 38.95, 31.31.

LC-MS (ESI) Calculated for $C_{10}H_{10}BrN_2O_2$ $[M + H]^+$= 270.1. Found: 270.1

1-(4-bromophenyl) dihydropyrimidine-2,4(1H,3H)-dione

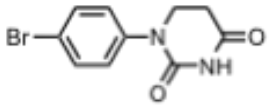

^{1}H NMR (400 MHz, DMSO) δ 10.43 (s, 1H), 7.62 – 7.54 (m, 2H), 7.35 – 7.27 (m, 2H), 3.79 (t, *J* = 6.7 Hz, 2H), 2.71 (t, *J* = 6.7 Hz, 2H).

^{13}C NMR (101 MHz, DMSO) δ 171.01, 152.51, 141.79, 131.91, 127.75, 118.56, 44.75, 40.59, 40.38, 40.17, 39.96, 39.76, 39.55, 39.34, 31.44.

LC-MS (ESI) Calculated for $C_{10}H_{10}BrN_2O_2$ $[M + H]^+$= 270.1. Found: 270.1

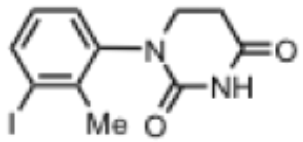

^{1}H NMR (400 MHz, $CDCl_3$) δ 7.78 (dd, *J* = 8.0, 1.1 Hz, 1H), 7.63 (s, 1H), 7.12 (d, *J* = 7.8 Hz, 1H), 6.90 (t, *J* = 7.9 Hz, 1H), 3.73 (ddd, *J* = 12.7, 8.6, 6.0 Hz, 1H), 3.56 (dt, *J* = 12.5, 6.1 Hz, 1H), 2.87 – 2.70 (m, 2H), 2.32 (s, 3H).

^{13}C NMR (101 MHz, $CDCl_3$) δ 169.25, 151.32, 139.54, 139.50, 139.23, 128.58, 127.28, 102.63, 77.35, 77.04, 76.72, 45.33, 31.38, 23.89.

LC-MS (ESI) Calculated for $C_{11}H_{12}IN_2O_2$ $[M + H]^+$= 331.1. Found: 331.1

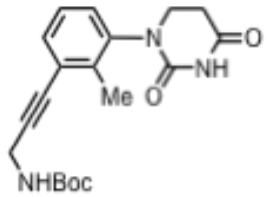

^{1}H NMR (400 MHz, DMSO) δ 10.38 (s, 1H), 7.68 – 7.51 (m, 1H), 7.42 – 7.20 (m, 4H), 4.02 (dd, *J* = 13.5, 6.4 Hz, 2H), 3.78 (ddd, *J* = 12.2, 9.7, 5.2 Hz, 1H), 3.52 (dt, *J* = 12.1, 5.9 Hz, 1H), 3.30 (s, 1H), 2.80 (ddd, *J* = 16.1, 9.8, 6.1 Hz, 1H), 2.68 (dt, *J* = 16.7, 5.5 Hz, 1H), 2.25 (s, 3H), 1.41 (s, 9H).

LC-MS (ESI) Calculated for $C_{19}H_{24}N_3O_4$ $[M + H]^+$= 357.2. Found: 357.2

***N*-(3-(3-(2,4-dioxotetrahydropyrimidin-1(2*H*)-yl)-2-methylphenyl)prop-2-yn-1-yl)-4-formylbenzamide**

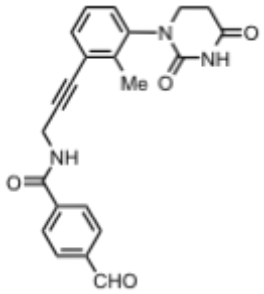

^{1}H NMR (400 MHz, DMSO) δ 10.38 (s, 1H), 10.10 (s, 1H), 9.33 (t, *J* = 5.3 Hz, 1H), 8.11 – 7.99 (m, 4H), 7.35 (ddd, *J* = 29.5, 7.8, 1.5 Hz, 2H), 7.28 – 7.18 (m, 1H), 4.43 – 4.37 (m, 2H), 3.77 (ddd, *J* = 12.1, 9.8, 5.3 Hz, 1H), 3.51 (dt, *J* = 12.0, 5.9 Hz, 1H), 2.79 (ddd, *J* = 18.8, 9.7, 6.1 Hz, 1H), 2.73 – 2.62 (m, 1H), 2.26 (d, *J* = 7.9 Hz, 3H).

^{13}C NMR (101 MHz, DMSO) δ 193.38, 171.17, 165.76, 152.23, 141.77, 139.33, 138.43, 130.40, 130.02, 129.97, 128.54, 127.20, 123.91, 91.62, 80.70, 65.08, 52.42, 47.81, 44.37, 37.47, 34.02, 29.41.

LC-MS (ESI) Calculated for $C_{22}H_{20}N_3O_4[M + H]^+$= 390.1. Found: 390.1

***N*-(3-(3-(2,4-dioxotetrahydropyrimidin-1(2*H*)-yl)-2-methylphenyl)prop-2-yn-1-yl)-3-formylbenzamide**

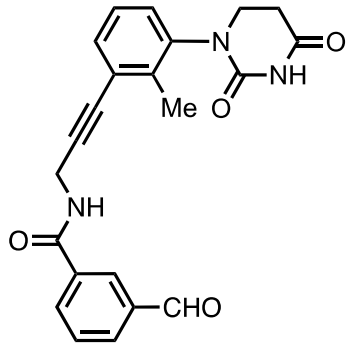

^{1}H NMR (400 MHz, DMSO) δ 10.38 (s, 1H), 9.88 (s, 1H), 7.88 (d, *J* = 8.7 Hz, 2H), 7.40 – 7.20 (m, 5H), 7.16 (d, *J* = 8.7 Hz, 2H), 4.24 (d, *J* = 5.4 Hz, 2H), 3.80 (d, *J* = 13.9 Hz, 1H), 3.52 – 3.47 (m, 1H), 2.82 – 2.73 (m, 1H), 2.72 – 2.65 (m, 2H), 2.27 (s, 1H).

^{13}C NMR (101 MHz, DMSO) δ 193.32, 171.17, 165.58, 152.23, 141.78, 136.74, 135.29, 133.51, 130.81, 129.93, 128.70, 127.21, 123.93, 91.69, 80.66, 65.08, 52.42, 47.82, 44.37, 37.47, 34.02, 29.42.

LC-MS (ESI) Calculated for $C_{22}H_{20}N_3O_4[M + H]^+$= 390.1. Found: 390.1

_N_-(3-(3-(2,4-dioxotetrahydropyrimidin-1(2_H_)-yl)-2-methylphenyl)prop-2-yn-1-yl)-2-formylbenzamide

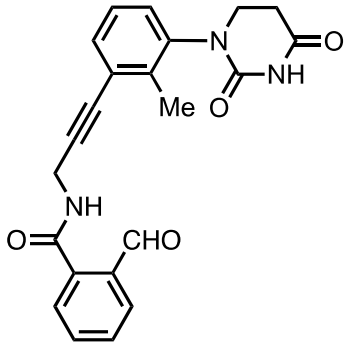

^{1}H NMR (400 MHz, DMSO) δ 10.29 (s, 1H), 9.99 (d, *J* = 2.1 Hz, 1H), 8.17 (s, 1H), 7.84 (ddt, *J* = 32.3, 25.4, 12.8 Hz, 4H), 7.70 – 7.63 (m, 1H), 7.64 – 7.46 (m, 4H), 7.27 – 7.03 (m, 3H), 3.72 (t, *J* = 6.7 Hz, 1H), 2.81 (s, 1H), 2.64 (dd, *J* = 12.4, 5.8 Hz, 1H), 2.28 – 1.98 (m, 1H).

^{13}C NMR (101 MHz, DMSO) δ 194.87, 185.13, 162.53, 153.04, 148.97, 136.81, 124.63, 114.33, 111.64, 108.24, 103.00, 98.02, 90.50, 86.65, 81.25, 76.58, 66.37, 59.13, 45.94, 40.56, 40.35, 40.14, 39.94, 39.73, 39.60, 39.52, 39.31, 37.24, 29.08, 16.99.

LC-MS (ESI) Calculated for $C_{22}H_{20}N_3O_4[M + H]^+$= 390.1. Found: 390.1

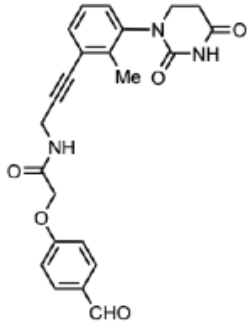

^{1}H NMR (400 MHz, DMSO) δ 10.38 (s, 1H), 9.88 (s, 1H), 8.82 (t, *J* = 5.6 Hz, 1H), 7.91 – 7.84 (m, 2H), 7.33 (ddd, *J* = 15.5, 7.8, 1.6 Hz, 2H), 7.24 (t, *J* = 7.7 Hz, 1H), 7.16 (d, *J* = 8.6 Hz, 2H), 4.71 (s, 2H), 4.24 (d, *J* = 5.6 Hz, 2H), 3.83 – 3.69 (m, 1H), 3.51 (dt, *J* = 12.0, 5.9 Hz, 1H), 2.87 – 2.75 (m, 1H), 2.70 (d, *J* = 5.8 Hz, 1H), 2.24 (s, 3H).

^{13}C NMR (101 MHz, DMSO) δ 191.86, 171.20, 167.54, 163.02, 152.24, 141.75, 138.25, 132.19, 130.61, 128.25, 127.20, 123.87, 115.70, 91.51, 80.54, 67.35, 52.39, 47.78, 44.94, 37.43, 33.99, 31.54, 29.13.

LC-MS (ESI) Calculated for $C_{23}H_{22}N_3O_5$ $[M + H]^+$= 420.2. Found: 420.2

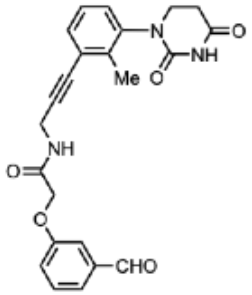

^{1}H NMR (400 MHz, DMSO) δ 10.37 (s, 1H), 9.97 (s, 1H), 8.77 (t, *J* = 5.7 Hz, 1H), 7.56 (d, *J* = 4.8 Hz, 2H), 7.47 (d, *J* = 2.6 Hz, 1H), 7.33 (dd, *J* = 15.2, 7.5 Hz, 3H), 7.24 (t, *J* =

7.7 Hz, 1H), 4.66 (s, 2H), 4.24 (d, *J* = 5.6 Hz, 2H), 3.83 – 3.69 (m, 1H), 3.51 (dt, *J* = 12.0, 5.9 Hz, 1H), 2.84 – 2.77 (m, 2H), 2.23 (s, 3H).

^{13}C NMR (101 MHz, DMSO) δ 193.31, 171.19, 167.82, 158.67, 152.23, 141.75, 138.05, 130.90, 128.25, 127.18, 123.75, 121.91, 114.44, 91.56, 80.50, 67.38, 52.40, 47.79, 44.94, 37.45, 34.00, 31.55, 29.39.

LC-MS (ESI) Calculated for $C_{23}H_{22}N_3O_5$ $[M + H]^+$= 420.2. Found: 420.2

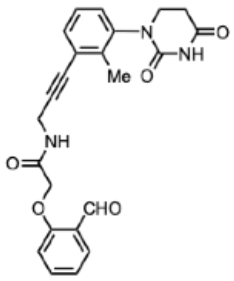

^{1}H NMR (400 MHz, DMSO) δ 10.51 (s, 1H), 10.38 (s, 1H), 8.76 (t, *J* = 5.7 Hz, 1H), 7.75 (dd, *J* = 7.6, 1.8 Hz, 1H), 7.68 – 7.59 (m, 1H), 7.33 (ddd, *J* = 16.1, 7.7, 1.6 Hz, 2H), 7.25 (t, *J* = 7.7 Hz, 1H), 7.19 – 7.09 (m, 2H), 4.76 (s, 2H), 4.26 (d, *J* = 5.6 Hz, 2H), 3.83 – 3.70 (m, 1H), 3.51 (dt, *J* = 12.0, 5.9 Hz, 1H), 2.81 (dd, *J* = 16.6, 6.2 Hz, 1H), 2.79 – 2.68 (m, 1H), 2.24 (s, 3H).

^{13}C NMR (101 MHz, DMSO) δ 190.45, 171.20, 167.66, 160.20, 152.24, 141.76, 138.25, 131.27, 127.20, 124.97, 121.89, 114.02, 91.53, 80.52, 67.67, 52.39, 47.78, 44.94, 37.43, 33.99, 31.54, 29.14.

LC-MS (ESI) Calculated for $C_{23}H_{22}N_3O_5$ $[M + H]^+$= 420.2. Found: 420.2

tert-butyl 4-(3-(2,4-dioxotetrahydropyrimidin-1(2H)-yl)phenyl)-3,6-dihydropyridine-1(2H)-carboxylate

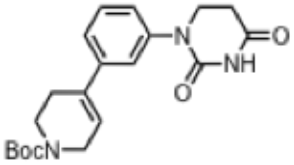

^{1}H NMR (400 MHz, $CDCl_3$) δ 7.56 (s, 1H), 7.31 (t, *J* = 7.8 Hz, 1H), 7.26 – 7.18 (m, 2H), 7.15 – 7.07 (m, 1H), 5.98 (s, 1H), 4.00 (d, *J* = 3.6 Hz, 2H), 3.81 (t, *J* = 6.6 Hz, 2H), 3.56 (t, *J* = 5.7 Hz, 2H), 2.77 (t, *J* = 6.7 Hz, 2H), 2.44 (s, 2H), 1.42 (s, 9H).

^{13}C NMR (101 MHz, $CDCl_3$) δ 169.32, 151.67, 142.13, 141.23, 129.30, 123.72, 123.64, 121.99, 79.80, 77.35, 77.23, 77.03, 76.71, 75.05, 45.31, 31.44, 28.50, 24.87, 24.57.

LC-MS (ESI) Calculated for $C_{20}H_{26}N_3O_4$ $[M + H]^+$= 372.4. Found: 372.4

***tert*-butyl 4-(4-(2,4-dioxotetrahydropyrimidin-1(2*H*)-yl)phenyl)-3,6-dihydropyridine-1(2*H*)-carboxylate**

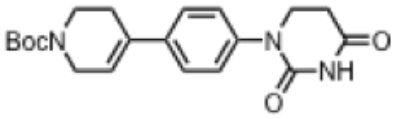

^{1}H NMR (400 MHz, $CDCl_3$) δ 7.53 (s, 1H), 7.42 – 7.28 (m, 2H), 7.27 – 7.06 (m, 4H), 5.97 (s, 1H), 4.03 (d, *J* = 13.9 Hz, 2H), 3.81 (t, *J* = 6.7 Hz, 2H), 3.57 (t, *J* = 5.7 Hz, 2H), 2.77 (t, *J* = 6.7 Hz, 2H), 1.42 (s, 9H).

^{13}C NMR (101 MHz, $CDCl_3$) δ 169.25, 154.96, 151.61, 139.93, 139.42, 125.77, 124.86, 83.43, 79.77, 79.45, 77.35, 77.23, 77.03, 76.71, 45.16, 31.40, 28.50, 26.15, 24.87, 24.80, 24.58.

LC-MS (ESI) Calculated for $C_{20}H_{26}N_3O_4$ $[M + H]^+$= 372.4. Found: 372.4

4-(4-(3-(2-methylene-4-oxotetrahydropyrimidin-1(2*H*)-yl)phenyl)piperidine-1-carbonyl)benzaldehyde

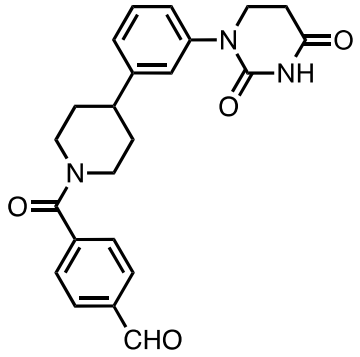

^{1}H NMR (400 MHz, DMSO) δ 10.28 (s, 1H), 9.98 (d, *J* = 8.5 Hz, 1H), 8.32 (s, 2H), 8.11 (d, *J* = 7.6 Hz, 1H), 7.95 – 7.87 (m, 2H), 7.81 (d, *J* = 7.6 Hz, 1H), 7.71 (d, *J* = 7.6 Hz, 1H), 7.62 (t, *J* = 7.6 Hz, 1H), 7.47 (t, *J* = 7.6 Hz, 1H), 7.30 – 7.17 (m, 2H), 7.14 – 7.07 (m, 2H), 3.72 (t, *J* = 6.6 Hz, 2H), 2.63 (t, *J* = 6.7 Hz, 2H), 1.92 (s, 1H), 1.61 (s, 3H).
^{13}C NMR (101 MHz, DMSO) δ 193.70, 171.60, 168.66, 167.43, 164.02, 163.28, 152.67, 146.65, 142.36, 139.07, 136.80, 130.35, 130.22, 130.02, 129.25, 127.74, 125.10, 124.19, 45.18, 36.43, 34.81, 31.37, 28.91, 25.20.

LC-MS (ESI) Calculated for $C_{23}H_{24}N_3O_4$ $[M + H]^+$= 406.2. Found: 406.2

3-(4-(3-(2,4-dioxotetrahydropyrimidin-1(2*H*)-yl)phenyl)piperidine-1-carbonyl)benzaldehyde

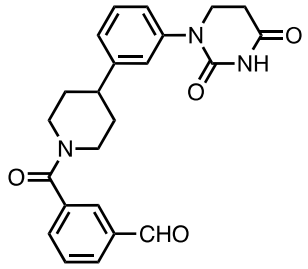

^{1}H NMR (400 MHz, DMSO) δ 10.29 (s, 1H), 10.08 – 9.98 (m, 2H), 8.10 (d, *J* = 8.2 Hz, 3H), 7.98 (dd, *J* = 8.4, 6.8 Hz, 3H), 7.65 – 7.58 (m, 1H), 7.34 – 7.11 (m, 2H), 3.79 – 3.61

(m, 2H), 2.70 (d, *J* = 7.7 Hz, 2H), 2.50 (s, 4H), 1.88 (d, *J* = 14.1 Hz, 1H), 1.70 (d, *J* = 12.8 Hz, 1H), 1.61 (d, *J* = 12.8 Hz, 1H).

^{13}C NMR (101 MHz, DMSO) δ 193.64, 186.22, 178.45, 155.79, 151.92, 147.27, 142.64, 138.66, 130.40, 128.39, 124.15, 119.68, 104.13, 102.35, 86.70, 69.26, 64.90, 56.16, 45.14, 37.98, 34.63, 31.44, 20.96.

LC-MS (ESI) Calculated for $C_{23}H_{24}N_3O_4$ $[M + H]^+$= 406.2. Found: 406.2

2-(4-(3-(2,4-dioxotetrahydropyrimidin-1(2*H*)-yl)phenyl)piperidine-1-carbonyl)benzaldehyde

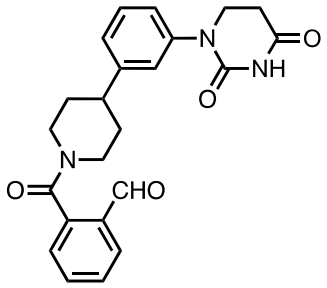

^{1}H NMR (400 MHz, DMSO) δ 10.35 (s, 1H), 10.03 (s, 1H), 7.83 (dq, *J* = 21.0, 10.1 Hz, 2H), 7.71 – 7.51 (m, 5H), 7.36 – 7.21 (m, 2H), 7.16 (t, *J* = 8.6 Hz, 2H), 4.71 (d, *J* = 13.3 Hz, 1H), 3.78 (s, 1H), 3.54 (s, 2H), 2.74 – 2.66 (m, 2H), 1.99 (s, 1H), 1.90 (d, *J* = 12.7 Hz, 1H), 1.68 (dd, *J* = 24.3, 12.6 Hz, 2H).

^{13}C NMR (101 MHz, DMSO) δ 192.21, 171.11, 160.64, 152.73, 142.62, 134.84, 132.84, 131.60, 131.10, 129.79, 127.47, 125.35, 124.18, 114.34, 107.83, 97.50, 69.77, 56.90, 47.50, 45.13, 33.15, 31.56, 23.89.

LC-MS (ESI) Calculated for $C_{23}H_{24}N_3O_4$ $[M + H]^+$= 406.2. Found: 406.2

4-(4-(4-(2,4-dioxotetrahydropyrimidin-1(2*H*)-yl)phenyl)piperidine-1-carbonyl)benzaldehyde

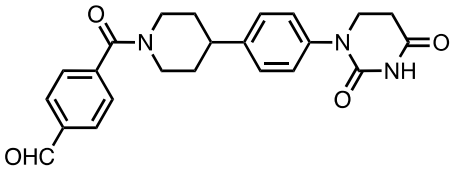

^{1}H NMR (400 MHz, DMSO) δ 10.27 (d, *J* = 5.2 Hz, 1H), 10.02 – 9.95 (m, 2H), 8.25 (s, 1H), 8.07 – 7.78 (m, 5H), 7.66 – 7.48 (m, 2H), 7.30 – 7.16 (m, 2H), 7.11 (dd, *J* = 6.1, 4.1 Hz, 1H), 4.57 (s, 1H), 3.71 (q, *J* = 7.1 Hz, 1H), 2.79 (d, *J* = 13.4 Hz, 2H), 2.63 (td, *J* = 6.7, 3.6 Hz, 2H), 1.81 (s, 1H), 1.60 (s, 2H).

^{13}C NMR (101 MHz, DMSO) δ 193.56, 171.10, 164.95, 148.68, 147.44, 144.98, 143.71, 142.43, 140.79, 137.95, 137.66, 130.14, 129.48, 127.81, 125.79, 112.57, 99.32, 83.39, 76.52, 59.15, 45.06, 31.58, 24.16.

LC-MS (ESI) Calculated for $C_{23}H_{24}N_3O_4$ $[M + H]^+$= 406.2. Found: 406.2

3-(4-(4-(2,4-dioxotetrahydropyrimidin-1(2*H*)-yl)phenyl)piperidine-1-carbonyl)benzaldehyde

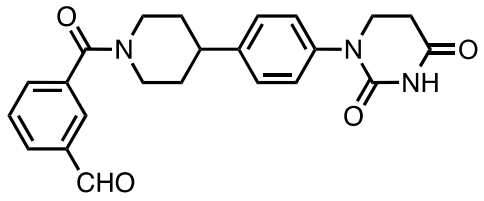

^{1}H NMR (400 MHz, DMSO) δ 10.35 (d, *J* = 5.4 Hz, 1H), 10.07 (s, 1H), 8.24 (dt, *J* = 7.7, 1.5 Hz, 7H), 8.13 (dt, *J* = 7.7, 1.5 Hz, 7H), 8.05 – 7.92 (m, 2H), 7.74 (s, 3H), 3.78 (q, *J* = 7.1 Hz, 1H), 2.70 (dd, *J* = 8.5, 4.8 Hz, 1H).

^{13}C NMR (101 MHz, DMSO) δ 193.35, 176.65, 167.03, 136.85, 135.28, 133.33, 132.76, 130.83, 130.06, 127.48, 125.79, 114.06, 79.12, 73.67, 63.31, 50.36, 45.06, 41.78, 23.73.

LC-MS (ESI) Calculated for $C_{23}H_{24}N_3O_4$ $[M + H]^+$= 406.2. Found: 406.2

2-(4-(4-(2,4-dioxotetrahydropyrimidin-1(2*H*)-yl)phenyl)piperidine-1-carbonyl)benzaldehyde

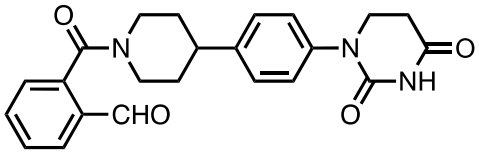

^{1}H NMR (400 MHz, DMSO) δ 10.34 (s, 1H), 10.04 (d, *J* = 7.0 Hz, 2H), 7.77 (t, *J* = 7.5 Hz, 2H), 7.66 (t, *J* = 7.2 Hz, 1H), 7.62 – 7.40 (m, 6H), 7.37 – 7.27 (m, 4H), 3.81 (d, *J* = 6.6 Hz, 2H), 2.72 (d, *J* = 6.5 Hz, 3H), 2.36 – 2.31 (m, 2H).

^{13}C NMR (101 MHz, DMSO) δ 197.62, 181.73, 181.27, 165.07, 162.10, 159.00, 156.61, 148.82, 145.06, 140.61, 134.67, 129.22, 119.39, 107.15, 103.18, 89.33, 63.72, 59.14, 45.57, 23.00, 19.40, 9.85.

LC-MS (ESI) Calculated for $C_{23}H_{24}N_3O_4$ $[M + H]^+$= 406.2. Found: 406.2

3.6.2 BTK Ligands

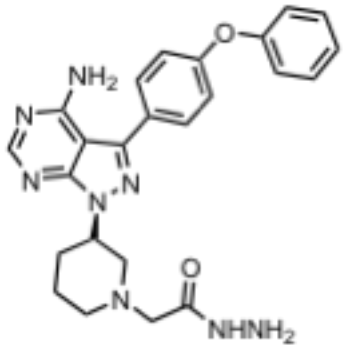

^{1}H NMR (400 MHz, $CDCl_3$) δ 8.28 (s, 1H), 7.57 (dd, *J* = 7.2, 5.0 Hz, 2H), 7.32 (t, *J* = 8.0 Hz, 2H), 7.14 – 7.05 (m, 4H), 7.03 – 6.97 (m, 2H), 5.69 (s, 3H), 4.91 (tt, *J* = 9.5, 4.3 Hz, 1H), 3.71 (s, 2H), 3.28 – 3.13 (m, 1H), 3.07 (d, *J* = 12.2 Hz, 2H), 2.98 (dd, *J* = 11.0, 4.0 Hz, 1H), 2.90 – 2.71 (m, 2H), 2.33 – 2.23 (m, 1H), 2.19 – 2.05 (m, 1H), 1.85 (td, *J* = 10.6, 5.8 Hz, 1H).

^{13}C NMR (101 MHz, DMSO) δ 171.12, 169.85, 158.61, 130.67, 129.25, 127.46, 127.06, 126.49, 125.59, 121.32, 119.56, 117.57, 88.78, 77.69, 72.97, 62.73, 55.83, 47.78, 44.33, 37.42, 33.98, 29.37, 19.02, 16.72.

LC-MS (ESI) Calculated for $C_{24}H_{27}N_8O_2[M + H]^+$= 459.2. Found: 459.2

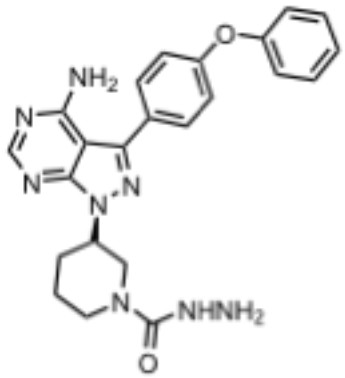

^{1}H NMR (400 MHz, $CDCl_3$) δ 8.27 (s, 1H), 7.61 – 7.50 (m, 2H), 7.32 (t, *J* = 8.0 Hz, 2H), 7.14 – 7.04 (m, 4H), 7.04 – 6.98 (m, 2H), 6.33 (s, 1H), 5.84 (s, 3H), 4.84 – 4.72 (m, 1H), 4.04 (dd, *J* = 13.2, 4.2 Hz, 1H), 3.88 (d, *J* = 13.3 Hz, 1H), 3.44 (dd, *J* = 13.0, 10.3 Hz,

1H), 2.99 – 2.87 (m, 1H), 2.31 (qd, *J* = 12.2, 4.1 Hz, 1H), 2.15 (dd, *J* = 13.4, 4.2 Hz, 1H), 1.85 (dt, *J* = 14.1, 3.5 Hz, 1H), 1.67 (t, *J* = 12.8 Hz, 1H).

^{13}C NMR (101 MHz, $CDCl_3$) δ 171.58, 162.04, 161.66, 160.54, 160.09, 155.54, 151.63, 147.26, 130.16, 129.65, 124.70, 120.04, 119.18, 119.00, 116.96, 114.10, 77.34, 77.23, 77.02, 76.70, 60.59, 53.43, 47.79, 44.48, 29.41, 21.07, 14.18.

LC-MS (ESI) Calculated for $C_{23}H_{25}N_8O_2[M + H]^+$= 445.2. Found: 445.2

3.7 NMR Spectra

3.7.1 Partial PROTAC Library based on Achiral Ligands

[1]H NMR (400 MHz, DMSO-d)

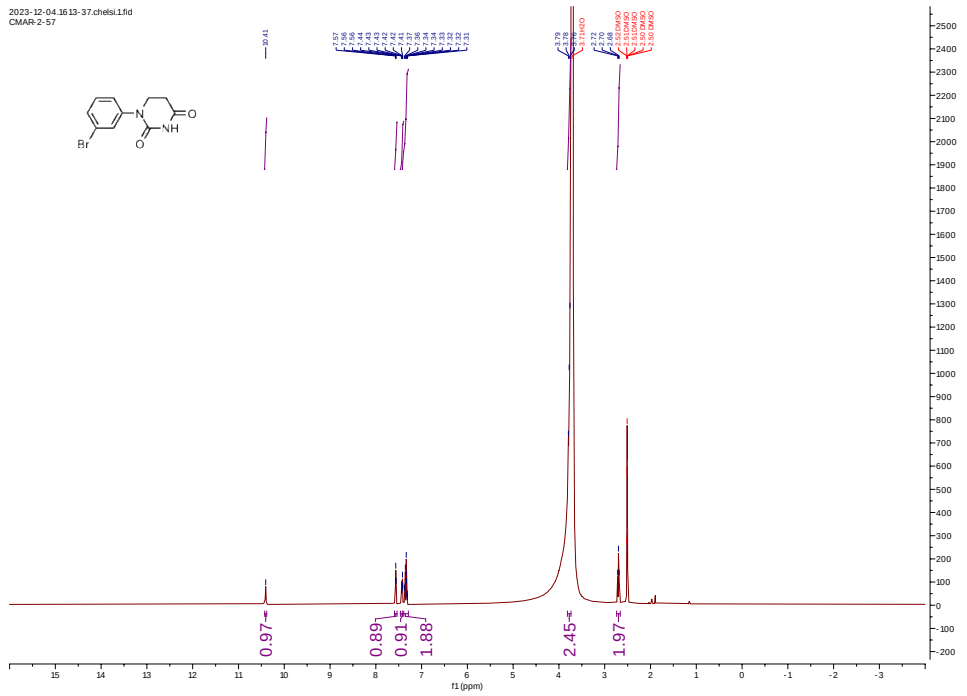

[13]C NMR (101 MHz, DMSO-d)

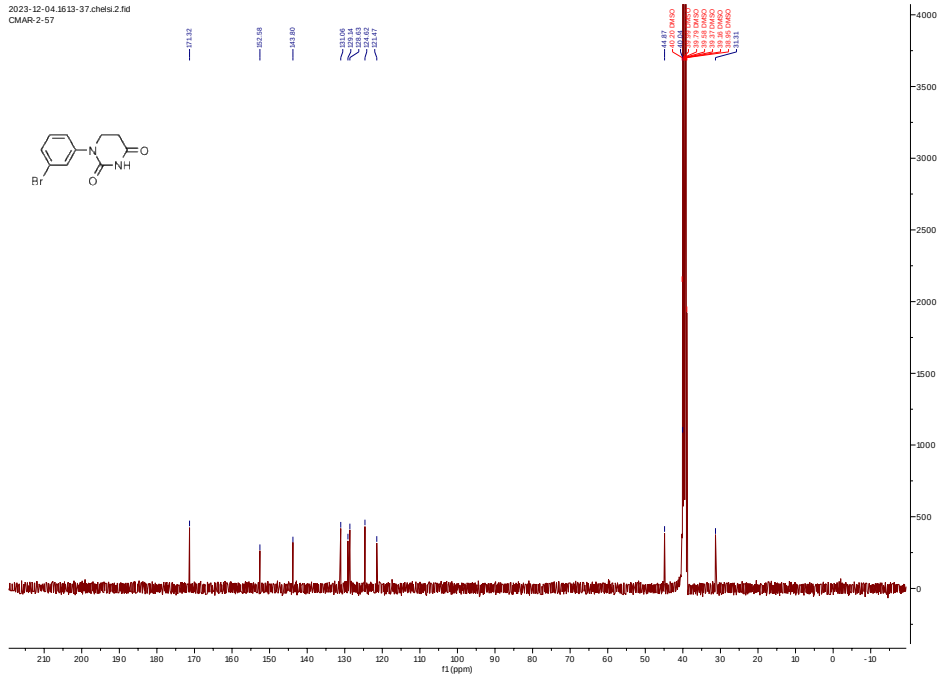

[1]H NMR (400 MHz, DMSO-d)

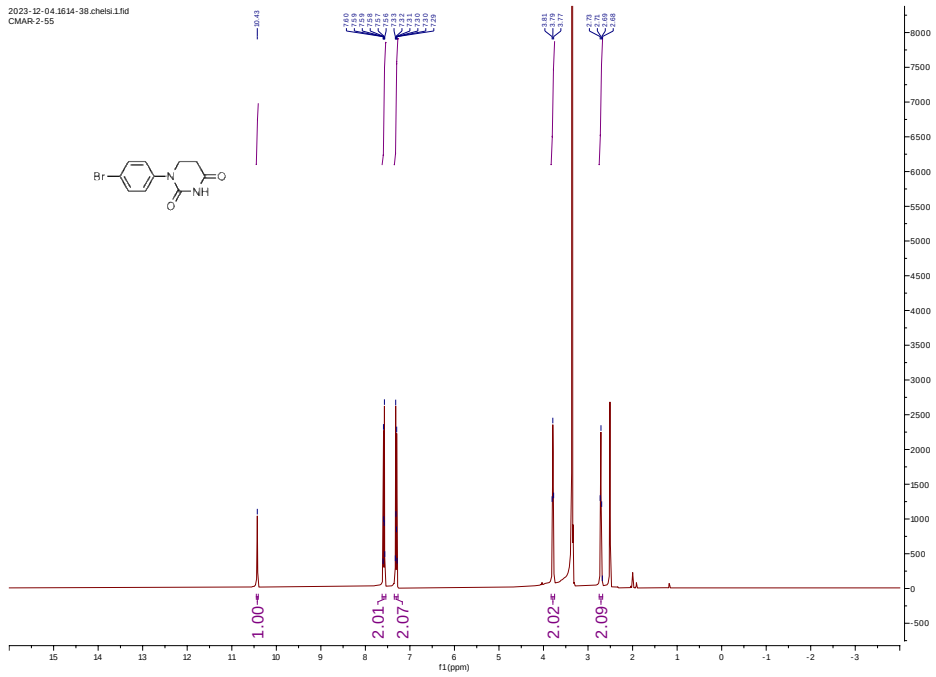

[13]C NMR (101 MHz, DMSO-d)

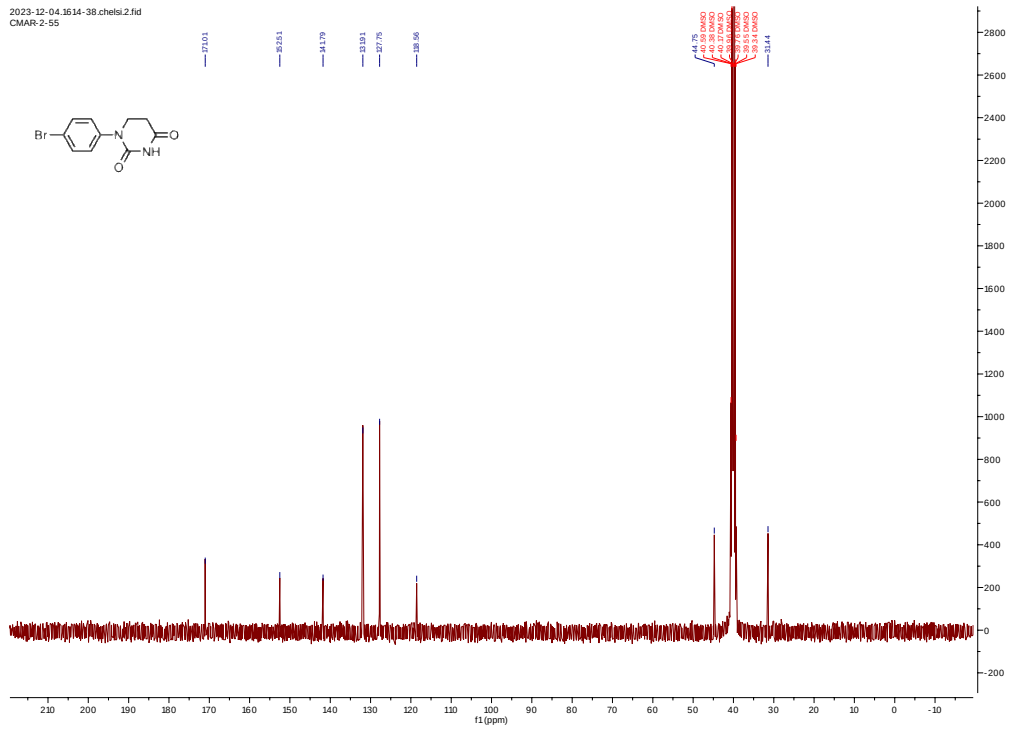

^{1}H NMR (400 MHz, DMSO-d)

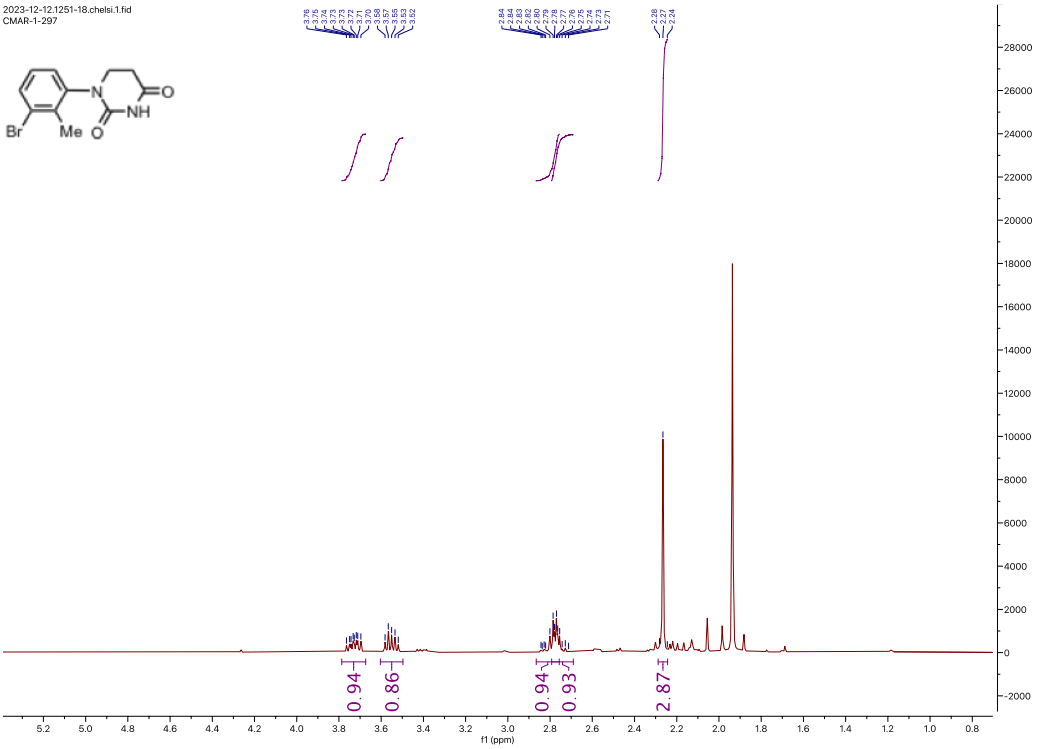

^{1}H NMR (400 MHz, DMSO-d)

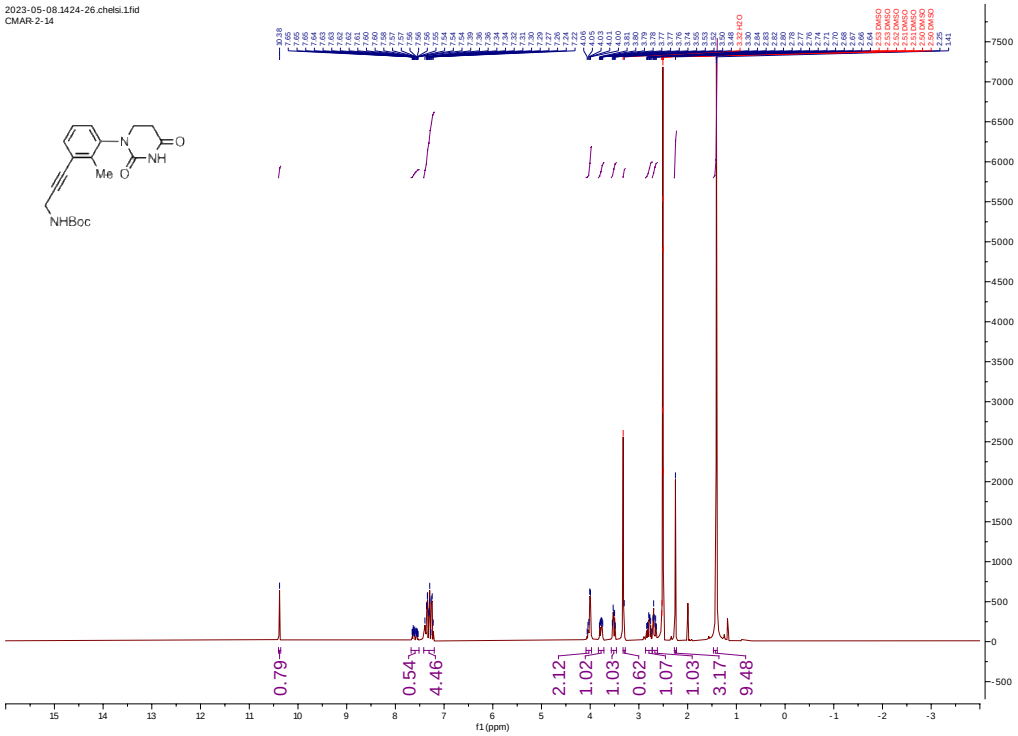

^{1}***H NMR*** (400 MHz, DMSO-d)

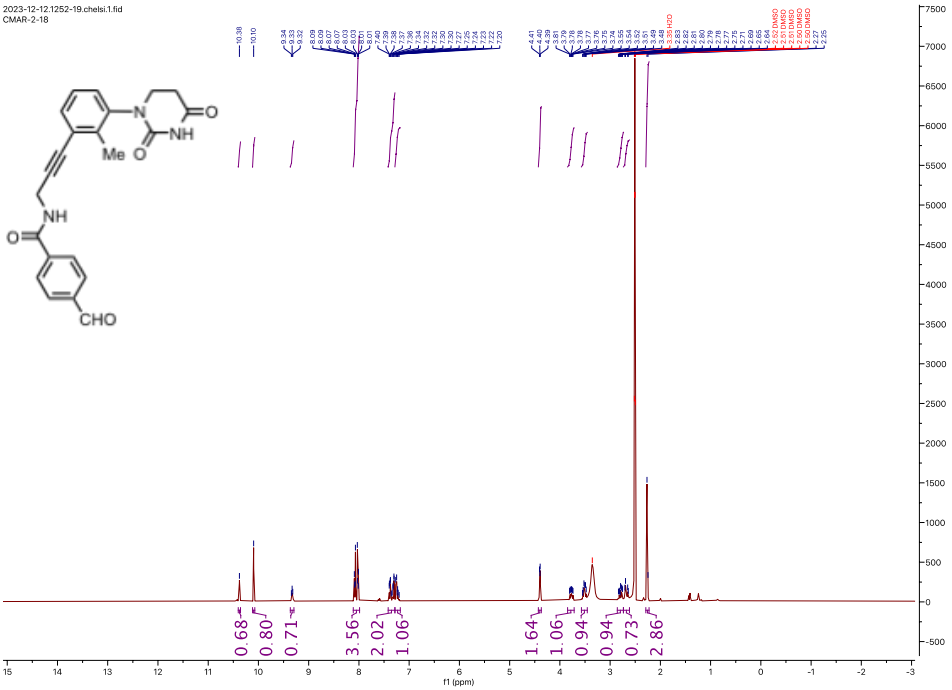

^{13}***C NMR*** (101 MHz, DMSO-d)

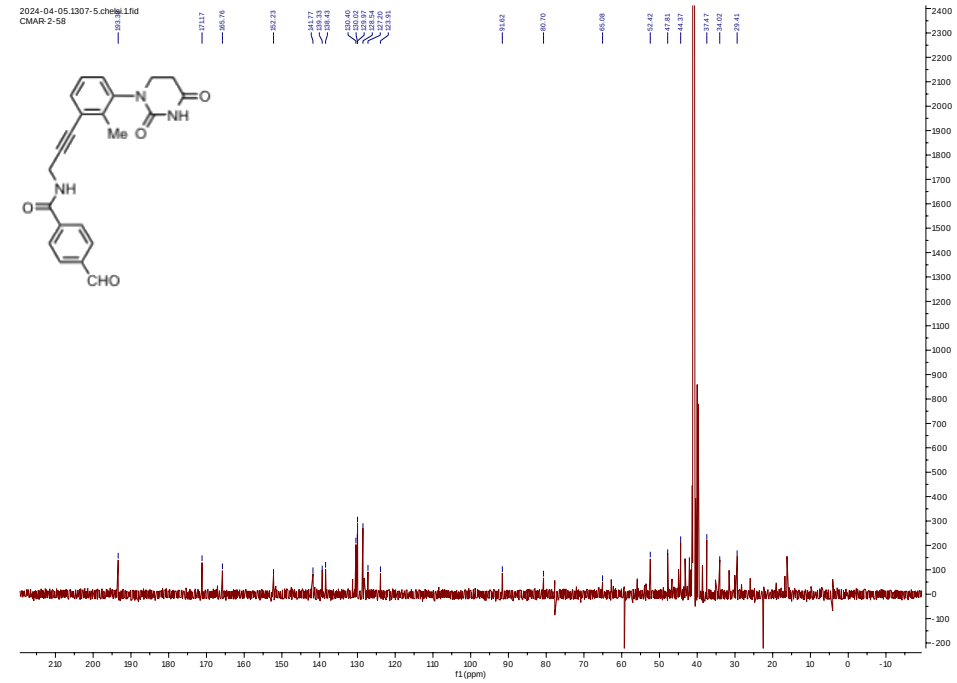

[1]H NMR (400 MHz, DMSO-d)

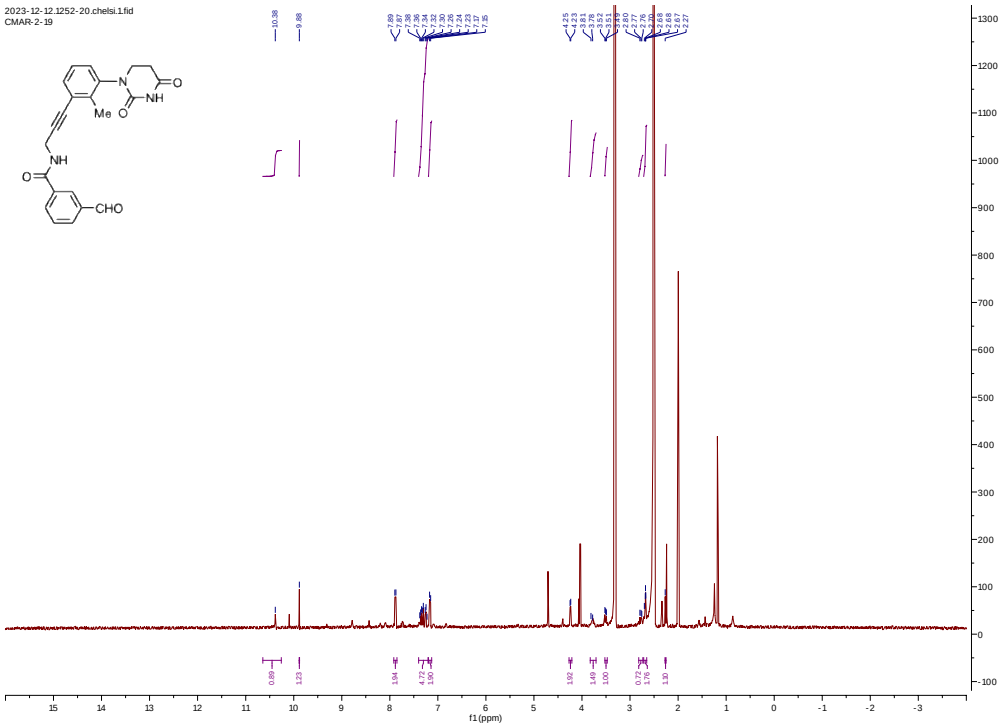

[13]C NMR (101 MHz, DMSO-d)

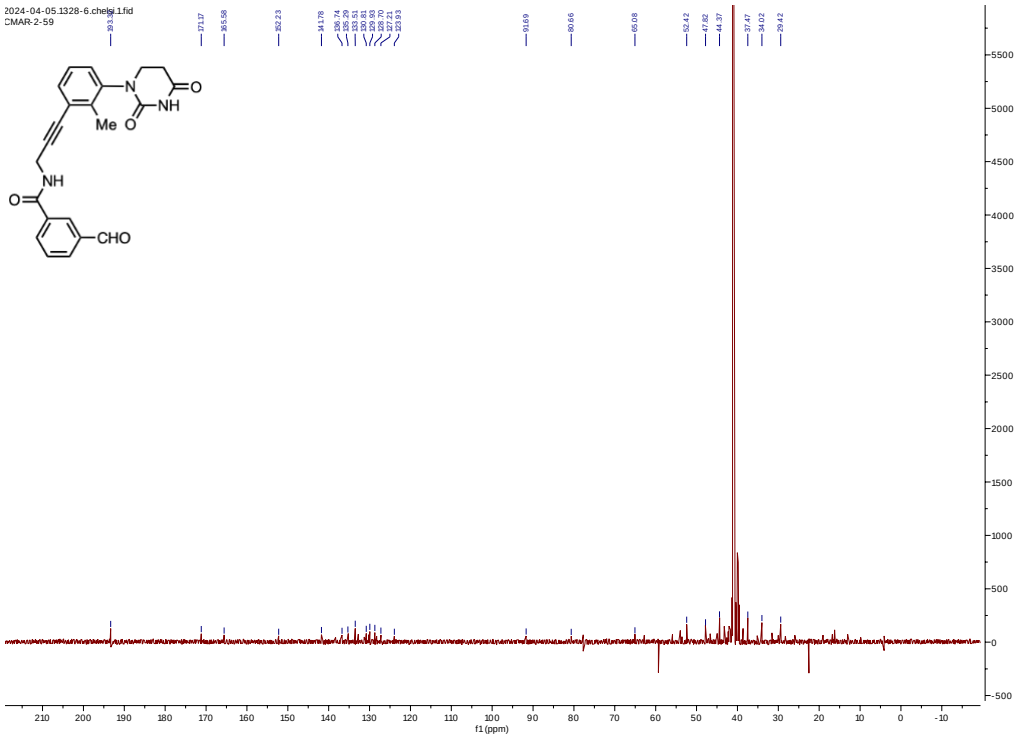

[1]H NMR (400 MHz, DMSO-d)

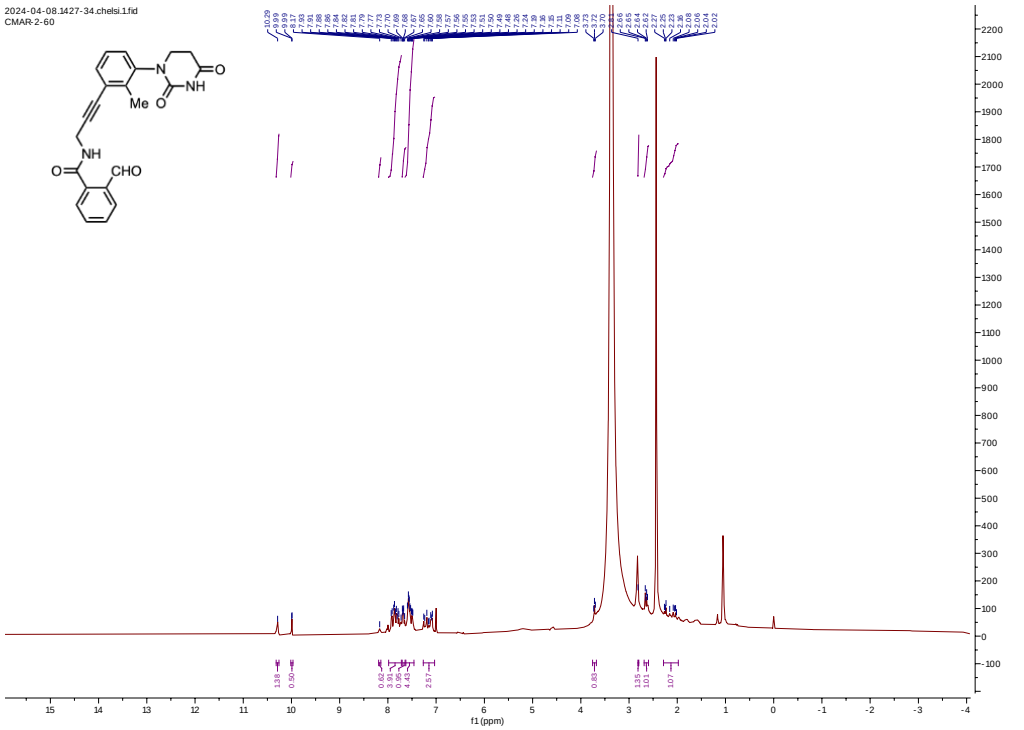

[13]C NMR (101 MHz, DMSO-d)

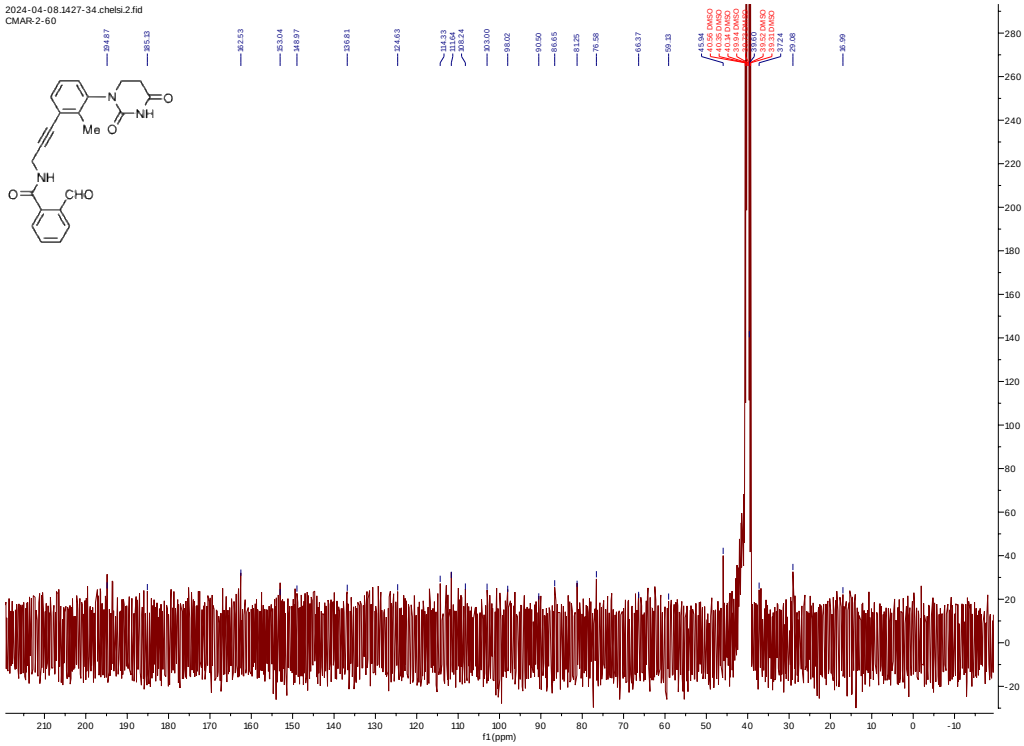

^{1}H NMR (400 MHz, DMSO-d)

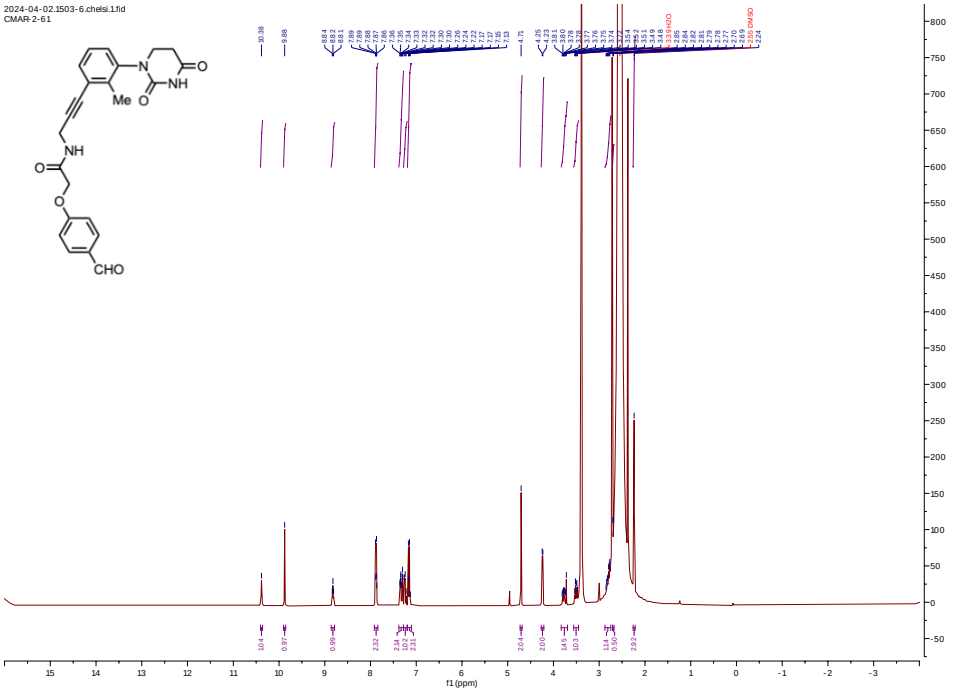

^{13}C NMR (101 MHz, DMSO-d)

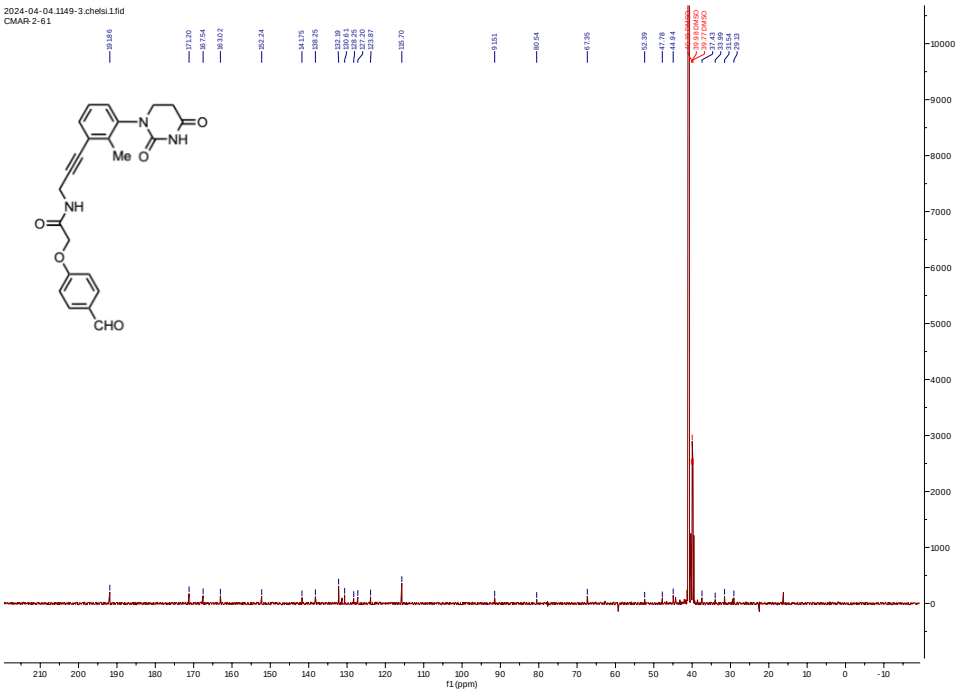

[1]H NMR (400 MHz, DMSO-d)

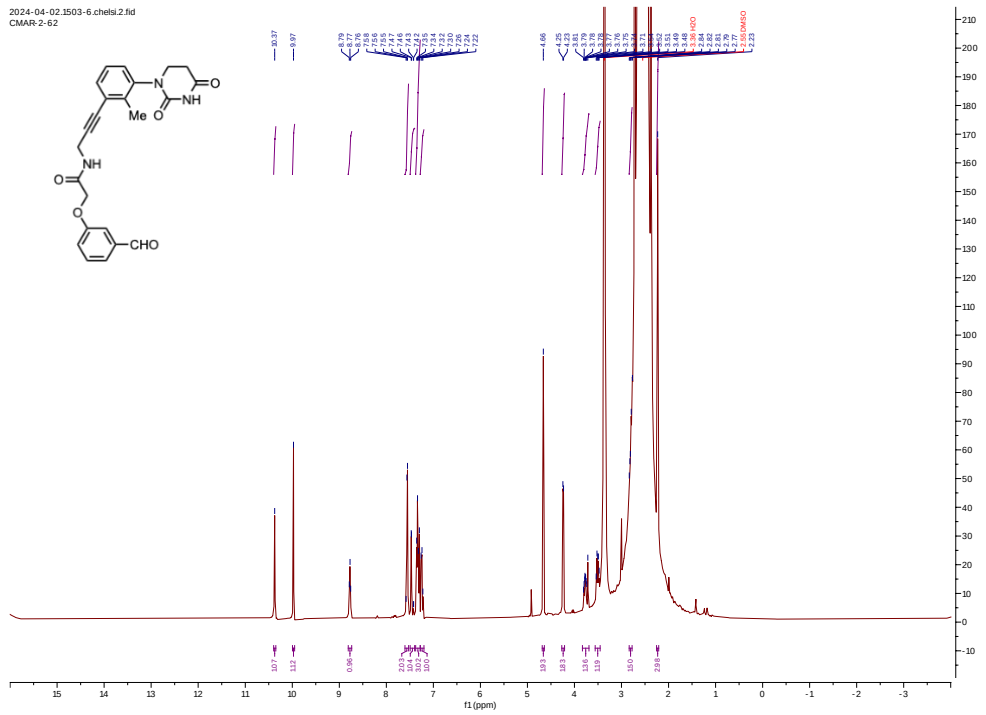

[13]C NMR (101 MHz, DMSO-d)

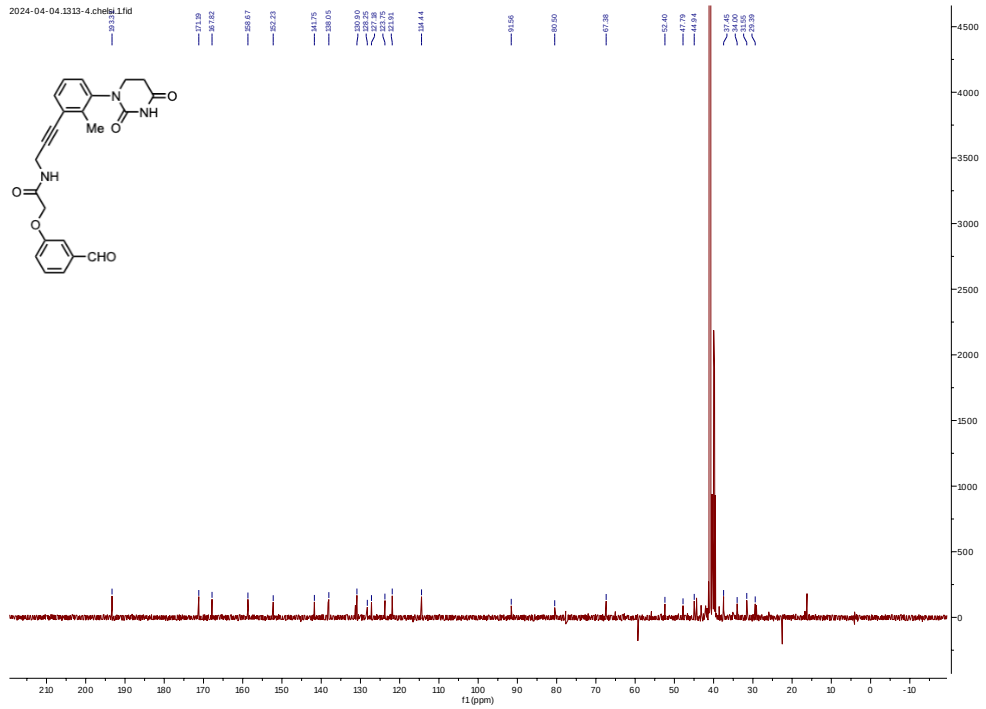

[1]H NMR (400 MHz, DMSO-d)

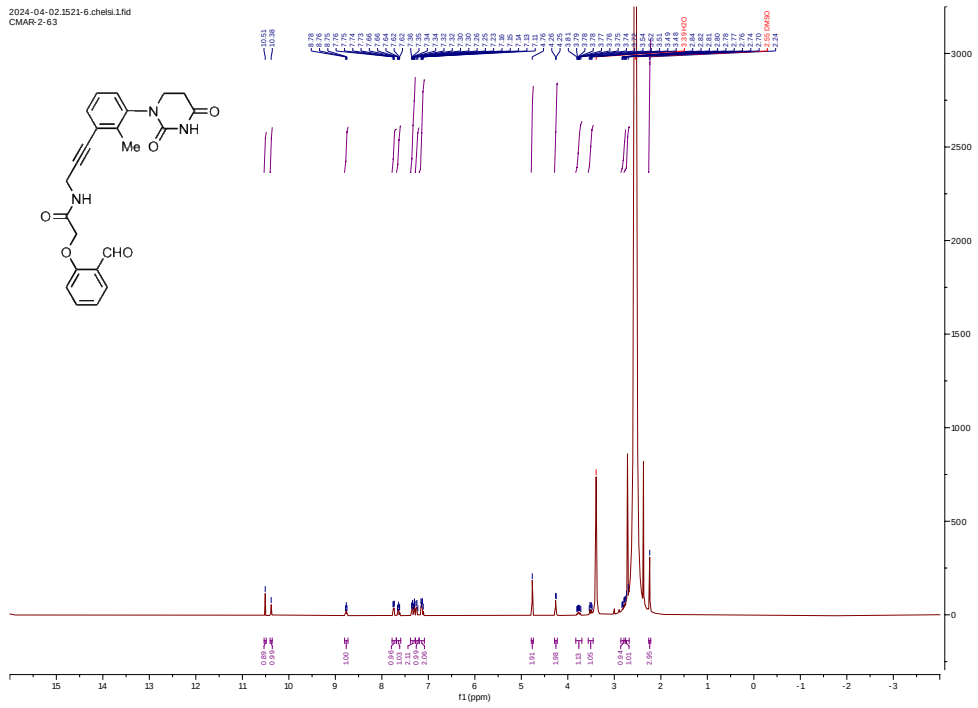

[13]C NMR (101 MHz, DMSO-d)

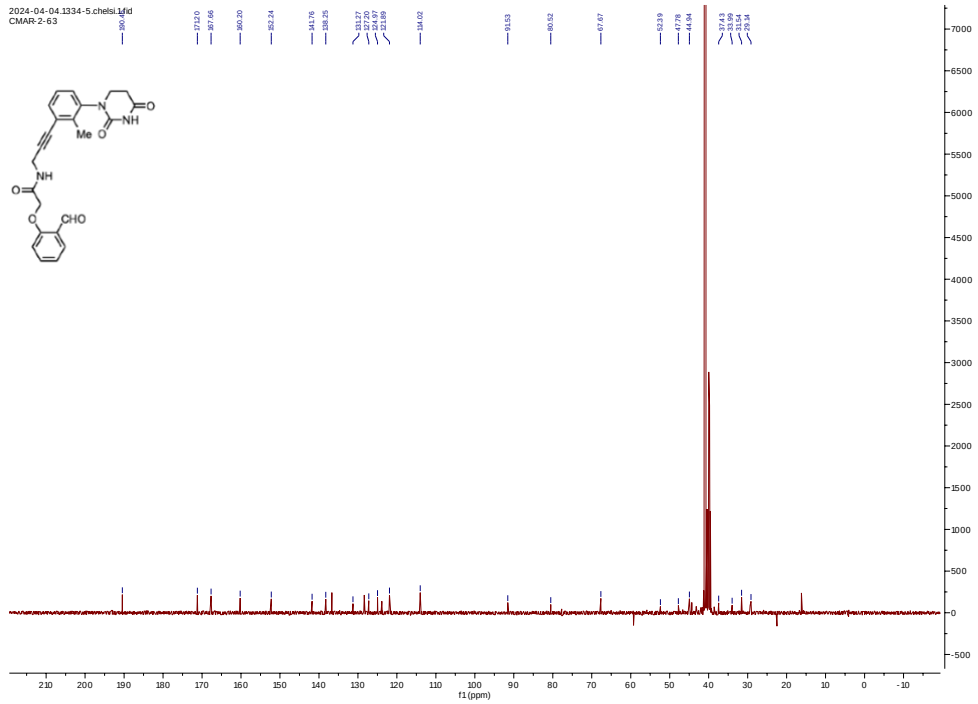

[1]H NMR (400 MHz, DMSO-d)

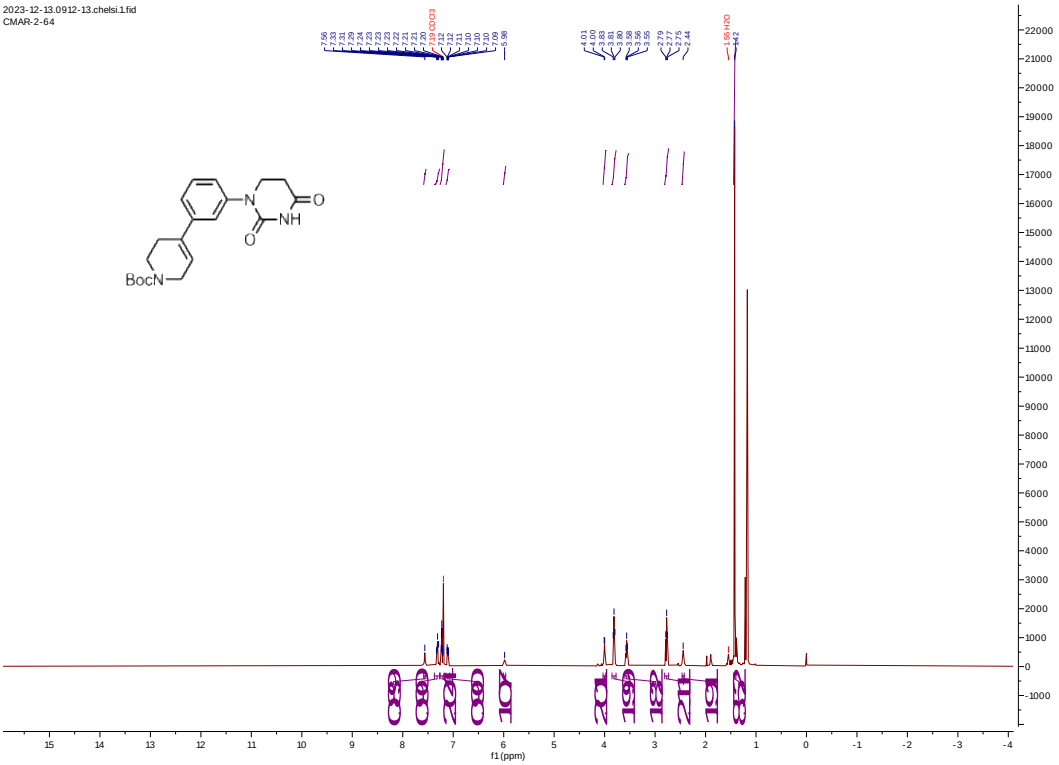

[13]C NMR (101 MHz, DMSO-d)

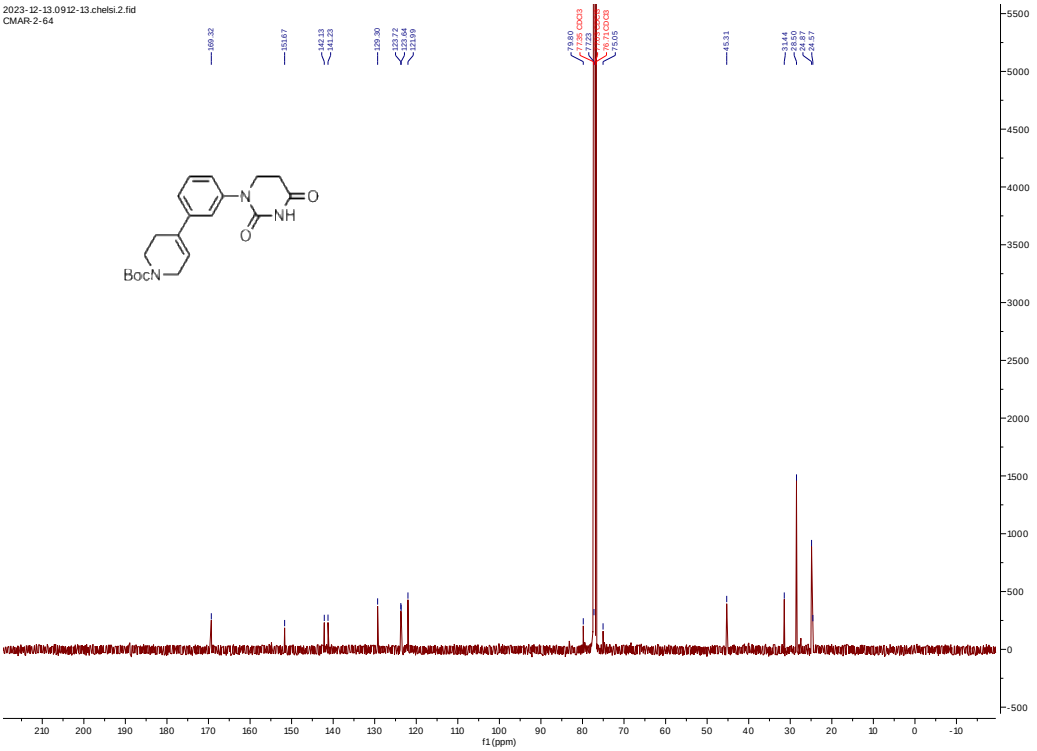

[1]H NMR (400 MHz, DMSO-d)

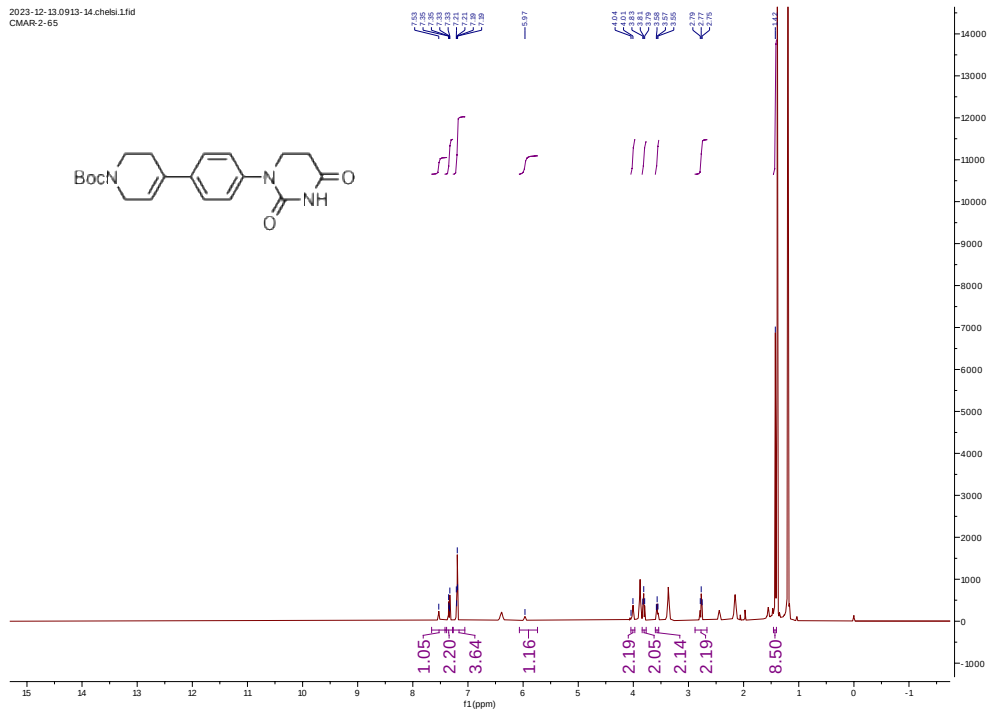

[13]C NMR (101 MHz, DMSO-d)

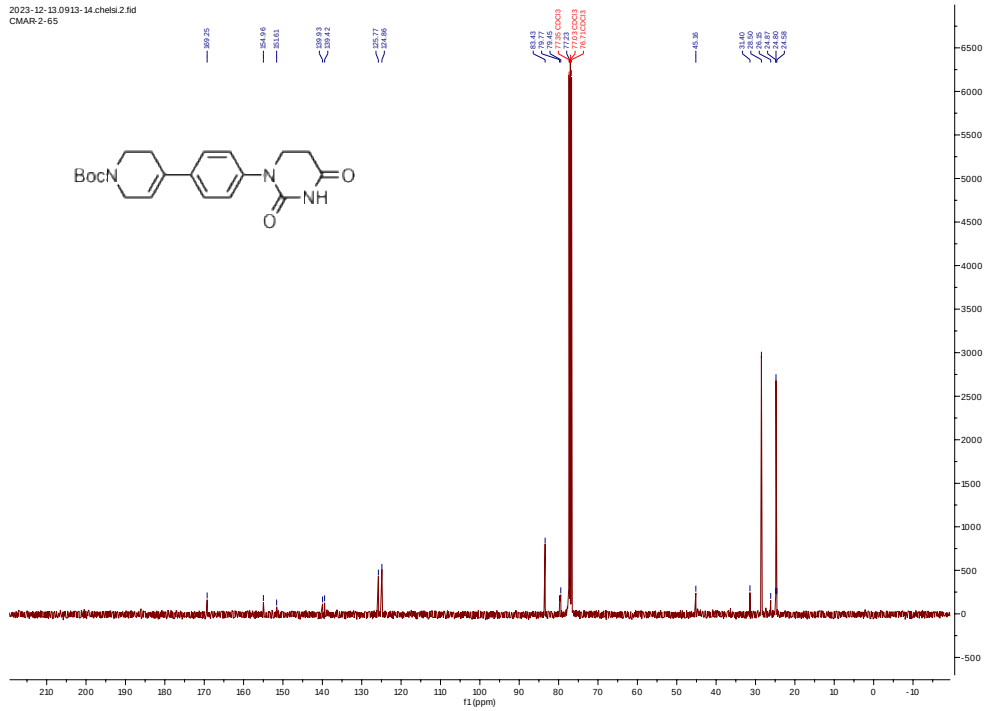

[1]H NMR (400 MHz, DMSO-d)

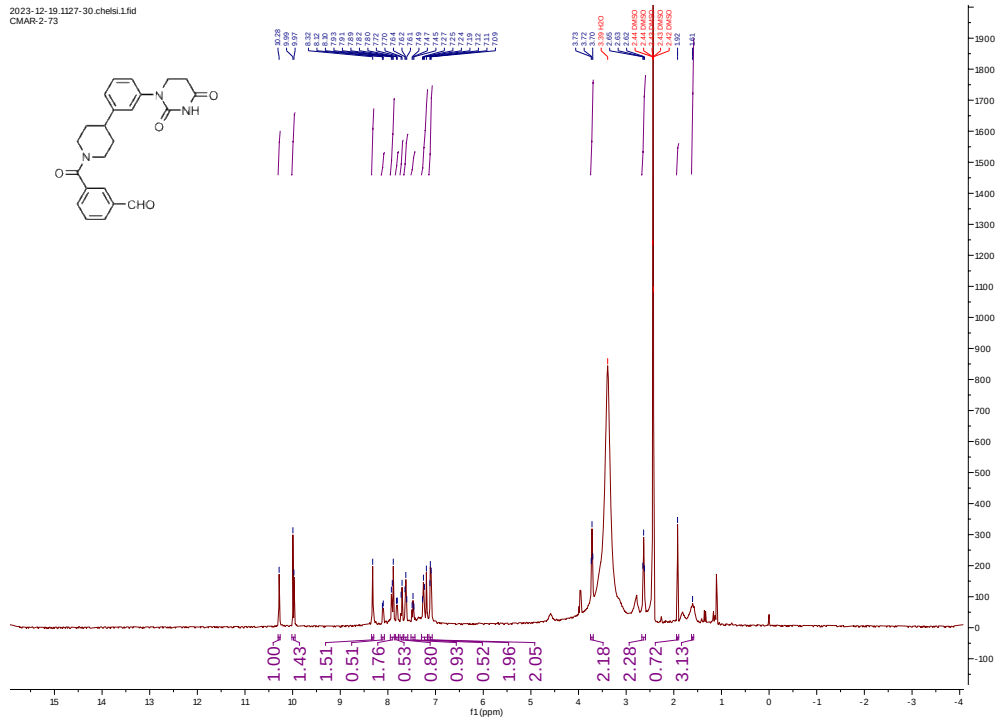

[13]C NMR (101 MHz, DMSO-d)

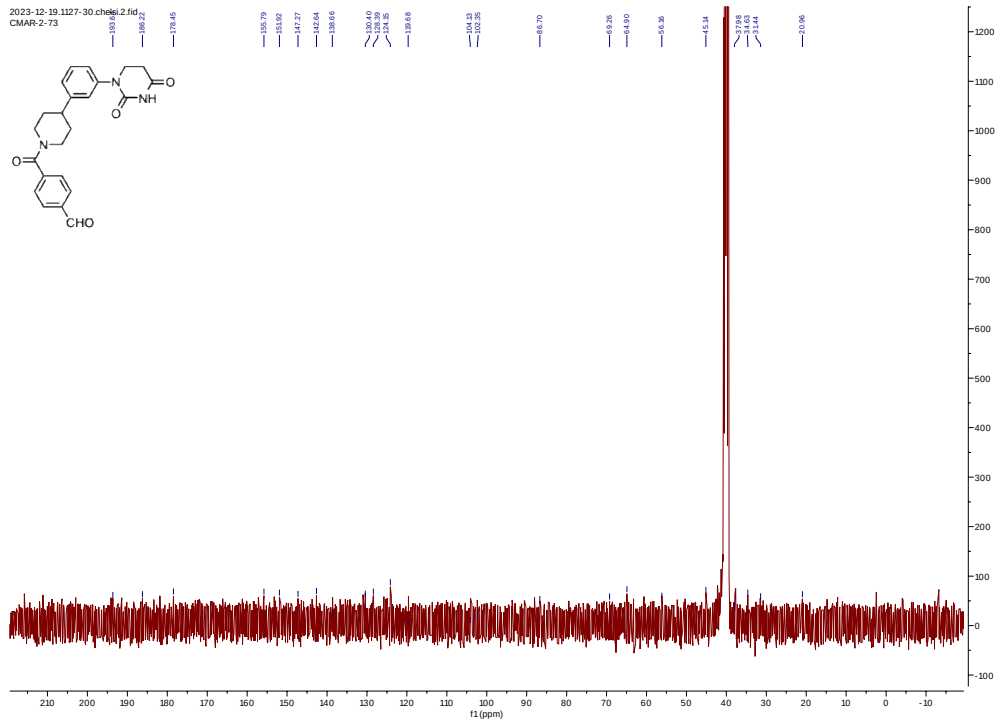

^{1}***H NMR*** (400 MHz, DMSO-d)

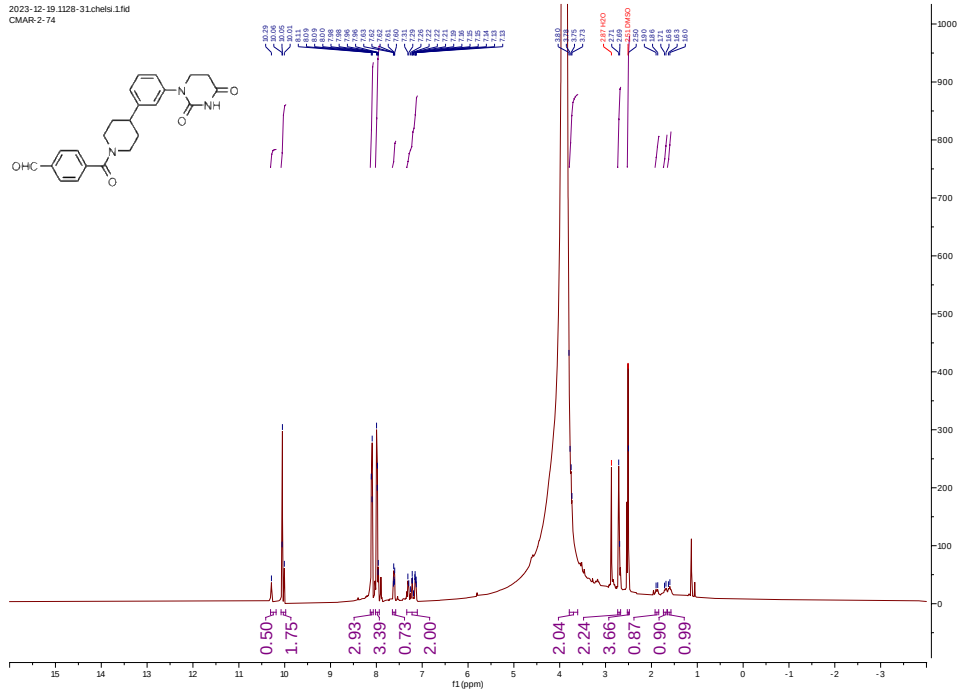

^{13}***C NMR*** (101 MHz, DMSO-d)

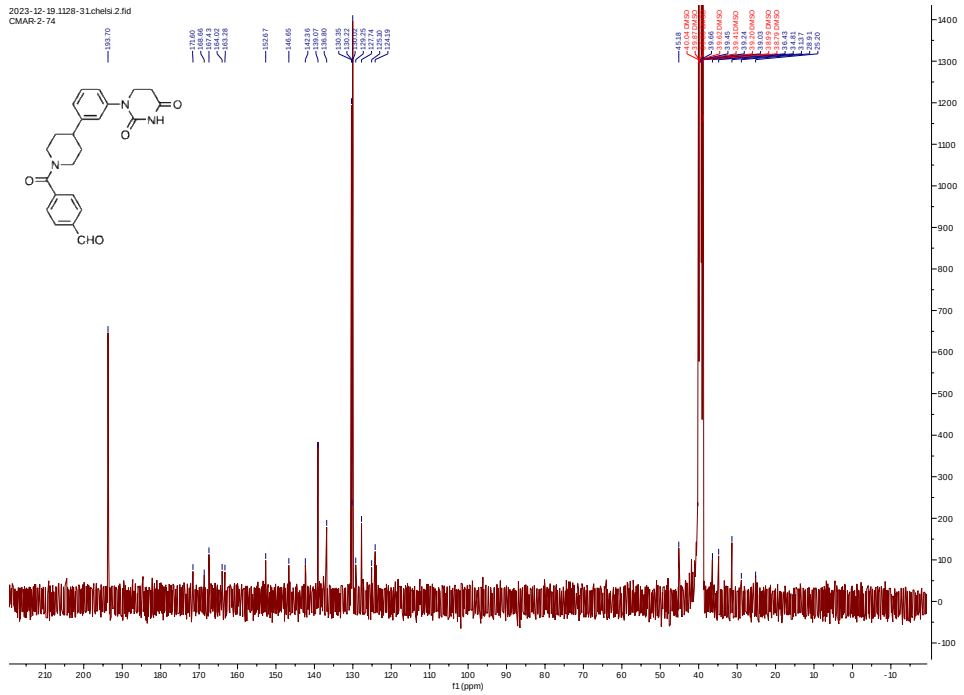

^{1}***H NMR*** (400 MHz, DMSO-d)

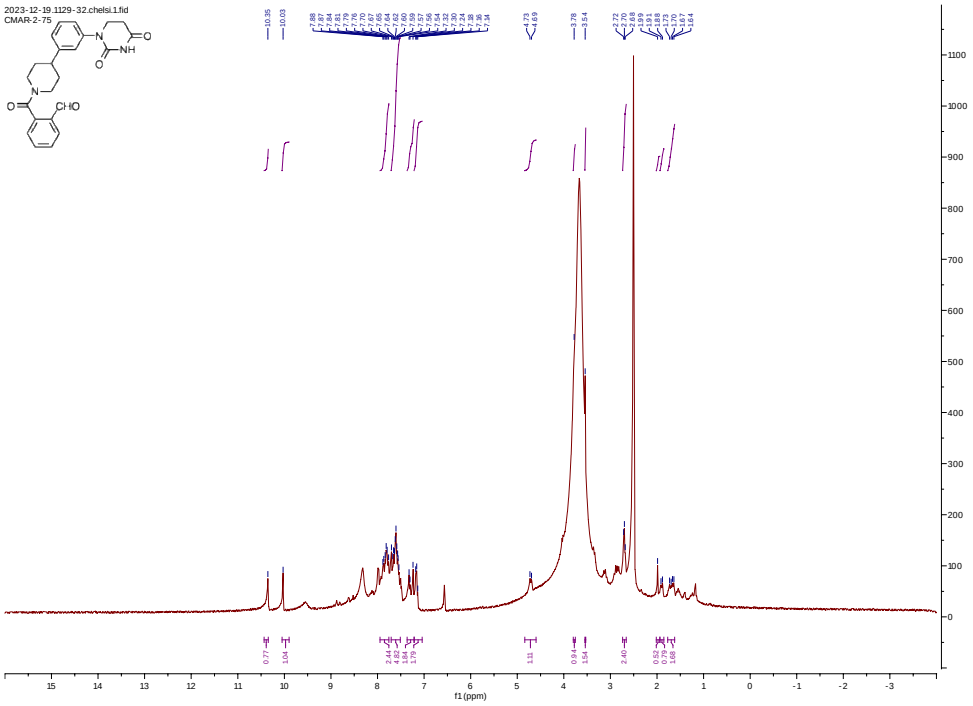

^{13}***C NMR*** (101 MHz, DMSO-d)

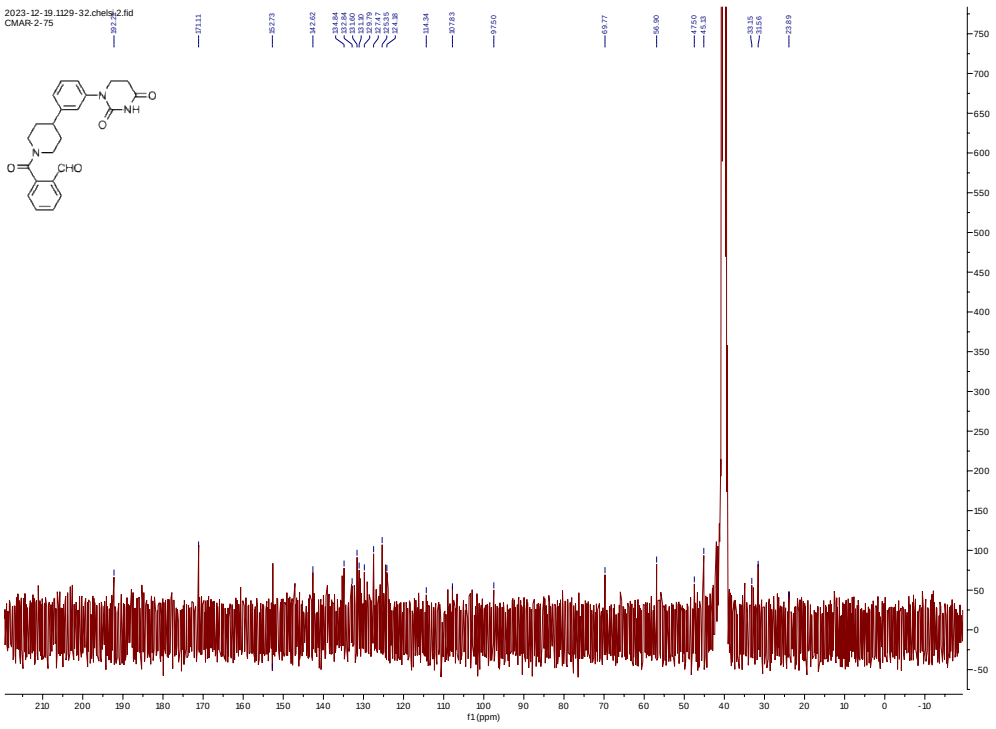

^{1}***H NMR*** (400 MHz, DMSO-d)

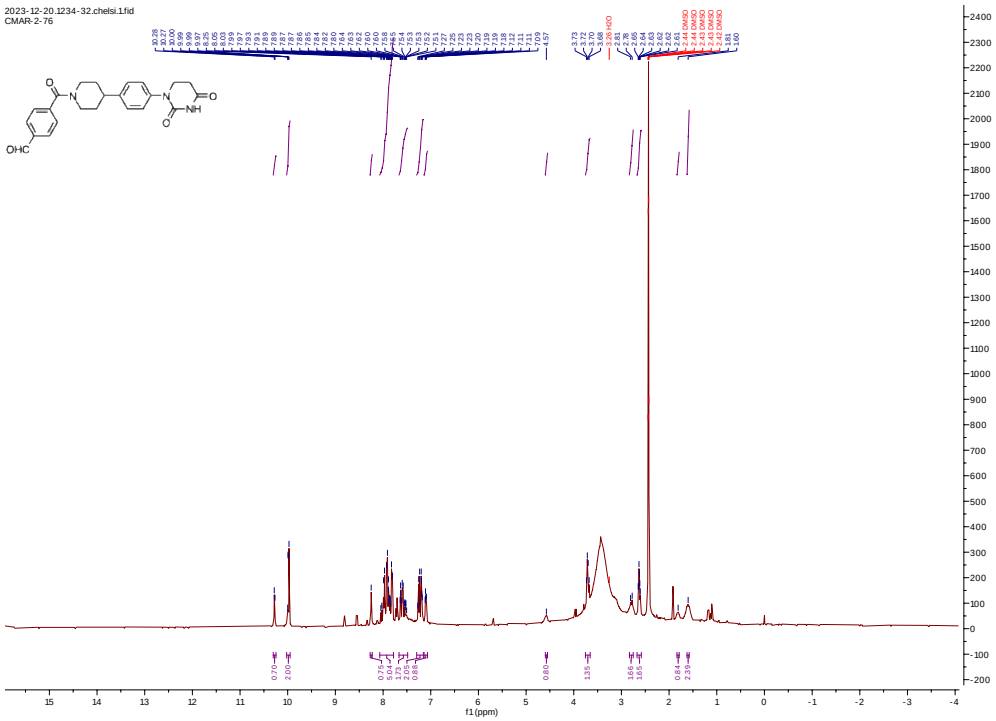

^{13}***C NMR*** (101 MHz, DMSO-d)

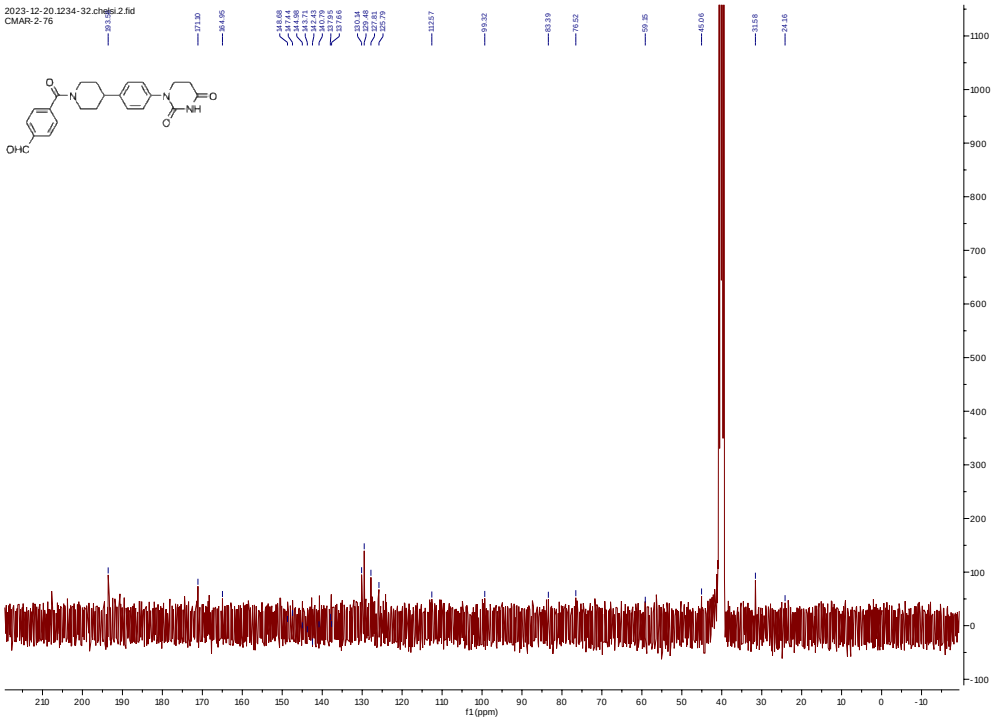

[1]H NMR (400 MHz, DMSO-d)

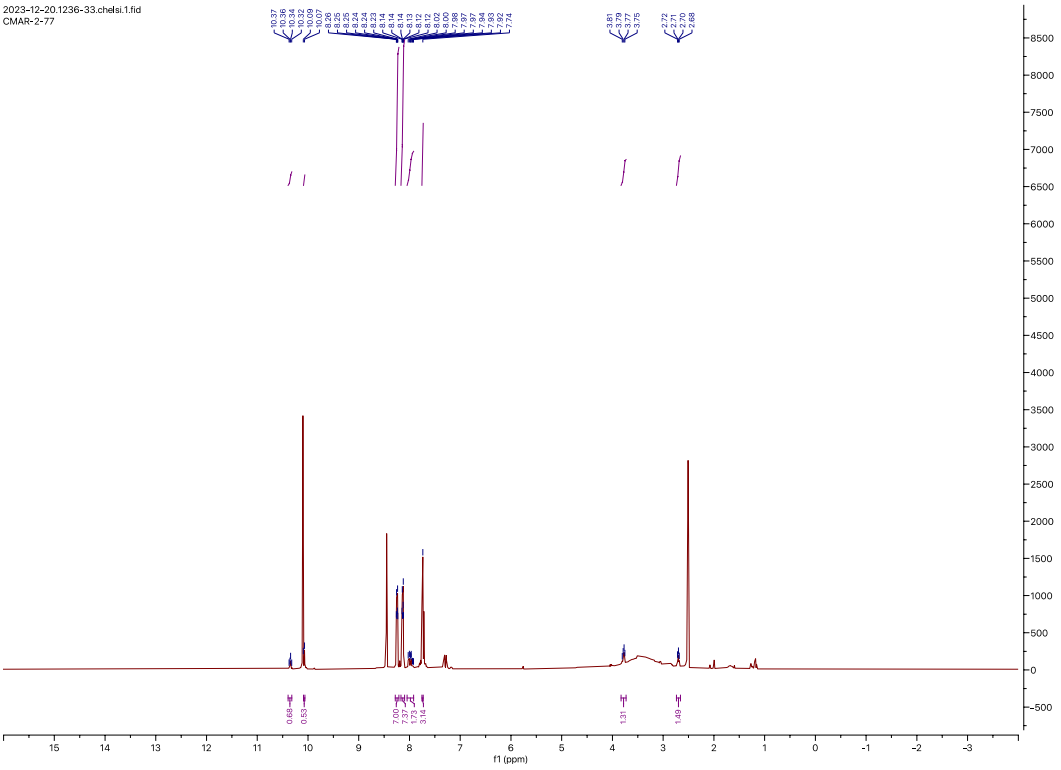

[13]C NMR (101 MHz, DMSO-d)

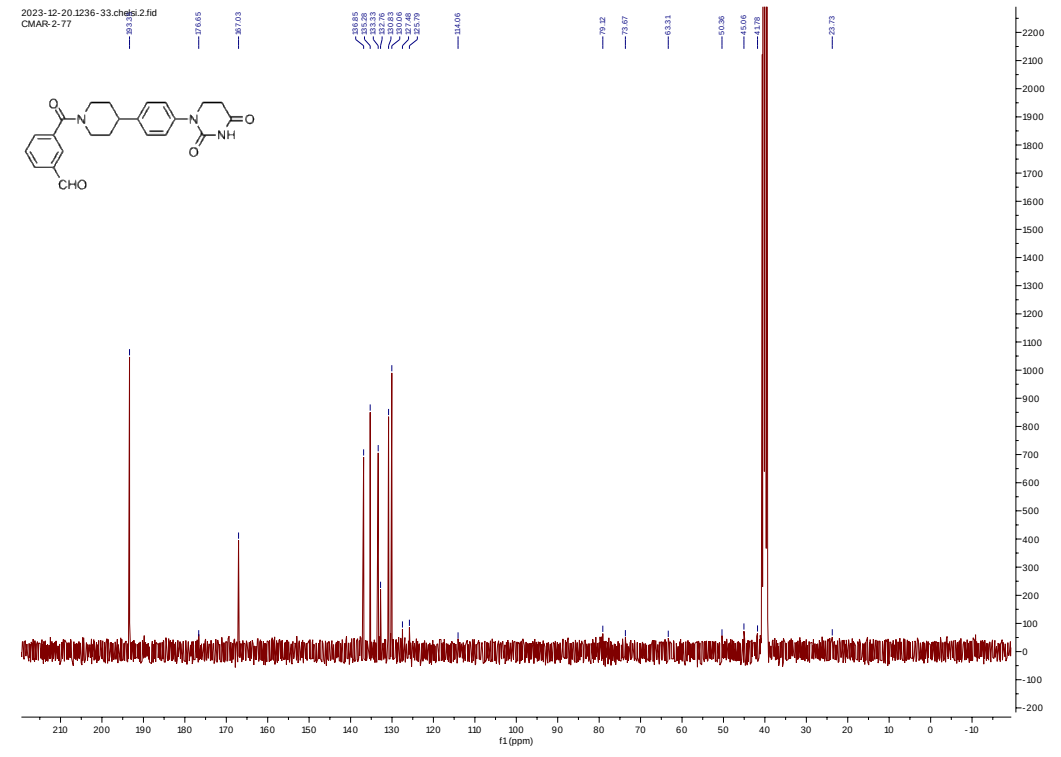

[1]H NMR (400 MHz, DMSO-d)

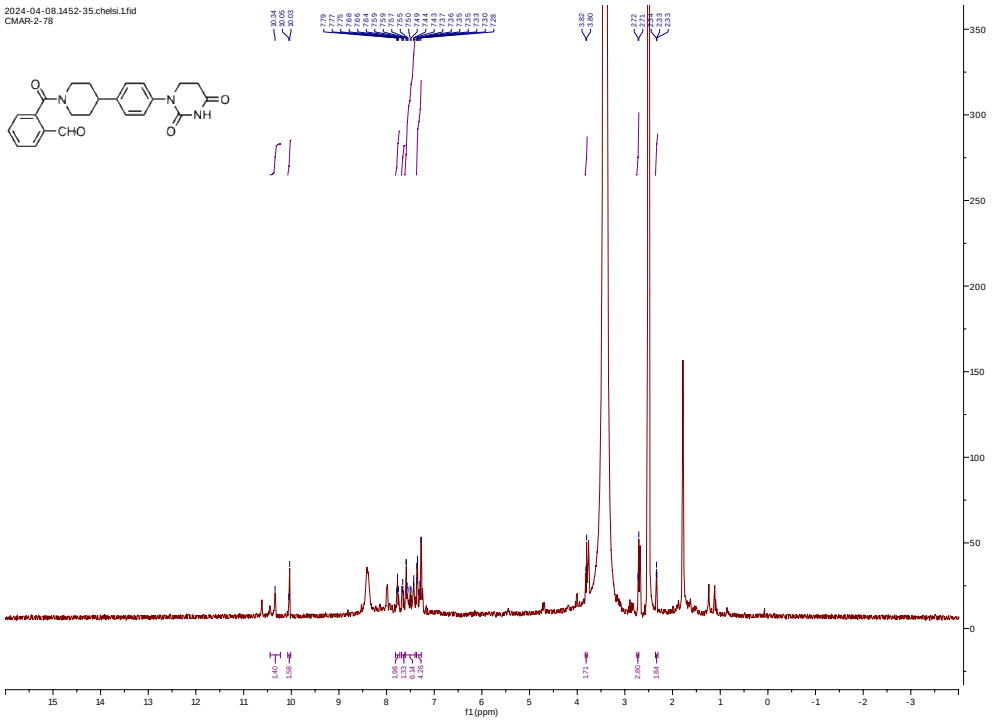

[13]C NMR (101 MHz, DMSO-d)

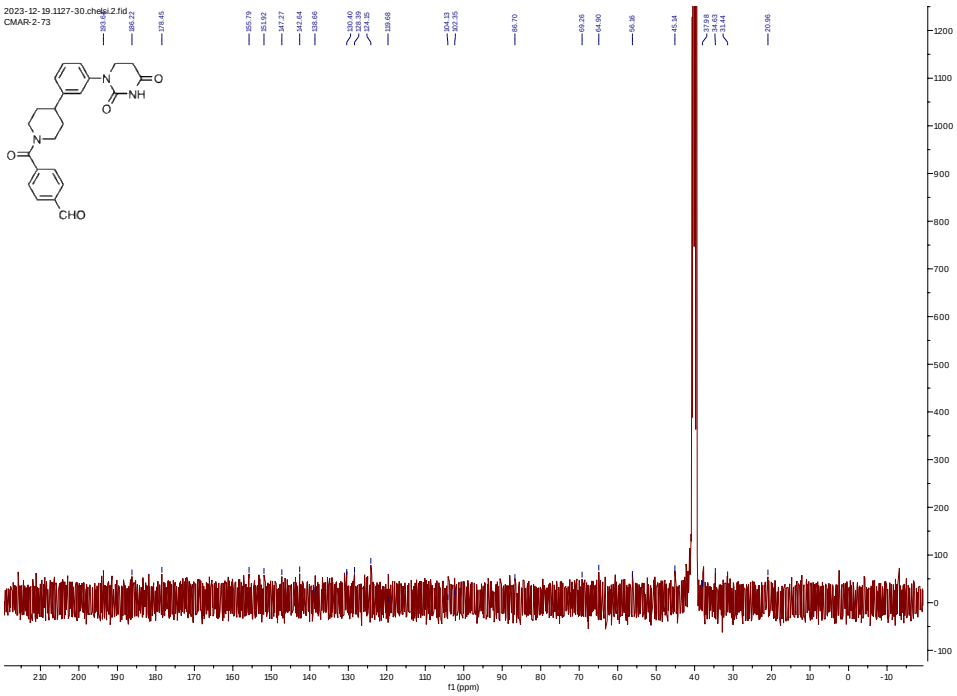

3.7.2 BTK Ligands

^{1}H NMR (400 MHz, $CDCl_3$)

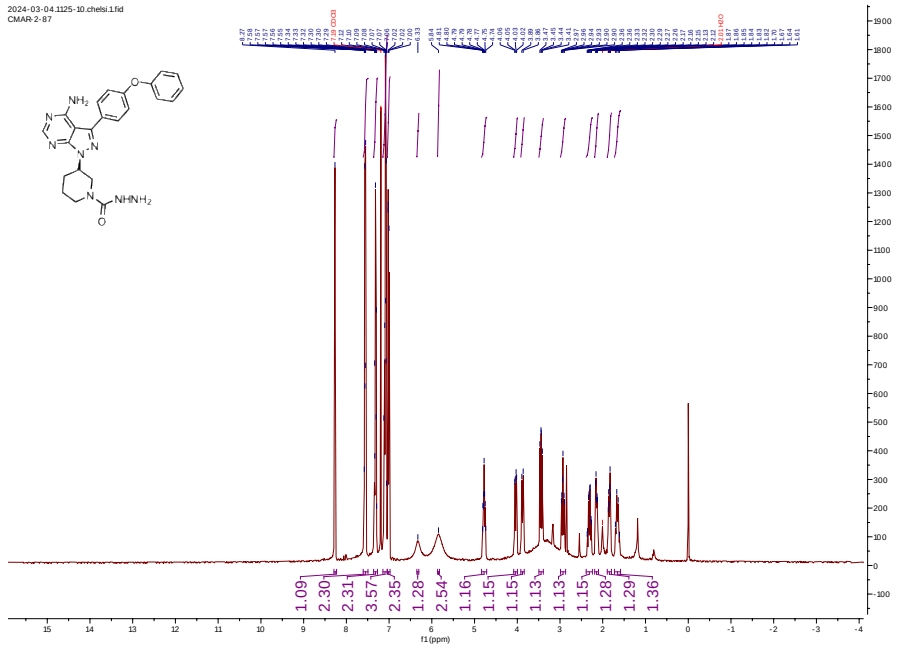

^{13}C NMR (101 MHz, $CDCl_3$)

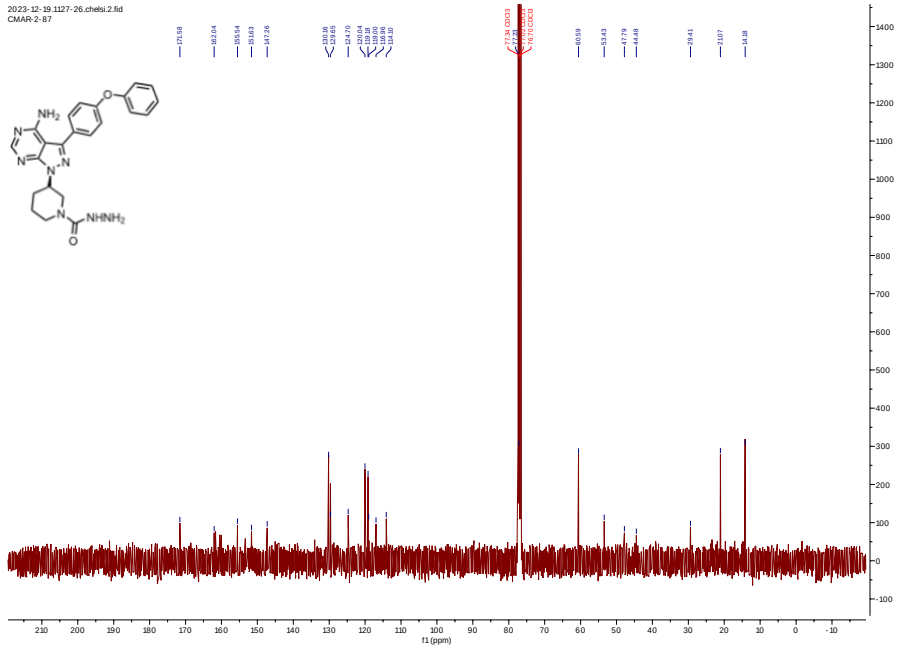

^{1}H NMR (400 MHz, $CDCl_3$)

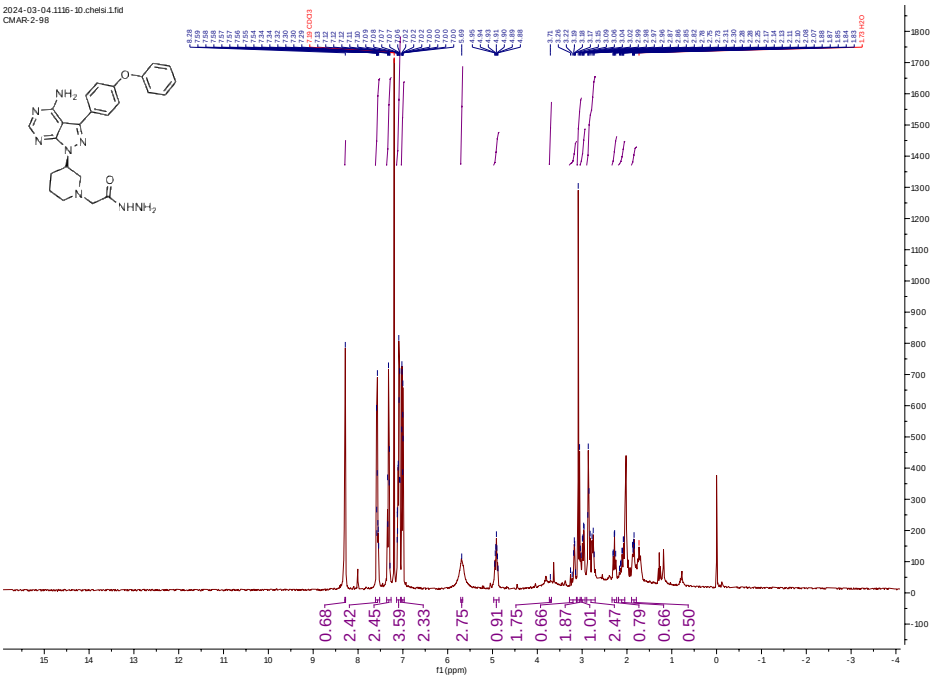

^{13}C NMR (101 MHz, $CDCl_3$)

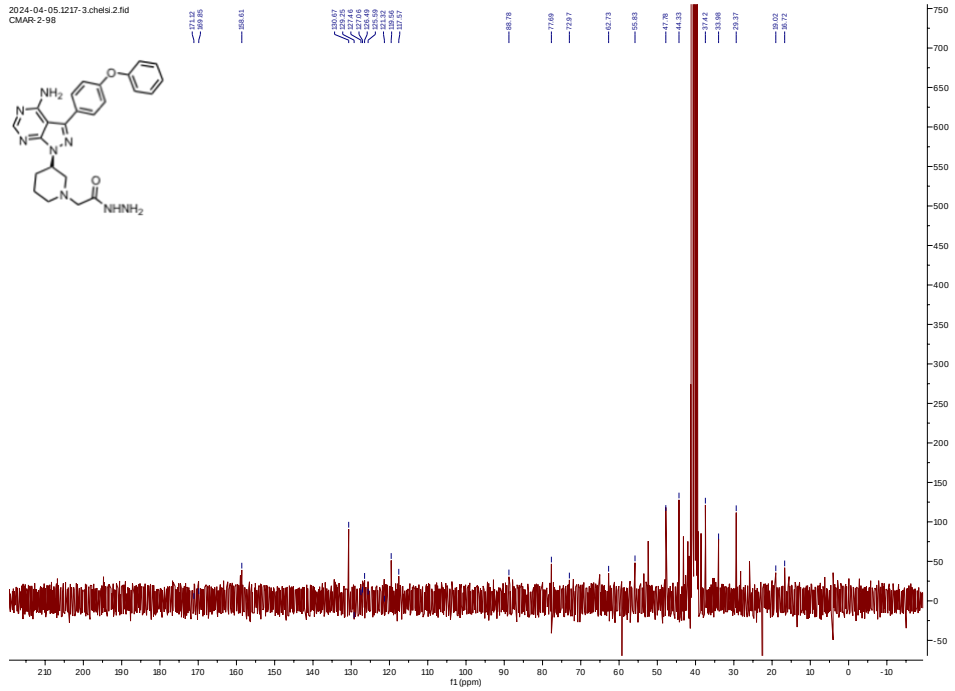

CHAPTER 4

Third Generation Rapid-TAC Platform Using the Thiol-Ene "Click" Chemistry

4.1 Introduction

High throughput experimentation is an advantageous tool in drug discovery for accelerating the optimization of drug molecules.[25] It enables the rapid synthesis and biological examination of libraries of hundreds to thousands compounds in over a few days. Proteolysis Targeting Chimeras (PROTACs) are a therapeutic approach to promote the degradation of intracellular proteins. PROTACs are heterobifunctional degraders composed of a linker bound by two ligands allowing the proximity of a POI and E3 ligase.[9,60] The process leads to polyubiquitination of the target protein and subsequent proteasomal degradation in a catalytic manner.[9] Although PROTACs have been used for a variety of protein targets, rapid optimization of these molecules still holds several challenges.

For instance, linker optimization plays a pivotal role in the degradation efficiency of PROTACs, where spatial orientation and linker length can enable efficient ternary complex formation. However, the synthesis of PROTACs is a time-consuming and challenging process due to the overall complexity of the molecules. Thus, strategies for fast development of active PROTAC degraders has been a priority in the TPD field.

Our lab developed the first generation of the rapid synthesis of PROTAC (Rapid-TAC) platform consisting of a combinatorial strategy that allow the couple a preassembled E3 ligase ligand library with a library of the POI ligands to yield an acylhydrazone linkage without further manipulations including purifications.[11,23] The noticeable advantage of this

chemistry allowed for faster access to full PROTAC products with more than 90% purity and direct biological screening.[11,23] Importantly, the reaction can be carried out under DMSO with the only by-product being water. Nevertheless, one key limitation of the approach is the hydrolytic liability of the acylhydrazone bond.[11,23] After the screening of the initial library and identification of a potent hit, a second stage is required where the acylhydrazone is further changed to more stable isosteres such as an amide bond to improve its stability and drug-like properties.[11,23] In most cases, the more stable amide-containing analogues could retain degradation potency that is comparable to the parent compound.[11,23] After the initial success with ER and FGFR, the approach was also validated for several targets including CARM1 recently.[70] Moreover, since only acylhydrazones derived from aryl aldehydes are stable enough for assays in aqueous solutions, it is required to have an aryl ring in the linker region (**Figure 1**).

The second generation of Rapid-TAC was later reported by our group to overcome some of the limitations of the first generation. In the second generation Rapid-TAC platform, a single step reaction can lead to the creation of active and stable PROTACs, while most advantages of the previous Rapid-TAC platform could be maintained.[24] The reaction involves the formation of a phthalimidine moiety from *ortho* thalaldehyde and a primary alkyl amine. [24] Similar to the first generation, the reaction is achieved under miniaturized conditions without further manipulations including purification.[24] The strategy was validated by creating full PROTAC libraries for the androgen receptor (AR) and the bromodomain containing protein 4 (BRD4).[24] However, alike the first generation Rapid-TAC, the second generation also requires the addition of an aromatic ring in the linker

region (**Figure 1**). To overcome this limitation, the third generation Rapid-TAC strategy should be considered for the rapid development of PROTACs, where an aryl ring is not required to be in the linker region.

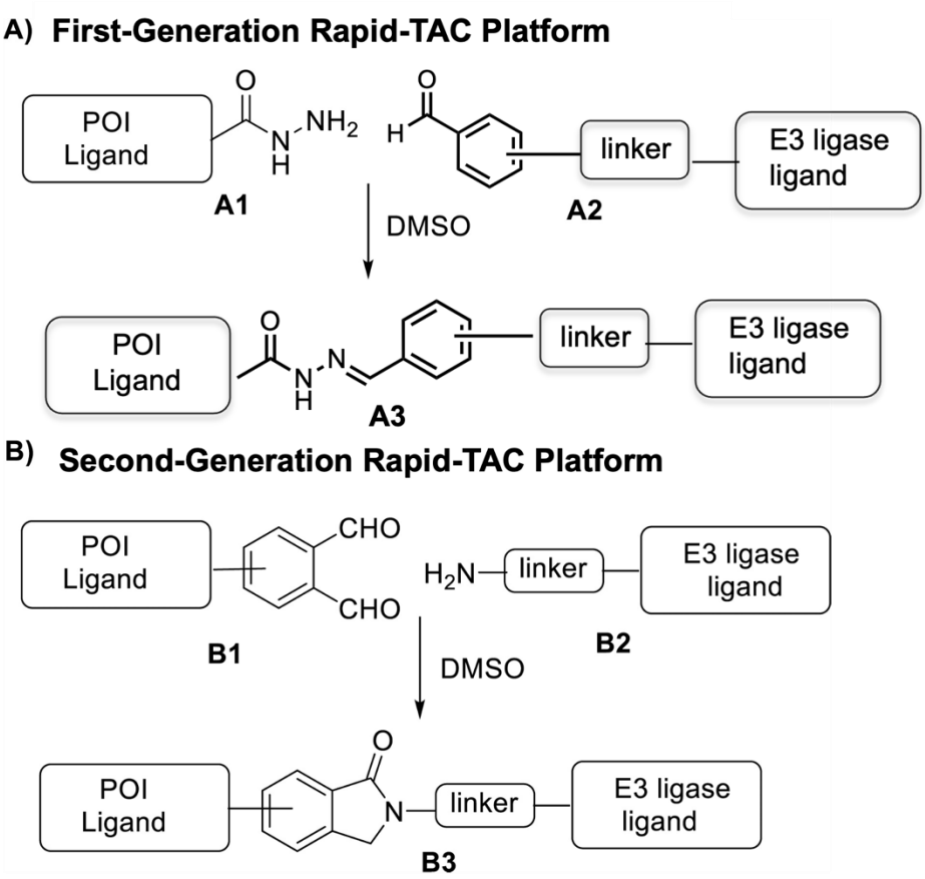

Figure 1. First and second generations of Rapid-TAC platforms previously developed by our lab.[11,24] *The figure was adapted from Guo et al.*[24]

The thiol-ene reaction, also known as thiol-ene coupling, has made ground in traditional synthetic organic chemistry and chemical biology applications including the synthesis of carbohydrates and peptides.[71,72] The mechanism involves a radical thyil from a thiol that undergoes an anti-Markovnikov addition to the alkene, leading to the formation of a

carbon-centered radical (**Figure 2**).[71] This way, the carbon-centered radical extracts a hydrogen from another thiol molecule to achieve a stable thiolether product.[71] Specifically, thermal or photo radical initiators can be used to generate the radical formation.[71] Currently, 2,2,-dimethoxy-2-acetophenone (DPAP) and 2,2'-azobis[2-(2-imidazolin-2-yl)]-dihydrochloride (VA044) are commonly used as photo radical initiators.[71] Interestingly, due to the absence of a metal catalyst, high reaction conversion, and minimal by-products, the thiol-ene reaction is considered to be part of "click" chemistry.[71] Thus, it is particularly attractive for bio-orthogonal applications.

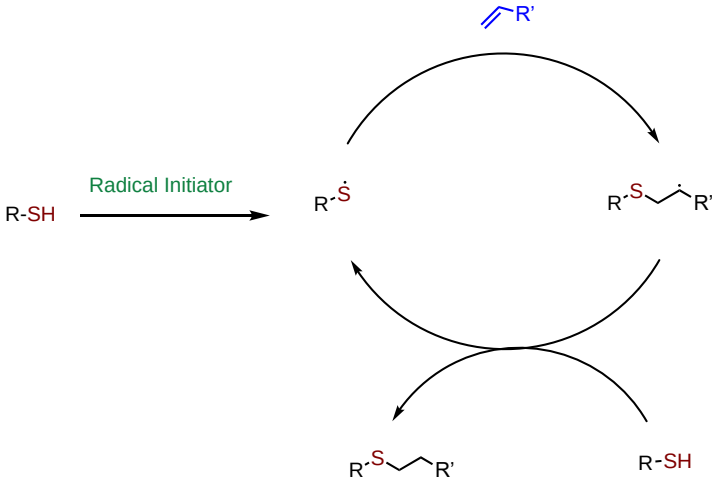

Figure 2. Thiol-ene "click" chemistry radical cycle.

The click chemistry strategy has been also applied to PROTACs.[20,21] Lebraud and coworkers developed a cell penetrating PROTAC molecule from small ligand precursors using a tetrazine/*trans*-cyclooctane "click" chemistry.[22] Moreover, various groups have also utilized the Cu(I)-catalyzed cycloaddition to create and evaluate full PROTAC libraries.[20,21] Herein, inspired by these and our previous studies[11,26], we proposed to utilize the thiol-ene click chemistry strategy for the generation of a third-generation Rapid-

TAC platform. Notably, the thiol-ene “click” chemistry would allow us to synthesize full PROTAC libraries containing a less complex and stable thioether linkage while also keeping the benefits of the prior generations, where direct biological analysis can be achieved with crude samples.

4.2 Results and Discussion

We started with a model test reaction to optimize the thiol-ene “click” chemistry conditions. Essentially, we used two commercially available starting materials and tested different concentrations, solvents, and reaction times. In this case, we decided to use DPAP (10 mol%) in catalytic amount as our photo initiator. The products were examined by LC-MS and TLC. It was observed that using THF as solvent allowed for optimal formation of the desired product after 4 h. However, since our goal is to directly apply the reaction to the generation of PROTACs, THF was changed to a mixture of DMSO/H_2O. Nonetheless, starting material was still observed even after 4 h.

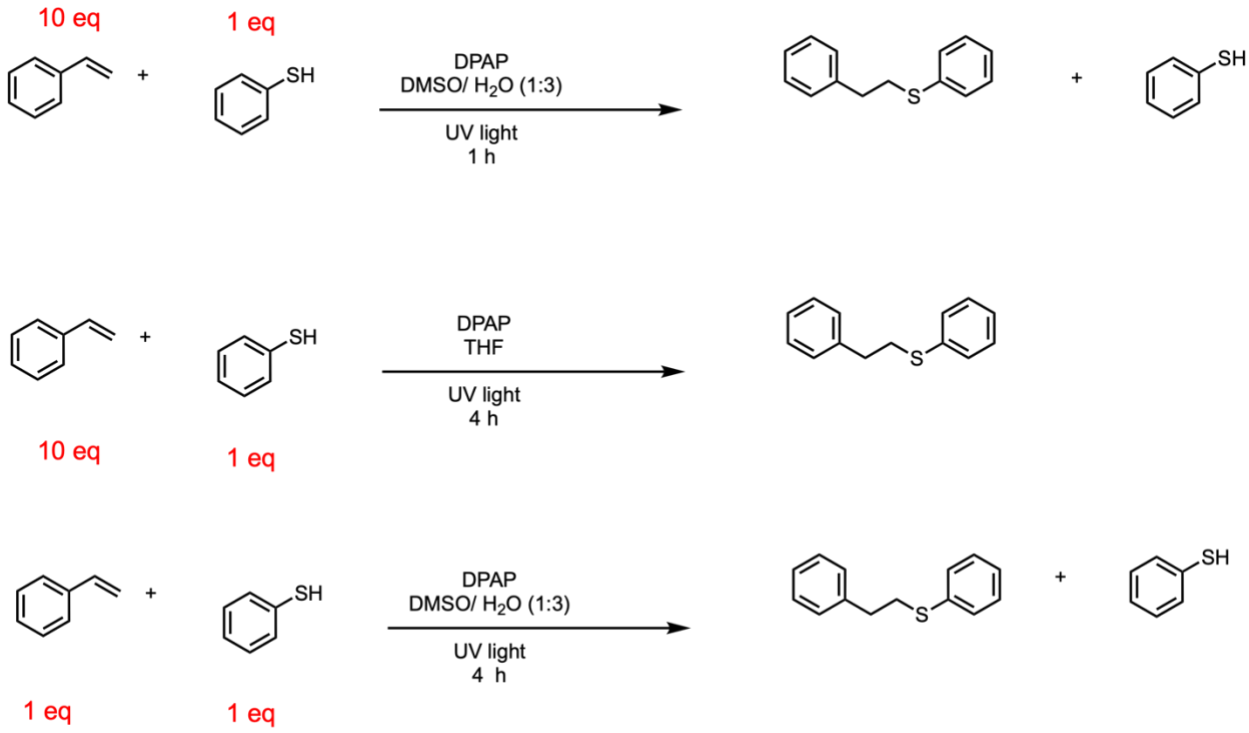

Scheme 1. Model reaction thiol-ene "click" chemistry conditions screening.

To continue our screening of reactions in a more relevant system, we then decided to test the thiol-ene conditions using a functionalized E3 ligase ligand. We started with the reaction between compound **b** containing an achiral CRBN ligand bearing a terminal olefin and a commercially available starting material (thiophenol). The reaction was performed in collaboration with Dr. Kui Zheng. It is worth to note that poor solubility was seen using a mixture DMSO/H_2O. We then decided to continue our reaction screenings only with DMSO as solvent. The reaction progression was analyzed by TLC and LC-MS and the presence of two compounds (**c** and **d**) was observed. Since the reaction undergoes a radical mechanism, we hypothesized that leaving the reaction for 40 h allowed the radical propagation and formation of the by-product **d** (**Scheme 2**). To

minimize the formation of byproduct **d**, we decided to further evaluate the same reaction conditions up until 4 h. Interestingly, high conversion of the desired product **c** was observed by TLC and LC-MS and no formation of **d** was detected.

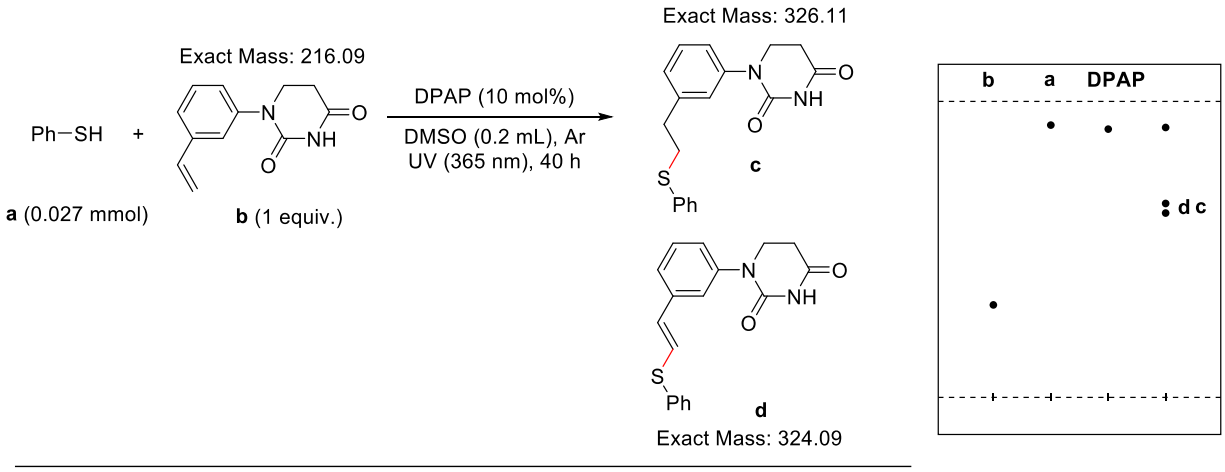

Scheme 2. Thiol-ene "click" chemistry reaction using a relevant meta-substituted CRBN E3 ligase ligand performed with Dr. Kui Zheng.

Later, we tested the thiol-ene conditions employing a para-substituted achiral CRBN ligand. Particularly, **e** was reacted with the commercially available thiophenol (**f**) (1:1 ratio). The reaction was also analyzed by TLC and LC-MS. The presence of the desired product was observed after 4 h with high conversion to the desired product (**g**) and no starting material was observed. We further estimated the NMR yield using the crude compound. However, only 36% yield was obtained by NMR, which is not consistent to our observed high conversion. We hypothesized that it could be due to the reaction workup, where some of our compound remained in the aqueous phase during our extraction procedure. Thus, we repeated the same reaction without the extraction step and calculated the NMR yield of the crude material which significantly increased to 74%.

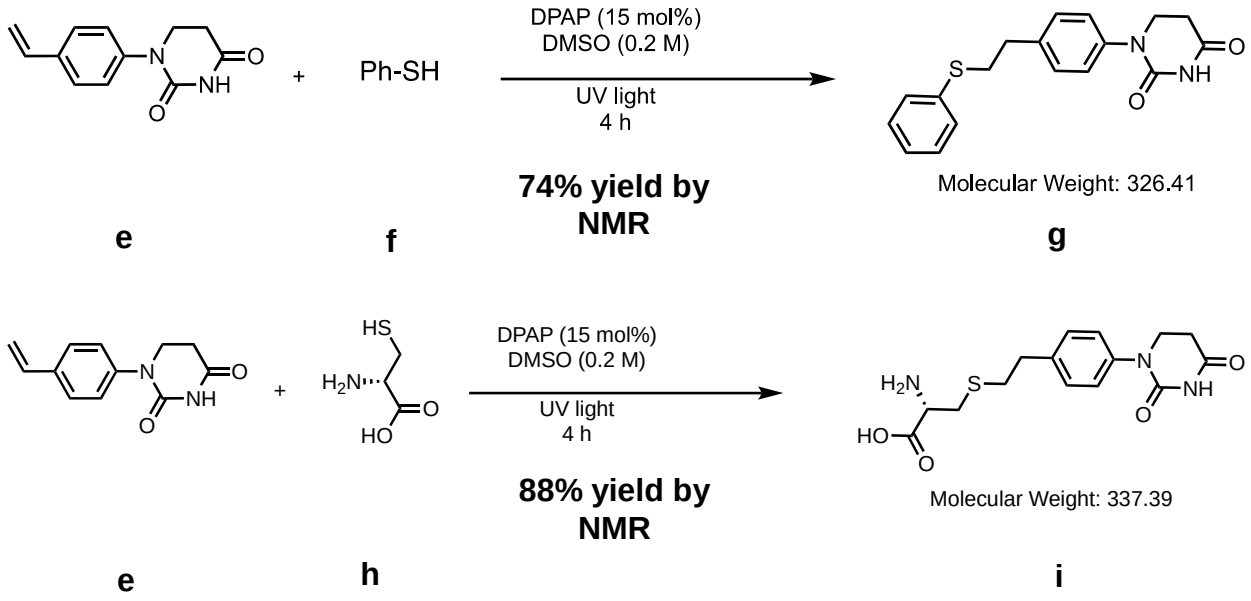

Scheme 3. A) Thiol-ene "click" chemistry reaction screening between a relevant para-substituted CRBN E3 ligase ligand and an aromatic substrate (thiophenol). B) Thiol-ene "click" chemistry reaction screening between a relevant para-substituted CRBN E3 ligase ligand and an aliphatic substrate (cysteine).

Finally, we examined the thiol-ene conditions employing a para-substituted achiral CRBN ligand and an aliphatic CRBN E3 ligase ligand. The reaction was analyzed by TLC and LC-MS. The presence of the desired product (**i**) was also observed after 4 h with high conversion and no starting material was left. Consistent with our previous observations, we determined the NMR yield of the product to be 88%. Further analysis will be done to evaluate the utility of the thiol-ene reaction conditions for the develop a library of a full PROTAC library for any target of interest.

4.3 Conclusion

In conclusion, here we described the preliminary screening of a third-generation Rapid-TAC platform using a thiol-ene “click” chemistry reaction. We evaluated various model reactions to optimize the reaction conditions. Our results indicated that the reaction can be completed after 4 h using DMSO as solvent and a 1:1 ratio of the starting materials. We further analyzed the utility of these reaction conditions with a relevant achiral CRBN E3 ligase ligand, where we achieved up to 88% yield (NMR yield) with the crude product and no by-products were observed. These results suggest the possibility of applying this reaction conditions for the development of partial and full PROTAC libraries using the thiol-ene “click” chemistry strategy for any protein of interest.

4.4 Future Directions

Full PROTAC libraries for different target proteins will need to be synthesized to demonstrate the utility of the new Rapid-TAC strategy. A terminal aryl or alkyl thiol moiety will be attached to a protein of interest ligand and the more stable alkene group will be appended to known E3 ligase ligand by various linkers. We will need to test the scope of different alkenes with aryl or alkyl thiols before building the partial PROTAC library, which is composed of an alkene functional group, various linkers and E3 ligase ligands.

4.5 Experimental Procedures

4.5.1 General Procedure of Thiol-ene “Click” Chemistry

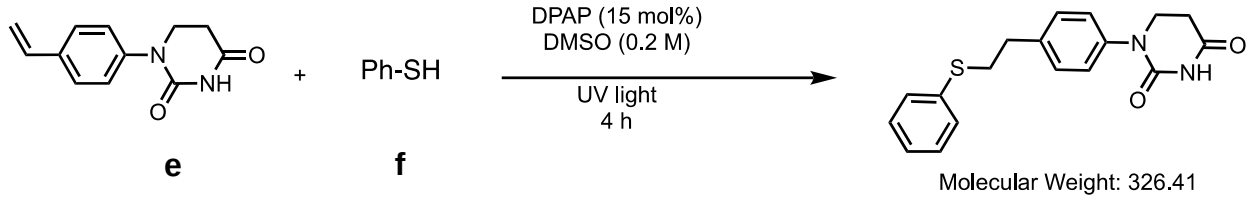

e **f** **g**

To a solution of **e** (10 mg) in DMSO (0.2 M) was added the corresponding thiophenol (1 eq), DPAP (15 mol%) and erradiated UV light and cover with aluminum foil. The reaction mixture was stirred for 4 h and the crude was directly analyzed by NMR.

4.6 Characterization

4.6.1 LC-MS Data

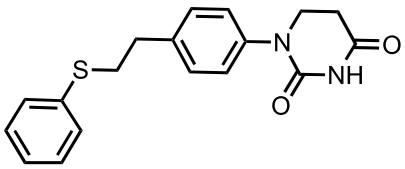

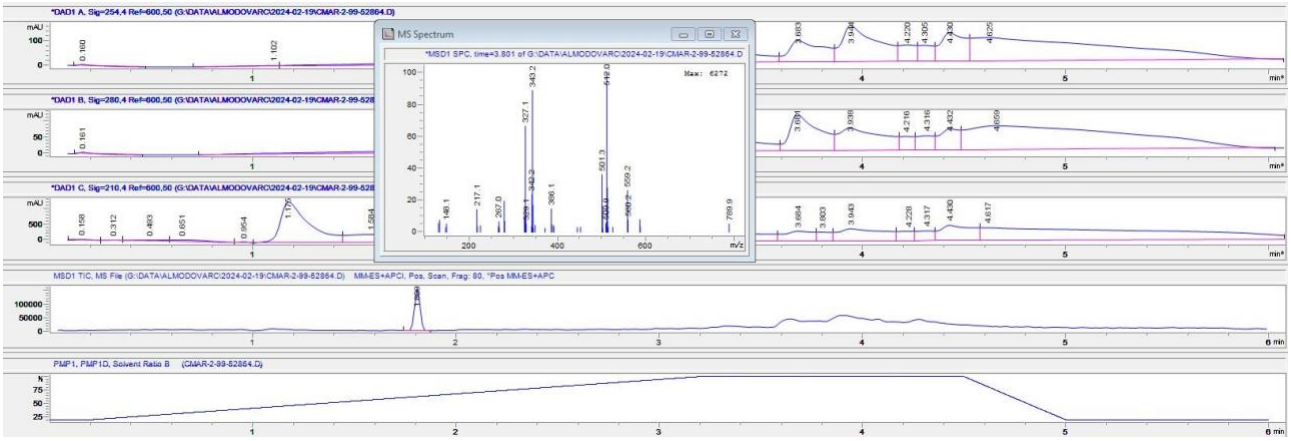

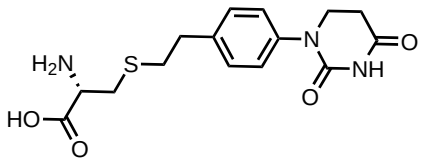

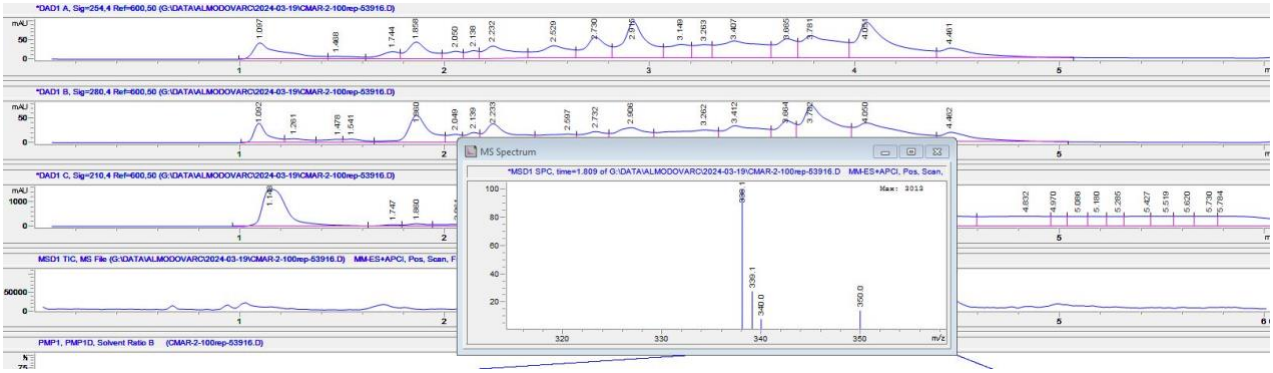

4.6.2 NMR Data

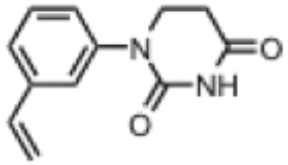

^{1}H NMR (400 MHz, $CDCl_3$) δ 7.94 (s, 1H), 7.35 – 7.15 (m, 4H), 6.62 (dd, *J* = 17.6, 10.9 Hz, 1H), 5.68 (d, *J* = 17.6 Hz, 1H), 5.22 (d, *J* = 10.9 Hz, 1H), 3.79 (q, *J* = 7.0 Hz, 2H), 2.75 (td, *J* = 6.7, 2.7 Hz, 2H).

^{13}C NMR (101 MHz, $CDCl_3$) δ 170.16, 162.78, 152.40, 138.83, 135.96, 130.35, 128.13, 124.45, 115.05, 82.97, 77.45, 77.13, 76.81, 45.23, 36.56, 31.50, 24.78.

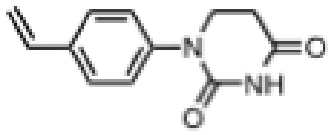

^{1}H NMR (400 MHz, $CDCl_3$) δ 10.01 (s, 1H), 7.57 – 7.41 (m, 1H), 7.41 – 7.29 (m, 1H), 7.29 – 6.97 (m, 2H), 3.80 (td, *J* = 6.7, 3.2 Hz, 1H), 3.64 (pd, *J* = 6.6, 3.9 Hz, 2H), 3.07 (qd, *J* = 7.4, 3.9 Hz, 2H), 2.83 – 2.72 (m, 2H).

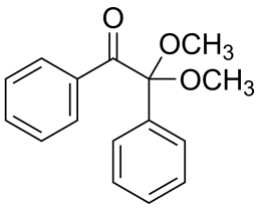

^{1}H NMR (400 MHz, DMSO-d) δ 8.02 – 7.95 (m, 2H), 7.58 – 7.48 (m, 3H), 7.46 – 7.30 (m, 5H), 3.13 (s, 6H).

*4.7*NMR Spectra

^{1}H NMR (400 MHz, $CDCl_3$)- *DPAP*

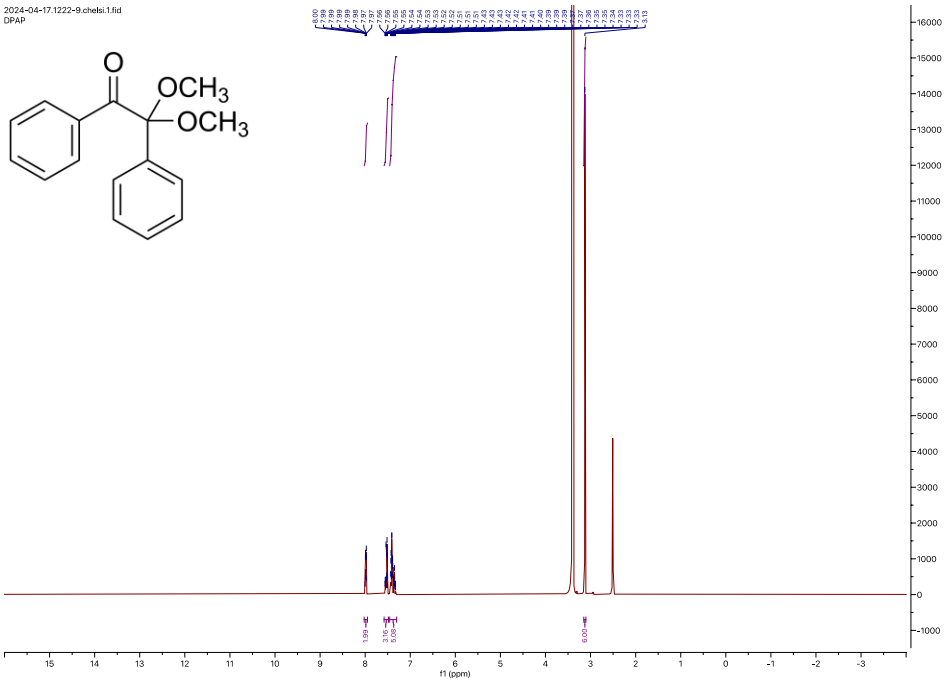

^{1}H NMR (400 MHz, $CDCl_3$)

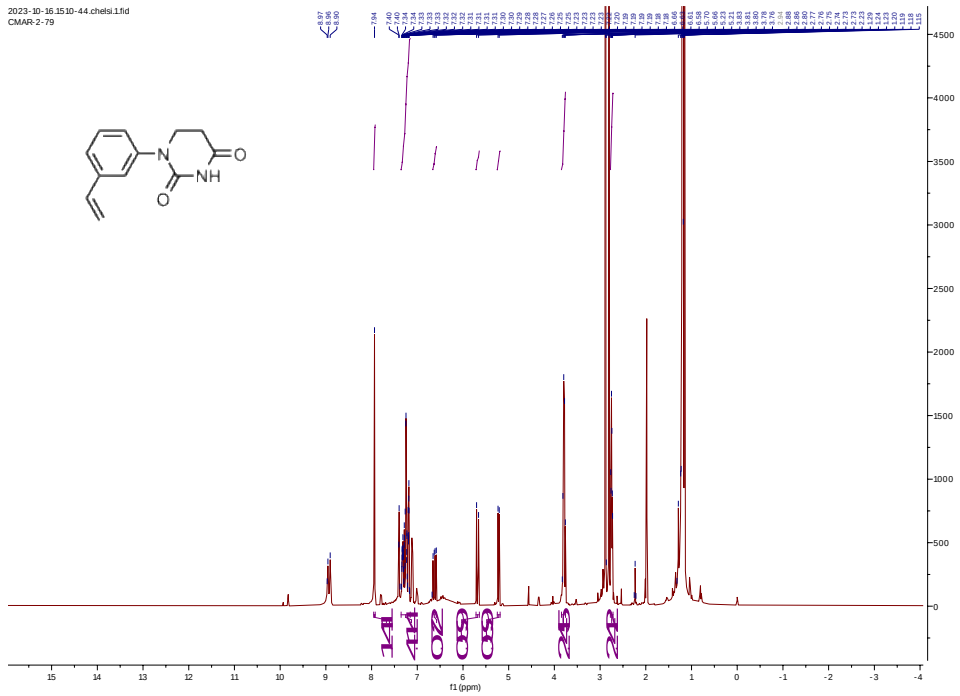

^{13}C NMR (101 MHz, $CDCl_3$)

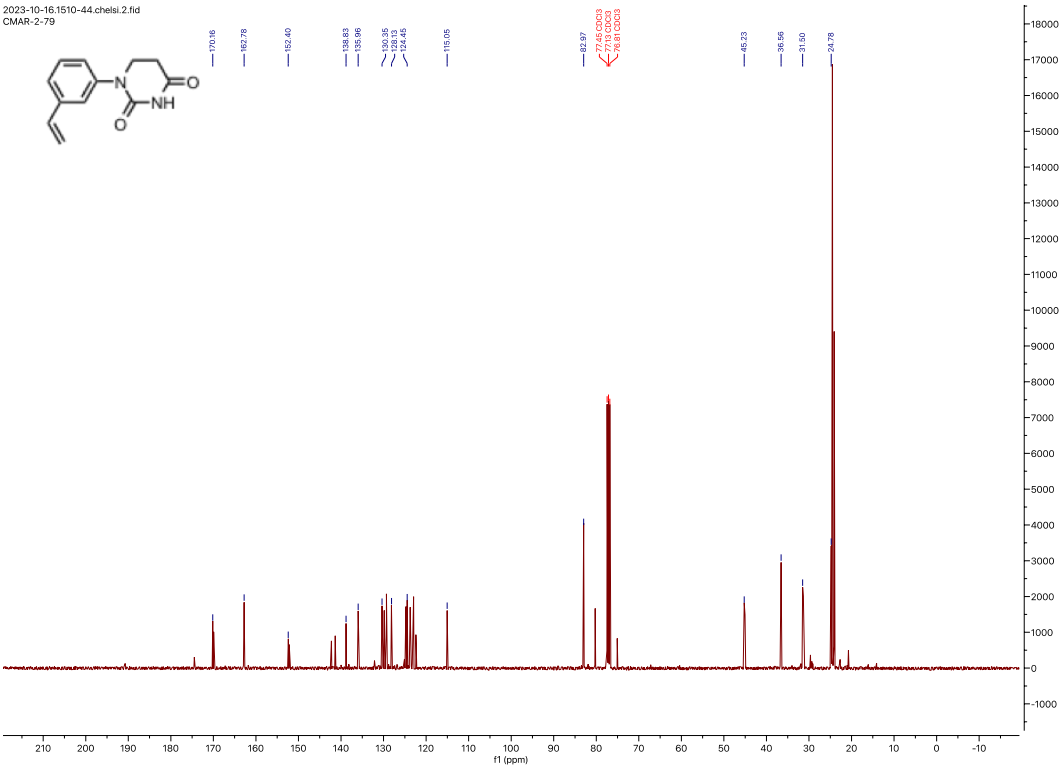

^{1}H NMR (400 MHz, $CDCl_3$)

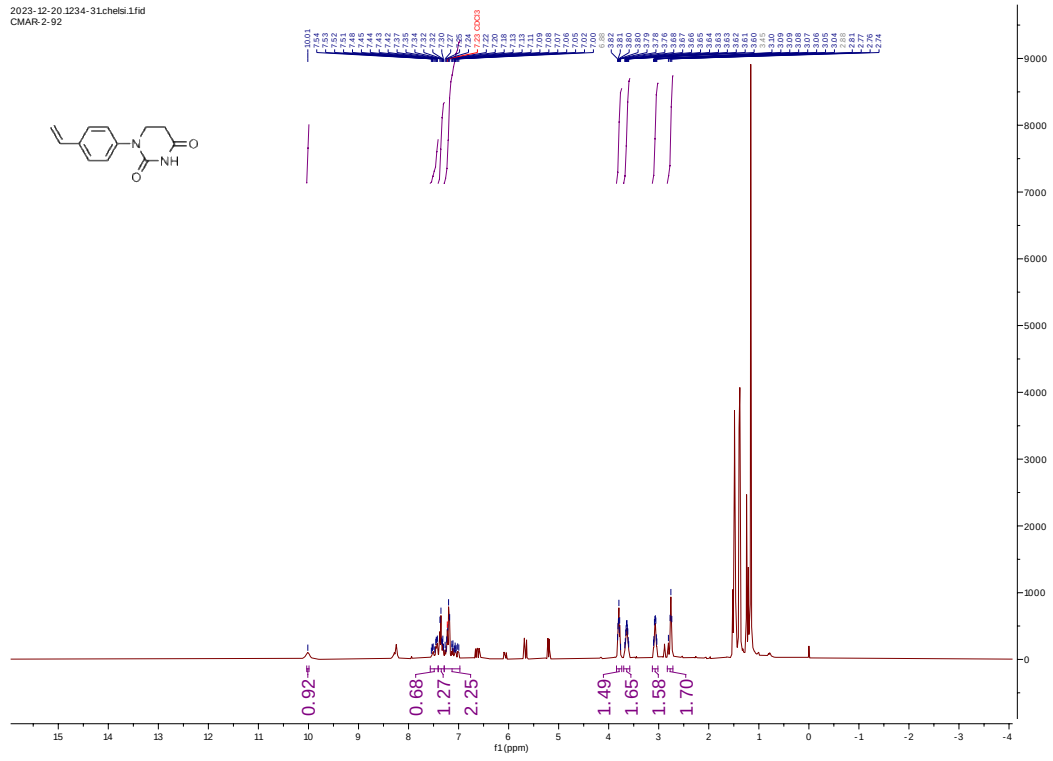

^{1}H NMR (400 MHz, DMSO-d) -Crude material for NMR yield (CH_2Br_2 was used as an internal standard)

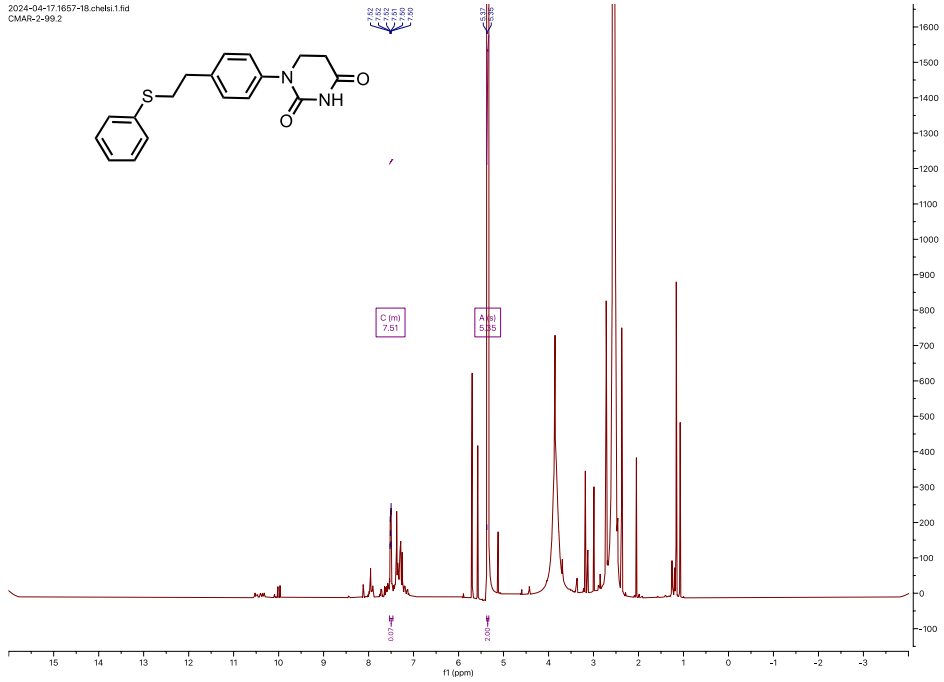

^{1}H NMR (400 MHz, DMSO-d) -Crude material for NMR yield (CH_2Br_2 was used as an internal standard)

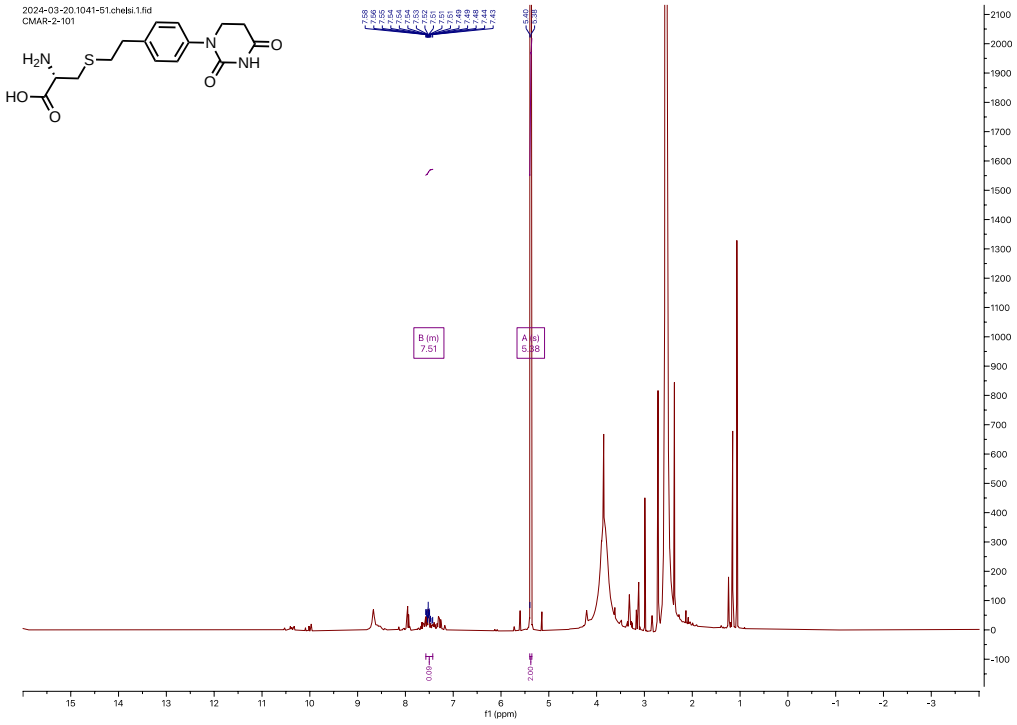

References

(1) Bondeson, D. P.; Crews, C. M. Targeted Protein Degradation by Small Molecules. *Annu. Rev. Pharmacol. Toxicol.* **2017**, *57* (1), 107–123. https://doi.org/10.1146/annurev-pharmtox-010715-103507.

(2) Mostofian, B.; Martin, H.-J.; Razavi, A.; Patel, S.; Allen, B.; Sherman, W.; Izaguirre, J. A. Targeted Protein Degradation: Advances, Challenges, and Prospects for Computational Methods. *J. Chem. Inf. Model.* **2023**, *63* (17), 5408–5432. https://doi.org/10.1021/acs.jcim.3c00603.

(3) Damgaard, R. B. The Ubiquitin System: From Cell Signalling to Disease Biology and New Therapeutic Opportunities. *Cell Death Differ.* **2021**, *28* (2), 423–426. https://doi.org/10.1038/s41418-020-00703-w.

(4) Sakamoto, K. M.; Kim, K. B.; Kumagai, A.; Mercurio, F.; Crews, C. M.; Deshaies, R. J. Protacs: Chimeric Molecules That Target Proteins to the Skp1–Cullin–F Box Complex for Ubiquitination and Degradation. *Proc. Natl. Acad. Sci.* **2001**, *98* (15), 8554–8559. https://doi.org/10.1073/pnas.141230798.

(5) Wang, S.; He, F.; Tian, C.; Sun, A. From PROTAC to TPD: Advances and Opportunities in Targeted Protein Degradation. *Pharmaceuticals* **2024**, *17* (1), 100. https://doi.org/10.3390/ph17010100.

(6) Chirnomas, D.; Hornberger, K. R.; Crews, C. M. Protein Degraders Enter the Clinic — a New Approach to Cancer Therapy. *Nat. Rev. Clin. Oncol.* **2023**, *20* (4), 265–278. https://doi.org/10.1038/s41571-023-00736-3.

(7) *Arvinas and Pfizer's Vepdegestrant (ARV-471) Receives FDA Fast Track Designation for the Treatment of Patients with ER+/HER2- Metastatic Breast Cancer*. https://www.pfizer.com/news/announcements/arvinas-and-pfizers-vepdegestrant-arv-471-receives-fda-fast-track-designation.

(8) Gao, H.; Sun, X.; Rao, Y. PROTAC Technology: Opportunities and Challenges. *ACS Med. Chem. Lett.* **2020**, *11* (3), 237–240. https://doi.org/10.1021/acsmedchemlett.9b00597.

(9) Liu, Z.; Hu, M.; Yang, Y.; Du, C.; Zhou, H.; Liu, C.; Chen, Y.; Fan, L.; Ma, H.; Gong, Y.; Xie, Y. An Overview of PROTACs: A Promising Drug Discovery Paradigm. *Mol. Biomed.* **2022**, *3* (1), 46. https://doi.org/10.1186/s43556-022-00112-0.

(10) Hendrick, C. E.; Jorgensen, J. R.; Chaudhry, C.; Strambeanu, I. I.; Brazeau, J.-F.; Schiffer, J.; Shi, Z.; Venable, J. D.; Wolkenberg, S. E. Direct-to-Biology Accelerates PROTAC Synthesis and the Evaluation of Linker Effects on Permeability and Degradation. *ACS Med. Chem. Lett.* **2022**, *13* (7), 1182–1190. https://doi.org/10.1021/acsmedchemlett.2c00124.

(11) Roberts, B. L.; Ma, Z.-X.; Gao, A.; Leisten, E. D.; Yin, D.; Xu, W.; Tang, W. Two-Stage Strategy for Development of Proteolysis Targeting Chimeras and Its Application for Estrogen Receptor Degraders. *ACS Chem. Biol.* **2020**, *15* (6), 1487–1496. https://doi.org/10.1021/acschembio.0c00140.

(12) Wang, B.; Wu, S.; Liu, J.; Yang, K.; Xie, H.; Tang, W. Development of Selective Small Molecule MDM2 Degraders Based on Nutlin. *Eur. J. Med. Chem.* **2019**, *176*, 476–491. https://doi.org/10.1016/j.ejmech.2019.05.046.

(13) Lee, J.; Lee, Y.; Jung, Y. M.; Park, J. H.; Yoo, H. S.; Park, J. Discovery of E3 Ligase Ligands for Target Protein Degradation. *Molecules* **2022**, *27* (19), 6515. https://doi.org/10.3390/molecules27196515.
(14) Li, L.; Mi, D.; Pei, H.; Duan, Q.; Wang, X.; Zhou, W.; Jin, J.; Li, D.; Liu, M.; Chen, Y. In Vivo Target Protein Degradation Induced by PROTACs Based on E3 Ligase DCAF15. *Signal Transduct. Target. Ther.* **2020**, *5* (1), 129. https://doi.org/10.1038/s41392-020-00245-0.
(15) Lucas, S. C. C.; Ahmed, A.; Ashraf, S. N.; Argyrou, A.; Bauer, M. R.; De Donatis, G. M.; Demanze, S.; Eisele, F.; Fusani, L.; Hock, A.; Kadamur, G.; Li, S.; Macmillan-Jones, A.; Michaelides, I. N.; Phillips, C.; Rehnström, M.; Richter, M.; Rodrigo-Brenni, M. C.; Shilliday, F.; Wang, P.; Storer, R. I. Optimization of Potent Ligands for the E3 Ligase DCAF15 and Evaluation of Their Use in Heterobifunctional Degraders. *J. Med. Chem.* **2024**, *67* (7), 5538–5566. https://doi.org/10.1021/acs.jmedchem.3c02136.
(16) Bricelj, A.; Steinebach, C.; Kuchta, R.; Gütschow, M.; Sosič, I. E3 Ligase Ligands in Successful PROTACs: An Overview of Syntheses and Linker Attachment Points. *Front. Chem.* **2021**, *9*, 707317. https://doi.org/10.3389/fchem.2021.707317.
(17) Yao, T.; Xiao, H.; Wang, H.; Xu, X. Recent Advances in PROTACs for Drug Targeted Protein Research. *Int. J. Mol. Sci.* **2022**, *23* (18), 10328. https://doi.org/10.3390/ijms231810328.
(18) Troup, R. I.; Fallan, C.; Baud, M. G. J. Current Strategies for the Design of PROTAC Linkers: A Critical Review. *Explor. Target. Anti-Tumor Ther.* **2020**, *1* (5). https://doi.org/10.37349/etat.2020.00018.
(19) Zografou-Barredo, N. A.; Hallatt, A. J.; Goujon-Ricci, J.; Cano, C. A Beginner's Guide to Current Synthetic Linker Strategies towards VHL-Recruiting PROTACs. *Bioorg. Med. Chem.* **2023**, *88–89*, 117334. https://doi.org/10.1016/j.bmc.2023.117334.
(20) Schiedel, M.; Herp, D.; Hammelmann, S.; Swyter, S.; Lehotzky, A.; Robaa, D.; Oláh, J.; Ovádi, J.; Sippl, W.; Jung, M. Chemically Induced Degradation of Sirtuin 2 (Sirt2) by a Proteolysis Targeting Chimera (PROTAC) Based on Sirtuin Rearranging Ligands (SirReals). *J. Med. Chem.* **2018**, *61* (2), 482–491. https://doi.org/10.1021/acs.jmedchem.6b01872.
(21) Wurz, R. P.; Dellamaggiore, K.; Dou, H.; Javier, N.; Lo, M.-C.; McCarter, J. D.; Mohl, D.; Sastri, C.; Lipford, J. R.; Cee, V. J. A "Click Chemistry Platform" for the Rapid Synthesis of Bispecific Molecules for Inducing Protein Degradation. *J. Med. Chem.* **2018**, *61* (2), 453–461. https://doi.org/10.1021/acs.jmedchem.6b01781.
(22) Lebraud, H.; Wright, D. J.; Johnson, C. N.; Heightman, T. D. Protein Degradation by In-Cell Self-Assembly of Proteolysis Targeting Chimeras. *ACS Cent. Sci.* **2016**, *2* (12), 927–934. https://doi.org/10.1021/acscentsci.6b00280.
(23) Guo, L.; Liu, J.; Nie, X.; Wang, T.; Ma, Z.; Yin, D.; Tang, W. Development of Selective FGFR1 Degraders Using a Rapid Synthesis of Proteolysis Targeting Chimera (Rapid-TAC) Platform. *Bioorg. Med. Chem. Lett.* **2022**, *75*, 128982. https://doi.org/10.1016/j.bmcl.2022.128982.
(24) Guo, L.; Zhou, Y.; Nie, X.; Zhang, Z.; Zhang, Z.; Li, C.; Wang, T.; Tang, W. A Platform for the Rapid Synthesis of Proteolysis Targeting Chimeras (Rapid-TAC)

under Miniaturized Conditions. *Eur. J. Med. Chem.* **2022**, *236*, 114317. https://doi.org/10.1016/j.ejmech.2022.114317.
(25) Stephens, R.; Bendito-Moll, E.; Battersby, D.; Miah, A.; Wellaway, N.; Law, R.; Stacey, P.; Klimaszewska, D.; Macina, J.; Burley, G.; Harling, J. An Integrated Direct-to-Biology Platform for the Nanoscale Synthesis and Biological Evaluation of PROTACs. September 1, 2023. https://doi.org/10.26434/chemrxiv-2023-1b47d.
(26) Li, J.; Li, C.; Zhang, Z.; Zhang, Z.; Wu, Z.; Liao, J.; Wang, Z.; McReynolds, M.; Xie, H.; Guo, L.; Fan, Q.; Peng, J.; Tang, W. A Platform for the Rapid Synthesis of Molecular Glues (Rapid-Glue) under Miniaturized Conditions for Direct Biological Screening. *Eur. J. Med. Chem.* **2023**, *258*, 115567. https://doi.org/10.1016/j.ejmech.2023.115567.
(27) Sasso, J. M.; Tenchov, R.; Wang, D.; Johnson, L. S.; Wang, X.; Zhou, Q. A. Molecular Glues: The Adhesive Connecting Targeted Protein Degradation to the Clinic. *Biochemistry* **2023**, *62* (3), 601–623. https://doi.org/10.1021/acs.biochem.2c00245.
(28) Wu, J.; Wang, W.; Leung, C.-H. Computational Strategies for PROTAC Drug Discovery. *Acta Mater. Medica* **2023**, *2* (1). https://doi.org/10.15212/AMM-2022-0041.
(29) Liao, J.; Nie, X.; Unarta, I. C.; Ericksen, S. S.; Tang, W. In Silico Modeling and Scoring of PROTAC-Mediated Ternary Complex Poses. *J. Med. Chem.* **2022**, *65* (8), 6116–6132. https://doi.org/10.1021/acs.jmedchem.1c02155.
(30) Qiu, X.; Sun, N.; Kong, Y.; Li, Y.; Yang, X.; Jiang, B. Chemoselective Synthesis of Lenalidomide-Based PROTAC Library Using Alkylation Reaction. *Org. Lett.* **2019**, *21* (10), 3838–3841. https://doi.org/10.1021/acs.orglett.9b01326.
(31) Sun, X.; Gao, H.; Yang, Y.; He, M.; Wu, Y.; Song, Y.; Tong, Y.; Rao, Y. PROTACs: Great Opportunities for Academia and Industry. *Signal Transduct. Target. Ther.* **2019**, *4* (1), 64. https://doi.org/10.1038/s41392-019-0101-6.
(32) Sosič, I.; Bricelj, A.; Steinebach, C. E3 Ligase Ligand Chemistries: From Building Blocks to Protein Degraders. *Chem. Soc. Rev.* **2022**, *51* (9), 3487–3534. https://doi.org/10.1039/D2CS00148A.
(33) Yao, T.; Xiao, H.; Wang, H.; Xu, X. Recent Advances in PROTACs for Drug Targeted Protein Research. *Int. J. Mol. Sci.* **2022**, *23* (18), 10328. https://doi.org/10.3390/ijms231810328.
(34) Bricelj, A.; Steinebach, C.; Kuchta, R.; Gütschow, M.; Sosič, I. E3 Ligase Ligands in Successful PROTACs: An Overview of Syntheses and Linker Attachment Points. *Front. Chem.* **2021**, *9*, 707317. https://doi.org/10.3389/fchem.2021.707317.
(35) Kazantsev, A.; Krasavin, M. Ligands for Cereblon: 2017–2021 Patent Overview. *Expert Opin. Ther. Pat.* **2022**, *32* (2), 171–190. https://doi.org/10.1080/13543776.2022.1999415.
(36) Kong, N. R.; Liu, H.; Che, J.; Jones, L. H. Physicochemistry of Cereblon Modulating Drugs Determines Pharmacokinetics and Disposition. *ACS Med. Chem. Lett.* **2021**, *12* (11), 1861–1865. https://doi.org/10.1021/acsmedchemlett.1c00475.
(37) Min, J.; Mayasundari, A.; Keramatnia, F.; Jonchere, B.; Yang, S. W.; Jarusiewicz, J.; Actis, M.; Das, S.; Young, B.; Slavish, J.; Yang, L.; Li, Y.; Fu, X.; Garrett, S. H.; Yun, M.; Li, Z.; Nithianantham, S.; Chai, S.; Chen, T.; Shelat, A.; Lee, R. E.; Nishiguchi, G.; White, S. W.; Roussel, M. F.; Potts, P. R.; Fischer, M.; Rankovic, Z.

Phenyl-Glutarimides: Alternative Cereblon Binders for the Design of PROTACs. *Angew. Chem. Int. Ed.* **2021**, *60* (51), 26663–26670. https://doi.org/10.1002/anie.202108848.
(38) Xie, H.; Li, C.; Tang, H.; Tandon, I.; Liao, J.; Roberts, B. L.; Zhao, Y.; Tang, W. Development of Substituted Phenyl Dihydrouracil as the Novel Achiral Cereblon Ligands for Targeted Protein Degradation. *J. Med. Chem.* **2023**, *66* (4), 2904–2917. https://doi.org/10.1021/acs.jmedchem.2c01941.
(39) Hayhow, T. G.; Borrows, R. E. A.; Diène, C. R.; Fairley, G.; Fallan, C.; Fillery, S. M.; Scott, J. S.; Watson, D. W. A Buchwald–Hartwig Protocol to Enable Rapid Linker Exploration of Cereblon E3-Ligase PROTACs**. *Chem. – Eur. J.* **2020**, *26* (70), 16818–16823. https://doi.org/10.1002/chem.202003137.
(40) Liu, H.; Sun, R.; Ren, C.; Qiu, X.; Yang, X.; Jiang, B. Construction of an IMiD-Based Azide Library as a Kit for PROTAC Research. *Org. Biomol. Chem.* **2021**, *19* (1), 166–170. https://doi.org/10.1039/D0OB02120B.
(41) Bricelj, A.; Dora Ng, Y. L.; Ferber, D.; Kuchta, R.; Müller, S.; Monschke, M.; Wagner, K. G.; Krönke, J.; Sosič, I.; Gütschow, M.; Steinebach, C. Influence of Linker Attachment Points on the Stability and Neosubstrate Degradation of Cereblon Ligands. *ACS Med. Chem. Lett.* **2021**, *12* (11), 1733–1738. https://doi.org/10.1021/acsmedchemlett.1c00368.
(42) Hoffmann, M.; Kasserra, C.; Reyes, J.; Schafer, P.; Kosek, J.; Capone, L.; Parton, A.; Kim-Kang, H.; Surapaneni, S.; Kumar, G. Absorption, Metabolism and Excretion of [14C]Pomalidomide in Humans Following Oral Administration. *Cancer Chemother. Pharmacol.* **2013**, *71* (2), 489–501. https://doi.org/10.1007/s00280-012-2040-6.
(43) Yang, K.; Zhao, Y.; Nie, X.; Wu, H.; Wang, B.; Almodovar-Rivera, C. M.; Xie, H.; Tang, W. A Cell-Based Target Engagement Assay for the Identification of Cereblon E3 Ubiquitin Ligase Ligands and Their Application in HDAC6 Degraders. *Cell Chem. Biol.* **2020**, S2451945620301458. https://doi.org/10.1016/j.chembiol.2020.04.008.
(44) Xiao, D.; Wang, Y.; Wang, H.; Zhou, Y.; Li, J.; Lu, W.; Jin, J. Design and Synthesis of New Lenalidomide Analogs via Suzuki Cross-coupling Reaction. *Arch. Pharm. (Weinheim)* **2020**, *353* (7), 1900376. https://doi.org/10.1002/ardp.201900376.
(45) Li, Y.; Yang, J.; Aguilar, A.; McEachern, D.; Przybranowski, S.; Liu, L.; Yang, C.-Y.; Wang, M.; Han, X.; Wang, S. Discovery of MD-224 as a First-in-Class, Highly Potent, and Efficacious Proteolysis Targeting Chimera Murine Double Minute 2 Degrader Capable of Achieving Complete and Durable Tumor Regression. *J. Med. Chem.* **2019**, *62* (2), 448–466. https://doi.org/10.1021/acs.jmedchem.8b00909.
(46) Ishiyama, T.; Murata, M.; Miyaura, N. Palladium(0)-Catalyzed Cross-Coupling Reaction of Alkoxydiboron with Haloarenes: A Direct Procedure for Arylboronic Esters. *J. Org. Chem.* **1995**, *60* (23), 7508–7510. https://doi.org/10.1021/jo00128a024.
(47) Brown, J.; Su, S. C. K.; Shafer, J. A. The Hydrolysis and Cyclization of Some Phthalamic Acid Derivatives. *J. Am. Chem. Soc.* **1966**, *88* (19), 4468–4474. https://doi.org/10.1021/ja00971a031.

(48) Zagidullin, A.; Milyukov, V.; Rizvanov, A.; Bulatov, E. Novel Approaches for the Rational Design of PROTAC Linkers. *Explor. Target. Anti-Tumor Ther.* **2020**, *1* (5), 381–390. https://doi.org/10.37349/etat.2020.00023.
(49) Du, Y. Fluorescence Polarization Assay to Quantify Protein-Protein Interactions in an HTS Format. In *Protein-Protein Interactions*; Meyerkord, C. L., Fu, H., Eds.; Methods in Molecular Biology; Springer New York: New York, NY, 2015; Vol. 1278, pp 529–544. https://doi.org/10.1007/978-1-4939-2425-7_35.
(50) Ranawakage, D. C.; Takada, T.; Kamachi, Y. HiBiT-qIP, HiBiT-Based Quantitative Immunoprecipitation, Facilitates the Determination of Antibody Affinity under Immunoprecipitation Conditions. *Sci. Rep.* **2019**, *9* (1), 6895. https://doi.org/10.1038/s41598-019-43319-y.
(51) *HiBiT Blotting: A Fast and Sensitive Western Blot Alternative*.
(52) Vargesson, N. Thalidomide-Induced Teratogenesis: History and Mechanisms: Thalidomide-Induced Teratogenesis. *Birth Defects Res. Part C Embryo Today Rev.* **2015**, *105* (2), 140–156. https://doi.org/10.1002/bdrc.21096.
(53) Zhu, Y. X.; Kortuem, K. M.; Stewart, A. K. Molecular Mechanism of Action of Immune-Modulatory Drugs Thalidomide, Lenalidomide and Pomalidomide in Multiple Myeloma. *Leuk. Lymphoma* **2013**, *54* (4), 683–687. https://doi.org/10.3109/10428194.2012.728597.
(54) Shi, Q.; Chen, L. Cereblon: A Protein Crucial to the Multiple Functions of Immunomodulatory Drugs as Well as Cell Metabolism and Disease Generation. *J. Immunol. Res.* **2017**, *2017*, 1–8. https://doi.org/10.1155/2017/9130608.
(55) Kowalski, T. W.; Gomes, J. do A.; Garcia, G. B. C.; Fraga, L. R.; Paixao-Cortes, V. R.; Recamonde-Mendoza, M.; Sanseverino, M. T. V.; Schuler-Faccini, L.; Vianna, F. S. L. CRL4-Cereblon Complex in Thalidomide Embryopathy: A Translational Investigation. *Sci. Rep.* **2020**, *10* (1), 851. https://doi.org/10.1038/s41598-020-57512-x.
(56) Angers, S.; Li, T.; Yi, X.; MacCoss, M. J.; Moon, R. T.; Zheng, N. Molecular Architecture and Assembly of the DDB1–CUL4A Ubiquitin Ligase Machinery. *Nature* **2006**, *443* (7111), 590–593. https://doi.org/10.1038/nature05175.
(57) Nishimura, K.; Hashimoto, Y.; Iwasaki, S. (S)-Form of .ALPHA.-Methyl-N(.ALPHA.)-Phthalimidoglutarimide, but Not Its (R)-Form, Enhanced Phorbol Ester-Induced Tumor Necrosis Factor-.ALPHA. Production by Human Leukemia Cell HL-60: Implication of Optical Resolution of Thalidomidal Effects. *Chem. Pharm. Bull. (Tokyo)* **1994**, *42* (5), 1157–1159. https://doi.org/10.1248/cpb.42.1157.
(58) Hansen, J. D.; Correa, M.; Nagy, M. A.; Alexander, M.; Plantevin, V.; Grant, V.; Whitefield, B.; Huang, D.; Kercher, T.; Harris, R.; Narla, R. K.; Leisten, J.; Tang, Y.; Moghaddam, M.; Ebinger, K.; Piccotti, J.; Havens, C. G.; Cathers, B.; Carmichael, J.; Daniel, T.; Vessey, R.; Hamann, L. G.; Leftheris, K.; Mendy, D.; Baculi, F.; LeBrun, L. A.; Khambatta, G.; Lopez-Girona, A. Discovery of CRBN E3 Ligase Modulator CC-92480 for the Treatment of Relapsed and Refractory Multiple Myeloma. *J. Med. Chem.* **2020**, *63* (13), 6648–6676. https://doi.org/10.1021/acs.jmedchem.9b01928.
(59) Lim, Y. S.; Yoo, S.-M.; Patil, V.; Kim, H. W.; Kim, H.-H.; Suh, B.; Park, J. Y.; Jeong, N.; Park, C. H.; Ryu, J. H.; Lee, B.-H.; Kim, P.; Lee, S. H. Orally Bioavailable BTK PROTAC Active against Wild-Type and C481 Mutant BTKs in Human Lymphoma

CDX Mouse Models. *Blood Adv.* **2023**, *7* (1), 92–105. https://doi.org/10.1182/bloodadvances.2022008121.
(60) Huang, J.; Ma, Z.; Peng, X.; Yang, Z.; Wu, Y.; Zhong, G.; Ouyang, T.; Chen, Z.; Liu, Y.; Wang, Q.; Chen, J.; Chen, T.; Zeng, Z. Discovery of Novel Potent and Fast BTK PROTACs for the Treatment of Osteoclasts-Related Inflammatory Diseases. *J. Med. Chem.* **2024**, *67* (4), 2438–2465. https://doi.org/10.1021/acs.jmedchem.3c01414.
(61) Chen, S.; Chen, Z.; Lu, L.; Zhao, Y.; Zhou, R.; Xie, Q.; Shu, Y.; Lin, J.; Yu, X.; Wang, Y. Discovery of Novel BTK PROTACs with Improved Metabolic Stability via Linker Rigidification Strategy. *Eur. J. Med. Chem.* **2023**, *255*, 115403. https://doi.org/10.1016/j.ejmech.2023.115403.
(62) Pal Singh, S.; Dammeijer, F.; Hendriks, R. W. Role of Bruton's Tyrosine Kinase in B Cells and Malignancies. *Mol. Cancer* **2018**, *17* (1), 57. https://doi.org/10.1186/s12943-018-0779-z.
(63) Montoya, S.; Bourcier, J.; Noviski, M.; Lu, H.; Thompson, M. C.; Chirino, A.; Jahn, J.; Sondhi, A. K.; Gajewski, S.; Tan, Y. S. (May); Yung, S.; Urban, A.; Wang, E.; Han, C.; Mi, X.; Kim, W. J.; Sievers, Q.; Auger, P.; Bousquet, H.; Brathaban, N.; Bravo, B.; Gessner, M.; Guiducci, C.; Iuliano, J. N.; Kane, T.; Mukerji, R.; Reddy, P. J.; Powers, J.; Sanchez Garcia De Los Rios, M.; Ye, J.; Barrientos Risso, C.; Tsai, D.; Pardo, G.; Notti, R. Q.; Pardo, A.; Affer, M.; Nawaratne, V.; Totiger, T. M.; Pena-Velasquez, C.; Rhodes, J. M.; Zelenetz, A. D.; Alencar, A.; Roeker, L. E.; Mehta, S.; Garippa, R.; Linley, A.; Soni, R. K.; Skånland, S. S.; Brown, R. J.; Mato, A. R.; Hansen, G. M.; Abdel-Wahab, O.; Taylor, J. Kinase-Impaired BTK Mutations Are Susceptible to Clinical-Stage BTK and IKZF1/3 Degrader NX-2127. *Science* **2024**, *383* (6682), eadi5798. https://doi.org/10.1126/science.adi5798.
(64) Yuan, H.; Zhu, Y.; Cheng, Y.; Hou, J.; Jin, F.; Li, M.; Jia, W.; Cheng, Z.; Xing, H.; Liu, M.; Han, T. BTK Kinase Activity Is Dispensable for the Survival of Diffuse Large B-Cell Lymphoma. *J. Biol. Chem.* **2022**, *298* (11), 102555. https://doi.org/10.1016/j.jbc.2022.102555.
(65) Gabizon, R.; Shraga, A.; Gehrtz, P.; Livnah, E.; Shorer, Y.; Gurwicz, N.; Avram, L.; Unger, T.; Aharoni, H.; Albeck, S.; Brandis, A.; Shulman, Z.; Katz, B.-Z.; Herishanu, Y.; London, N. Efficient Targeted Degradation via Reversible and Irreversible Covalent PROTACs. *J. Am. Chem. Soc.* **2020**, *142* (27), 11734–11742. https://doi.org/10.1021/jacs.9b13907.
(66) Guo, W.-H.; Qi, X.; Yu, X.; Liu, Y.; Chung, C.-I.; Bai, F.; Lin, X.; Lu, D.; Wang, L.; Chen, J.; Su, L. H.; Nomie, K. J.; Li, F.; Wang, M. C.; Shu, X.; Onuchic, J. N.; Woyach, J. A.; Wang, M. L.; Wang, J. Enhancing Intracellular Accumulation and Target Engagement of PROTACs with Reversible Covalent Chemistry. *Nat. Commun.* **2020**, *11* (1), 4268. https://doi.org/10.1038/s41467-020-17997-6.
(67) Schiemer, J.; Maxwell, A.; Horst, R.; Liu, S.; Uccello, D. P.; Borzilleri, K.; Rajamohan, N.; Brown, M. F.; Calabrese, M. F. A Covalent BTK Ternary Complex Compatible with Targeted Protein Degradation. *Nat. Commun.* **2023**, *14* (1), 1189. https://doi.org/10.1038/s41467-023-36738-z.
(68) Toriki, E. S.; Papatzimas, J. W.; Nishikawa, K.; Dovala, D.; Frank, A. O.; Hesse, M. J.; Dankova, D.; Song, J.-G.; Bruce-Smythe, M.; Struble, H.; Garcia, F. J.; Brittain, S. M.; Kile, A. C.; McGregor, L. M.; McKenna, J. M.; Tallarico, J. A.; Schirle, M.;

Nomura, D. K. Rational Chemical Design of Molecular Glue Degraders. *ACS Cent. Sci.* **2023**, *9* (5), 915–926. https://doi.org/10.1021/acscentsci.2c01317.
(69) Almodóvar-Rivera, C. M.; Zhang, Z.; Li, J.; Xie, H.; Zhao, Y.; Guo, L.; Mannhardt, M. G.; Tang, W. A Modular Chemistry Platform for the Development of a Cereblon E3 Ligase-Based Partial PROTAC Library. *ChemBioChem* **2023**, e202300482. https://doi.org/10.1002/cbic.202300482.
(70) Xie, H.; Bacabac, M. S.; Ma, M.; Kim, E.-J.; Wang, Y.; Wu, W.; Li, L.; Xu, W.; Tang, W. Development of Potent and Selective Coactivator-Associated Arginine Methyltransferase 1 (CARM1) Degraders. *J. Med. Chem.* **2023**, *66* (18), 13028–13042. https://doi.org/10.1021/acs.jmedchem.3c00982.
(71) Nolan, M. D.; Scanlan, E. M. Applications of Thiol-Ene Chemistry for Peptide Science. *Front. Chem.* **2020**, *8*, 583272. https://doi.org/10.3389/fchem.2020.583272.
(72) Hoyle, C. E.; Lee, T. Y.; Roper, T. Thiol–Enes: Chemistry of the Past with Promise for the Future. *J. Polym. Sci. Part Polym. Chem.* **2004**, *42* (21), 5301–5338. https://doi.org/10.1002/pola.20366.